frontiers | Research Topics

Diagnosis, epidemiology and treatment of salivary gland carcinomas

Edited by
Stefano Cavalieri, Pierluigi Bonomo, Ester Orlandi and Andreas Mock

Published in
Frontiers in Oncology

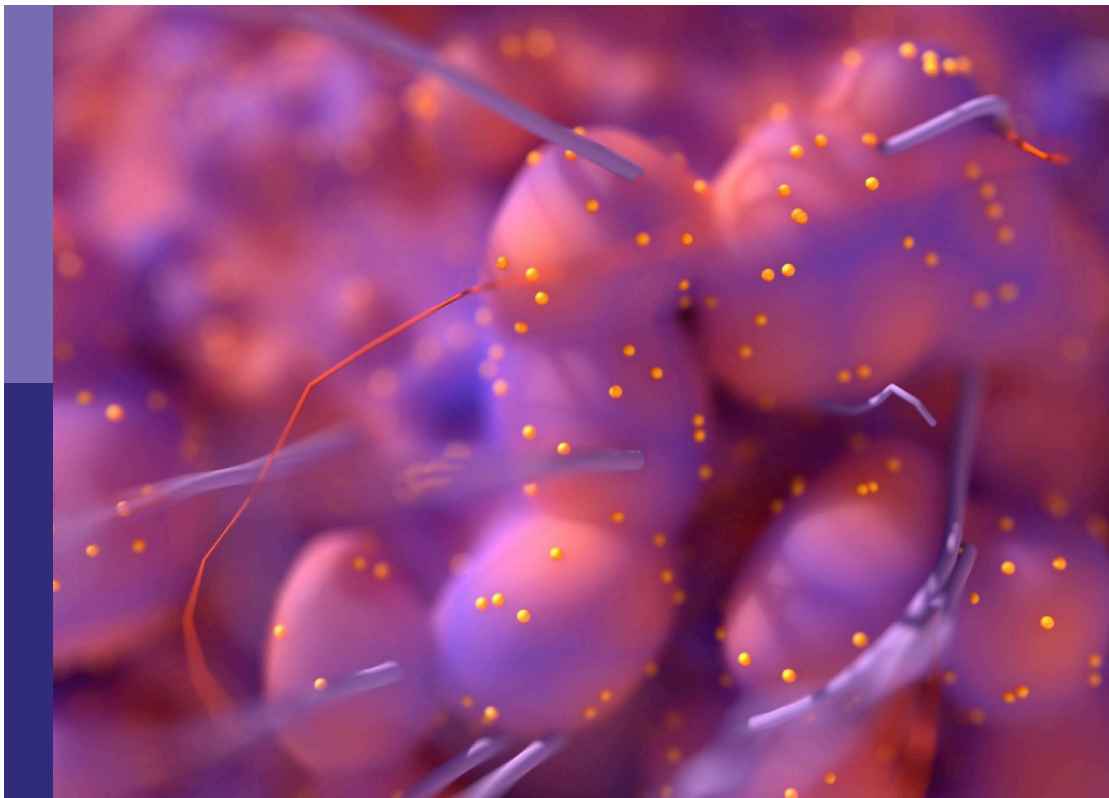

ISSN 1664-8714
ISBN 978-2-8325-4540-9
DOI 10.3389/978-2-8325-4540-9

About Frontiers

Frontiers is more than just an open access publisher of scholarly articles: it is a pioneering approach to the world of academia, radically improving the way scholarly research is managed. The grand vision of Frontiers is a world where all people have an equal opportunity to seek, share and generate knowledge. Frontiers provides immediate and permanent online open access to all its publications, but this alone is not enough to realize our grand goals.

Frontiers journal series

The Frontiers journal series is a multi-tier and interdisciplinary set of open-access, online journals, promising a paradigm shift from the current review, selection and dissemination processes in academic publishing. All Frontiers journals are driven by researchers for researchers; therefore, they constitute a service to the scholarly community. At the same time, the *Frontiers journal series* operates on a revolutionary invention, the tiered publishing system, initially addressing specific communities of scholars, and gradually climbing up to broader public understanding, thus serving the interests of the lay society, too.

Dedication to quality

Each Frontiers article is a landmark of the highest quality, thanks to genuinely collaborative interactions between authors and review editors, who include some of the world's best academicians. Research must be certified by peers before entering a stream of knowledge that may eventually reach the public - and shape society; therefore, Frontiers only applies the most rigorous and unbiased reviews. Frontiers revolutionizes research publishing by freely delivering the most outstanding research, evaluated with no bias from both the academic and social point of view. By applying the most advanced information technologies, Frontiers is catapulting scholarly publishing into a new generation.

What are Frontiers Research Topics?

Frontiers Research Topics are very popular trademarks of the *Frontiers journals series*: they are collections of at least ten articles, all centered on a particular subject. With their unique mix of varied contributions from Original Research to Review Articles, Frontiers Research Topics unify the most influential researchers, the latest key findings and historical advances in a hot research area.

Find out more on how to host your own Frontiers Research Topic or contribute to one as an author by contacting the Frontiers editorial office: frontiersin.org/about/contact

Diagnosis, epidemiology and treatment of salivary gland carcinomas

Topic editors

Stefano Cavalieri — Head and Neck Medical Oncology Department, Fondazione IRCCS Istituto Nazionale dei Tumori, Italy

Pierluigi Bonomo — Careggi University Hospital, Italy

Ester Orlandi — National Center of Oncological Hadrontherapy, Italy

Andreas Mock — National Center for Tumor Diseases Heidelberg (NCT), Germany

Citation

Cavalieri, S., Bonomo, P., Orlandi, E., Mock, A., eds. (2024). *Diagnosis, epidemiology and treatment of salivary gland carcinomas*. Lausanne: Frontiers Media SA.

doi: 10.3389/978-2-8325-4540-9

Table of contents

frontiers | Frontiers in Oncology

TYPE Editorial
PUBLISHED 20 February 2024
DOI 10.3389/fonc.2024.1379584

OPEN ACCESS

EDITED AND REVIEWED BY
Jan Baptist Vermorken,
University of Antwerp, Belgium

*CORRESPONDENCE
Stefano Cavalieri
stefano.cavalieri@istitutotumori.mi.it

RECEIVED 31 January 2024
ACCEPTED 07 February 2024
PUBLISHED 20 February 2024

CITATION
Nuzzolese I, Bonomo P, Orlandi E, Mock A and Cavalieri S (2024) Editorial: Diagnosis, epidemiology and treatment of salivary gland carcinomas.
Front. Oncol. 14:1379584.
doi: 10.3389/fonc.2024.1379584

Editorial: Diagnosis, epidemiology and treatment of salivary gland carcinomas

Imperia Nuzzolese[1], Pierluigi Bonomo[2], Ester Orlandi[3,4], Andreas Mock[5,6] and Stefano Cavalieri[1,7]*

[1]Head and Neck Medical Oncology Department, Fondazione IRCCS Istituto Nazionale dei Tumori di Milano, Milan, Italy, [2]Radiation Oncology, Azienda Ospedaliero-Universitaria Careggi, Florence, Italy, [3]Clinical Department, National Center for Oncological Hadrontherapy (Fondazione CNAO), Pavia, Italy, [4]Department of Clinical, Surgical, Diagnostic, and Pediatric Sciences, University of Pavia, Pavia, Italy, [5]Division of Translational Medical Oncology, National Center for Tumor Diseases (NCT) Heidelberg and German Cancer Research Center (DKFZ), Heidelberg, Germany, [6]Institute of Pathology, Ludwig-Maximilians-Universität (LMU) München, Munich, Germany, [7]Department of Oncology and Hemato-oncology, University of Milan, Milan, Italy

KEYWORDS

salivary gland carcinoma, multidisciplinarity, head and neck, rare cancers, adenoid cystic carcinoma

Editorial on the Research Topic
Diagnosis, epidemiology and treatment of salivary gland carcinomas

Salivary gland cancers (SGC) are heterogeneous entities representing less than 5% of head and neck (HN) tumors. The majority of benign SGC are amenable to curative surgery, while the over 20 malignant epithelial SGC subtypes (1) typically require multimodal treatment approaches, combining surgery with radiotherapy to treat local and loco-regional advanced disease. Recent advances in molecular profiling of malignant SGC let to biology-guided treatment paths in the recurrent/metastatic (R/M) setting. While early studies primarily compared adenoid cystic carcinomas (ACCs), one of the most common salivary malignancies, with non-ACC SGCs, a growing list of emerging biomarkers shape a continuously finer grained molecular understanding of the histological subtypes. This Research Topic aimed to promote these developments towards precision oncology trials and new drug developments in SGC. The articles published within the Research topic focused on both ACC and the wide and heterogeneous group of non-ACCs.

On 24 June 2022, in the meeting "Current management and future challenges in salivary gland cancers" held at the National Cancer Center for Oncological hadrontherapy in Italy, several international experts discussed the most significant innovations in molecular profiling, local treatments (i.e., surgery, radiotherapy [RT]), and the development of novel systemic drugs. The expert panel highlighted that it is essential to engage in collaborative research networks to enhance efficiency. Networks play a vital role in facilitating the organization and management of international clinical trials for rare malignancies, such as SGCs. Tailored research plans are needed to foster advancements of care in this setting. The conference proceedings, citing more than 100 articles, contributed to this Research Topic reflecting the rapid evolution of the current SGC scenario, focusing on the exciting progress that has been made in many research domains in the last few years (Locati et al.).

In the pre-operative setting, Wang et al. showed the diagnostic potential of amide proton transfer-weighted (APTw) magnetic resonance imaging adopting endogenous contrast by chemical exchange saturation transfer to indirectly reveal mobile peptides in tissues, which seems to correlate to tumor metabolism. The differences in average and, especially, maximum values of APTw distinguished benign and malignant parotid gland tumors. This may help define the nature of parotid lesions better and rationalize the pre-surgical setting.

Given the relevant discrepancies that emerged in the prognostic evaluation of the current classification systems, researchers focused on better risk stratification, thus considering the nodal status for disease management. The current neck nodal status for major SGC was extrapolated from HN squamous cell carcinomas, with a growing number of studies investigating the need for an adapted lymph node (LN) evaluation method in patients with SGC (2–7).

In a retrospective study, LN metastases significantly affected overall survival and recurrence-free survival in submandibular non-ACC, and the impact was established mainly by the number of positive LNs rather than LN size as defined in the current TNM staging (Wang and Shi).

The heterogeneity of these cancers is further reflected in terms of even unusual clinical behavior, sometimes demonstrated by some more indolent forms, as described by Miserocchi et al., who report a singular case of high-grade transformation of polymorphous adenocarcinoma of the oral floor after 20 years from the primary treatment.

Regarding ACC histology, research is moving towards more detailed knowledge of the disease, and different behaviors were found to be evident according to the primary site of the same histology.

Single-cell RNA sequencing was applied to observe the evolution of individual ACC cells in paracarcinoma and carcinoma tissues. Lin et al. reported their examination of ACC at the transcriptome level, identifying special populations of inter-duct cells and pre-malignant cells that could explain the possible origin of ACC cells and the peculiarly high recurrence rate of this histology.

A single-center retrospective analysis combined with available international databases confirmed recent evidence of a worse prognosis of submandibular ACC compared with parotid ACC, associated with early cervical LN and distant metastases along with rapid progression (Zhou et al.). This behavior may be connected to a high MYB/MYBL1 mutation rate and abnormal upregulation of the phosphatidylinositol-3 kinase pathway, which emerged by analyzing their molecular expression patterns.

Furthermore, in a retrospective analysis from the SEER database based on the number of positive LNs in subjects surgically treated for parotid ACC, Han defined three prognostic categories, thus possibly defining a different treatment plan for high-risk patients.

Regarding the R/M setting, in the last few years, the importance of assessing molecular targets has emerged to drive treatment choices in SGC. A comprehensive meta-analysis including more than 3300 patients showed a diversified prevalence of HER2 positivity (HER2+) ranging from 0% to 43% across sixteen subtypes of SGC (Egeberg et al.). Authors observed a trend towards increasing frequency of HER2+ in cancers derived from salivary gland ducts. As seven different definitions of HER2+ emerged from the evaluated studies, researchers suggested prospective clinical trials to determine the optimal definition of HER2+ based on therapy response in SGC with HER2+.

Moreover, in contrast to previous evidence (8), HER2+ appeared to be a negative prognostic factor in androgen receptor (AR)-positive cancers, at least in the recurrent/metastatic setting. In a retrospective study of 74 subjects with salivary duct carcinoma (SDC) and adenocarcinoma not otherwise specified AR+, Cavalieri et al. showed worse outcomes in HER2+ patients compared to HER2- ones. On the other hand, a non-statistically significant higher risk of developing central nervous system metastases emerged in this cohort, thus deriving the importance of assessing the brain at baseline. A possible crosstalk between the two altered pathways suggests evaluating a treatment combination in the future.

Available data further support comprehensive molecular profiling for a more aggressive form as salivary duct carcinoma (SDC). A collection of patients with AR+, HRAS/PIK3CA co-mutated SDC from a single center experience and a systematic literature search showed multiple targeted treatment strategies and their outcomes. Given the lack of data, Rieke et al. suggested further specific studies to define the best treatment sequences for this disease subtype.

Despite this precision medicine approach, chemotherapy can still have a role in SCG, as demonstrated by Onaga et al. in a subgroup analysis of the retrospective study of 40 patients. The authors demonstrated a favorable efficacy of docetaxel plus cisplatin compared to paclitaxel plus carboplatin, which is confirmed to be mainly not effective in ACC histology.

The eleven papers published in this Research Topic constitute a vital contribution to the field. New interesting results are included, new topics and challenges are approached. In particular, this Research Topic aimed to offer a platform to improve our knowledge of SGC to move their treatment into the future finally but, at the same time, highlighted some controversies present in the current research planning, probably due to the rarity of this disease and the lack of uniformity in the research efforts.

In line with major guidelines (9, 10), the diagnosis must be based on histology and immunohistochemistry findings. Molecular characterization has a supplementary role and can help define poorly differentiated or atypical lesions better and provide information on biological behavior, disease management, and possible targeted treatments.

While some studies focus on this molecular approach, defining possible subtypes of the same histology, others still consider SGC a unique disease. As many of these studies are small and retrospective, we promote an international effort to realize better-designed and prospective trials for the future, which could represent a further step forward to the knowledge of the SGC.

Author contributions

IN: Conceptualization, Methodology, Writing – original draft, Writing – review & editing. PB: Conceptualization, Methodology,

Writing – original draft, Writing – review & editing. EO: Conceptualization, Methodology, Writing – original draft, Writing – review & editing. AM: Conceptualization, Methodology, Writing – original draft, Writing – review & editing. SC: Conceptualization, Methodology, Supervision, Writing – original draft, Writing – review & editing.

Conflict of interest

The authors declare that the research was conducted in the absence of any commercial or financial relationships that could be construed as a potential conflict of interest.

The author(s) declared that they were an editorial board member of Frontiers, at the time of submission. This had no impact on the peer review process and the final decision.

Publisher's note

References

1. IARC. Available online at: https://publications.iarc.fr/.

2. Aro K, Ho AS, Luu M, Kim S, Tighiouart M, Clair JM, et al. Development of a novel salivary gland cancer lymph node staging system. *Cancer*. (2018) 124:3171–80. doi: 10.1002/cncr.31535

3. Lee H, Roh JL, Cho KJ, Choi SH, Nam SY, Kim SY. Positive lymph node number and extranodal extension for predicting recurrence and survival in patients with salivary gland cancer. *Head Neck*. (2020) 42:1994–2001. doi: 10.1002/hed.26135

4. Qian K, Sun W, Guo K, Zheng X, Sun T, Chen L, et al. The number and ratio of positive lymph nodes are independent prognostic factors for patients with major salivary gland cancer: Results from the surveillance, epidemiology, and End Results dataset. *Eur J Surg Oncol*. (2019) 45:1025–32. doi: 10.1016/j.ejso.2018.11.008

5. Terada H, Suzuki H, Hanai N, Nishikawa D, Koide Y, Hasegawa Y. Prognostic value of lymph node density for major salivary gland carcinoma without clinical lymph node metastasis. *Am J Otolaryngol*. (2020) 41:102304. doi: 10.1016/j.amjoto.2019.102304

6. Lombardi D, Tomasoni M, Paderno A, Mattavelli D, Ferrari M, Battocchio S, et al. The impact of nodal status in major salivary gland carcinoma: A multicenter experience and proposal of a novel N–classification. *Oral Oncol*. (2021) 112:105076. doi: 10.1016/j.oraloncology.2020.105076

7. de Morais EF, da Silva LP, Moreira DGL, Mafra RP, Rolim LSA, de Moura Santos E, et al. Prognostic factors and survival in adenoid cystic carcinoma of the head and neck: A retrospective clinical and histopathological analysis of patients seen at a cancer center. *Head Neck Pathol*. (2021) 15:416–24. doi: 10.1007/s12105-020-01210-7

8. Sousa LG, Wang K, Torman D, Binks BJ, Rubin ML, Andersen CR, et al. Treatment patterns and outcomes of palliative systemic therapy in patients with salivary duct carcinoma and adenocarcinoma, not otherwise specified. *Cancer*. (2022) 128:509–18. doi: 10.1002/CNCR.33968

9. Geiger JL, Ismaila N, Beadle B, Caudell JJ, Chau N, Deschler D, et al. Management of salivary gland Malignancy: ASCO guideline. *J Clin Oncol*. (2021) 39:1909–41. doi: 10.1200/JCO.21.00449

10. van Herpen C, Vander Poorten V, Skalova A, Terhaard C, Maroldi R, van Engen A, et al. Salivary gland cancer: ESMO-European Reference Network on Rare Adult Solid Cancers (EURACAN) Clinical Practice Guideline for diagnosis, treatment and follow-up. *ESMO Open*. (2022) 7:100602. doi: 10.1016/j.esmoop.2022.100602

frontiers in Oncology

SYSTEMATIC REVIEW
published: 24 June 2021
doi: 10.3389/fonc.2021.693394

HER2 Positivity in Histological Subtypes of Salivary Gland Carcinoma: A Systematic Review and Meta-Analysis

Kristian Egebjerg[1], Cecilie Dupont Harwood[2], Nina Claire Woller[3], Claus Andrup Kristensen[1] and Morten Mau-Sørensen[1]*

[1] Department of Oncology, Copenhagen University Hospital, Rigshospitalet, Copenhagen, Denmark, [2] Department of Otorhinolaryngology, Head & Neck Surgery and Audiology, Copenhagen University Hospital, Rigshospitalet, Copenhagen, Denmark, [3] Department of Pathology, Copenhagen University Hospital, Rigshospitalet, Copenhagen, Denmark

OPEN ACCESS

Edited by:
Vincent Vander Poorten, KU Leuven, Belgium

Reviewed by:
Laura Deborah Locati, Istituto Nazionale dei Tumori (IRCCS), Italy
Alena Skalova, Charles University, Czechia

****Correspondence:***
Kristian Egebjerg
kristian.egebjerg@gmail.com

Specialty section:
This article was submitted to Head and Neck Cancer, a section of the journal Frontiers in Oncology

Received: *10 April 2021*
Accepted: *19 May 2021*
Published: *24 June 2021*

Citation:
Egebjerg K, Harwood CD, Woller NC, Kristensen CA and Mau-Sørensen M (2021) HER2 Positivity in Histological Subtypes of Salivary Gland Carcinoma: A Systematic Review and Meta-Analysis. Front. Oncol. 11:693394. doi: 10.3389/fonc.2021.693394

Background: HER2 aberrations in salivary gland carcinomas (SGC) as well as benefit of HER2 directed therapy have been reported in small studies. However, reliable estimates of the prevalence of HER2 positivity in SGC and its various histological subtypes are lacking.

Objective: To assess the prevalence of HER2 positivity in histological subtypes of salivary gland carcinomas (SGC).

Methods: Studies were identified by a systematic review of the literature. Data on *in situ* hybridization (ISH) and immunohistochemistry (IHC) were extracted to derive pooled prevalence estimates calculated by a random effects model. Characteristics of the studies were extracted for subgroup analysis.

Results: Fifty studies including 3372 patients were identified, providing data on sixteen histological subtypes. Based on the meta-analysis, the estimated prevalence of HER2 positivity were 43% (95% CI: 36% – 51%) in salivary duct carcinoma (SDC), 39% (95% CI: 32% – 45%) in carcinoma ex pleomorphic adenoma (CEP), 17% (95% CI: 7.5% – 33%) in squamous cell carcinoma (SCC), 13% (95% CI: 7.6% – 21%) in adenocarcinoma NOS (ADC), 6.7% (95% CI: 0.17%-32%) in poorly differentiated carcinoma, 5.5% (95% CI: 2.9% – 9.6%) in mucoepidermoid carcinoma, 4.3% (95% CI: 1.4% – 13%) in myoepithelial carcinoma, 1.8% (95% CI: 0.04%-9.6%) in epithelial-myoepithelial carcinoma, 0.45% (95% CI: 0.0097% – 18%) in acinic cell carcinoma and 0.15% (0.037% – 5.4%) in adenoid cystic carcinoma. Estimates for five additional subtypes were assessed.

Conclusion: Prevalence of HER 2 positivity in SGC varies greatly based on histological subtype, with SDC, CEP, SCC, and ADC displaying the highest rates.

Keywords: HER2, salivary gland (S.G) tumors, ERBB2, salivary duct carcinoma, prevalence

INTRODUCTION

Salivary gland carcinomas (SGC) are relatively rare tumors with an annual worldwide incidence of 0.07% corresponding to 52,799 cases each year according to the Global Cancer Observatory (1). The most recent WHO classification divide SGC into 21 histological subtypes (2). The incidence of the most common histopathological subtypes vary between countries, but mucoepidermoid carcinoma is the most prevalent subtype making up 12%-29% of the total cases, adenoid cystic carcinomas accounts for 10%-22%, acinic cell carcinoma for 8%-14%, while salivary duct carcinomas (SDC) only account for 5%-10%. SDC represents the most aggressive type (3–5). The prognosis of metastasizing SGC remains poor, and response rates to chemotherapy are modest (4). Consequently, oncologists and patients alike are faced with a clear unmet medical need for improvements in the treatment of this disease (6).

HER2 is a human epidermal receptor 2 tyrosine kinase of the epidermal growth factor receptor (EGFR) class coded by an oncogene *ERBB2* located on chromosome 17. HER2 is overexpressed in various subtypes of SGC, but clinical trials on HER2 targeted therapy with trastuzumab or lapatanib without chemotherapy in SGC have failed to show significant clinical benefit, maybe because only a subset of the lapatinib treated patients harbored tumors with HER2 overexpression (7, 8). However, a Japanese study combining trastuzumab and docetaxel found an overall response rate of 70% in patients with HER2 positive SDC defined as IHC3+ or gene amplification by FISH (9). Recently, novel HER2 targeted therapies such as ado-trastuzumab emtansine and combinations of trastuzumab and pertuzumab have reached relevant response rate of 90% and 60%, respectively (10, 11).

HER2 protein overexpression is measured semi-quantitatively by immunohistochemistry (IHC) and gene amplification is measured by fluorescence/silver/dual *in situ* hybridization (FISH, SISH and DISH). Various scoring systems exist for other cancer types, such as breast carcinoma and gastric esophageal adenocarcinoma (12, 13). Although specific criteria for SGC have been proposed, the breast cancer carcinoma criteria are the most commonly used for scoring HER2 expression in SGC (14). This is partially due to morphological similarities to invasive ductal carcinoma of the breast and molecular resemblance with apocrine breast cancer and because studies validating HER2 scoring systems in SGC are lacking (15).

HER2 overexpression or gene amplification seems to be a prerequisite for response to trastuzumab. Currently there is no systematic review or meta-analysis investigating the prevalence of HER2 in SGC. The aims of this review and meta-analysis are to evaluate the literature and provide prevalence estimates for HER2 in various histological subtypes of SGC.

METHODS

PRISMA Reporting guidelines were used.

Eligibility

Inclusion Criteria: Only studies examining human SGC tissue were included. Studies allowed were clinical trials, prospective and retrospective observational studies provided the study population was not a preselected HER2 positive cohort. HER2 status had to be evaluated by *either* IHC reporting semi-quantitative scores of 0, 1+, 2+, 3+ *or* quantitative ratios of HER2 gene copy number relative to chromosome 17 by ISH *or* by both IHC and ISH. Studies reporting HER2 status dichotomously (HER2 positive/negative) using the above mentioned semi-quantitative or quantitative data were eligible.

Exclusion criteria: Studies not listing which quantitative scoring methods of IHC 0 to 3+ or ISH were used to define HER2 positivity were not included. Studies not discriminating between histological subtype and HER2 status were not included. If the same dataset of patients was reported by the same author in two different publications only the newest was included. Studies reported in languages other than English, unpublished studies, case studies, conference abstracts, cell line and animal studies were all considered ineligible.

Rationale for criteria: The above-mentioned inclusion criteria were chosen to gather sufficient data to evaluate HER2 positivity in specific histological subtypes, and to assess whether criteria of HER2 positivity affect the prevalence estimates.

Identifying Studies

PubMed, Embase, Web of Science were searched up to September 19th, 2020 using the search string ((salivary gland tumor[Title/Abstract] OR carcinoma of the salivary gland[Title/Abstract] OR salivary gland cancer[Title/Abstract])) AND (HER2 or c-ERB2). The search syntaxes were adapted to those used by each respective search engine. All time periods were included. Exact search-syntax used for each search engine can be seen in **Supplemental S2**. No limitations were set regarding the date of coverage. In addition, hand searching of references list of obtained articles was conducted.

Study Selection Process

Titles were identified by the above-mentioned search strategy, screened and assessed for inclusion in the final meta-analysis independently by KE and CDH. Discrepancies were solved by consensus. A full list of texts screened but not included as well as the reason for exclusion is listed in **Supplement S3**.

Risk of Bias in the Individual Studies and Across Studies

The eligibility criteria were designed to minimize risk of bias – especially selection bias, across studies.

As the studies included are observational and not randomized controlled trials or interventional in nature, risks of bias were assessed using recommendations from COSMOS-E (Conducting Systematic Reviews and Meta-Analyses of Observational Studies of Etiology) (16).

Information bias was assessed by registering methods potentially affecting how frequently the outcome were registered: Prospectively collected or archival samples, HER2

positivity criteria, IHC assay and ISH probe type. The latter were also treated as confounders together with Geographic Region.

Data Items and Collection

A data extraction form was used to extract equivalent information from each paper. First author, published year, geographical region, prospectively collected or archival samples, HER2 positivity criteria, IHC assay, ISH probe type and ISH type: FISH, DISH, SISH. In addition, number of patients with each histological subtype and number of HER2 positive patients as well as data on, IHC0, IHC1+, IHC2+, IHC3+, and HER2 amplification were collected.

Specification of Endpoints

The following endpoints were predefined:

The primary endpoint was HER2 positivity for each SGC histological subtype. Specific IHC data (0, 1+, 2+, 3+) and gene amplification status was extracted when possible. During the data collection it became clear that this specific data was only available for SDC.

Analysis and Statistics and Synthesis Methods

Studies were included in each respective meta-analysis depending on the available data. Meta-analyses were conducted using a random effects model. The Wilson score interval method was used to calculate confidence intervals. Maximum likelihood estimator was used to estimate between study variance tau^2 with the inverse variance method. Generalized linear mixed models were used for pooled prevalence estimates, forest plots were created and sorted based on number of patients included. Whenever sufficient data were available, subgrouping based on HER2 definition was plotted, and subgroup analysis based on probe, assay, geographical region was also conducted.

A threshold of n>60 patients was chosen for each tissue type to conduct meta-analysis, as we believe a lower number of patients would not yield a meaningful meta-analysis.

The Clopper-Pearson interval was used to calculate 95% confidence intervals in tissue types not eligible for inclusion in meta-analysis.

R version 4.0.0 and package meta was used.

HER2 Positivity

Various criteria were employed by studies to characterize tumor tissue as "HER2 positive", and each study was labelled according to criteria employed. When data on both IHC and FISH status were reported, IHC2+ confirmed by gene amplification or IHC3+ was preferentially defined as HER2 positive.

IHC and FISH Prevalence Among SDC

Data for SDC, both *de novo* and carcinoma ex pleomorphic adenoma were sufficient to conduct analysis for specific IHC status sand gene amplification. Two studies (17, 18) reported combined estimates of IHC0 and IHC1+; this estimate was divided by two and each half was included in the IHC0 and IHC1+ analysis respectively.

RESULTS

By the indicated method of study selection (**Figure 1**), 50 studies were identified including a total number of 3,372 patients to study the prevalence of HER2 positivity in SGC (**Table 1**, full characteristics of studies, **Supplemental S1**). Archival tissue was used in all studies except one; in this study information about tissue sampling was not available. Nineteen studies were conducted in Europe, 12 studies in the Americas, eight in Asia, two in Oceania and one study conducted in both Europe and the Americas. The following criteria were used in the studies included to define HER2 positivity: (1) IHC2+ or IHC3+, (2) IHC3+, (3) IHC2+ and HER2 amplification assessed by ISH or IHC3+, (4) IHC2+ or IHC3+ or HER2 amplification assessed by ISH, (5) IHC3+ or HER2 amplification assessed by ISH, (6) HER2 amplification assessed by ISH, (7) IHC2+ and ISH or IHC3 and ISH.

Salivary Duct Carcinoma: IHC

Eighteen studies were included in the analysis of prevalence of protein expression as assessed by IHC in SDC patients. The estimated prevalence of HER2 scores of IHC0 was 31% (95% CI: 21% - 44%), IHC1+ 10% (95% CI: 6.4% – 15%), IHC2+ 14% (95% CI: 8.9%-20%), and IHC3+ 37% (95% CI: 28%-47%) as presented in **Figure 2**. There was significant ($p<0.01$) and marked heterogeneity in the IHC0 and IHC3+ data with I^2 of 59% and 67%, respectively, but no significant heterogeneity in the IHC1+ and IHC2+ data. There was significant difference between assays used for all four IHC HER2 scores, for further information see **Supplemental S4**.

Salivary Duct Carcinoma: HER2 Gene Amplification

Eighteen studies were included in the analysis. HER2 amplification rate in SDC was found to be 39% (95% CI: 31-49) as shown in **Figure 3**. There was significant ($p<0.01$) and marked (I^2 66%) heterogeneity between studies. There was no significant difference in the estimated prevalence between studies applying various probes (p=0.12).

Salivary Duct Carcinoma: HER2 Positivity

Thirty-seven studies with a total of 1,105 patients were included in the random effects model. The model predicted a prevalence of HER2 positivity in SDC patients to be 43% (95% CI: 36% – 51%) depicted in **Figure 4**. The heterogeneity between the studies was significant $p<0.01$, and substantial, $I^2 = 80\%$. There was significant difference between assays p=0.0017, although the differences seemed to level off for the most commonly used assays: Prevalence of 46% (95% CI: 32%- 62%) and 44% (95% CI: 36%- 53%) were estimated for 19 and 11 studies using DAKO and Ventana assays, respectively. Prevalence of less commonly used assays are shown in **Supplemental S5**.

There were no differences in the prevalence between studies using varying criteria for HER2 positivity (p=0.61) or conducted in different geographical regions (p=0.16).

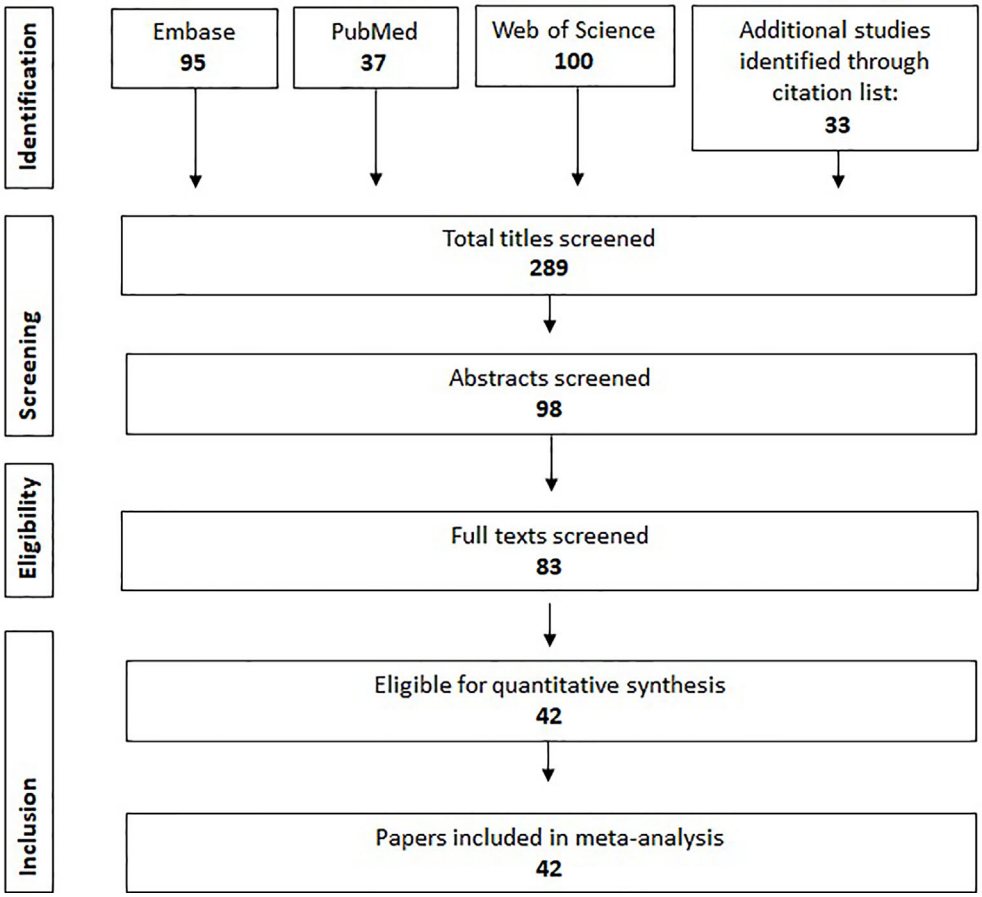

FIGURE 1 | Flowchart describing the methodology of article selection.

Carcinoma Ex Pleomorphic Adenoma (CEP): HER2 Positivity

Fourteen studies were included in the random effects model with a total of 218 patients. The model predicted a prevalence of HER2 positivity in CEP patients to be 39% (95% CI: 32% – 45%) depicted in **Figure 4**. The heterogeneity between studies was not significant. There were no statistical differences based on the applied criteria for HER2 positivity (p=0.95), used assays (p=0.46) or the geographical regions (p=0.48).

Adenocarcinoma NOS (ADC NOS): HER2 Positivity

Fifteen studies were included in the random effects model with a total of 275 patients. The model predicted a prevalence of HER2 positivity in ADC NOS tumors of 13% (95% CI: 7.6% – 21%) as shown in **Figure 5**. The heterogeneity between studies was not significant. The prevalence were significantly different when comparing studies using different criteria for HER2 positivity (p=0.0052). However, the estimated prevalence was higher in those studies using the narrowest criteria for HER2 positivity. Neither geographical region (p=0.47) nor assay (p=0.30) used was associated with differences in prevalence.

Mucoepidermoid Carcinoma: HER2 Positivity

Fifteen studies with a total of 591 patients were included in the random effects model. The model predicted a prevalence of HER2 positivity in mucoepidermoid carcinoma patients to be 5.5% (95% CI: 2.9% – 9.6%) as seen in **Figure 5**. The heterogeneity between studies was moderate I^2 = 51% and statistically significant p=0.050. There were significant differences in the prevalence between subgroups based on criteria for HER2 positivity (p=0.0014) and geographical region (p=0.0002). The broadest criteria defining HER2 positivity as IHC2+ and IHC3+ reached prevalence estimates of 12% (95% CI: 6.4% -21%). Two American studies resulted in prevalence estimates by the random effect model of 19% (95% CI: 0.16% – 97%), four Asian studies in prevalence estimates of 4.1 (95% CI: 0.41%-30%) and nine studies from Europe in prevalence estimates of 3.3% (95% CI: 1.8% - 5.9). There was no significant difference between assays used (p=0.56).

Myoepithelial Carcinoma: HER2 Positivity

Nine studies were included in the random effects model with a total of 70 patients. The model predicted a prevalence of HER2

TABLE 1 | Studies included in the meta-analysis.

First Author	Year	Geographic Region	Criteria for HER2 Positivity Criteria	Number of patients
Khan (19)	2001	America	IHC3	29
Skálová (20)	2001	Europe	IHC2 or IHC3	29
Dori (21)	2002	Asia	IHC3	32
Skalova (22)	2003	Europe	IHC2 and ISH or IHC3	11
Glisson (17)	2004	America	IHC2 or IHC3	136
Weed (23)	2004	America	IHC2 or IHC3	28
Di Palma (24)	2005	Europe	IHC3	11
Jaehne (25)	2005	Europe	IHC3	34
Cornolti (26)	2007	Europe	IHC3 or ISH	13
Nabili (27)	2007	America	IHC3	7
Tapia (28)	2007	Europe	IHC2 and ISH or IHC3	12
Williams (29)	2007	America	IHC3	59
Ettl (30)	2008	Europe	IHC2 or IHC3	91
Shang (31)	2008	Asia	IHC2 or IHC3	46
Locati (32)	2009	Europe	IHC2 and ISH or IHC3	123
Luukkaa (33)	2010	Europe and America	ISH	11
Williams (34)	2010	America	IHC2 and ISH or IHC3	66
Clauditz (35)	2011	Europe	IHC3 or ISH	915
Di Palma (36)	2012	Europe	IHC2 and ISH or IHC3	42
Ettl (37)	2012	Europe	IHC3	235
Hashimoto (38)	2012	Asia	IHC2 and ISH or IHC3	31
Suzuki (39)	2012	Asia	IHC2 or IHC3	45
Cros (40)	2013	Europe	IHC3	28
Nakano (41)	2013	Asia	IHC2 or IHC3	31
Nardi (42)	2013	America	ISH	19
Kondo (43)	2014	Asia	IHC2 and ISH or IHC3	13
Masubuchi (44)	2014	Asia	ICH3 and ISH	32
Han (45)	2015	Asia	IHC2 and ISH or IHC3	25
Jakob (46)	2015	America	IHC2 or IHC3	16
Nishijima (47)	2015	Asia	IHC2 or IHC3	50
Kusafuka (48)	2016	Asia	IHC2 and ISH or IHC3	9
Locati (49)	2016	Europe	IHC2 and ISH or IHC3	11
Lemound (50)	2016	Europe	IHC3 or ISH	37
Luk (51)	2016	Oceania	IHC2 and ISH or IHC3	23
Hashimoto (52)	2017	Asia	IHC2 and ISH or IHC3	221
Khoo (53)	2017	Oceania	ISH	15
Locati (54)	2017	Europe	IHC2 and ISH or IHC3	28
Takase (55)	2017	Asia	ICH3 or ISH	151
Andreasen (56)	2018	Europe	IHC2 and ISH or IHC3 and ISH	73
Beck (57)	2018	Europe	IHC2 and ISH or IHC3	15
Boon (58)	2018	Europe	IHC2 and ISH or IHC3	153
Kanazawa (59)	2018	Asia	IHC3	34
Ryu (60)	2018	Asia	ISH	28
Gargano (61)	2019	America	IHC3	28
Liang (62)	2019	America	IHC3	86
Santana (63)	2019	Europe	IHC2 and ISH or IHC3	24
Szewczyk (64)	2019	Europe	IHC2 and ISH or IHC3	115
Villeplet (18)	2019	Europe	IHC2 and ISH or IHC3	36
Chatzopoulos (14)	2020	America	IHC2 and ISH or IHC3	32
Hsieh (65)	2020	Europe	IHC2 and ISH or IHC3	33

positivity in myoepithelial carcinoma patients to be 4.3% (95% CI: 1.4% – 13%) depicted in **Figure 6**. The heterogeneity between studies was not statistically significant.

Acinic Cell Carcinoma: HER2 Positivity

Ten studies with 274 patients were included in the random effects model. The model predicted a prevalence of HER2 positivity in acinic cell carcinoma patients to be 0.45% (95% CI: 0.0097% – 18%) depicted in **Figure 6**. The heterogeneity between studies was not statistically significant but two studies reported prevalence in the range of 5.4% to 27% while 8 studies reported a prevalence of 0%.

Adenoid Cystic Carcinoma: HER2 Positivity

Fifteen studies were included in the random effects model with a total of 614 patients. The model predicted the prevalence of

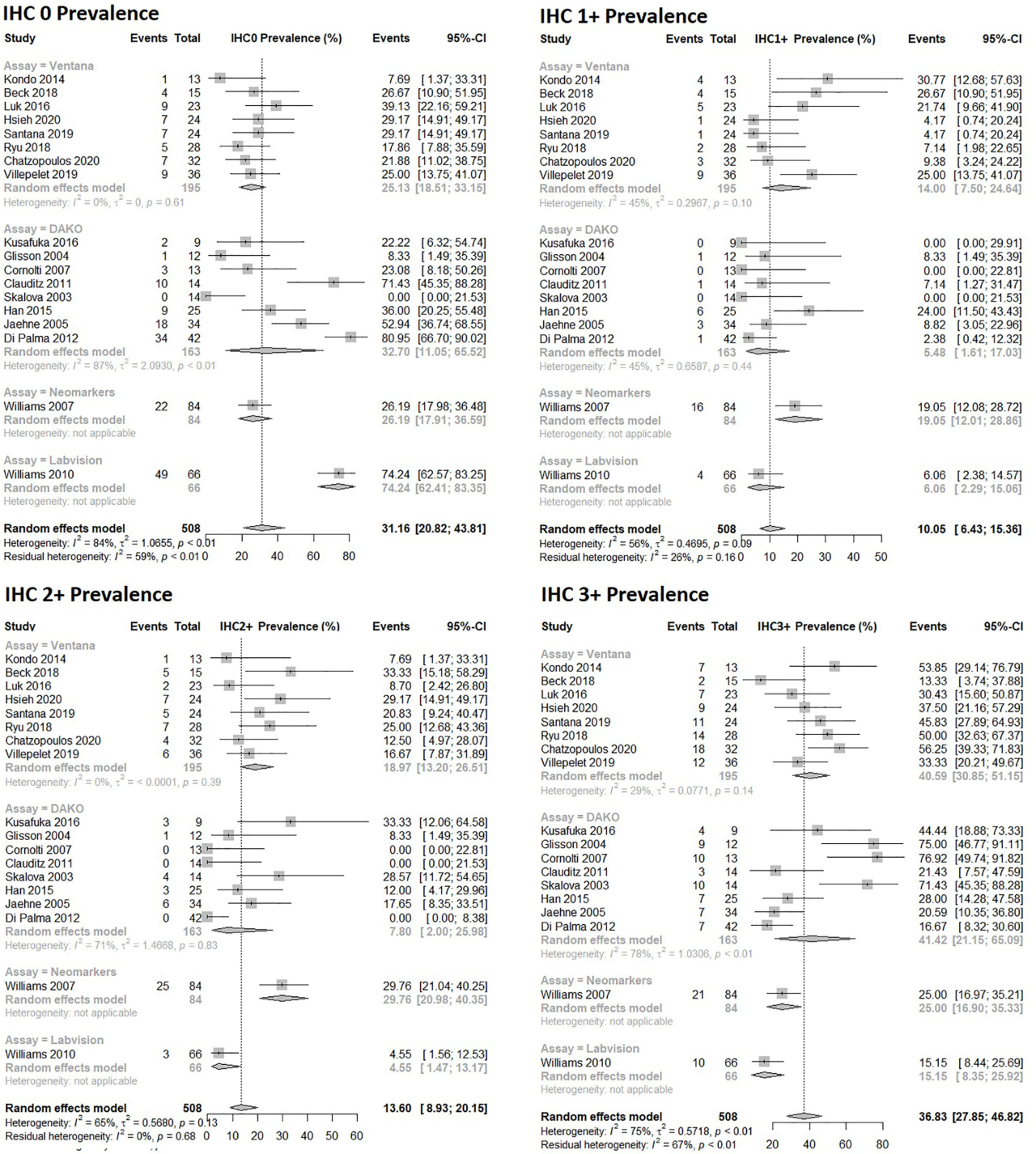

FIGURE 2 | Forrest plot of prevalence estimates for HER2 protein expression assessed by IHC in salivary duct carcinomas.

HER2 positivity in adenoid cystic carcinoma patients to be 0.15% (95% CI: 0.037% – 5.4%) depicted in **Figure 6**. The heterogeneity between studies was not statistically significant but three studies reported prevalence of 4.3%, 6.9% and 36% while 12 studies reported a prevalence of 0%.

HER2 Positivity of Other Histological Subtypes

The low number of patients precluded the conduction of meaningful meta-analysis for the following histological subtypes (Full details of studies in **Supplemental S5**): For

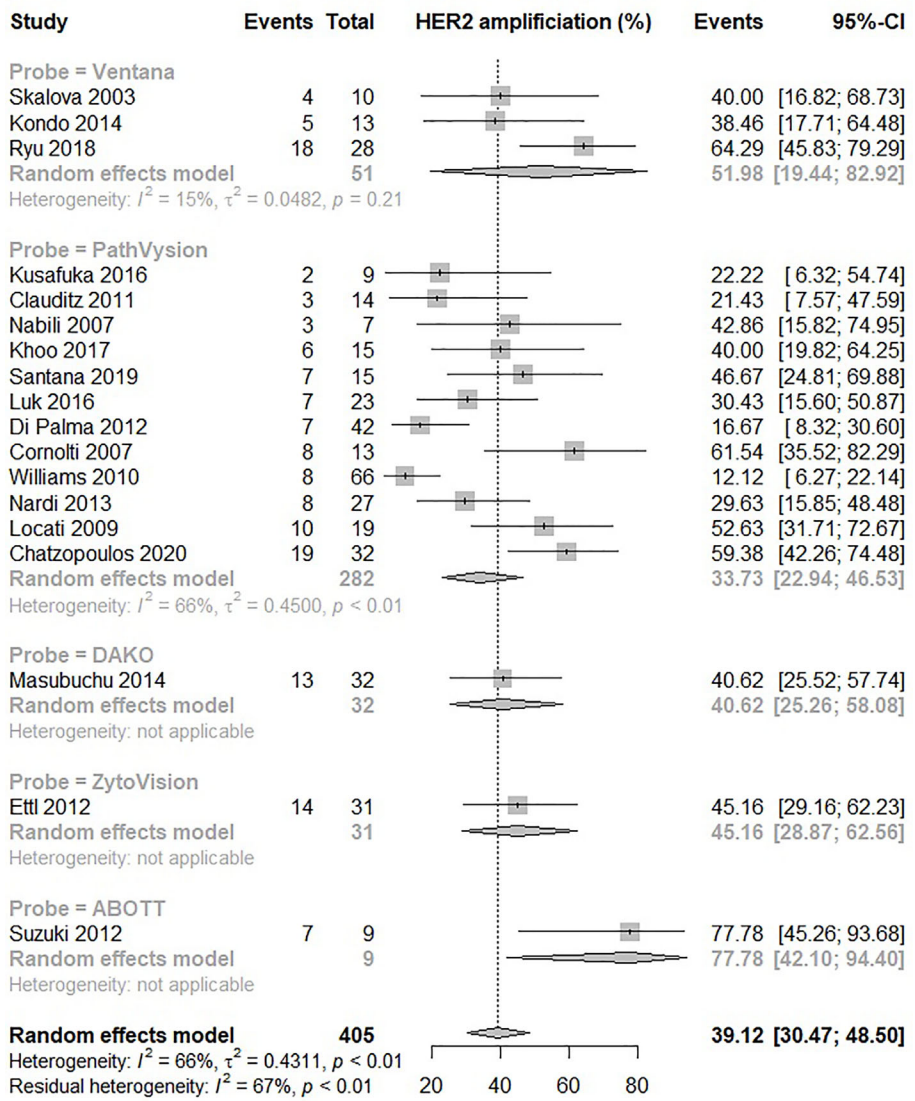

FIGURE 3 | Forrest plot of HER2 gene amplification rate in SDC assessed by in situ hybridization.

epithelial-myoepithelial carcinoma, 56 patients were included in two studies reporting a single HER2 positive tumor corresponding to a prevalence of 1.8% (95% CI: 0.04%-9.6%).

Seven out of 39 patients with *squamous cell carcinoma* in five studies had HER2 positive tumor corresponding to a prevalence of 17% (95% CI: 7.5%-33%). For *poorly differentiated carcinoma*, 15 patients were included in four studies with one HER2 positive tumor corresponding to 6.7% (95% CI: 0.17%-32%).

One study reported on nine patients with *intraductal carcinoma* with one HER2 positive case corresponding to 11% (95% CI: 0.28% – 48%).

Three studies included 50 patients *with polymorphous adenocarcinoma*, five studies included 33 patients with *basal cell carcinoma*, and three studies included 14 patients with *oncocytic carcinoma*. In all three tumor types, no HER2 positive cases were identified. Two studies reported a total of five patients with *lymphoepithelial carcinoma* of which zero were HER2 positive.

One study reported one patient with *clear cell carcinoma* which was not HER2 positive.

DISCUSSION

The present work is the first comprehensive meta-analysis providing reliable estimates of the prevalence of HER2 positivity in salivary gland carcinomas including its histological subtypes. The results are summarized in **Tables 2** and **3**. Our results show that salivary gland tumors are very heterogeneous with respect to HER2 positivity ranging from 0% up to 43% with

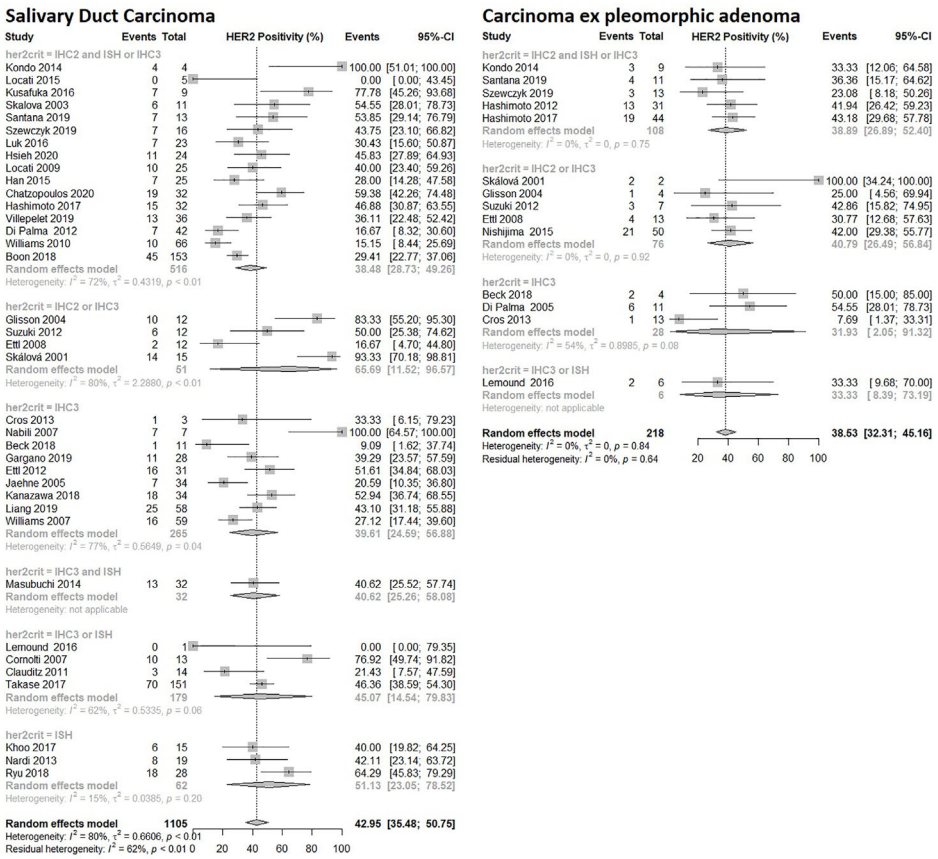

FIGURE 4 | Forrest plot of HER2 Prevalence among SGC subtypes: Salivary Duct Carcinoma and Carcinoma ex pleomorphic adenoma.

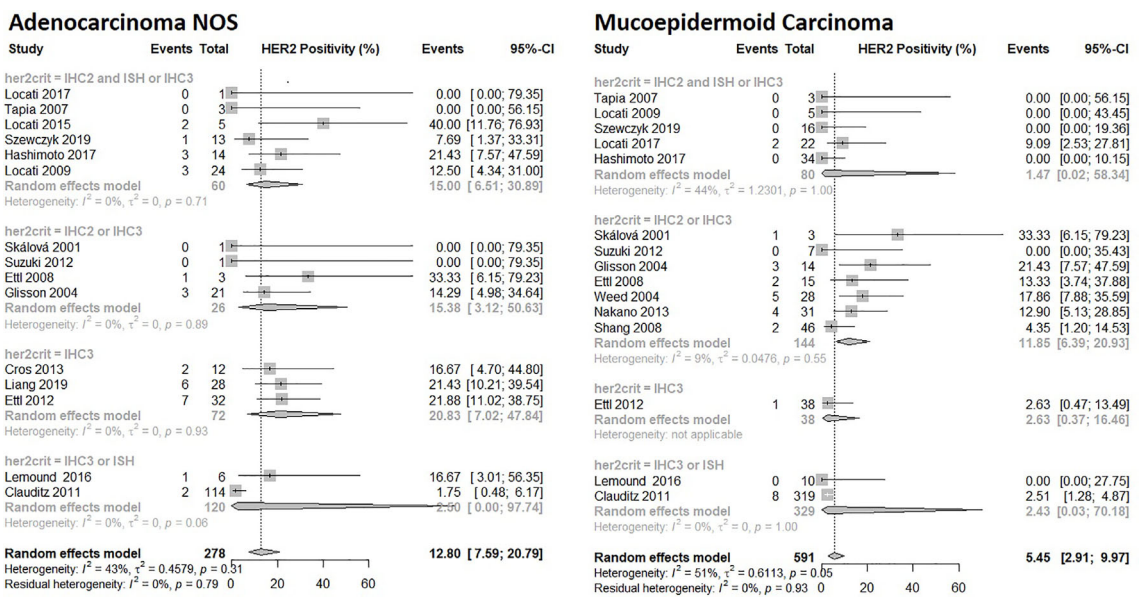

FIGURE 5 | Forrest plot of HER2 Prevalence among SGC subtypes: Adenocarcinoma NOS and Mucoepidermoid Carcinoma.

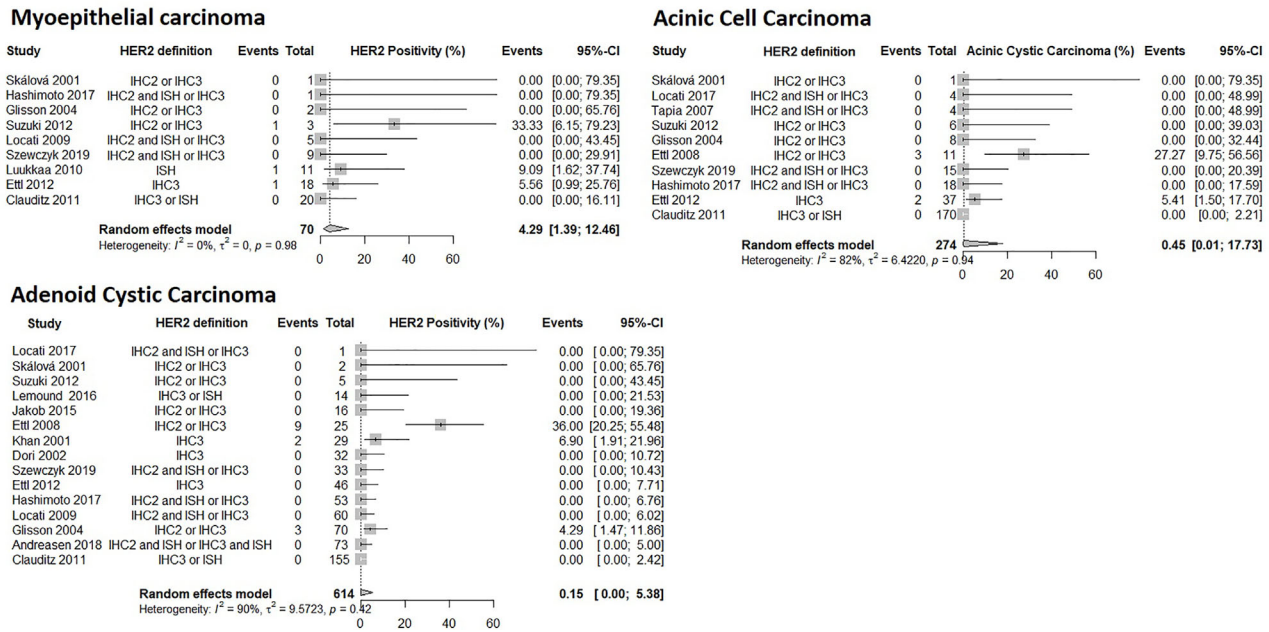

FIGURE 6 | Forrest plot of HER2 Prevalence among SGC subtypes: Myoepithelial carcinoma, Acinic Cell Carcinoma, Adenoid Cystic Carcinoma.

TABLE 2 | Summary of results.

Histological Subtype	Study Included	Number of patients	HER2 positivity estimate (95% CI)
Salivary duct carcinoma	37	1105	43% (95% CI: 36% – 51%)
Carcinoma ex pleomorphic adenoma	14	218	39% (95% CI: 32% – 45%)
Squamous cell carcinoma	5	39	17% (7.5%-33%)
Adenocarcinoma NOS	14	274	13% (7.6% – 21%)
Intraductal carcinoma	1	9	11% (0.28% – 48%)
Poorly differentiated carcinoma	4	15	6.7% (0.17%-32%).
Mucoepidermoid carcinoma	15	591	5.5% (2.9% – 9.6%).
Myoepithelial carcinoma	9	70	4.3% (1.4% – 13%)
Epithelial-myoepithelial carcinoma	2	56	1.8% (0.04%-9.6%)
Acinic cell carcinoma	10	274	0.45% (0.0097% – 18%)
Adenoid cystic carcinoma	14	541	0.15% (0.037% – 5.4%)
Polymorphus adenocarcinoma	3	50	0%
Basal cell carcinoma	5	33	0%
Oncocytic carcinoma	3	14	0%
Lymphoepithelial carcinoma	2	5	0%
Clear cell carcinoma	1	1	0%
Total	50	3372	

the highest prevalence in SDC which both genomically and morphologically resembles invasive ductal carcinoma of the breast (15). Interestingly, similar frequency measures were seen in histologically related tumors, since both SDC and CEP, as well as epithelial-myoepithelial and myoepithelial carcinoma have comparable estimates. Furthermore, a tendency was noted towards increasing frequency of HER2 positivity in tumor types derived from salivary gland ducts compared to tumors

TABLE 3 | Summary of HER2 protein expression assessed by IHC and HER2 amplification assessed by ISH among SDC patients in the meta-analysis.

Scores of HER2 protein expression	Rate of prevalence (95% CI)	Rate of prevalence of overall HER2 amplification by ISH (95% CI)
IHC0	31% (21-44)	39% (95% CI: 31-49)
IHC1+	10% (6.4-15)	
IHC2+	14% (8.9-20)	
IHC3+	37% (28-47)	

with origin from cells with exocrine function. Accordingly, SDC and SCC displayed high prevalence compared to acinic cell carcinomas and adenoid cystic carcinomas with virtually no HER2 expression. Caution should be advised when evaluating the prevalence estimates of rare histological subtypes with small number of patients and no identified HER2 positive cases.

There was sufficient data in four histological subtypes, SDC, CEP, ADC NOS and mucoepidermoid carcinoma to conduct subgroup analyses of the IHC assay used and its correlation with HER2 prevalence. In three of the subgroup analyses: CEP, ADC NOS and mucoepidermoid carcinoma there was no significant difference between the IHC assays used. However, in SDC there was a significant difference based on the IHC assay used, but no difference between probes used in ISH analysis of HER2 amplification (**Figures 2**, **3**). The difference based on IHC assay used may in part be due to inter-observer variability which is thought to be higher when scoring IHC, compared to ISH scoring which is more objective and quantitative (66). Of note, differences disappeared when comparison was restricted to the two most commonly used IHC assays, DAKO and Ventana. There was similarity in frequency measures in IHC and ISH derived estimates of HER2 positivity and amplification of 43% (95% CI: 36% – 51%) and 39% (95% CI: 31-49) respectively.

The criteria used to define HER2 positivity varied among studies with seven different definitions being employed. Subgroup differences between criteria applied to define HER2 positivity were also analyzed (**Figures 4**, **5**). A significant difference depending on the criteria used was observed in ADC NOS and mucoepidermoid carcinoma, in the latter the broadest definition of HER2 positivity of IHC2+ and IHC3+ also yielded the highest prevalence estimate, but this pattern was not as clear in the ADC NOS subgroup analysis. In subtypes with higher prevalence i.e. SDC and CEP subgroup analyses, use of varying criteria did not seem to result in differences in estimated prevalence. Our estimates are limited by these varying criteria for HER2 positivity used in the included studies.

In recent years, it has become common to use IHC2+ confirmed by ISH or IHC3+ as the definition of HER2 positivity as a threshold for using HER2 targeted therapies. In SGC HER2 is often evaluated by use of a HER2 scoring system developed in breast cancer with the use of a threshold chosen based upon clinical response in patients with breast cancer (67).

Another quite unique application of HER2 testing in SGC is its use in the diagnosis of SDC, since this subtype has a higher prevalence of HER2 overexpression and gene amplification than other subtypes.

There is no generally accepted standard treatment of metastatic SGC, and the role of HER2 targeted therapy in this setting is still unclear. Currently there is not sufficient data on newer HER2 targeted drugs in SGC to further define which patient population benefits from the treatment. As such, defining the specific cut-off value to decide which patients should be regarded as "HER2 positive" to receive HER2 targeted therapy remains to be answered. One step in this direction may be the HER2 scoring criteria for SGC proposed by Chatzopoulos et al. (14).

While HER2 treatment results in survival benefits in breast, gastric and esophageal ADC, only limited data are available in SGC. Single agent HER2 directed therapy antitumor effect in patients with HER2 positive SGC is at best modest (7, 8). Several resistance mechanisms have been proposed for HER2 targeted therapy including HER2 receptors lacking extracellular trastuzumab binding domain, upregulation of other tyrosine kinase receptors or alteration of downstream components resulting in aberrant PI3K/Akt/mTOR pathways (68).

But an exact reason to why response with these drugs seem lower in SGC compared to breast cancer and gastric and esophageal ADC has yet to be found. However, HER2 still remains an important potential target for therapies. Thus, promising strategies have emerged applying dual HER2 blockage with trastuzumab and pertuzumab or combining with chemotherapy (trastuzuamb/docetaxel) or as a drug-antibody-conjugate (ado-trastuzumab-emtasine) (9–11).

In summary, the expression of HER2 in SGC is very heterogeneous between and within histological subtypes. The prevalence of HER2 positivity ranged from 0% to 43% in 3,372 patients with sixteen subtypes of SGC. HER2 positivity was most prevalent in SDC and in some tumor subtypes derived from exocrine cells virtually no HER2 expression was reported. Prospective clinical trials are needed to further evaluate novel HER2 directed therapy and to establish the optimal definition of HER2 positivity based on treatment response in SGC with high prevalence of HER2 positivity.

DATA AVAILABILITY STATEMENT

The original contributions presented in the study are included in the article/**Supplementary Material**. Further inquiries can be directed to the corresponding author.

AUTHOR CONTRIBUTIONS

KE and MM-S conceived the project idea. KE and CH reviewed the literature and included studies. KE undertook data analysis. All authors assisted in writing the manuscript and interpreting results. NW, CK, and MM-S provided advice and guidance. All authors contributed to the article and approved the submitted version.

SUPPLEMENTARY MATERIAL

The Supplementary Material for this article can be found online at: https://www.frontiersin.org/articles/10.3389/fonc.2021.693394/full#supplementary-material

REFERENCES

1. Bray F, Ferlay J, Soerjomataram I, Siegel RL, Torre LA, Jemal A. Global Cancer Statistics 2018: GLOBOCAN Estimates of Incidence and Mortality Worldwide for 36 Cancers in 185 Countries. *CA: A Cancer J Clin* (2018) 68 (6):394–424. doi: 10.3322/caac.21492
2. El-Naggar Chan JKC, Grandis JR, Takata T, Slootweg PJ. *Who Classification of Head and Neck Tumours, 4th ed*, Vol. Vol 9. IARC Publications (2017).
3. Dimas K, Ulukaya E, Sakellaridis N. Salivary Gland Tumors☆. In: *Reference Module in Biomedical Sciences*. Elsevier (2015). doi: 10.1016/B978-0-12-801238-3.99478-9
4. Son E, Panwar A, Mosher CH, Lydiatt D. Cancers of the Major Salivary Gland. *J Oncol Pract* (2018) 14(2):99–108. doi: 10.1200/JOP.2017.026856
5. Nakaguro M, Tada Y, Faquin WC, Sadow PM, Wirth LJ, Nagao T. Salivary Duct Carcinoma: Updates in Histology, Cytology, Molecular Biology, and Treatment. *Cancer Cytopathol* (2020) 128(10):693–703. doi: 10.1002/cncy.22288
6. Wang X, Luo Y, Li M, Yan H, Sun M, Fan T. Management of Salivary Gland Carcinomas - A Review. *Oncotarget* (2017) 8(3):3946–56. doi: 10.18632/oncotarget.13952
7. Haddad R, Colevas AD, Krane JF, Cooper D, Glisson B, Amrein PC, et al. Herceptin in Patients With Advanced or Metastatic Salivary Gland Carcinomas. A Phase II Study. *Oral Oncol* (2003) 39(7):724–7. doi: 10.1016/S1368-8375(03)00097-6
8. Agulnik M, Cohen EWE, Cohen RB, Chen EX, Vokes EE, Hotte SJ, et al. Phase II Study of Lapatinib in Recurrent or Metastatic Epidermal Growth Factor Receptor and/or erbB2 Expressing Adenoid Cystic Carcinoma and Non-Adenoid Cystic Carcinoma Malignant Tumors of the Salivary Glands. *J Clin Oncol* (2007) 25(25):3978–84. doi: 10.1200/JCO.2007.11.8612
9. Takahashi H, Tada Y, Saotome T, Akazawa K, Ojiri H, Fushimi C, et al. Phase II Trial of Trastuzumab and Docetaxel in Patients With Human Epidermal Growth Factor Receptor 2-Positive Salivary Duct Carcinoma. *J Clin Oncol* (2019) 37(2):125–34. doi: 10.1200/JCO.18.00545
10. Li BT, Shen R, Offin M, Buonocore DJ, Myers ML, Venkatesh A, et al. Ado-Trastuzumab Emtansine in Patients With HER2 Amplified Salivary Gland Cancers (SGCS): Results From a Phase II Basket Trial. *J Clin Oncol* (2019) 37 (15_suppl):6001–1. doi: 10.1200/jco.2019.37.15_suppl.6001
11. Kurzrock R, Bowles DW, Kang H, Meric-Bernstam F, Hainsworth J, Spigel DR, et al. Targeted Therapy for Advanced Salivary Gland Carcinoma Based on Molecular Profiling: Results From MyPathway, a Phase IIa Multiple Basket Study. *Ann Oncol* (2020) 31:412–21. doi: 10.1016/j.annonc.2019.11.018
12. Wolff AC, Hammond MEH, Allison KH, Harvey BE, McShane LM, Dowsett M. HER2 Testing in Breast Cancer: American Society of Clinical Oncology/College of American Pathologists Clinical Practice Guideline Focused Update Summary. *J Oncol Pract* (2018) 14(7):437–41. doi: 10.1200/JOP.18.00206
13. Bartley AN, Washington MK, Colasacco C, Ventura CB, Ismaila N, Benson AB, et al. Her2 Testing and Clinical Decision Making in Gastroesophageal Adenocarcinoma: Guideline From the College of American Pathologists, American Society for Clinical Pathology, and the American Society of Clinical Oncology. *J Clin Oncol* (2017) 35(4):446–64. doi: 10.1200/JCO.2016.69.4836
14. Chatzopoulos K, Collins AR, Sotiriou S, Keeney MG, Visscher DW, Rivera M, et al. Increased ERBB2 Gene Copy Numbers Reveal a Subset of Salivary Duct Carcinomas With High Densities of Tumor Infiltrating Lymphocytes and PD-L1 Expression. *Head Neck Pathol* (2020) 14.4:1–15. doi: 10.1007/s12105-020-01163-x
15. Dalin MG, Desrichard A, Katabi N, Makarov V, Walsh LA, Lee KW, et al. Comprehensive Molecular Characterization of Salivary Duct Carcinoma Reveals Actionable Targets and Similarity to Apocrine Breast Cancer. *Clin Cancer Res* (2016) 22(18):4623–33. doi: 10.1158/1078-0432.CCR-16-0637
16. Dekkers OM, Vandenbroucke JP, Cevallos M, Renehan AG, Altman DG, Egger M. Cosmos-E: Guidance on Conducting Systematic Reviews and Meta-Analyses of Observational Studies of Etiology. *PloS Med* (2019) 16(2): e1002742. doi: 10.1371/journal.pmed.1002742
17. Glisson B, Colevas AD, Haddad R, Krane J, El-Naggar A, Kies M, et al. Her2 Expression in Salivary Gland Carcinomas: Dependence on Histological Subtype. *Clin Cancer Res* (2004) 10(3):944–6. doi: 10.1158/1078-0432.CCR-03-0253
18. Villepelet A, Lefèvre M, Verillaud B, Janot F, Garrel R, Vergez S, et al. Salivary Duct Carcinoma: A Prospective Multicenter Study of 61 Cases of the Réseau D'expertise Français Des Cancers Orl Rares. *Head Neck* (2018) 41(3):584–91. doi: 10.1002/hed.25194
19. Khan AJ, Digiovanna MP, Ross DA, Sasaki CT, Carter D, Son YH, et al. Adenoid Cystic Carcinoma: A Retrospective Clinical Review. *Int J Cancer* (2001) 96(3):149–58. doi: 10.1002/ijc.1013
20. Skálová A, Stárek I, Kuerová V, Szépe P, Plank L. Salivary Duct Carcinoma - a Highly Aggressive Salivary Gland Tumor With HER-2/neu Oncoprotein Overexpression. *Pathol Res Pract* (2001) 197(9):621–6. doi: 10.1078/0344-0338-00136
21. Dori S, Vered M, David R, Buchner A. *HER2/Neu* Expression in Adenoid Cystic Carcinoma of Salivary Gland Origin: An Immunohistochemical Study. *J Oral Pathol Med* (2002) 31(8):463–7. doi: 10.1034/j.1600-0714.2002.00017.x
22. Skálová A, Stárek I, Vanecek T, Kucerová V, Plank L, Szépe P, et al. Expression of HER-2/neu Gene and Protein in Salivary Duct Carcinomas of Parotid Gland as Revealed by Fluorescence in-Situ Hybridization and Immunohistochemistry. *Histopathology* (2003) 42(4):348–56. doi: 10.1046/j.1365-2559.2003.01600.x
23. Weed DT, Gomez-Fernandez C, Pacheco J, Ruiz J, Hamilton-Nelson K, Arnold DJ, et al. MUC4 and ERBB2 Expression in Major and Minor Salivary Gland Mucoepidermoid Carcinoma. *Head Neck* (2004) 26(4):353–64. doi: 10.1002/hed.10387
24. Di Palma S, Skálová A, Vanìèek T, Simpson RHW, Stárek I, Leivo I. Non-Invasive (Intracapsular) Carcinoma Ex Pleomorphic Adenoma: Recognition of Focal Carcinoma by HER-2/neu and MIB1 Immunohistochemistry. *Histopathology* (2005) 46(2):144–52. doi: 10.1111/j.1365-2559.2005.02058.x
25. Jaehne M, Roeser K, Jaekel T, David Schepers J, Albert N, Löning T. Clinical and Immunohistologic Typing of Salivary Duct Carcinoma: A Report of 50 Cases. *Cancer* (2005) 103(12):2526–33. doi: 10.1002/cncr.21116
26. Cornolti G, Ungari M, Morassi ML, Facchetti F, Rossi E, Lombardi D, et al. Amplification and Overexpression of Her2/neu Gene and HER2/neu Protein in Salivary Duct Carcinoma of the Parotid Gland. *Arch Otolaryngol - Head Neck Surg* (2007) 133(10):1031–6. doi: 10.1001/archotol.133.10.1031
27. Nabili V, Tan JW, Bhuta S, Sercarz JA, Head CS. Salivary Duct Carcinoma: A Clinical and Histologic Review With Implications for Trastuzumab Therapy. *Head Neck* (2007) 29(10):907–12. doi: 10.1002/hed.20614
28. Tapia C, Glatz K, Novotny H, Lugli A, Horcic M, Seemayer CA, et al. Close Association Between HER-2 Amplification and Overexpression in Human Tumors of Non-Breast Origin. *Mod Pathol* (2007) 20(2):192–8. doi: 10.1038/modpathol.3800729
29. Williams MD, Roberts D, Blumenschein GR, Temam S, Kies MS, Rosenthal DI, et al. Differential Expression of Hormonal and Growth Factor Receptors in Salivary Duct Carcinomas: Biologic Significance and Potential Role in Therapeutic Stratification of Patients. *Am J Surg Pathol* (2007) 31(11):1645–52. doi: 10.1097/PAS.0b013e3180caa099
30. Ettl T, Schwarz S, Kleinsasser N, Hartmann A, Reichert TE, Driemel O. Overexpression of EGFR and Absence of C-KIT Expression Correlate With Poor Prognosis in Salivary Gland Carcinomas. *Histopathology* (2008) 53 (5):567–77. doi: 10.1111/j.1365-2559.2008.03159.x
31. Shang J, Shui Y, Sheng L, Wang K, Hu Q, Wei Q. Epidermal Growth Factor Receptor and Human Epidermal Growth Receptor 2 Expression in Parotid Mucoepidermoid Carcinoma: Possible Implications for Targeted Therapy. *Oncol Rep* (2008) 19(2):435–40. doi: 10.3892/or.19.2.435
32. Locati LD, Perrone F, Losa M, Mela M, Casieri P, Orsenigo M, et al. Treatment Relevant Target Immunophenotyping of 139 Salivary Gland Carcinomas (Sgcs). *Oral Oncol* (2009) 45(11):986–90. doi: 10.1016/j.oraloncology.2009.05.635
33. Luukkaa H, Klemi P, Leivo I, Mäkitie AA, Irish J, Gilbert R, et al. Expression of Matrix metalloproteinase-1, -7, -9, -13, Ki-67, and HER-2 in Epithelial-Myoepithelial Salivary Gland Cancer. *Head Neck* (2010) 32(8):1019–27. doi: 10.1002/hed.21277
34. Williams MD, Roberts DB, Kies MS, Mao L, Weber RS, El-Naggar AK. Genetic and Expression Analysis of HER-2 and EGFR Genes in Salivary Duct Carcinoma: Empirical and Therapeutic Significance. *Clin Cancer Res* (2010) 16(8):2266–74. doi: 10.1158/1078-0432.CCR-09-0238
35. Clauditz TS, Reiff M, Gravert L, Gnoss A, Tsourlakis MC, Münscher A, et al. Human Epidermal Growth Factor Receptor 2 (HER2) in Salivary Gland Carcinomas. *Pathology* (2011) 43(5):459–64. doi: 10.1097/PAT.0b013e3283484a60
36. Di Palma S, Simpson RHW, Marchió C, Skálová A, Ungari M, Sandison A, et al. Salivary Duct Carcinomas Can Be Classified Into Luminal Androgen Receptor-Positive, HER2 and Basal-Like Phenotypes. *Histopathology* (2012) 61(4):629–43. doi: 10.1111/j.1365-2559.2012.04252.x

37. Ettl T, Stiegler C, Zeitler K, Agaimy A, Zenk J, Reichert TE, et al. Egfr, HER2, Survivin, and Loss of pSTAT3 Characterize High-Grade Malignancy in Salivary Gland Cancer With Impact on Prognosis. *Hum Pathol* (2012) 43 (6):921–31. doi: 10.1016/j.humpath.2011.08.006
38. Hashimoto K, Yamamoto H, Shiratsuchi H, Nakashima T, Tamiya S, Nishiyama KI, et al. Her-2/neu Gene Amplification in Carcinoma Ex Pleomorphic Adenoma in Relation to Progression and Prognosis: A Chromogenic In-Situ Hybridization Study. *Histopathology* (2012) 60(6 B): E131–42. doi: 10.1111/j.1365-2559.2012.04201.x
39. Suzuki S, Dobashi Y, Minato H, Tajiri R, Yoshizaki T, Ooi A. EGFR and HER2-Akt-mTOR Signaling Pathways Are Activated in Subgroups of Salivary Gland Carcinomas. *Virchows Arch* (2012) 461(3):271–82. doi: 10.1007/s00428-012-1282-3
40. Cros J, Sbidian E, Hans S, Roussel H, Scotte F, Tartour E, et al. Expression and Mutational Status of Treatment-Relevant Targets and Key Oncogenes in 123 Malignant Salivary Gland Tumours. *Ann Oncol* (2013) 24(10):2624–9. doi: 10.1093/annonc/mdt338
41. Nakano T, Yamamoto H, Hashimoto K, Tamiya S, Shiratsuchi H, Nakashima T, et al. HER2 and EGFR Gene Copy Number Alterations are Predominant in High-Grade Salivary Mucoepidermoid Carcinoma Irrespective of MAML2 Fusion Status. *Histopathology* (2013) 63(3):378–92. doi: 10.1111/his.12183
42. Nardi V, Sadow PM, Juric D, Zhao D, Cosper AK, Bergethon K, et al. Detection of Novel Actionable Genetic Changes in Salivary Duct Carcinoma Helps Direct Patient Treatment. *Clin Cancer Res* (2013) 19(2):480–90. doi: 10.1158/1078-0432.CCR-12-1842
43. Kondo Y, Kikuchi T, Esteban JC, Kumaki N, Ogura G, Inomoto C, et al. Intratumoral Heterogeneity of HER2 Protein and Amplification of HER2 Gene in Salivary Duct Carcinoma. *Pathol Int* (2014) 64(9):453–9. doi: 10.1111/pin.12195
44. Masubuchi T, Tada Y, Maruya Si, Osamura Y, Kamata Se, Miura K, et al. Clinicopathological Significance of Androgen Receptor, HER2, Ki-67 and EGFR Expressions in Salivary Duct Carcinoma. *Int J Clin Oncol* (2015) 20 (1):35–44. doi: 10.1007/s10147-014-0674-6
45. Han MW, Roh JL, Choi SH, Nam SY, Lee HJ, Cho KJ, et al. Prognostic Factors and Outcome Analysis of Salivary Duct Carcinoma. *Auris Nasus Larynx* (2015) 42(6):472–7. doi: 10.1016/j.anl.2015.04.005
46. Jakob JA, Kies MS, Glisson BS, Kupferman ME, Liu DD, Lee JJ, et al. Phase II Study of Gefitinib in Patients With Advanced Salivary Gland Cancers. *Head Neck* (2015) 37(5):644–9. doi: 10.1002/hed.23647
47. Nishijima T, Yamamoto H, Nakano T, Nakashima T, Taguchi KI, Masuda M, et al. Dual Gain of HER2 and EGFR Gene Copy Numbers Impacts the Prognosis of Carcinoma Ex Pleomorphic Adenoma. *Hum Pathol* (2015) 46 (11):1730–43. doi: 10.1016/j.humpath.2015.07.014
48. Kusafuka K, Kawasaki T, Maeda M, Yamanegi K, Baba S, Ito Y, et al. Salivary Duct Carcinoma With Rhabdoid Features: A Salivary Counterpart of Pleomorphic Lobular Carcinoma of the Breast. *Histopathology* (2017) 70 (2):164–73. doi: 10.1111/his.12987
49. Locati LD, Perrone F, Cortelazzi B, Lo Vullo S, Bossi P, Dagrada G, et al. Clinical Activity of Androgen Deprivation Therapy in Patients With Metastatic/Relapsed Androgen Receptor-Positive Salivary Gland Cancers. *Head Neck* (2016) 38(5):724–31. doi: 10.1002/hed.23940
50. Lemound J, Schenk M, Keller G, Stucki-Koch A, Witting S, Kreipe H, et al. Cytogenetic and Immunohistochemical Biomarker Profiling of Therapy-Relevant Factors in Salivary Gland Carcinomas. *J Oral Pathol Med* (2016) 45(9):655–63. doi: 10.1111/jop.12429
51. Luk PP, Weston JD, Yu B, Selinger CI, Ekmejian R, Eviston TJ, et al. Salivary Duct Carcinoma: Clinicopathologic Features, Morphologic Spectrum, and Somatic Mutations. *Head Neck* (2016) 38:E1838–47. doi: 10.1002/hed.24332
52. Hashimoto K, Hayashi R, Mukaigawa T, Yamazaki M, Fujii S. Concomitant Expression of Ezrin and HER2 Predicts Distant Metastasis and Poor Prognosis of Patients With Salivary Gland Carcinomas. *Hum Pathol* (2017) 63:110–9. doi: 10.1016/j.humpath.2017.02.017
53. Khoo TK, Yu B, Smith JA, Clarke AJ, Luk PP, Selinger CI, et al. Somatic Mutations in Salivary Duct Carcinoma and Potential Therapeutic Targets. *Oncotarget* (2017) 8(44):75893–903. doi: 10.18632/oncotarget.18173
54. Locati LD, Collini P, Imbimbo M, Barisella M, Testi A, Licitra LF, et al. Immunohistochemical and Molecular Profile of Salivary Gland Cancer in Children. *Pediatr Blood Cancer* (2017) 64(9). doi: 10.1002/pbc.26468
55. Takase S, Kano S, Tada Y, Kawakita D, Shimura T, Hirai H, et al. Biomarker Immunoprofile in Salivary Duct Carcinomas: Clinicopathological and Prognostic Implications With Evaluation of the Revised Classification. *Oncotarget* (2017) 8(35):59023–35. doi: 10.18632/oncotarget.19812
56. Andreasen S, Tan Q, Agander TK, Steiner P, Bjørndal K, Høgdall E, et al. Adenoid Cystic Carcinomas of the Salivary Gland, Lacrimal Gland, and Breast are Morphologically and Genetically Similar But Have Distinct microRNA Expression Profiles. *Mod Pathol* (2018) 31(8):1211–25. doi: 10.1038/s41379-018-0005-y
57. Beck AJCC, Lohuis PJFM, Al-Mamgani A, Smit LA, Klop WMC. Salivary Duct Carcinoma: Evaluation of Treatment and Outcome in a Tertiary Referral Institute. *Eur Arch Oto-Rhino-Laryngol* (2018) 275(7):1885–92. doi: 10.1007/s00405-018-5000-x
58. Boon E, Bel M, van Boxtel W, van der Graaf WTA, van Es RJJ, Eerenstein SEJ, et al. A Clinicopathological Study and Prognostic Factor Analysis of 177 Salivary Duct Carcinoma Patients From The Netherlands. *Int J Cancer* (2018) 143(4):758–66. doi: 10.1002/ijc.31353
59. Kanazawa T, Misawa K, Fukushima H, Misawa Y, Sato Y, Maruta M, et al. Epigenetic Inactivation of Galanin Receptors in Salivary Duct Carcinoma of the Parotid Gland: Potential Utility as Biomarkers for Prognosis. *Oncol Lett* (2018) 15(6):9043–50. doi: 10.3892/ol.2018.8525
60. Ryu HJ, Koh YW, Yoon SO. The Implications of TrkA and MET Aberrations in Novo Salivary Duct Carcinoma. *Hum Pathol* (2018) 81:18–25. doi: 10.1016/j.humpath.2018.04.027
61. Gargano SM, Senarathne W, Feldman R, Florento E, Stafford P, Swensen J, et al. Novel Therapeutic Targets in Salivary Duct Carcinoma Uncovered by Comprehensive Molecular Profiling. *Cancer Med* (2019) 8(17):7322–9. doi: 10.1002/cam4.2602
62. Liang L, Williams MD, Bell D. Expression of PTEN, Androgen Receptor, HER2/Neu, Cytokeratin 5/6, Estrogen Receptor-Beta, HMGA2, and PLAG1 in Salivary Duct Carcinoma. *Head Neck Pathol* (2019) 13(4):529–34. doi: 10.1007/s12105-018-0984-5
63. Santana T, Pavel A, Martinek P, Steiner P, Grossmann P, Baněčková M, et al. Biomarker Immunoprofile and Molecular Characteristics in Salivary Duct Carcinoma: Clinicopathological and Prognostic Implications. *Hum Pathol* (2019) 93:37–47. doi: 10.1016/j.humpath.2019.08.009
64. Szewczyk M, Marszałek A, Sygut J, Golusiński P, Golusiński W. Prognostic Markers in Salivary Gland Cancer and Their Impact on Survival. *Head Neck* (2019) 41(9):3338–47. doi: 10.1002/hed.25857
65. Hsieh MS, Lee YH, Jin YT, Kuo YJ. Clinicopathological Study of Intraductal Carcinoma of the Salivary Gland, With Emphasis on the Apocrine Type. *Virchows Arch* (2020) 477(4):581–92. doi: 10.1007/s00428-020-02823-7
66. Perez EA, Cortés J, Gonzalez-Angulo AM, Bartlett JMS. HER2 Testing: Current Status and Future Directions. *Cancer Treat Rev* (2014) 40(2):276–84. doi: 10.1016/j.ctrv.2013.09.001
67. Rakha EA, Pinder SE, Bartlett JMS, Ibrahim M, Starczynski J, Carder PJ, et al. Updated UK Recommendations for HER2 Assessment in Breast Cancer. *J Clin Pathol* (2015) 68(2):93–9. doi: 10.1136/jclinpath-2014-202571
68. Luque-Cabal M, García-Teijido P, Fernández-Pérez Y, Sánchez-Lorenzo L, Palacio-Vázquez I. Mechanisms Behind the Resistance to Trastuzumab in HER2-Amplified Breast Cancer and Strategies to Overcome it. *Clin Med Insights Oncol* (2016) 10s1:21–30. doi: 10.4137/CMO.S34537

Conflict of Interest: CK has served in advisory boards for MSD, Bristol-Myers Squibb, and Merck Serono. MM-S has served in advisory boards for Roche, Genmab, Bayer, and Karyopharm Therapeutics and received research grants from Karyopharm Therapeutic, Puma Biotechnologies and MSD.

The remaining authors declare that the research was conducted in the absence of any commercial or financial relationships that could be construed as a potential conflict of interest.

frontiers | Frontiers in Oncology

TYPE Original Research
PUBLISHED 17 November 2022
DOI 10.3389/fonc.2022.1063477

OPEN ACCESS

EDITED BY
Ester Orlandi,
National Center of Oncological Hadrontherapy, Italy

REVIEWED BY
Yingying Jiang,
Affiliated Hospital of Weifang Medical University, China
Gennaro Gambardella,
Telethon Institute of Genetics and Medicine (TIGEM), Italy

*CORRESPONDENCE
Hongzhu Qu
quhongzhu@big.ac.cn
Xiangdong Fang
fangxd@big.ac.cn
Qing Xi
xiqing301@163.com

†These authors have contributed equally to this work

SPECIALTY SECTION
This article was submitted to Head and Neck Cancer, a section of the journal Frontiers in Oncology

RECEIVED 07 October 2022
ACCEPTED 27 October 2022
PUBLISHED 17 November 2022

CITATION
Lin Q, Fang Z, Sun J, Chen F, Ren Y, Fu Z, Yang S, Feng L, Wang F, Song Z, Chen W, Yu W, Wang C, Shi Y, Liang Y, Zhang H, Qu H, Fang X and Xi Q (2022) Single-cell transcriptomic analysis of the tumor ecosystem of adenoid cystic carcinoma. *Front. Oncol.* 12:1063477. doi: 10.3389/fonc.2022.1063477

Single-cell transcriptomic analysis of the tumor ecosystem of adenoid cystic carcinoma

Quanquan Lin[1†], Zhanjie Fang[2†], Jinlong Sun[1†], Fei Chen[1†], Yipeng Ren[1], Zhenhong Fu[1], Sefei Yang[1], Lin Feng[1], Feng Wang[1], Zhigang Song[1], Wei Chen[1], Wenjun Yu[1], Chen Wang[2], Yixin Shi[2], Yue Liang[2], Haizhong Zhang[1], Hongzhu Qu[2*], Xiangdong Fang[2*] and Qing Xi[1*]

[1]Department of Stomatology, Chinese People's Liberation Army General Hospital, Beijing, China, [2]Key Laboratory of Genome Sciences and Information, Beijing Institute of Genomics, Chinese Academy of Sciences/China National Center for Bioinformation, Beijing, China

Adenoid cystic carcinoma (ACC) is a malignant tumor that originates from exocrine gland epithelial cells. We profiled the transcriptomes of 49,948 cells from paracarcinoma and carcinoma tissues of three patients using single-cell RNA sequencing. Three main types of the epithelial cells were identified into myoepithelial-like cells, intercalated duct-like cells, and duct-like cells by marker genes. And part of intercalated duct-like cells with special copy number variations which altered with MYB family gene and EN1 transcriptomes were identified as premalignant cells. Developmental pseudo-time analysis showed that the premalignant cells eventually transformed into malignant cells. Furthermore, MYB and MYBL1 were found to belong to two different gene modules and were expressed in a mutually exclusive manner. The two gene modules drove ACC progression into different directions. Our findings provide novel evidence to explain the high recurrence rate of ACC and its characteristic biological behavior.

KEYWORDS

adenoid cystic carcinoma, head and neck cancer, single-cell transcriptomic analysis, MYB, EN1

1 Introduction

Adenoid cystic carcinoma is a kind of malignant tumor of the exocrine glands. The annual incidence of salivary gland ACC has been reported to be 0.16 to 0.14 per 100,000 populations (1). Compared with other solid tumors, ACC is characterized by more aggressive behavior, perineural invasion, early pulmonary metastasis, and a higher rate of positive incision edge (2).The current clinical treatment for ACC is surgery and adjuvant radiotherapy but recurrence or metastasis still occurs in more than 50% ACCs (3). The survival rates of 5 years, 10 years, and 20 years is 68%, 52%, and 28% respectively, indicating the bad prognosis (4).

Histopathologically, ACC is a type of epithelial tumor comprised of ductal and myoepithelial cells. The expression of MYB is the gold standard for diagnosis of ACC (4, 5). With the widespread use of whole exome sequencing (WES) and whole genome sequencing (WGS), its internal oncogenic mechanism has been gradually revealed, such as the MYB family gene translocation (6), the Notch signal pathway (7), and the DNA damage repair (8) and epigenetic molecular mutation pathways (9). However, the underlying molecular mechanisms of tumor development remain unexplained clearly.

Single-cell RNA sequencing (scRNA-seq) (10) can be used to observe the evolution of individual cells in various paracarcinoma and carcinoma tissues. It is widely used in breast cancer (11), ovarian cancer (12), non-small-lung cancer (13), pancreatic ductal adenocarcinoma (14), and other cancers. Nevertheless, scRNA-seq is poorly reported in ACC.

In this study, we analyzed the epithelial cell clusters in the paracarcinoma and carcinoma tissues of three patients and aimed to elucidate the mechanisms of ACC at the single-cell transcriptional level. Our findings revealed the possible origin of ACC cells and mapped the progression of tumor development at the transcriptional level.

2 Results

2.1 Overview of cell population in the ACC tumor ecosystem

The tumor ecosystem of ACC was examined using scRNA-seq of digested living cells derived from ACC paracarcinoma and carcinoma tissues using a 10x Genomics-based platform (Figure 1A). A total of 49,948 cells from the parcarcinoma and carcinoma tissues of three ACC patients were captured using the sequencer and 42,714 cells were retained for downstream analysis after quality control filtering (Supplementary Table 1). The results of the staining pathologic sections of three patients are shown in Supplementary Figure 1. The clinicopathological characteristics of three patients are listed in Supplementary Table 2.

Unsupervised clustering of the cells identified 13 cell types, including fibroblasts, epithelial cells, endothelial cells, basal cells, T or natural killer cells, smooth muscle cells, myeloid cells, muscle satellite cells, mast cells, skeletal muscle cells, lymphatic endothelial cells, Schwann cells, and an unknown cell cluster, which was a mixture of plasma cells, B cells, and fibroblasts (Figure 1B and Supplementary Figure 2B).

Uniform manifold approximation and projection (UMAP) visualization of the hallmark genes expressed in each cell subtype was performed (Figure 1C). The dot plots show the well-expressed marker genes in corresponding cell types (Supplementary Figures 2A, C). The complex tumor ecosystem comprised 40.1% epithelial cells, 27.9% fibroblasts, 11.3% T/NK cells, 10.8% endothelial cells, and a small number of other cells (Figure 1D). Notably, basal cells only existed in sample 0222 paracarcinoma tissue, whereas smooth muscle cells, muscle satellite cells, unknown cells, skeletal muscle cells, and Schwann cells only existed in sample 7420 paracarcinoma and carcinoma tissues (Figure 1E).

The proportion of cell types in the paracarcinoma and carcinoma tissues were examined. The proportion of epithelial cells was 9.3% in paracarcinoma, while in carcinoma was 40.1%. In contrast, the proportion of endothelial cells in paracarcinoma and carcinoma were 24.0% and 10.8%, respectively (Figures 1D, E). Considering ACC is a malignant tumor that originates from epithelial cells, the transcriptome characteristics of epithelial cells were further evaluated in the study.

2.2 Various subtypes of epithelial cells play different roles in tumor progression

The 9,685 epithelial cells present were categorized as three subtypes (Figure 2A): myoepithelial-like cells (MECs, $ACTA2^{+}$/$MYH11^{+}$/$CNN1^{+}$), intercalated duct-like cells (Inter-Duct 1–7, KRT19+/AQP5+/KIT+), and duct-like cells (Duct 1 and Duct 2, KRT19+/AQP5-/KIT-). MUC5B, which is a mucinous acinar marker, was expressed at lower levels in a few subtypes, such as Inter-Duct 5. Moreover, MUC7, which is a serious acinar marker, was barely expressed in any subtypes (Figure 2B). In the paracarcinoma tissues, Inter-Duct 1, Inter-Duct 3, Duct 1, Inter-Duct 4, and MECs accounted for 34.7%, 21.9%, 15.6%, 12.2%, and 8.0% of the epithelial cells, respectively. In the carcinoma tissues, MECs, Inter-Duct 5, and Duct 2 accounted for 18.7%, 7.0%, and 3.4% of the epithelial cells, respectively (Figure 2C).

Each cluster was analyzed to identify differentially expressed genes. HES1 and ID4 were highly expressed in Inter–Duct 3 cells. CENPF, TOP2A, and MK167 were highly expressed in

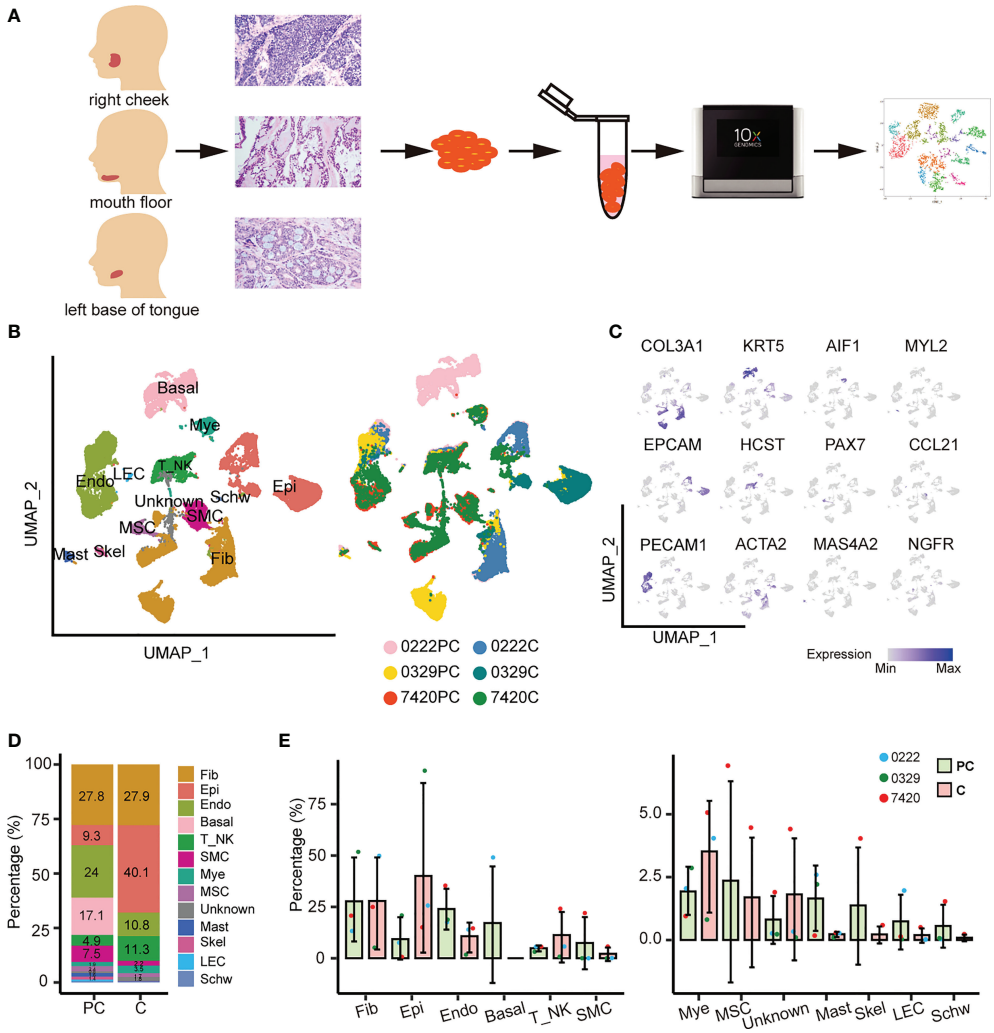

FIGURE 1
Overview of THE ACC tumor microenvironment. **(A)** Workflow for collecting clinical samples and processing scRNA-Seq data. **(B)** UMAP of 13 cell populations from six samples. PC, paracarcinoma; C, carcinoma. **(C)** Cell subtypes were labeled in the UMAP plot using typical markers. **(D)** The abundance of each cell population in the paracarcinoma and carcinoma tissues. **(E)** The relative abundance of 13 cell clusters in the paracarcinoma and carcinoma tissues. Error bars are presented as mean values ± SD.

Inter–Duct 4 cells. ACTA2 and TP63 were highly expressed in MECs. SCGB3A1, MMP7, and ZG16B were highly expressed in Inter–Duct 5 cells. SRGN, CCL5, and CREM were highly expressed in Inter–Duct6 cells. PLVAP and PECAM1 were highly expressed in Inter–Duct 7 cells (Figure 2D).

Gene set variation analysis (GSVA) revealed the function of the different epithelial clusters. Notch signaling pathway, MYC targets, DNA replication process, oxidative phosphorylation, Wnt β-catenin, and Pi3k-Akt-mTOR signaling pathway were upregulated in Inter-Duct 3–4 cells. Duct 2 and MECs were involved in epithelial–mesenchymal transformation, angiogenesis, myogenesis, and apical junction. Inter-Duct 5–7 cells showed high expression of immune-related genes and were enriched for pathways including interferon α/γ response, allograft rejection, and IL6 JAK STAT3 signaling (Figure 2E).

These results suggested that each epithelial cluster was enriched for different signaling pathways. Inter-Duct 3–4 cells were enriched for activation of tumor progression pathways and Inter-Duct 5–7 cells may be involved in the immune response.

Differences in gene expression programs of three main epithelial cell clusters were performed by non-negative matrix decomposition. Hierarchical clustering identified five expression programs that varied within the Inter-Duct cells, including cell cycle, extracellular matrix organization, epidermal development, stress response, and regulation of neuron death. Three gene expression programs were found in MECs, including epithelial

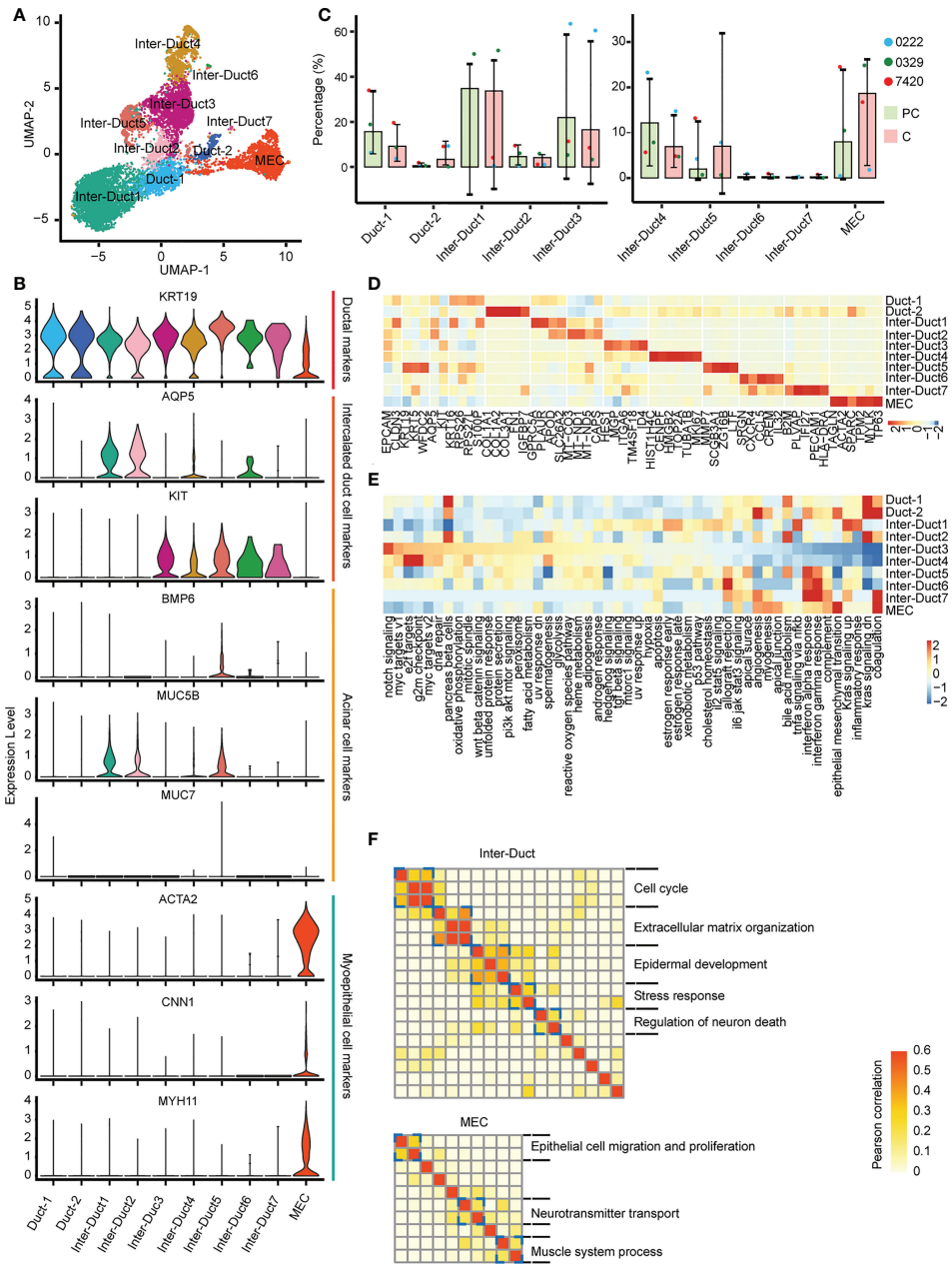

FIGURE 2
Different epithelial cell subtypes with specific functions. **(A)** UMAP visualization of 10 epithelial cell subtypes across the three patients. **(B)** Violin plots showing the expression of duct, acinar, and myoepithelial cells markers in epithelial cells subtypes. **(C)** The relative abundance of 10 epithelial cell subtypes in the paracarcinoma (PC) and carcinoma (C) tissues. **(D)** Heatmap of differentially expressed genes in epithelial cell clusters. **(E)** Heatmap showing differences in 50 hallmark pathways enrichment scores among each epithelial cell subtype. **(F)** Heatmap showing pairwise correlations of intratumoral programs derived from Inter-Duct (top) and myoepithelial-like cells (bottom). Coherent expression programs across tumors are marked on the right.

cell migration and proliferation, neurotransmitter transport, and muscle system process (Figure 2F). We identified the dominant gene sets in the different expression programs of three main epithelial cell clusters and performed GO (Gene Ontology) enrichment analysis on specific genesets to support above findings (Supplementary Table 3, Supplementary Figures 3, 4).

These results suggested that Inter-Duct cells may be directly involved in tumor development and myoepithelial cells play a contributory role in this process.

2.3 The underlying regulatory network in epithelial cell clusters

The potential molecular basis driving the distinct epithelial clusters was examined using SCENIC (Single-cell Regulatory Network Inference and Clustering) to identify the underlying regulatory network in epithelial cells.

Each cluster was driven by different transcription factors (TFs). Notably, coexpression of MYB and EN1 was observed in the upstream TFs of Inter-Duct 3–4 cells (Figure 3A). In addition, genes involved in DNA repair and cell cycle transition, such as E2F2, TFDP1, E2F3, BRCA1, POLE3, E2F1, EZH2, and RB1, showed aggregation (Figure 3B). Prediction of genes downstream of MYB and EN1 identified 10 coregulated downstream target genes, including COLEC12, ELAVL2, FRS2, IL17RD, ITGA6, LAMB1, LRIG1, NAV2, NCALD, and HOMER3 (Figure 3C), which are predominantly associated with the nervous system (15–21). Genemania (22) was used to predict possible functions coregulated by MYB and EN1, which are involved in cell–substrate junctions and neuronal guidance. (Figure 3D)

Gene Ontology (GO) enrichment analysis of the TFs drove different expression programs. Duct 1 and Duct 2 cells were enriched for G1/S transition of the mitotic cell cycle, protein–DNA complex subunit organization, and intracellular receptor signaling pathway. Inter-Duct 3 cells were enriched for regulation of neuron death, histone deacetylation, and eyelid development in camera-type. Inter-Duct 4 were enriched for negative regulation of G0/G1 transition, cell cycle regulation, and transcription regulation involved in the G1/S transition of the mitotic cell cycle. Inter-Duct 5 cells were enriched for cellular response to type I interferon and transcription initiation from RNA polymerase II promoter. MECs were enriched for maintenance of the somatic cell population and steroid hormone-mediated signaling pathway (Figure 3E). These results indicate that Inter-Duct 3 cells were regulated by the upstream TFs, MYB and EN1.

2.4 Copy number variation in epithelial cells derived from paracarcinoma and carcinoma tissues

The large-scale chromosome CNV status of all the cells from the paracarcinoma and carcinoma tissues was examined using infercnv (Figure 4A). Comparing with the endothelial cells and fibroblasts from the paracarcinoma, all epithelial cells showed complex CNV changes, suggesting a malignant tendency in most cells (Supplementary Figure 5A). Moreover, different clusters of epithelial cells from the paracarcinoma tissue underwent the massive copy number amplification in 6q, 8q, 12q, and 17p, and chromosomal deletions in 14q (Figure 4C). We assume that the majority of tumor tissue derived from epithelial cells with similar CNV pattern are malignant, while epithelial cells that do not conform to that pattern, which were mainly identified in the paracarcinoma tissue are considered to be premalignant (Pre-M) cells. (Figure 4B).

Examination of the paracarcinoma and carcinoma tissues revealed that 47.6% of epithelial cells in paracarcinoma tissues were pre-M cells (Figure 4D). Moreover, among the pre-M cells, 26.2% were Duct 1 cells, 40.3% were Inter-Duct 1 cells, 5.4% were Inter-Duct 3 cells, 1.4% were Inter-Duct 5 cells and 9.7% were MECs. In comparison, the proportion of Inter-Duct 3 cells in malignant cells was 19.9%, which was significantly higher than the pre-M cells 5.4%. In addition, nearly 17.3% malignant cells were MECs (Figure 4E). The percentage of the pre-M cells in the Duct cells, Inter-Duct cells, and MECs were 32.8%, 12.8%, and 8.9%, respectively. On the contrary, the proportion of malignant cells in each cell clusters were 67.2%, 87.2%, and 91.1%, respectively. (Figure 4F).

MYB and EN1 were identified as the upstream TFs and MYB was identified as the hallmark ACC gene. MYB/MYBL1/EN1 were only highly expressed in epithelial cells (Supplementary Figure 5B). MYB and EN1 were highly expressed in malignant Inter-Duct 3–7 cells, and MYBL1 was highly expressed in Inter-Duct 1 cells, Inter-Duct 2 cells and MECs. (Supplementary Figure 5C). Moreover, among three main epithelial cell types, MYB was highly expressed in malignant Inter-Duct cells, MYBL1 was highly expressed in malignant MECs, and EN1 was highly expressed in all of them (Supplementary Figure 5E). These findings were consistent with previous studies that reported that the expression of MYB and MYBL1 were mutually exclusive (11) (Supplementary Figures 5C, D).

Importantly, the stem cell gene score of pre-M cells was higher than that of malignant cells, reflecting the accuracy of our method (Supplementary Figure 5F).

2.5 Different gene modules defined the developmental trajectory states

Differentiation trajectory analysis was used to examine the evolution of epithelial cells. The nodes of pre-M cells with a higher stemness score were set as the root node of pseudo-time. Most of the pre-M cells were gathered initially and evolved into malignant cells by the end of the pseudo-time. Notably, MECs, which were used as an independent differentiation group, were not involved in these processes (Figure 5A).

The pseudo-time axis was divided into four stages according to its lower quartile, median, and upper quartile. Graph-autocorrelation analysis revealed coregulated genes in the modules within the four stages. MYB and MYBL1 were highly expressed in modules 5 and 13 (Figure 5B, Supplementary Table 4), originated from the same root node, and showed

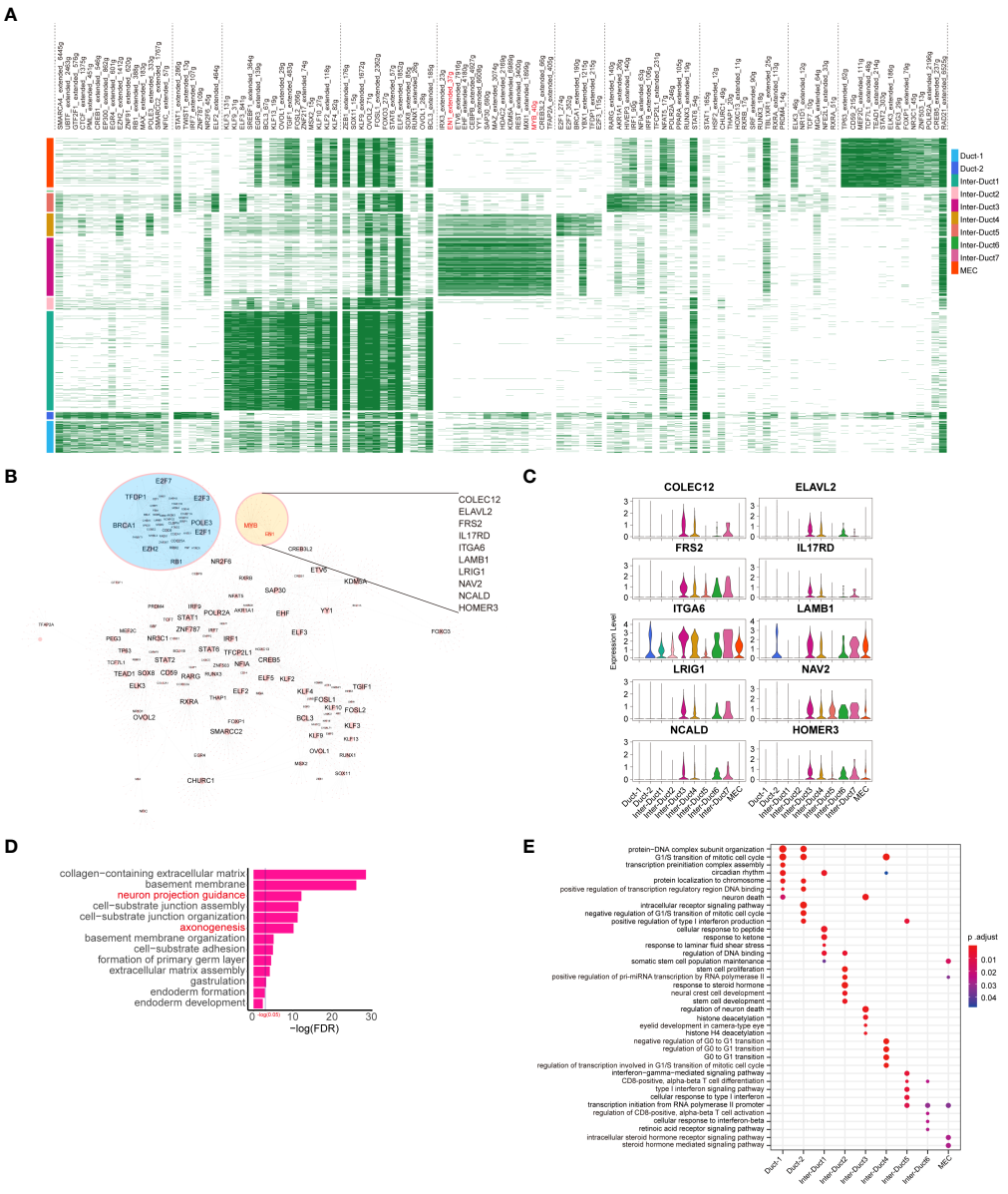

FIGURE 3
Development of epithelial cell subtypes is driven by distinct TFs. **(A)** Heatmap showing differentially expressed transcriptional regulons in different epithelial cell subtypes. **(B)** Epithelial cell transcription factor regulatory network, of which significant clusters or regulons with their targets are labeled. **(C)** Violin plots showing the relative expression of downstream target genes coregulated by MYB and EN1 in each epithelial cell subtype. **(D)** The result of GO enrichment analysis for target genes coregulated by MYB and EN1 and genes interacting with them. Biological processes terms associated with the peripheral nervous system are highlighted in red font. **(E)** Dot plot showing the results of GO enrichment analysis for predominant TFs of different epithelial cell subtypes.

increased expression along the pseudo-time trajectory, evolving toward two completely different branches (Figure 5C). Consistent with the above-mentioned results, during tumor evolution, gene MYB and MYBL1 showed opposite trends in expression (Figure 5D).

In addition, GO enrichment analysis of these two gene modules showed that the genes in Module 5 were involved in the rhythmic process, regulation of cellular component size, and dopaminergic neuron differentiation (Figure 5E). Furthermore, the genes in Module 13 were associated with diverse and complex biological processes, such as cellular response to external stimulus (Figure 5F). Taken together, these findings indicate that genes coregulated with MYB or MYBL1 may drive the two different evolutionary directions of ACC.

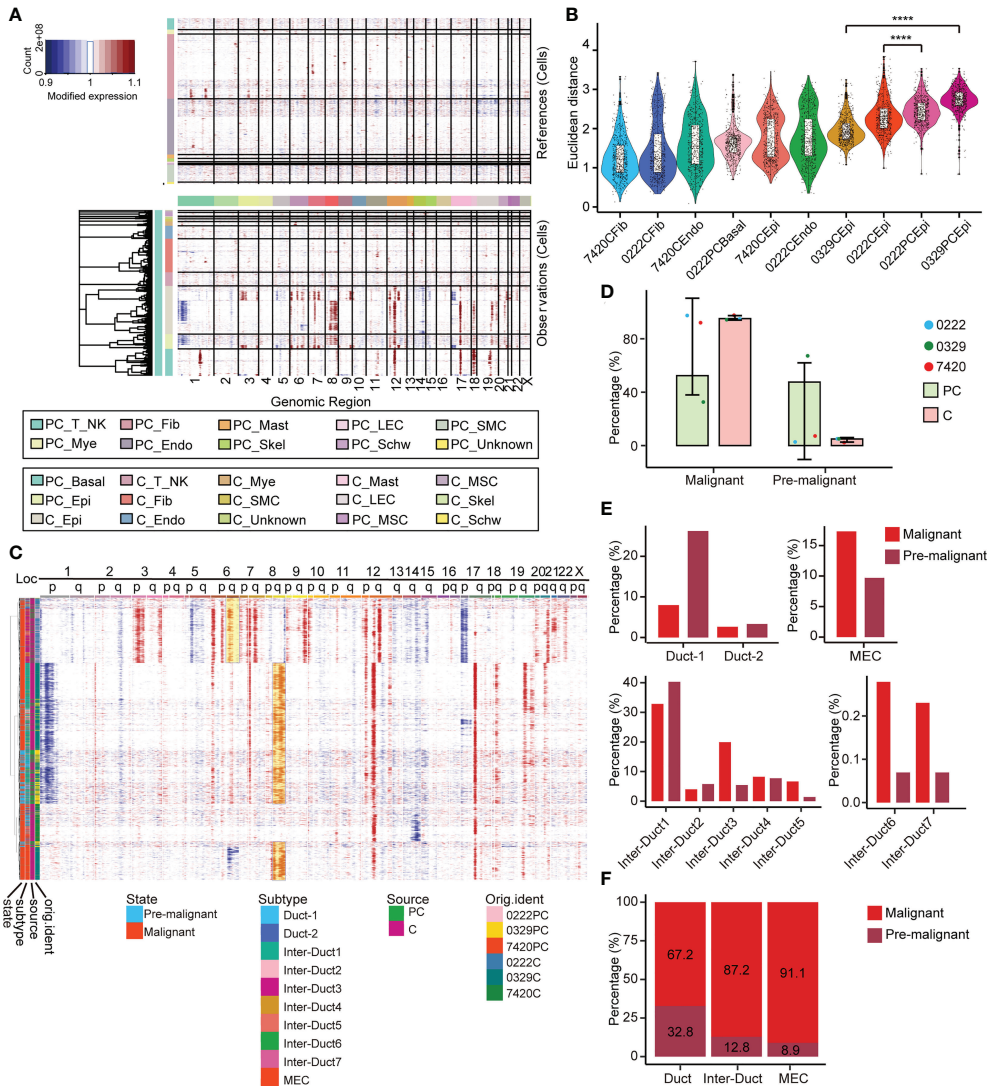

FIGURE 4
Multilayer heterogeneity of CNVs in epithelial cells. **(A)** Nonmalignant cells were used as references (top) and large-scale CNVs were observed in epithelial and basal cells (bottom). **(B)** A total of 600 epithelial cells, endothelial cells, basal cells, and fibroblasts were randomly selected from each corresponding sample and the Euclidean distance between the CNV score of which and the median CNV score of fibroblasts in adjacent samples was calculated and ranked respectively and presented as a scatterplot. All p-values were calculated by Wilcoxon rank sum test, **** $p \leq 0.0001$. **(C)** Reclustering the CNV score matrix of the epithelial cells. Cell grouping information is annotated below. **(D)** The relative abundance of pre-M and malignant cells in PT and tumor tissues. Error bars are presented as mean ± SD. **(E)** The relative abundance of 10 epithelial cell subtypes in the pre-M and malignant cells. **(F)** The relative abundance of the three main epithelial cell populations in the pre-M and malignant cells. pre-M: pre-malignant, PC: paracarcinoma, C: carcinoma.

2.6 Intercellular communications in the ACC tumor microenvironment

The tumor microenvironment is essential for the proliferation, migration, survival, anti-immune killing of malignant cells. Thus, we applied CellPhoneDB to infer cell-cell communication from combined expression of multi-subunit ligand-receptor complexes from scRNA-seq data. We found that malignant_inter_duct, Basal cells, endothelial cells, fibroblasts, myeloid cells, malignant_MEC were the dominant communication hubs (Figure 6A).

We classified cell communication pairs into 12 categories according to malignancy grade, predominant epithelial subset, and molecular origin. A significant upregulation in the expression of a number of receptors and ligands has been observed in malignant Inter-Duct and malignant MECs. Moreover, compared with preM cells, MIF-TNFRSF14, CD74-MIF and CD74-APP were generally highly up-regulated in the

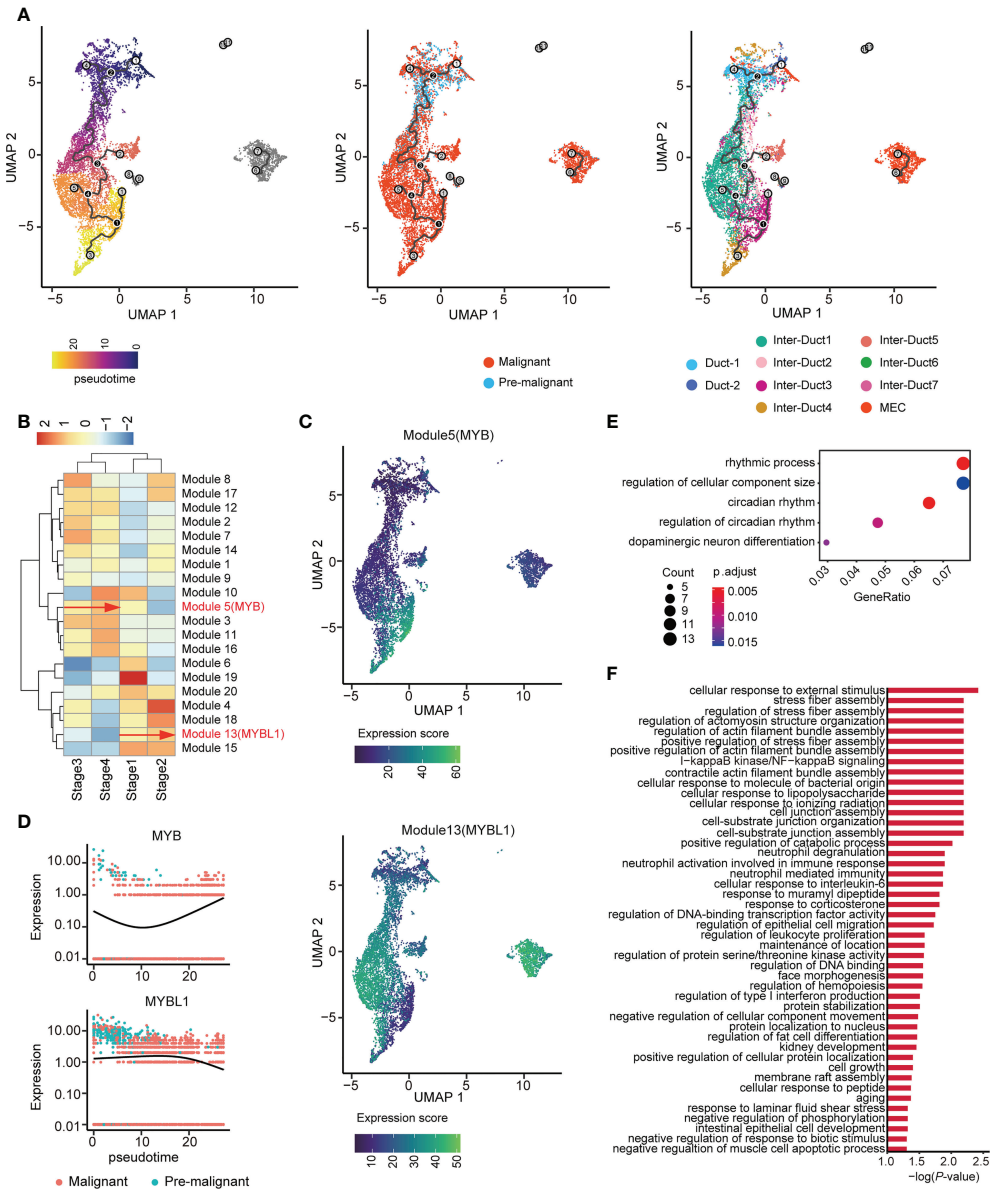

FIGURE 5
Two distinct evolutionary directions of ACC. **(A)** UMAP visualization of epithelial cells colored by pseudo-time (left), malignant state (middle), and subtype (right). **(B)** Unsupervised clustering heatmap showing the heterogeneity of gene modules expression over the pseudo-time. MYB and MYBL1 belong to Modules 5 and 13, respectively. **(C)** UMAP plot shows the gene expression score of Modules 5 (upper) and 13 (lower) among epithelial cells. **(D)** Dynamics of MYB (upper) and MYBL1 (lower) along pseudo-time. **(E)** Dot plot showing the results of GO enrichment analysis for genes in Module 5. **(F)** Bar chart showing the results of GO enrichment analysis for genes in Module 13.

communications between malignant Inter-Duct cells or MECs and other cells.

MIF (Macrophage Migration Inhibitory Factor) plays an import dual role of pro-inflammatory and pro-oncogenic (23). TNFRSF14 is a member of tumor necrosis factor (TNF) receptor superfamily, functioning in activating inflammatory and inhibitory T-cell immune response (24). The up-regulation of MIF-CD74 were found in many cancers, such as cervical squamous cell carcinoma (25), hepatocellular carcinoma (26) and prostatic cancer (27). Studies have shown that MIF-CD74 may enhance the proliferation and inhibit the apoptosis of tumors by promoting angiogenesis of tumor microenvironment. In addition, it has been reported that MIF may be a novel prognostic marker for human oral squamous cell carcinoma (28). This suggested that inflammation and immunosuppression in tumor microenvironment may provide

10.3389/fonc.2022.1063477

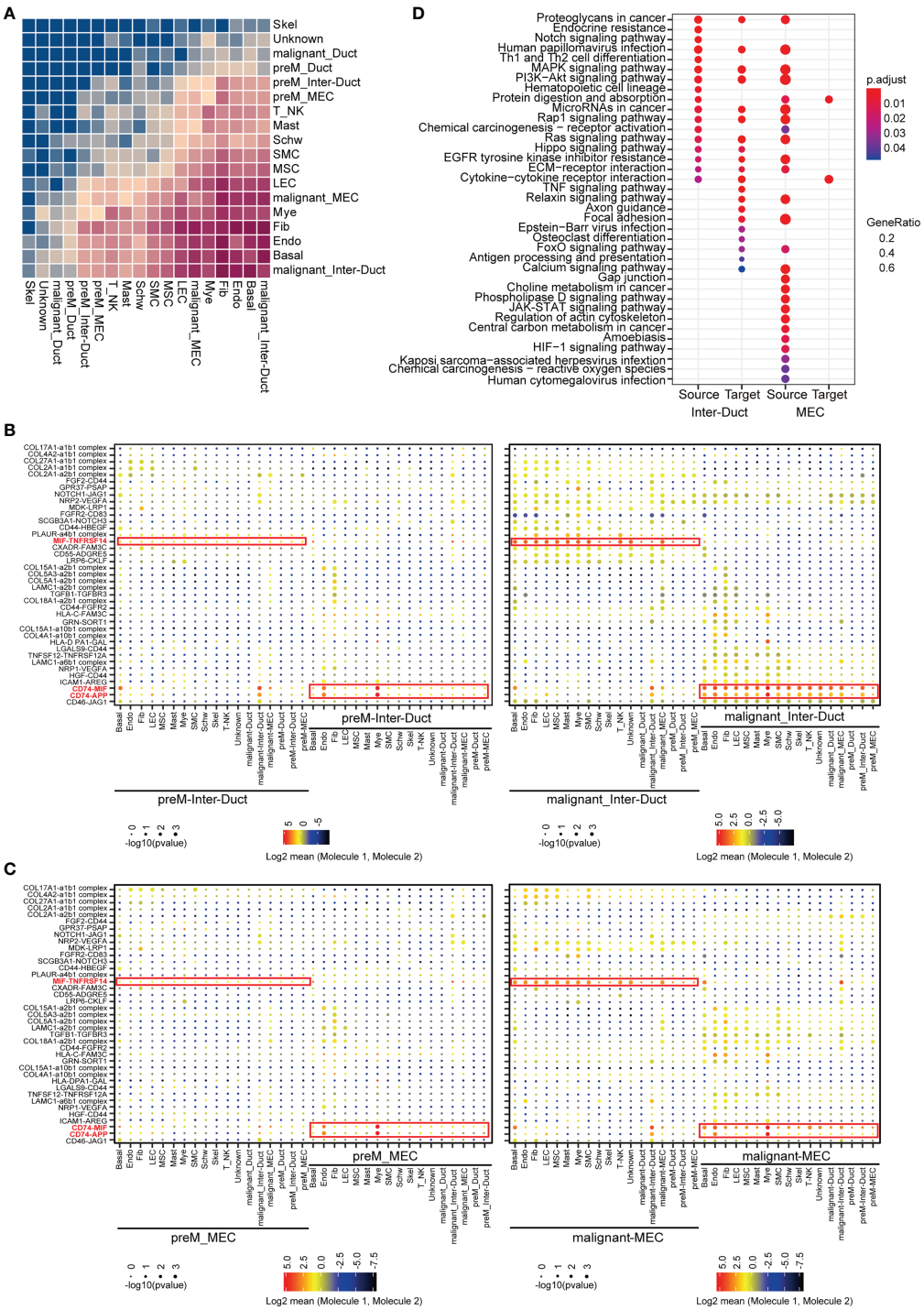

FIGURE 6
Intercellular interactions in ACC. **(A)** Heatmap showing the relative strength of cellular communication between different cell types. The depth of rectangular color is positively correlated with the number of interacting receptors-ligand pairs between cell types. **(B)** Dot plot showing the mean expression level and p-values for the selected interacting partners between other cells and intercalated duct-like cells. The interacting communication with Pre-M Inter-Duct was shown in left and those with malignant Inter-Duct was shown in right figure. **(C)** Dot plot showing the mean expression level and p-values for the selected interacting partners between other cells and myoepithelial-like cells. The interacting communication with Pre-M MEC was shown in left and those with malignant MEC was shown in right figure. **(D)** Dot plot showing the results of KEGG enrichment analysis for upregulated receptor and ligand genes in different groups, which were cell pairs with malignant Inter-Duct-like cells or MEC-like cells as "Source" or "Target".

favorable conditions for ACC proliferation and invasion (Figures 6B, C).

The upregulated receptor–ligand genes in different groups were implicated in different Kyoto Encyclopedia of Genes and Genomes (KEGG) pathways strongly associated with cancerization (Figure 6D). Overall, the enhanced communications between malignant and stromal cells in the tumor microenvironment further indicate the complexity of tumor behavior. The tumor microenvironment is essential for the proliferation, migration, survival, and anti-immune killing of malignant cells and the combined expression of multisubunit ligand–receptor complexes identified in the scRNA-seq data may infer cell–cell communication.

3 Discussion

The epithelial structures of normal salivary gland tissue are divided into four parts: acinus, intercalated duct, striated duct, and excretory duct (29). However, it is difficult to distinguish between the intercalated duct cells and other duct cells at the cellular level. Intercalated duct cells have been reported to act as stem cells with the potential to differentiate into ductal cells, which has not been shown at the cellular level (30). This is the first study to identify the epithelial cells from the perspective of scRNA-seq in ACC, which is essential to further clarify its pathogenesis route.

3.1 Transcriptome characteristics of epithelial cells in ACC

The dynamic changes in the homologous subpopulations of the Inter-Duct 1 and 7 cells from paracarcinoma and carcinoma tissues may be related to the different biological functions of each cell subpopulation in tumor progression.

GSVA showed that each Inter-Duct cell clusters were enriched for different signaling pathway, including Notch signaling pathway, MYC, and immune response-related pathways (31, 32). The results indicated that different homologous cell clusters had different biological functions.

We used SCENIC to identify the TFs for each epithelial cell cluster. GO enrichment analysis of the dominant TFs showed that they controlled different expression programs.

MYB and EN1, as upstream TFs, regulated downstream genes related to domain neural activity together (33), histone deacetylation, and other tumor processes (34, 35) in Inter-Duct 3–4 cells. This is the first time we identified EN1 as a TF in ACC, may regulate the activity of different cell types in scRNA-seq at the transcription level.

The clustering of TFs, POLE3 (DNA Polymerase Epsilon 3), TFDP1, RB1, and E2F transcription factor families (E2F3, E2F3, and EF7) were associated with cell cycle transition (36), suggesting possible disruption of the normal epithelial cell division cycle (Figure 3B). Duct 1 and Duct 2 cells shared many biological processes, which were mostly related to transcription. Inter-Duct 1 cells were enriched for stress response-related pathways, such as response to peptide and laminar shear stress. Inter-Duct 2 cells were associated with stem cell proliferation and differentiation. Inter-Duct 5 and Inter-Duct 6 cells were associated with immune processes, such as T cell activation and interferon response. MECs were enriched for maintenance of somatic cell populations and steroid hormone-mediated signaling pathways (Figure 3E).

Our findings contribute to further understanding of the heterogeneity of biological functions by different TFs. Furthermore, these can explain the neural invasion from a scRNA-seq perspective in ACC.

3.2 Identified and verified premalignant cells in paracarcinoma tissues

Large-scale CNV analysis validated an intermediate state between precancer and cancer in the transcriptional profile of samples from exocrine glandular malignancies, such as breast cancer, prostate cancer, and their paracarcinoma tissues (37–39).

In our study, the complex CNVs were found in the epithelial cells from the paracarcinoma tissues. We speculated that there was an abundant population of specialized cells with abnormal transcription. They will transform into malignant cells in the paracarcinoma tissues in the future but cannot be accurately determined at the cellular or protein levels. This may be relevant to the frequently positive incisal edge in ACC. We tried to identify and define this unique cell population as pre-M cells.

Sample 0222 and 0329 showed a long arm amplification at chromosomes 6 (40) and 8 (41), respectively. As previously reported (42), MYB and MYBL1 were located at 6q23 and 8q13.1, respectively. This suggested that the expression of these two genes may affect copy number changes at the chromosomal level. In addition, translocation fusion of MYB family genes with NFIB is the gold standard for diagnosis of ACC, in which the expression rate is about 65%–85% (43). Previous study reported that EN1 was a potential biomarker for worse prognosis in ACC (44). This may explain the association of EN1 with poor prognosis from the single cell transcriptome level.

The distribution of the pre-M and malignant cells in each cell cluster was observed.

We attempted to calculate the stemness gene score of pre-M and malignant cells as it may be useful to determine the potential for transforming cells from pre-malignant to malignant states. Assuming that about 95% of the epithelial cells in carcinoma tissues are malignant, we observed a relatively equal proportion of pre-M and malignant cells in paracarcinoma tissues. This may suggest that pre-M cells may transform into malignant cells.

Comparing with the different cluster, more malignant cells were found in Inter-Duct 3, which activated tumor-associated signaling pathways by upstream TFs, MYB and EN1.

Subsequently, MYB family genes and EN1 were expressed in both pre-M and malignant Inter-Duct cells. MYB was previously shown to be highly expressed in only duct cells by immunohistochemistry and fluorescence *in situ* hybridization (45). Notably, the stemness gene score of pre-M was higher, suggesting its potential cancer transforming characteristics. These findings fully validate the pre-M cells in the paracarcinoma tissues. It can be a more accurate explanation for the false-negative incision edge and high recurrence rate from a single-cell transcriptome perspective in ACC.

3.3 Pseudo-time analysis of epithelial cell trajectory development from pre-M to malignant cells

The abnormal manifestation of complex CNVs verified the presence of specific pre-M cells in the paracarcinoma tissues and the expression of MYB verified its accuracy. We used scRNA-seq pseudo-time analysis to infer the differentiation trajectory of the epithelial cells and evolution of the cell subtypes to explain how the pre-M cells eventually become malignant throughout tumor progression.

The pseudo-time was divided into four stages. At the beginning of the time, a considerable number of cells were pre-M, which was mainly enriched in the Duct 1 cluster. As the timeline progressed, they gradually transformed into malignant cells and overlapped with Inter-Duct 3/4/6. Inter-Duct 3–4 cells were regulated by the TFs, MYB and EN1, and underwent activation of tumor-associated pathways. Myoepithelial cells were separated from the rest of the epithelial cell population and similarly transformed over time into a malignant cell population. This finding is fully consistent with the pathological features of ACC.

Graph-autocorrelation analysis revealed that MYB gene expression was progressively enhanced during the transition from stage 3 to 4, whereas MYBL1 showed high gene expression during the transition from stage1 to 2. UMAP (Uniform Manifold Approximation and Projection) analysis of the pseudo-time showed that MYB and MYBL1 showed exclusive expression at the end of the proposed time, which is consistent with the findings of previous studies (41, 46). GO enrichment analysis of these two gene modules showed that these two modules may drive two different evolutionary directions of ACC. This could explain the further development of ACC under the regulation of MYB homologous genes from a single-cell transcriptional perspective.

To sum up, the study is the first to report the use of scRNA-seq to examine ACC at the transcriptome level. We identified a special population of Inter-Duct cells. Inter-Duct 3–4 cells were coregulated by the upstream TFs, MYB, and EN1, which were enriched for tumor progression pathways. In addition, pre-M cells were found in paracarcinoma tissues, which was verified by the presence of MYB gene, and were highly expressed mainly in malignant Inter-Duct cells, including Inter-Duct 3–7. In addition, MYBL1 was highly expressed in malignant Inter-Duct and myoepithelial cells. Finally, pseudo-time analysis revealed that different cell clusters eventually transformed from a pre-M to malignant state in the ACC progression. Two modules containing MYB and MYBL1 drove different trajectories. Our findings further explain the high recurrence rate and unique biological characteristics of ACC.

4 Materials and methods

4.1 Ethical statement

The present study was approved by the Ethics Committee of Chinese People's Liberation Army (PLA) General Hospital and was performed according to the guidelines of the Declaration of Helsinki. Written informed consent was obtained from each patient prior to sample collection.

4.2 Human specimens

Preoperatively, the CT data of patients were imported into the Robotic-assisted navigation system. The surgeon could locate the tumor precisely by the robot. We removed the paracarcinoma and carcinoma tissues by enlargement. Samples were obtained from the paracarcinoma and carcinoma tissues of three ACC patients who underwent surgery at the Chinese PLA General Hospital Stomatology department. The primary foci were on the minor salivary gland. The sample 7420 and 0329 were both cribriform types, in addition sample 0222 was cribriform type in 2019 and recurrence to be solid type in 2021 in pathology.

The tissues from sample 0222 for scRNA-seq was incised for recurrence in 2021. And then we compared pathological sections of 0222 samples between 2019 and 2021 for further study. Each sample was carefully reviewed by two experienced pathologists to confirm the pathology. Single-cell data information of the six samples in shown in Supplementary Table 1. The clinical data are summarized in Supplementary Table 2.

4.3 Cell preparation for scRNA-seq

4.3.1 Tissue collection

The patients who underwent the surgery received the informed consent for the specimen. Preoperative head skin preparation was performed on the three patients and robotic

positioning patches were applied on surgery morning. The CT data were scanned and imported into the robotic navigation system. After the patients were successfully intubated through the nasal cavity, the Mayfield 3-peg head frame was placed, and after checking the stability of each mechanical joint fixation. The robot was matched with the patient's head positioning marker points and the navigation system was activated after successful fusion. Under the precise guidance and positioning of the navigation robot, the patient's paracarcinoma and carcinoma tissues were removed. A part of the tissue obtained during surgery was placed in 10% neutral formalin solution at room temperature and sent to pathology for definitive patient diagnosis. The other tissues were submerged in 4°C tissue preservation solution and put into ice box for immediate transport to the laboratory for single cell transcriptome study.

4.3.2 Tissue dissociation

Tissue samples were cut into small pieces of around 1 mm^3 in size and placed in petri dish and covered with PBS (Gibco). Each sample was then transferred to centrifuge tube with adding 2mL digestive system (Adult Brain Dissociation Kit, mouse and rat NO.130-107-677), 750μL Enzyme mix 1 (Enzyme P 50μL and Buffer Z 1900μL) and 30μL Enzyme mix 2 (Buffer Z 20 μL and Enzyme A 10μL). After running the gentle MACS Program m _brain_01 program on the tissue. the tissues were incubated in water bath at 37°C for 15 min, and then filtered the cell suspension, centrifuged at 300×g for 10 min at 4°C to completely remove the supernatant.

The samples were left to stand for 2–3 min and collected the supernatant. The supernatant was removed, and the cells were resuspended in red blood cell lysis buffer, according to the ratio of cell suspension to red blood cell lysate at 1:3, and incubated for 2–3 min at room temperature prior to centrifugation at 120× *g* at 4 °C for 3 min. Finally, the cells were resuspended in PBS.

4.4 10X Genomics scRNA-Seq

4.4.1 Cell capture and cDNA synthesis

Cell capture and cDNA synthesis were performed using a Chromium Single-Cell 3' Gene Expression library and Gel Bead Kit V3.1 (10x Genomics, 1000075). Cell profiling was performed using a Single-Cell B Chip Kit (10x Genomics, 1000074). Cell suspension containing 300–600 living cells/μL (determined using Count Star) was loaded onto the Chromium single-cell controller (10x Genomics) to generate single-cell gel beads in the emulsion according to the manufacturer's protocol. In brief, single cells were suspended in PBS containing 0.04% bovine serum albumin.

Around 8,700 cells were added to each channel with a targeted cell recovery estimate of 8,000 cells. Captured cells were lysed and the released RNA was barcoded through reverse transcription in individual GEMs (Gel bead-In-EMulsions). GEMs were reverse transcribed in a C1000 Touch Thermal Cycler (Bio Rad) programmed at 53°C for 45 min, 85°C for 5 min, and held at 4°C. After reverse transcription, single-cell droplets were broken, and single-stranded cDNA was isolated and cleaned with Cleanup Mix containing DynaBeads (Thermo Fisher Scientific). cDNA was generated and amplified, and the quality was assessed using the Agilent 4200.

4.4.2 Preparation of the scRNA-Seq library

Single-cell RNA-seq libraries we reconstructed using Single-Cell 3' Library and Gel Bead Kit V3.1 according to the manufacturers' instructions. The libraries were finally sequenced using an IlluminaNovaseq6000 sequencer with a sequencing depth of at least 100,000 reads per cell with a pair-end 150 bp (PE150) reading strategy.

4.4.3 Processing of scRNA-Seq data

Raw data produced from the 10× Genomic platform were processed by Cell Ranger (v6.1.2) (47) and mapped to the human reference genome GRCH38. Pre-processed data were imported into R (v4.1.2) and analyzed using Seurat (v4.0.3) (48). The quality control thresholds for the number of genes detected and the proportion of mitochondrial and hemoglobin transcripts were the mean plus 2.58-fold standard deviation across all cells. As a supplement, in a single cell, the number of genes detected needed to be >200, and the ratio of mitochondrial genes and hemoglobin genes had to be <30 and 10, respectively. Cells that did not meet these criteria were discarded. A linear equation according to the corresponding table of the number of loading cells and the multiplet rate provided by 10× company was fitted. Then the doublets were identified with appropriate multiplet rates from the linear equation above by DoubletFinder (v2.0.3) (49) and will be removed subsequently. Each sample was subjected to quality control separately to ensure that high-quality cells were remained. The top 2,000 variable features were chosen for PCA, and the 50 most significant PCs were selected for subsequent cluster analysis. All cell types were manually identified and further examined by R package singleR (v1.6.1) (50). Epithelial cells were extracted and then batch effect across different samples was removed using the Harmony algorithm in R package harmony (v0.1.0) (51) before identifying neighbors and finding clusters.

4.5 Marker genes for cell populations

Differentially expressed genes were identified using the FindAllMarkers function of the Seurat package for each subcluster. Specific genes were selected to serve as a basis for artificially defining cell populations as follows (52–58): fibroblasts (COL3A1, DCN, COL1A1, LUM, COLA2, COL6A2, FBN1), epithelial cells (EPCAM, KRT19, CLDN3

and KRT8), endothelial cells (PECAM1, ENG, VWF), basal cells (KRT5, KRT14, TP63), T/NK cells (GZMA, HCST), smooth muscle cells (ACTA2, MYH11, ACTG2, CNN1, CALD1, MCAM, TAGLN, PDGFRB, MYL9), myeloid cells (AIF1, CD163, LYZ), muscle satellite cells (PAX7, CD82, NCAM1, MYF5), mast cells (MS4A2, TPSB2, GATA2), skeletal muscle cells (ACTA1, NEB, MYL2), lymphatic endothelial cells (PDPN, PROX1, LYVE1), Schwann cells (NGFR, SOX10, GAP43, CDH19), plasma cells (JCHAIN, IGKC, IGHA1, IGHA2), T cells (CD3G, CD3D, CD3E), and B cells (MS4A1, BANK1, CD37).

4.6 Identification of malignant cells

Large-scale chromosomal copy number alterations within cells were detected using the R package inferCNV (v1.8.1). Immune and stromal cells from paracarcinoma tissues were used as presumptive "normal" cells as a reference, and their CNV scores were set as baseline. A previously described method was used to distinguish malignant cells from all epithelial cells (59). In brief, 1,600 fibroblasts and endothelial cells were stochastically picked from paracarcinoma samples, among which 1,000 were regarded as a reference and the remaining cells and epithelial cells were considered as an observation. CNV analysis was performed using inferCNV. When most of the spiked "normal" stromal cells were gathered in a specific cluster on a dendrogram, the other cells in this cluster were considered as "normal epithelial cells". Correspondingly, cells not belonging to this cluster were identified as "malignant epithelial cells." Since only 29 epithelial cells were identified as normal epithelial cells, accounting for only 0.003% of all epithelial cells, we concluded that all epithelial cells show malignant characteristics. Epithelial cells with malignant features were further subclassified. The median CNV estimates of all fibroblasts in the paracancerous samples were defined as the baseline, and the Euclidean distance between the CNV estimates of all observation cells and the above baseline was calculated. We determined the range of Euclidean distances (median ± 2 SD) by assuming that most epithelial cells (95%) in the carcinoma samples were "malignant" in the true sense, whereas cells whose distance from the baseline was not within this range were considered pre-M cells. The signature genes used to distinguish subtypes of epithelial cells or to calculate the score of stemness of different class of epithelial cells are as follows (60–62): intercalated duct cells (KIT or AQP5), myoepithelial cell genes (ACTA2, MYH11, CNN1), and stemness genes (ALDH1A1, CD44, PROM1, NANOG, KIT, NES, KLF4, CD55, ALCAM, NOTCH4, WNT7A, PDPN). Each cell was scored for stemness activity using the function AddModuleScore in Seurat with default settings. A re-clustered heatmap of CNV scores of all epithelial cells was plotted using pheatmap (v1.0.12).

4.7 Pseudo-time analysis

The expression matrix and meta information of epithelial cells migrated from Seurat object were subsequently imported into R and analyzed using monocle3 (v1.0.0) (63) using the default parameters and a standard pipeline. After graph-autocorrelation analysis, the top 3,000 genes that varied with the trajectory were selected and collected into the gene module divided by pseudo-time. The graph of the change of key gene expression over the pseudo-time was drawn using the plot_genes_in_pseudo-time function.

4.8 Transcriptional regulator analysis

The specific transcriptional drivers in each epithelial cell subtype were analyzed by using the R package, SCENIC (v1.2.4) (64), under the guidance of a tutorial from https://github.com/aertslab/SCENIC. The binary score matrix of intracellular regulator activities was processed using *limma* (v3.48.3) (65) to find TFs that were differentially expressed in different cell subpopulations (logFC > 0 & p.adjust < 0.05), and the results were displayed using pheatmap (v1.0.12). The interaction network construction of high confidence dominating transcription factor and their target genes in epithelial cells and final visualization were implemented using Cytoscape (v3.9.1) (66).

In order to predict the possible functions of genes co-regulated by MYB and EN1, we used an online tool called Genemania (http://genemania.org/), which can find other genes that are related to a set of input genes by using a large set of genome and proteome association data. The result of GO enrichment analysis of above genes can be download from the website directly.

4.9 Cell–cell communication analysis

Intercellular communication within the tumor microenvironment was predicted using the python package, CellPhoneDB (v3.0.0) (67), based on the expression of interacting ligand and receptor genes. The number of iterations for the statistical analysis was set as 1,000. Significant ($p < 0.05$) mean results were further processed as follows. Cell pairs containing Duct/InterDuct/MEC were selected and divided into "source" and "target" groups according to the sequence of which in cell pairs. The expression scores of receptor–ligand pairs were considered as "counts" and constructed as a Seurat object and the differentially expressed receptor–ligand pairs in each group were revealed using the FindAllMarkers function with default parameters. Receptor–ligand pairs were selected for plot as those with p.adjust value <0.05, average log2FC >1. Heatmaps and dot plots were plotted using CellPhoneDB.

4.10 Expression program heterogeneity analysis

All epithelial cells were extracted from six samples and divided into three subgroups and the expression matrix was then normalized and decomposed using python package cNMF (v1.3) (68). The high-quality expression programs in each sample were manually selected, the Pearson's correlation coefficients between them were calculated, and those with coefficients >0.18 and clustered together were considered as characteristic programs. In addition, correlation coefficients >0.6 were corrected to 0.6. The parameters, methods, and code used for data processing were adapted from a GitHub tutorial (https://github.com/dylkot/cNMF).

4.11 GSVA

GSVA was executed on hallmark gene sets, which were obtained from MSigDB (The Molecular Signatures Database) (69) and contained 50 well-defined pathways, using the R package, GSVA (v1.40.1) (70), with default settings. Differences between the pathway enrichment scores of the different groups was calculated by R package Limma (v3.48.3).

4.12 GO and KEGG enrichment analysis

GO and KEGG term enrichment analysis were performed using R packages clusterProfiler (v4.0.5) and org.Hs.eg.db (v3.13.0) with default settings (71).

4.13 Statistical analyses

The software, methods, and thresholds used for the statistical analyses are detailed in the Materials and Methods section. Wilcoxon test was used to reveal the statistical differences in Figures 1E, 2C and 4B. Two-tailed *t* test was used to reveal the statistical difference in Supplementary Figures 5E, F. A p.adjust-value or q-value <0.05 was considered significant.

Data availability statement

The data presented in the study are deposited in the CNCB-NGDC (National Genomics Data Center, China National Center for Bioinformation, https://ngdc.cncb.ac.cn/gsa-human/s/j2QOEb3S), accession number is PRJCA012307.

Ethics statement

The studies involving human participants were reviewed and approved by Ethics Committee Of Chinese PLA General Hospital. The patients/participants provided their written informed consent to participate in this study.

Author contributions

Conceptualization: QX, HQ, XF. Surgery: QL, QX, FC, YR, LF, YS, FW, WY, HZ. Robotic assistant: HZ. Methodology: QX, HQ, XF, QL, ZJF. Pathology: ZS, WC. Data analysis: ZJF, HQ, CW, YS, YL, XF. Supervision: QX, HQ and XF. Writing—original draft: QL, ZJF. Writing—review & editing: QL, ZJF, JS, FC, YR. All authors contributed to the article and approved the submitted version.

Funding

National Key Research and Development Program 2017YFB1304300 (HZ) National Key Research and Development Program 2020YFC2003405. National Natural Science Foundation of China Grant 81800939 (JS). Youth Incubation Program of Medical Science and Technology of PLA Grant 21QNPY114 (JS). The funders had no role in study design, data collection and analysis, decision to publish, or preparation of the manuscript.

Acknowledgments

We thank all the patients for their generous donation of tissue samples for analysis in this study.

Conflict of interest

The authors declare that the research was conducted in the absence of any commercial or financial relationships that could be construed as a potential conflict of interest.

Publisher's note

Supplementary material

The Supplementary Material for this article can be found online at: https://www.frontiersin.org/articles/10.3389/fonc.2022.1063477/full#supplementary-material

References

1. Hay AJ, Migliacci J, Karassawa Zanoni D, McGill M, Patel S, Ganly I. Minor salivary gland tumors of the head and neck-memorial Sloan Kettering experience: Incidence and outcomes by site and histological type. *Cancer* (2019) 125(19):3354–66. doi: 10.1002/cncr.32208

2. Pelak MJ, Walser M, Bachtiary B, Hrbacek J, Lomax AJ, Kliebsch UL, et al. Clinical outcomes of head and neck adenoid cystic carcinoma patients treated with pencil beam-scanning proton therapy. *Oral Oncol* (2020) 107:104752. doi: 10.1016/j.oraloncology.2020.104752

3. Dillon PM, Chakraborty S, Moskaluk CA, Joshi PJ, Thomas CY. Adenoid cystic carcinoma: A review of recent advances, molecular targets, and clinical trials. *Head Neck* (2016) 38(4):620–7. doi: 10.1002/hed.23925

4. Bjørndal K, Krogdahl A, Therkildsen MH, Overgaard J, Johansen J, Kristensen CA, et al. Salivary gland carcinoma in Denmark 1990-2005: a national study of incidence, site and histology. results of the Danish head and neck cancer group (DAHANCA). *Oral Oncol* (2011) 47(7):677–82. doi: 10.1016/j.oraloncology.2011.04.020

5. Yarbrough WG, Panaccione A, Chang MT, Ivanov SV. Clinical and molecular insights into adenoid cystic carcinoma: Neural crest-like stemness as a target. *Laryngoscope Investig Otolaryngol* (2016) 1(4):60–77. doi: 10.1002/lio2.22

6. Pattabiraman DR, Gonda TJ. Role and potential for therapeutic targeting of MYB in leukemia. *Leukemia* (2013) 27(2):269–77. doi: 10.1038/leu.2012.225

7. Xie J, Lin LS, Huang XY, Gan RH, Ding LC, Su BH, et al. The NOTCH1-HEY1 pathway regulates self-renewal and epithelial-mesenchymal transition of salivary adenoid cystic carcinoma cells. *Int J Biol Sci* (2020) 16(4):598–610. doi: 10.7150/ijbs.36407

8. Gaillard H, García-Muse T, Aguilera A. Replication stress and cancer. *Nat Rev Cancer* (2015) 15(5):276–89. doi: 10.1038/nrc3916

9. Ho AS, Kannan K, Roy DM, Morris LGT, Ganly I, Katabi N, et al. The mutational landscape of adenoid cystic carcinoma. *Nat Genet* (2013) 45(7):791–8. doi: 10.1038/ng.2643

10. Grün D, van Oudenaarden A. Design and analysis of single-cell sequencing experiments. *Cell* (2015) 163(4):799–810. doi: 10.1016/j.cell.2015.10.039

11. Savas P, Virassamy B, Ye C, Salim A, Mintoff CP, Caramia F, et al. Single-cell profiling of breast cancer T cells reveals a tissue-resident memory subset associated with improved prognosis [published correction appears in nat med. 2018 Dec;24(12):1941]. *Nat Med* (2018) 24(7):986–93. doi: 10.1038/s41591-018-0078-7

12. Izar B, Tirosh I, Stover EH, Wakiro I, Cuoco MS, Alter I, et al. A single-cell landscape of high-grade serous ovarian cancer. *Nat Med* (2020) 26(8):1271–9. doi: 10.1038/s41591-020-0926-0

13. Guo X, Zhang Y, Zheng L, Zheng C, Song J, Zhang Q, et al. Global characterization of T cells in non-small-cell lung cancer by single-cell sequencing. *Nat Med* (2018) 24(7):978–85. doi: 10.1038/s41591-018-0045-3

14. Han J, DePinho RA, Maitra A. Single-cell RNA sequencing in pancreatic cancer. *Nat Rev Gastroenterol Hepatol* (2021) 18(7):451–2. doi: 10.1038/s41575-021-00471-z

15. D'Alessandro V, Muscarella LA, Copetti M, Zelante L, Carella M, Vendemiale G. Molecular detection of neuron-specific ELAV-like-positive cells in the peripheral blood of patients with small-cell lung cancer. *Cell Oncol* (2008) 30 (4):291–7. doi: 10.3233/clo-2008-0424

16. Ong SH, Guy GR, Hadari YR, Laks S, Gotoh N, Schlessinger J, et al. FRS2 proteins recruit intracellular signaling pathways by binding to diverse targets on fibroblast growth factor and nerve growth factor receptors. *Mol Cell Biol* (2000) 20 (3):979–89. doi: 10.1128/MCB.20.3.979-989.2000

17. Chen Z, Shen G, Tan X, Qu L, Zhang C, Ma L, et al. ID1/ID3 mediate the contribution of skin fibroblasts to local nerve regeneration through Itga6 in wound repair. *Stem Cells Transl Med* (2021) 10(12):1637–49. doi: 10.1002/sctm.21-0093

18. Chang IA, Kim KJ, Namgung U. α6 and β1 integrin heterodimer mediates schwann cell interactions with axons and facilitates axonal regeneration after peripheral nerve injury. *Neuroscience* (2018) 371:49–59. doi: 10.1016/j.neuroscience

19. Chen ZL, Strickland S. Laminin gamma1 is critical for schwann cell differentiation, axon myelination, and regeneration in the peripheral nerve. *J Cell Biol* (2003) 163(4):889–99. doi: 10.1083/jcb.200307068

20. McNeill EM, Roos KP, Moechars D, Clagett-Dame M. Nav2 is necessary for cranial nerve development and blood pressure regulation. *Neural Dev* (2010) 5:6. doi: 10.1186/1749-8104-5-6

21. Upadhyay A, Hosseinibarkooie S, Schneider S, Kaczmarek A, Torres-Benito L, Mendoza-Ferreira N, et al. Neurocalcin delta knockout impairs adult neurogenesis whereas half reduction is not pathological. *Front Mol Neurosci* (2019) 12:19. doi: 10.3389/fnmol.2019.00019

22. Warde-Farley D, Donaldson SL, Comes O, Zuberi K, Badrawi R, Chao P, et al. The GeneMANIA prediction server: biological network integration for gene prioritization and predicting gene function. *Nucleic Acids Res* (2010) 38:W214–20. doi: 10.1093/nar/gkq537

23. Grieb G, Merk M, Bernhagen J, Bucala R. Macrophage migration inhibitory factor (MIF): a promising biomarker. *Drug News Perspect* (2010) 23(4):257–64. doi: 10.1358/dnp.2010.23.4.1453629

24. Steinberg MW, Cheung TC, Ware CF. The signaling networks of the herpesvirus entry mediator (TNFRSF14) in immune regulation. *Immunol Rev* (2011) 244(1):169–87. doi: 10.1111/j.1600-065X.2011.01064.x

25. Cheng RJ, Deng WG, Niu CB, Li YY, Fu Y. Expression of macrophage migration inhibitory factor and CD74 in cervical squamous cell carcinoma. *Int J Gynecologic Cancer* (2011) 21(6):1004–1012. doi: 10.1097/IGC.0b013e31821c45b7

26. Wirtz TH, Saal A, Bergmann I, Fischer P, Heinrichs D, Brandt EF, et al. Macrophage migration inhibitory factor exerts pro-proliferative and anti-apoptotic effects *via* CD74 in murine hepatocellular carcinoma. *Br J Pharmacol* (2021) 178 (22):4452–67. doi: 10.1111/bph.15622

27. Meyer-Siegler KL, Iczkowski KA, Leng L, Bucala R, Vera PL. Inhibition of macrophage migration inhibitory factor or its receptor (CD74) attenuates growth and invasion of DU-145 prostate cancer cells. *J Immunol* (2006) 177(12):8730–9. doi: 10.4049/jimmunol.177.12.8730

28. Kang Y, Zhang Y, Sun Y. Macrophage migration inhibitory factor is a novel prognostic marker for human oral squamous cell carcinoma. *Pathol Res Pract* (2018) 214(8):1192–8. doi: 10.1016/j.prp.2018.06.020

29. Bishop JA, Rooper LM, Sangoi AR, Gagan J, Thompson LDR, Inagaki H. The myoepithelial cells of salivary intercalated duct-type intraductal carcinoma are neoplastic: A study using combined whole-slide imaging, immunofluorescence, and RET fluorescence *In situ* hybridization. *Am J Surg Pathol* (2021) 45(4):507–15. doi: 10.1097/PAS.0000000000001605

30. Katsumata O, Sato Y, Sakai Y, Yamashina S. Intercalated duct cells in the rat parotid gland may behave as tissue stem cells. *Anat Sci Int* (2009) 84(3):148–54. doi: 10.1007/s12565-009-0019-0

31. Stoeck A, Lejnine S, Truong A, Pan L, Wang H, Zang C, et al. Discovery of biomarkers predictive of GSI response in triple-negative breast cancer and adenoid cystic carcinoma. *Cancer Discovery* (2014) 4(10):1154–67. doi: 10.1158/2159-8290.CD-13-0830

32. Miller AJ, Chang A, Cunningham PN. Chronic microangiopathy due to DCR-MYC, a myc-targeted short interfering RNA. *Am J Kidney Dis* (2020) 75 (4):513–6. doi: 10.1053/j.ajkd.2019.09.011

33. Phuchareon J, Overdevest JB, McCormick F, Eisele DW, van Zante A, Tetsu O. Fatty acid binding protein 7 is a molecular marker in adenoid cystic carcinoma of the salivary glands: implications for clinical significance. *Transl Oncol* (2014) 7 (6):780–7. doi: 10.1016/j.tranon.2014.10.003

34. Altieri SC, Zhao T, Jalabi W, Romito-DiGiacomo RR, Maricich SM. En1 is necessary for survival of neurons in the ventral nuclei of the lateral lemniscus. *Dev Neurobiol* (2016) 76(11):1266–74. doi: 10.1002/dneu.22388

35. Zhang Y, Zhang Y, Aman Y, Ng CT, Chau WH, Zhang Z, et al. Amyloid-β toxicity modulates tau phosphorylation through the PAX6 signalling pathway. *Brain* (2021) 144(9):2759–70. doi: 10.1093/brain/awab134

36. Kent LN, Leone G. The broken cycle: E2F dysfunction in cancer. *Nat Rev Cancer* (2019) 19(6):326–38. doi: 10.1038/s41568-019-0143-7

37. Shirahata M, Ono T, Stichel D, Schrimpf D, Reuss DE, Sahm F, et al. Novel, improved grading system(s) for IDH-mutant astrocytic gliomas. *Acta Neuropathol* (2018) 136(1):153–66. doi: 10.1007/s00401-018-1849-4

38. Aran D, Camarda R, Odegaard J, Paik H, Oskotsky B, Krings G, et al. Comprehensive analysis of normal adjacent to tumor transcriptomes. *Nat Commun* (2017) 8(1):1077. doi: 10.1038/s41467-017-01027-z

39. Graham K, de las Morenas A, Tripathi A, King C, Kavanah M, Mendez J, et al. Gene expression in histologically normal epithelium from breast cancer patients and from cancer-free prophylactic mastectomy patients shares a similar profile. *Br J Cancer* (2010) 102(8):1284–93. doi: 10.1038/sj.bjc.6605576

40. de Almeida-Pinto YD, Costa SFDS, de Andrade BAB, Altemani A, Vargas PA, Abreu LG, et al. t(6;9)(MYB-NFIB) in head and neck adenoid cystic carcinoma: A systematic review with meta-analysis. *Oral Dis* (2019) 25(5):1277–82. doi: 10.1111/odi.12984

41. Togashi Y, Dobashi A, Sakata S, Sato Y, Baba S, Seto A, et al. MYB and MYBL1 in adenoid cystic carcinoma: diversity in the mode of genomic

rearrangement and transcripts. *Mod Pathol* (2018) 31(6):934–46. doi: 10.1038/s41379-018-0008-8

42. Wagner VP, Bingle CD, Bingle L. MYB-NFIB fusion transcript in adenoid cystic carcinoma: Current state of knowledge and future directions. *Crit Rev Oncol Hematol* (2022) 176:103745. doi: 10.1016/j.critrevonc.2022.103745

43. Brayer KJ, Frerich CA, Kang H, Ness SA. Recurrent fusions in MYB and MYBL1 define a common, transcription factor-driven oncogenic pathway in salivary gland adenoid cystic carcinoma. *Cancer Discovery* (2016) 6(2):176–87. doi: 10.1158/2159-8290

44. Bell D, Bell A, Roberts D, Weber RS, El-Naggar AK. Developmental transcription factor EN1–a novel biomarker in human salivary gland adenoid cystic carcinoma. *Cancer* (2012) 118(5):1288–92. doi: 10.1002/cncr.26412

45. Li B, Jie W, He H. Myb immunohistochemical staining and fluorescence *in situ* hybridization in salivary rare basaloid lesions. *Front Oncol* (2020) 10:870. doi: 10.3389/fonc.2020.00870

46. Mitani Y, Liu B, Rao PH, Borra VJ, Zafereo M, Weber RS, et al. Novel MYBL1 gene rearrangements with recurrent MYBL1-NFIB fusions in salivary adenoid cystic carcinomas lacking t(6;9) translocations. *Clin Cancer Res* (2016) 22 (3):725–33. doi: 10.1158/1078-0432.CCR-15-2867-T

47. Zheng GX, Terry JM, Belgrader P, Ryvkin P, Bent ZW, Wilson R, et al. Massively parallel digital transcriptional profiling of single cells. *Nat Commun* (2017) 8:14049. doi: 10.1038/ncomms14049

48. Hao Y, Hao S, Andersen-Nissen E, Mauck WM3rd, Zheng S, Butler A, et al. Integrated analysis of multimodal single-cell data. *Cell* (2021) 184(13):3573–87. doi: 10.1016/j.cell.2021.04.048

49. McGinnis CS, Murrow LM, Gartner ZJ. DoubletFinder: Doublet detection in single-cell RNA sequencing data using artificial nearest neighbors. *Cell Syst* (2019) 8(4):329–37. doi: 10.1016/j.cels.2019.03.003

50. Aran D, Looney AP, Liu L, Wu E, Fong V, Hsu A, et al. Reference-based analysis of lung single-cell sequencing reveals a transitional profibrotic macrophage. *Nat Immunol* (2019) 20(2):163–72. doi: 10.1038/s41590-018-0276-y

51. Korsunsky I, Millard N, Fan J, Slowikowski K, Zhang F, Wei K, et al. Fast, sensitive and accurate integration of single-cell data with harmony. *Nat Methods* (2019) 16(12):1289–96. doi: 10.1038/s41592-019-0619-0

52. Baron M, Veres A, Wolock SL, Faust AL, Gaujoux R, Vetere A, et al. A single-cell transcriptomic map of the human and mouse pancreas reveals inter- and intra-cell population structure. *Cell Syst* (2016) 3(4):346–60. doi: 10.1016/j.cels.2016.08.011

53. Cortal A, Martignetti L, Six E, Rausell A. Gene signature extraction and cell identity recognition at the single-cell level with cell-ID. *Nat Biotechnol* (2021) 39 (9):1095–102. doi: 10.1038/s41587-021-00896-6

54. Relaix F, Bencze M, Borok MJ, Der Vartanian A, Gattazzo F, Mademtzoglou D, et al. Perspectives on skeletal muscle stem cells. *Nat Commun* (2021) 12(1):692. doi: 10.1038/s41467-020-20760-6

55. Lokmic Z. Isolation, identification, and culture of human lymphatic endothelial cells. *Methods Mol Biol* (2016) 1430:77–90. doi: 10.1007/978-1-4939-3628-1_5

56. Morrisey EE. Basal cells in lung development and repair. *Dev Cell* (2018) 44 (6):653–4. doi: 10.1016/j.devcel.2018.03.004

57. Xing X, Yang F, Huang Q, Guo H, Li J, Qiu M, et al. Decoding the multicellular ecosystem of lung adenocarcinoma manifested as pulmonary subsolid nodules by single-cell RNA sequencing. *Sci Adv* (2021) 7(5):eabd9738. doi: 10.1126/sciadv.abd9738

58. Zhang X, Lan Y, Xu J, Quan F, Zhao E, Deng C, et al. CellMarker: a manually curated resource of cell markers in human and mouse. *Nucleic Acids Res* (2019) 47 (D1):D721–8. doi: 10.1093/nar/gky900

59. Maynard A, McCoach CE, Rotow JK, Harris L, Haderk F, Kerr DL, et al. Therapy-induced evolution of human lung cancer revealed by single-cell RNA sequencing. *Cell* (2020) 182(5):1232–51. doi: 10.1016/j.cell.2020.07.017

60. Hauser BR, Aure MH, Kelly MCGenomics and Computational Biology Core, , Hoffman MP, Chibly AM. Generation of a single-cell RNAseq atlas of murine salivary gland development. *iScience* (2020) 23(12):101838. doi: 10.1016/j.isci.2020.101838

61. Costa-da-Silva AC, Aure MH, Dodge J, Martin D, Dhamala S, Cho M, et al. Salivary ZG16B expression loss follows exocrine gland dysfunction related to oral chronic graft-versus-host disease. *iScience* (2021) 25(1):103592. doi: 10.1016/j.isci.2021.103592

62. Ge G, Han Y, Zhang J, Li X, Liu X, Gong Y, et al. Single-cell RNA-seq reveals a developmental hierarchy super-imposed over subclonal evolution in the cellular ecosystem of prostate cancer. *Adv Sci* (2022) 9(15):e2105530. doi: 10.1002/advs.202105530

63. Cao J, Spielmann M, Qiu X, Huang X, Ibrahim DM, Hill AJ, et al. The single-cell transcriptional landscape of mammalian organogenesis. *Nature* (2019) 566(7745):496–502. doi: 10.1038/s41586-019-0969-x

64. Aibar S, González-Blas CB, Moerman T, Huynh-Thu VA, Imrichova H, Hulselmans G, et al. SCENIC: single-cell regulatory network inference and clustering. *Nat Methods* (2017) 14(11):1083–6. doi: 10.1038/nmeth.4463

65. Ritchie ME, Phipson B, Wu D, Hu Y, Law CW, Shi W, et al. Limma powers differential expression analyses for RNA-sequencing and microarray studies. *Nucleic Acids Res* (2015) 43(7):e47. doi: 10.1093/nar/gkv007

66. Shannon P, Markiel A, Ozier O, Baliga NS, Wang JT, Ramage D, et al. Cytoscape: a software environment for integrated models of biomolecular interaction networks. *Genome Res* (2003) 13(11):2498–504. doi: 10.1101/gr.1239303

67. Efremova M, Vento-Tormo M, Teichmann SA, Vento-Tormo R. CellPhoneDB: inferring cell-cell communication from combined expression of multi-subunit ligand-receptor complexes. *Nat Protoc* (2020) 15(4):1484–506. doi: 10.1038/s41596-020-0292-x

68. Kotliar D, Veres A, Nagy MA, Tabrizi S, Hodis E, Melton DA, et al. Identifying gene expression programs of cell-type identity and cellular activity with single-cell RNA-seq. *Elife* (2019) 8:e43803. doi: 10.7554/eLife.43803

69. Subramanian A, Tamayo P, Mootha VK, Mukherjee S, Ebert BL, Gillette MA, et al. Gene set enrichment analysis: a knowledge-based approach for interpreting genome-wide expression profiles. *Proc Natl Acad Sci USA* (2005) 102(43):15545–50. doi: 10.1073/pnas.0506580102

70. Hänzelmann S, Castelo R, Guinney J. GSVA: gene set variation analysis for microarray and RNA-seq data. *BMC Bioinf* (2013) 14:7. doi: 10.1186/1471-2105-14-7

71. Wu T, Hu E, Xu S, Chen M, Guo P, Dai Z, et al. clusterProfiler 4.0: A universal enrichment tool for interpreting omics data. *Innovation* (2021) 2 (3):100141. doi: 10.1016/j.xinn.2021.100141

frontiers | Frontiers in Oncology

TYPE Original Research
PUBLISHED 16 December 2022
DOI 10.3389/fonc.2022.1021169

OPEN ACCESS

EDITED BY
Ester Orlandi,
National Center of Oncological Hadrontherapy, Italy

REVIEWED BY
Huan Li,
Sun Yat-sen University Cancer Center (SYSUCC), China
Tobias Ettl,
University Medical Center Regensburg, Germany

*CORRESPONDENCE
Ruohui Song
song_0515@126.com
Xiaohong Chen
trchxh@163.com

†These authors have contributed equally to this work

SPECIALTY SECTION
This article was submitted to Head and Neck Cancer, a section of the journal Frontiers in Oncology

RECEIVED 17 August 2022
ACCEPTED 30 November 2022
PUBLISHED 16 December 2022

CITATION
Zhou M, Ma T, Wang X, Zhang S, Yang G, Song R and Chen X (2022) High-risk subtype: Clinical manifestations and molecular characteristics of submandibular gland adenoid cystic carcinoma. *Front. Oncol.* 12:1021169. doi: 10.3389/fonc.2022.1021169

High-risk subtype: Clinical manifestations and molecular characteristics of submandibular gland adenoid cystic carcinoma

Mengjiao Zhou[1†], Tingyao Ma[1†], Xuelian Wang[1], Shujing Zhang[1], Guoliang Yang[1], Ruohui Song[2*] and Xiaohong Chen[1*]

[1]Department of Otolaryngology, Head and Neck Surgery, Beijing Tongren Hospital, Capital Medical University, Key Laboratory of Otolaryngology Head and Neck Surgery, Ministry of Education, Capital Medical University, Beijing, China, [2]Department of Otolaryngology, the First Affiliated Hospital of Anhui University of Chinese Medicine, Hefei, Anhui, China

Objective: Adenoid cystic carcinoma of the head and neck mainly occurs in the major salivary glands, of which the parotid gland and submandibular gland are the most common. The purpose of this study was to clarify the site-specific differences in prognosis and molecular expression characteristics of the patients and to achieve stratified risk management of the clinical prognosis.

Materials: By performing a single-centre retrospective analysis combined with analyses of the Surveillance, Epidemiology, and End Results (SEER) database, cBioPortal and GEO databases, the clinical prognostic characteristics and the differences in molecular expression patterns of ACC in the submandibular gland and parotid gland were analysed. Cox regression analysis, the chi-square test, Fisher's test and the log-rank test were used to compare the significance of differences.

Results: Compared with patients with parotid gland ACC, the submandibular gland ACC is more likely to have metastases in the cervical lymph node (21.7% vs. 3.3%) and shows a higher rate of distant metastasis within 1 year after the primary site diagnosis (47.8% vs. 23.3%), a worse overall prognosis, more frequent mutations of *MYB/MYBL1* (50% vs. 25%) and abnormal upregulation of the phosphatidylinositol-3 kinase (PI3K) pathway.

Conclusions: Submandibular gland ACC is associated with site-specific early cervical lymph node metastasis and hidden distant metastasis, along with rapid progression and a poor prognosis. A high *MYB/MYBL1* mutation rate and abnormal upregulation of the PI3K pathway with MYB involvement were identified.

KEYWORDS

adenoid cystic carcinoma, lung metastasis, MYB, parotid gland, submandibular gland

1 Introduction

Adenoid cystic carcinoma (ACC), a rare malignant tumor originating from secretory glands, occurs most commonly in the head and neck. The main clinical features of ACC are relentless and slow growth, perineural invasion, and a high distant metastasis rate. ACC is composed of the epithelial and myoepithelial cells, which are arranged into three pathological subtypes: cribriform, tubular and solid (most of which are mixed). Therefore, the pathological manifestation of ACC is biphasic differentiation. Surgery combined with radiotherapy is the conventional treatment for the primary tumor. Distant metastasis developed in 52% of patients, mainly within the first 5 years following diagnosis, and the median time to metastasis was only 31.5 months (1). The most common site of distant metastasis is the lung, accounting for 67-85.9% of cases, followed by the bone and liver (2, 3). The 5-year overall survival rate(OS) is 68%, and once metastasis occurs, the median survival time is only 20-32 months (4). The special pathological subtypes (solid or high-grade transformation), T/N stages, and treatment of the primary sites are common clinical risk factors for ACC lung metastasis (5–8). The high incidence rate and uncontrollable continuous progression of distant metastasis are challenges in the treatment of this disease.

Achieving population stratification by screening high-risk factors and adopting different clinical intervention measures are very important. Renata Ferrarotto (2021) analysed two ACC molecular subtypes defined by MYC and P63 using RNA sequencing (RNA-seq) and revers-phase protein microarray (RPPA). The high-risk type of ACC-I showed substantial overexpression of MYC and MYC target genes, mRNA splicing, and enrichment for NOTCH-activating mutations, resulting in shorter median survival than patients with ACC-II (3.44 years vs. 23.2 years) (9). In addition to molecular typing, clinical characteristics might also identify high-risk groups for simple and effective risk stratification and management.

The parotid gland and submandibular gland are the most common salivary glands in the head and neck (64.8%) (10). The salivary glands site was a prognostic risk factor in the nomogram model developed by Xiaoli Mu (11), but the specific classification of salivary glands was not performed. Jason Tasoulas et al. found that the overall prognosis of patients with submandibular gland ACC in stage IV was worse than that of patients with ACC in the parotid gland and minor salivary glands (10), but the specific differences in the clinical prognosis presentation and molecular expression patterns were not clarified. We further confirmed whether the prognosis of patients with submandibular gland ACC and parotid gland ACC differed in a large multicentre sample, and analysed the reasons for the difference. Therefore, based on the retrospective case data from our hospital combined with the SEER, cBioPortal and GEO data, we analysed the specific clinical manifestations and molecular characteristics of submandibular gland ACC by comparing it with parotid gland ACC which has a similar gene expression background and acinar structure with submandibular gland (12).

2 Materials and methods

2.1 Data sources

2.1.1 SEER database

The dataset "Incidence-SEER Research Plus Data, 18 Registries, Nov 2020 Sub (2000-2018)" was downloaded from the SEER database using SEER Stat 8.4.0 software. Case screening criteria were based on the study by Jason Tasoulas et al. (10), as follows:

1. The screened tumor type was ACC in the classification of salivary gland tumors determined by the World Health Organization (WHO). The SEER database code was based on the International Classification of Cancer Diseases, the third edition (ICD-O-3) system (ACC = 8200), and patients with ACC were initially screened.
2. The main specific information included age, sex, race, primary site, TNM stage, surgery (primary site and cervical lymph node), radiotherapy, chemotherapy, SEER cause-specific death classification, survival in months, and extent of disease—SEER Combined Mets to DX-lung/liver/bone/brain.
3. As TNM staging was not available in the data before 2004, data collected after 2004 were selected. Cases from 2004 to 2009 were graded according to the American Joint Committee on Cancer (AJCC) 6th edition, while cases from 2010 and later were graded according to the AJCC 7th edition. The staging criteria for major salivary gland tumors were not significantly revised in the 7th edition; cases classified according to the 6th and 7th editions of the AJCC were merged. Invalid cases, which have multiple primary tumors, ambiguous survival time, or non-specific death classification, were removed. (Figure 1).

2.1.2 Collection of clinical data from patients

A retrospective analysis was performed on patients (including outpatients and inpatients) who were diagnosed with head and neck ACC in Beijing Tongren Hospital from January 2005 to March 2022, and the primary sites were the parotid gland and submandibular gland. The basic information was complete. Clinical and pathological characteristics, such as sex, symptoms at first diagnosis, TNM stage (based on the eighth edition of AJCC), treatment method, pathological grade, perineural invasion, and the Ki67 index, were collected. The pathological grading criteria used by Szanto et al. (13) were uniformly modified to grade I-II and grade III. Pulmonary

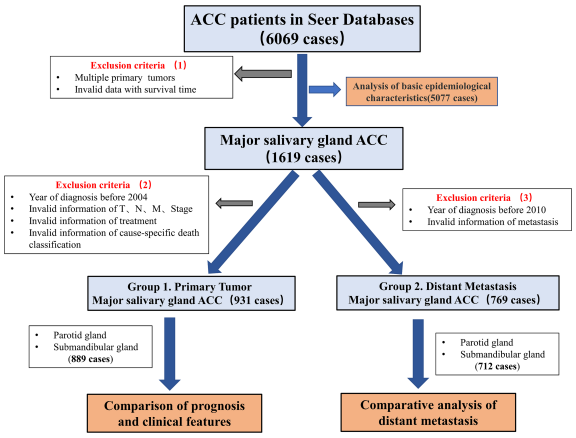

FIGURE 1
Flow chart showing the screening process for data from the SEER database. The dataset "Incidence-SEER Research Plus Data, 18 Registries, Nov 2020 Sub (2000-2018)", including a total of 6069 patients with ACC, was selected based on screening criteria 1. The basic epidemiological characteristics of 5077 ACC patients with complete information were analysed. Then, a total of 1619 patients with major salivary glands ACC were selected. According to screening criteria 2, patients with missing basic clinical characteristics were excluded from the 1619 patients for the analysis of the differences in clinical characteristics to determine the prognosis. According to screening criteria 3, 769 patients were selected from the original 1619 patients, and distant metastasis was analysed.

metastases were diagnosed by two or more lung CT reports (at intervals of 3 months or more) with the persistent progression of pulmonary nodules and after the exclusion of other diseases, and the diagnosis of extrapulmonary metastasis was made by performing a PET-CT evaluation.

2.1.3 Mutation and RNA-seq analyses

Data on mutations in parotid and submandibular glands ACC, including the mutation frequency and mutation type, were obtained from the cBioPortal database (https://www.cbioportal.org/). ACC was searched and the following datasets were selected: (J Clin Invest 2019), (Fmi. Am J Surg Pathl.2014), (JHU, Cancer Prev Res 2016), (MDA. Clin Cancer Res 2015), (MGH. Nat Gen 2016), (MSKCC. NAT Genet 2013), and (Sanger/Mda.jCI 2013). The information collected included the site, age, histological type, and perineural invasion. The histological type was uniformly modified into grade I-II and grade III according to (13) the pathological grading criteria. The mutational landscape was mapped using Microsoft Office Home and Student 2019. The parotid gland and submandibular gland were selected as the "Tumor Disease Anatomic Site". "Cancer Gene" was screened as defined by OncoKB from mutated genes/structural variant genes, and the number of mutations in each sample should be greater than 2.

The GSE88804 and GSE34816 datasets were screened in the GEO database and corrected for batch effects, and the parts were selected as parotid gland and submandibular gland ACC for the differential expression analysis. The differential expression analysis was performed using R 4.2.0 and the R limma package (|log fold change| > 0.585, P value < 0.05). Differentially expressed genes were selected for a Kyoto Encyclopedia of Genes and Genomes (KEGG) enrichment analysis using the HIPLOT enrichment database (public/db/kegg/hsa_kegg_20220424.rds) (https://hiplot.com.cn/). Bubble charts were drawn using the web tool Sangerbox3.0 (http://vip.sangerbox.com/home.html). Gene set enrichment analysis (GSEA) was performed using a web tool (http://www.webgestalt.org/). Venn diagrams were constructed and analysed using the web tool (https://hiplot.com.cn/basic/).

2.1.4 Statistical analysis

Cox regression analysis, the chi-square test, Fisher's test, and the log-rank test were performed on the data using SPSS 22.0 and GraphPad Prism 8.0 software. Survival curves were drawn using the Kaplan-Meier method. P<0.05 (*), P<0.01 (**), and P<0.001 (***) indicate a significant difference. The web tool Sangerbox3.0 was used to draw the forest map (http://vip.sangerbox.com/home.html).

3 Results

3.1 Epidemiological characteristics and prognosis of patients with submandibular gland ACC based on the SEER database

After downloading the dataset and performing the initial screening (Figure 1, Exclusion criteria 1), a total of 5077 ACC patients were screened, among which the patients with ACC of the major salivary glands accounted for 34%. The submandibular gland (41.0%, 712/1738) and parotid gland (48.2%, 838/1438) were the most common sites of tumors in the major salivary glands (Figure 2A). The age group with the highest proportion of ACC in the submandibular gland was 40-54 years old, and the incidence of ACC in the submandibular gland was higher in younger patients (P<0.05, Figure 2B, Table S1). The incidence rate of ACC in the major salivary glands and submandibular gland in females was approximately 1.5 times that in males, and white people were the most frequently affected (Figures 2C, D).

Two groups of data were obtained after screening based on two criteria (Figure 1). Group 1 was used to compare the clinical characteristics of 931 patients with primary site tumors after removing 42 patients with incomplete data. A total of 889 patients were obtained, including 477 patients with parotid gland ACC and 412 patients with submandibular gland ACC. The

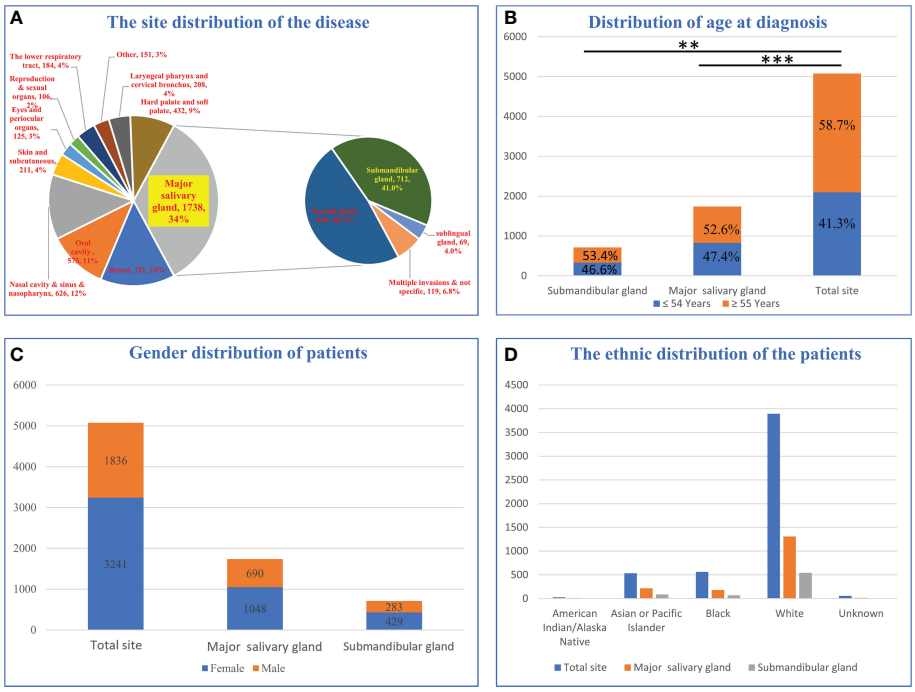

FIGURE 2
Epidemiological analysis of patients with submandibular gland ACC. **(A)** Distribution of disease sites in 5077 patients. **(B)** Age distribution of submandibular gland ACC compared with the major salivary glands and all parts of the body. **(C)** Sex distribution of patients with submandibular gland ACC compared with major salivary glands and body parts. **(D)** The racial distribution of submandibular gland ACC compared with major salivary glands and body parts (** P-value <0.01; *** P-value <0.001).

median follow-up times were 93 months and 100 months, respectively (the mean follow-up times were 95 months and 100 months, respectively).

The Cox regression analysis showed that age, site, T stage, N stage, M stage and chemotherapy were the related factors affecting the prognosis (P<0.05), and the overall prognosis of patients with submandibular gland ACC was poor (P<0.05) (Figures 3 and 4A). Basic clinical features were analysed and the log-rank test revealed that age, tumor stage, T stage, N stage, M stage, and surgical treatment at the primary site correlated with the prognosis (P<0.05, Table S2). However, differences in the prognosis of patients with parotid gland ACC and submandibular gland ACC were significant only in patients with stage IV tumors (P<0.001, Figure 4B), consistent with the results reported by Jason Tasoulas et al. (10). Further analysis of the distribution characteristics of the stage IV population showed that compared with patients with parotid gland ACC, the proportion of patients with stage T4 submandibular gland ACC was lower (50% vs. 87.8%), while the rates of lymph node metastasis (58.3% vs. 35.4%) and distant metastasis (35.7% vs. 17.1%) were higher (P<0.01, Figure 4C). Compared with patients with parotid gland ACC, patients with submandibular gland ACC showed mainly stage I-III tumors (79.6% vs. 65.6%) and T1-3 tumors (89.8% vs. 69.8%) (Table 1, P<0.05). Distant

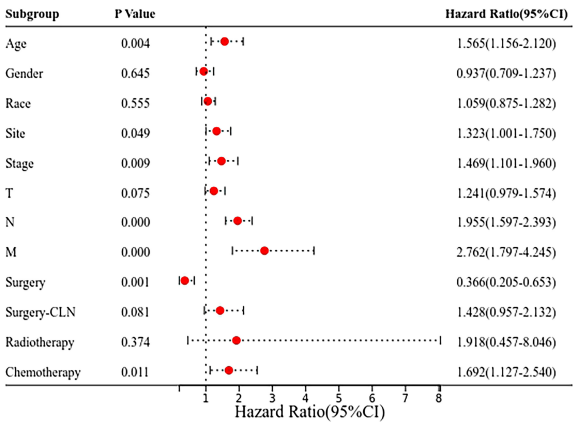

FIGURE 3
Forest plot of the Cox regression analysis of 899 patients with submandibular/parotid glands ACC in the SEER database. The clinical prognosis of 899 patients with parotid gland and submandibular gland ACC was determined using the Cox regression model to analyse the factors influencing the prognosis, such as the tumor site.

metastasis was evaluated in Group 2 (post-2010 dataset), including 383 patients with parotid gland ACC (mean follow-up time: 49 months, median follow-up time: 44 months) and 329

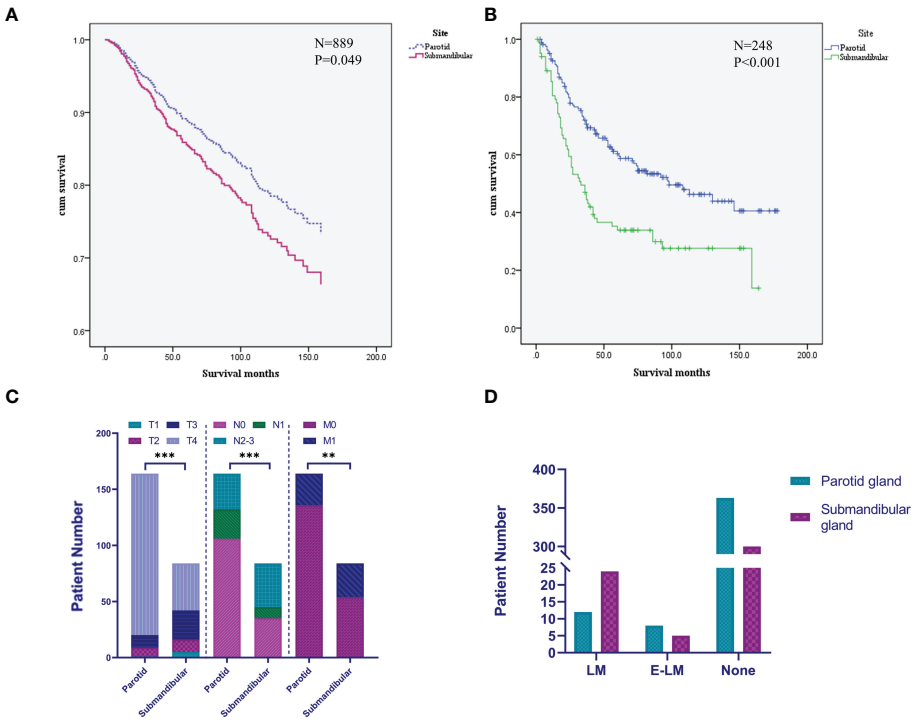

FIGURE 4
Differences in the prognosis and clinical characteristics of patients with submandibular/parotid gland ACC in the SEER database. **(A)** Survival curves for patients with submandibular and parotid glands ACC analysed using the Cox regression model. **(B)** Survival curves for patients with stage IV submandibular and parotid glands ACC analysed using the Kaplan-Meier method. **(C)** Difference in the distribution of TNM staging in patients with stage IV submandibular and parotid glands ACC. **(D)** Distribution of distant metastases of submandibular and parotid glands ACC. LM, lung metastasis; E-LM, extrapulmonary metastasis; None, no distant metastasis found (** P-value <0.01; *** P-value <0.001).

patients with submandibular gland ACC (mean follow-up time: 51 months, median follow-up time: 50 months). The overall distant metastasis rate of patients with submandibular gland ACC was higher than that of patients with parotid gland ACC (8.81% vs. 5.22%, Figure 4D), and the lung metastasis rate was higher (7% vs. 3%). In conclusion, compared with parotid gland ACC, submandibular gland ACC has a worse prognosis in general, with a higher rate of distant metastasis, mainly lung metastasis, at an early stage (within 1 year).

3.2 Clinicopathological features and manifestations of lung metastases of ACC of the submandibular gland (retrospective analysis of patients from a single centre)

Seventy-six patients with ACC (parotid gland ACC (30) and submandibular gland ACC (46)) were included in our analysis. The mean follow-up time was 66 months (median 55 months) for patients with parotid gland ACC and 58 months (median 47 months) for patients with submandibular gland ACC. Compared with patients with parotid gland ACC, more patients with submandibular gland ACC were older than 50 years of age (45.7%, 21/46) and had a higher rate of cervical lymph node metastasis (21.7% vs. 3.3%). No significant differences were observed in the pathological grade, neurotropic growth, Ki67 index or treatment methods (including general treatment, radiotherapy and neck dissection) (Table 2).

When comparing distant metastases at the first diagnosis and follow-up, patients with submandibular gland ACC had a mean distant metastasis-free survival (MFS) of 32 months (median 14 months), while those with parotid gland ACC had a mean value of 44 months (median 24 months); however, the log-rank test did not reveal a significant difference (P>0.05, Figure 5A). The rate of distant metastasis in patients with submandibular gland ACC (47.8%) was higher than that in patients with parotid gland ACC (23.3%) within 1 year after the primary diagnosis (P<0.05, Figure 5B). Compared with parotid gland ACC and submandibular gland ACC in the early stage (T1-2), the rate of distant metastasis of submandibular gland ACC was significantly higher at the first diagnosis (P<0.05), and the rate of cervical lymph node metastasis (N+) was slightly higher (Figure 5C).

10.3389/fonc.2022.1021169

TABLE 1 Differences in the clinical characteristics of patients with submandibular and parotid glands ACC from the SEER database.

		Major salivary gland (2004-2018)		X2
		Parotid	Submandibular	P value
Age	<50	182 (38.2%)	143 (34.7%)	0.287
	≥50	295 (61.8%)	269 (65.3%)	
Gender	Male	186 (39.0%)	152 (36.9%)	0.52
	Female	291 (61%)	260 (63.1%)	
Race	White	362 (75.9%)	308 (74.8%)	0.116
	Black	57 (11.9%)	35 (8.5%)	
	Other	54 (11.3%)	65 (15.8%)	
	NA	4 (0.8%)	4 (1%)	
Stage	I	126 (26.4%)	126 (30.6%)	**<0.001**
	II	104 (21.8%)	110 (26.7%)	
	III	83 (17.4%)	92 (22.3%)	
	IV	164 (34.4%)	84 (20.4%)	
T	T1	136 (28.5%)	134 (32.5%)	**<0.001**
	T2	117 (24.5%)	128 (31.1%)	
	T3	80 (16.8%)	108 (26.2%)	
	T4	144 (30.2%)	42 (10.2%)	
N	N0	399 (83.6%)	342 (83.0%)	0.196
	N1	46 (9.6%)	31 (7.5%)	
	N2-N3	32 (6.7%)	39 (9.5%)	
M	M0	449 (94.1%)	382 (92.7%)	0.395
	M1	28 (5.9%)	30 (7.3%)	
Surgery	None	33 (6.9%)	18 (4.4%)	0.103
	Yes	444 (93.1%)	394 (95.6%)	
Cervical lymph node dissection	None	141 (29.6%)	177 (43.0%)	**<0.001**
	Yes	336 (70.4%)	235 (57.0%)	
Radiotherapy	None/NA	7 (1.5%)	6 (1.5%)	0.989
	Yes	470 (98.5%)	406 (98.5%)	
Chemotherapy	None/NA	435 (91.2%)	376 (91.3%)	0.972
	Yes	42 (8.8%)	36 (8.7%)	
Total		477	412	

We subsequently screened and analysed patients with complete information on distant metastasis identified at the first diagnosis of primary early-stage (T1-2N0) ACC, including 8 patients with parotid gland ACC (62%, 8/17) and 19 patients with submandibular gland ACC (73%, 19/27) to compare the difference in disease status at the time of the first diagnosis of distant metastasis. We identified a significant difference in the risk level of the disease course of the first diagnosis of distant metastasis. The risk classification is as follows: low-risk, multiple nodules in both lungs and the largest diameter is <1 cm, without extrapulmonary metastasis; medium-risk, multiple nodules in both lungs and the largest is 1-3 cm in diameter, without extrapulmonary metastasis; and high-risk, multiple nodules in both lungs with a maximum diameter greater than 3 cm or with extrapulmonary metastasis. The analysis of the distribution of risk grades of distant metastasis in patients with parotid gland

10.3389/fonc.2022.1021169

TABLE 2 Differences in the overall clinical characteristics of patients with submandibular and parotid glands ACC based on a single-centre retrospective analysis.

		Major salivary gland (Stage IV)		X2
		Parotid	Submandibular	P value
Age	<50	23 (76.7%)	25 (54.3%)	**0.049**
	≥50	7 (23.3%)	21 (45.7%)	
Gender	Male	12 (40%)	15 (32.6%)	0.51
	Female	18 (60%)	31 (67.4%)	
Symptom	Painless mass	17 (56.7%)	37 (80.4%)	**0.026**
	Pain and other discomfort	13 (43.3%)	9 (19.6%)	
Histological grade	NA	4 (13.3%)	4 (8.7%)	0.839
	Grade I—II	16 (53.3%)	25 (54.3%)	
	Grade III	10 (33.3%)	17 (37.0%)	
Perineural invasion	NA	6 (20.0%)	9 (19.6%)	0.752
	None	5 (16.7%)	5 (10.9%)	
	Yes	19 (63.3%)	32 (69.6%)	
Ki67	NA	1 (3.3%)	10 (21.7%)	0.127
	<30%	19 (63.3%)	23 (50.0%)	
	30%-60%	9 (30.0%)	11 (23.9%)	
	>60%	1 (3.3%)	2 (4.3%)	
T	T1	3 (10.0%)	8 (17.4%)	0.317
	T2	14 (46.7%)	24 (52.2%)	
	T3	5 (16.7%)	9 (19.6%)	
	T4	8 (26.7%)	5 (10.9%)	
N	N0	29 (96.7%)	36 (78.3%)	**0.042**
	N+	1 (3.3%)	10 (21.7%)	
M	M0	27 (90.0%)	34 (73.9%)	0.085
	M1	3 (10.0%)	12 (26.1%)	
Treatment	S	3 (10%)	5 (10.9%)	0.1
	S+R	24 (80.0%)	26 (56.5%)	
	S+R+C	3 (10.0%)	10 (21.7%)	
	S+C	0 (0.0%)	5 (10.9%)	
Cervical lymph node dissection	None	20 (66.7%)	27 (58.7%)	0.484
	Yes	10 (33.3%)	19 (41.3%)	
Radiotherapy	None	3 (10.0%)	10 (21.7%)	0.256
	<60GY	6 (20.0%)	12 (26.1%)	
	≥60GY	21 (70.0%)	24 (52.2%)	
Total		30	46	

S, surgery; R, radiotherapy; C, chemotherapy.

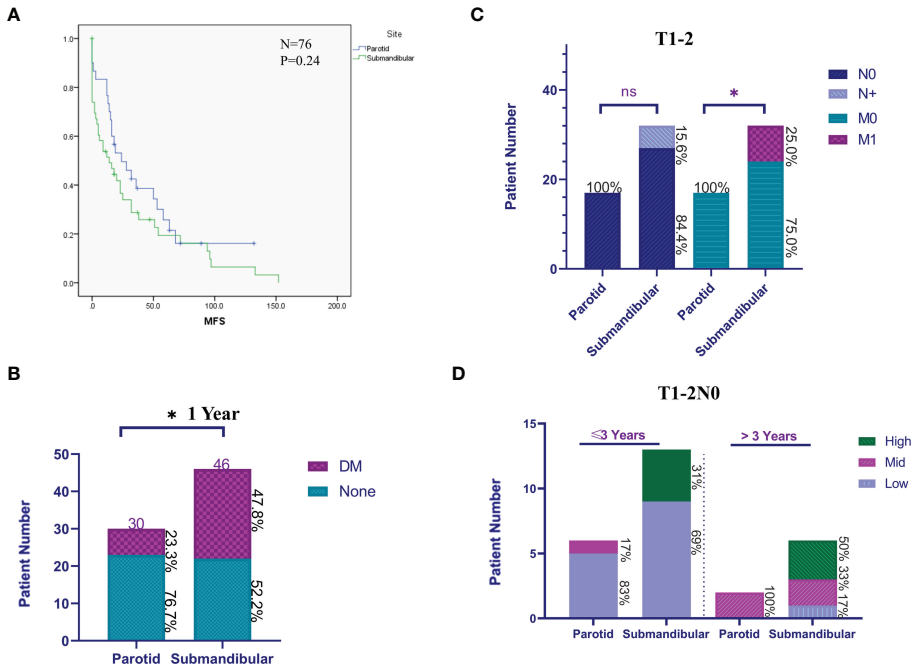

FIGURE 5
Clinical features of patients with submandibular/parotid glands ACC from a single-centre retrospective analysis. **(A)** The Kaplan-Meier method was used to analyse the differences in distant metastases from ACC of the submandibular and parotid glands. **(B)** The difference in distant metastases (DM) within 1 year after the primary diagnosis of submandibular and parotid glands ACC. **(C)** Cervical lymph node and distant metastasis ratio at the first diagnosis of early (T1-2) submandibular and parotid glands ACC. **(D)** Early (T1-2N0) differences in the rate of progression of distant metastases of submandibular and parotid glands ACC. High: prognostic high-risk status for distant metastasis; Mid: prognostic medium-risk status for distant metastasis; and Low: prognostic low-risk status for distant metastasis (ns: P-value> 0.05; * P-value <0.05).

ACC and submandibular gland ACC within 3 years and after 3 years showed that the high-risk grade of distant metastasis in patients with submandibular gland ACC was 31% and 50%, respectively, while the high-risk grade of distant metastasis in patients with parotid gland ACC was 0 (Figure 5D). In conclusion, patients with ACC of the submandibular gland are prone to early occult distant metastasis, and the disease progresses rapidly.

3.3 Mutation map and expression characteristics of ACC oncogene in submandibular gland

The dataset was searched using the cBioPortal database, and 22 cases of submandibular gland ACC and 36 cases of parotid gland ACC were screened for gene mutation analysis (Figure 6). The mutant genes were divided into four categories: *MYB/MYBL1-NFIB*-related fusion genes, Notch pathway-related genes, epigenetic modification-related genes, and others. The *MYB/MYBL1-NFIB* fusion had a higher mutation frequency in submandibular gland ACC compared with submandibular gland ACC (50% vs. 25%), and the fusion mutation of *MYBL1* only appeared in submandibular gland ACC (9%). *NOTCH1* mutation did not occur in ACC of the parotid gland, accounting for 9% of ACC of the submandibular gland; meanwhile, mutations in *SPEN* (a negative regulator of the Notch pathway) did not appear in ACC of the submandibular gland, and the mutation frequency in ACC of the parotid gland was 11%. Epigenetic modification-related genes included *ARID1A*, *ARID5B*, *SMARCA2*, *CHD2*, and *SF3B1*. Except for *CHD2* (9%), all of them were detected in parotid and submandibular gland ACC, and all of them had mutually exclusive mutations.

We further studied the differences in the molecular expression patterns of ACC tumor tissues in the parotid gland and submandibular gland and analysed the abnormal pathways in submandibular gland ACC by screening upregulated and downregulated genes in 10 cases of submandibular gland ACC and 16 cases of parotid gland ACC from the two GEO datasets. *MYB* gene expression was significantly upregulated in submandibular gland ACC compared with parotid gland ACC (Figure 7A). KEGG enrichment analysis of genes with $P<0.05$ and $|\log FC|>0.585$ showed that genes were significantly enriched in the PI3K pathway, including the *PDGFA, MYB, ITGA2, FN1, EGF, COL6A3, COL1A2*, and *COL1A1* genes (Figure 7B). According to GSEA, the activity of the PI3K

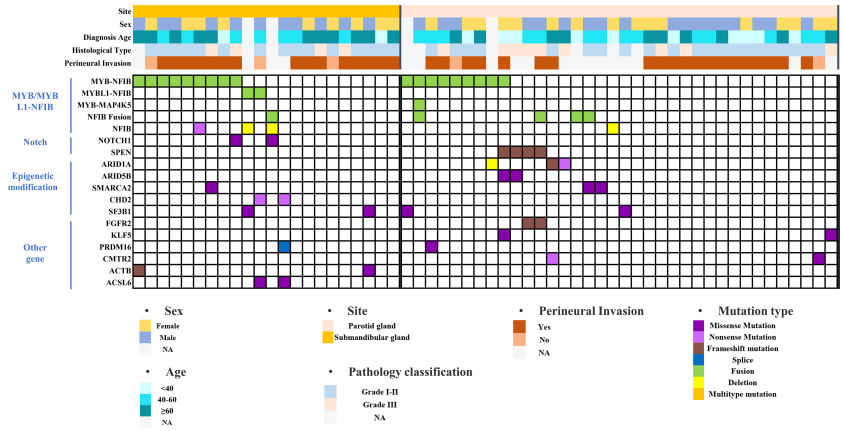

FIGURE 6
Mutation landscape of submandibular gland and parotid gland ACC based on the cBioPortal database.

pathway was upregulated (Figure 7C). Next, we aimed to exclude differences in the expression of genes related to the PI3K pathway in normal parotid and submandibular glands tissues, and 6311 differentially expressed genes ($P<0.05$, $|\log FC|>1$) in the normal parotid gland and submandibular gland tissues were downloaded from the supplementary materials of the study by Marie Saitou et al. (12) and intersected with the differentially expressed genes in the submandibular gland and parotid gland ACC obtained from the GEO dataset. No intersecting genes were identified (Figure 7D). This result excluded the possibility that differentially expressed genes in tumor genes were caused by differences in the genetic background of normal tissues. Therefore, based on the results from the cBioPortal and GEO databases, submandibular gland ACC has a higher frequency of *MYB/MYBL1* mutations, and genes in the PI3K pathway, including MYB, are upregulated.

4 Discussion

ACC is a rare malignant tumor of glandular origin that may occur systemically but is more common in the head and neck. The development of uncontrolled distant metastases after primary surgery has become a major challenge in disease treatment. Risk stratification based on differences in prognosis is a prerequisite for individualized treatment of the disease. Renata Ferrarotto proposed in 2017 that patients with *NOTCH1* mutations should be defined as a population with a poor prognosis who are prone to have extrapulmonary metastasis (14); In 2021, they proposed two risk subtypes defined by MYC and TP63: ACC-I (37%) and ACC-II (63%). High-risk ACC-I is characterized by the enrichment of NOTCH-activating mutations and overexpression of MYC target genes, and mRNA splicing. The continuous improvement of molecular typing is helpful for the precise treatment of diseases, and risk stratification based on clear clinical features can simply and effectively assist with clinical individual treatment. Moreover, molecular typing should be further defined and improved based on molecular expression characteristics in populations with varying clinical prognostic performance.

Identifying the site-specific clinical prognosis of patients with submandibular gland ACC is helpful for simple and effective clinical treatment stratification and an accurate risk assessment. In the nomogram prediction model constructed by Ian Ganly, tumors in the nasal cavity and paranasal sinuses had the highest risk, followed by the major salivary glands, while tumors in the larynx/pharynx/oral cavity had the lowest risk. However, none of the studies further analysed the prognostic risk weights for the three major salivary glands (15, 16). A log-rank univariate analysis performed by Jason Tasoulas using SEER data revealed that the prognosis of patients with submandibular gland ACC was worse than that of patients with parotid gland and minor salivary glands ACC which was only showed in stage IV. But the specific manifestation of the clinical prognosis difference has not been compared and expounded in detail (10). We screened 5077 patients with ACC from the SEER database, a large sample clinical database. Using Cox regression analysis, patients with submandibular gland ACC were found to have a worse prognosis than patients with parotid gland ACC, consistent with the research conclusions described above. Because normal tissues of the parotid and submandibular glands have similar gene expression patterns (12), the submandibular gland ACC can be compared with the parotid gland ACC to determine the specific clinical prognosis and abnormal molecular expression. Similar to the study by Jason Tasoulas et al, the same analysis showed that the prognosis of patients with stage IV submandibular gland ACC was significantly worse than the

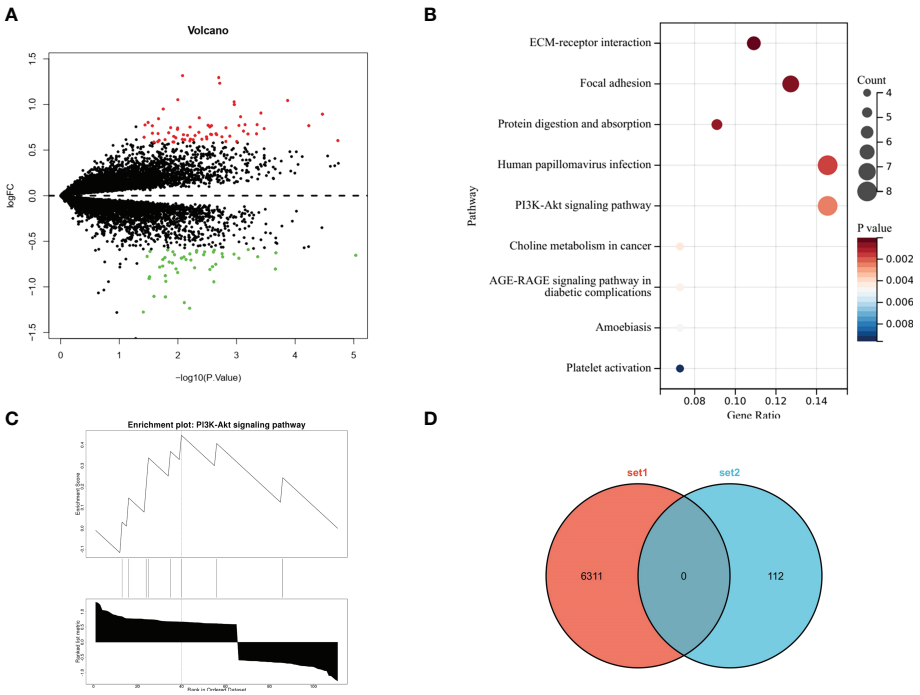

FIGURE 7
RNA sequencing results from the submandibular gland and parotid gland ACC based on the GEO database. **(A)** Volcano plot showing differentially expressed genes. Red dots and green dots indicate upregulated and downregulated genes, respectively, in submandibular gland ACC compared with parotid gland ACC. **(B)** Bubble diagram of the KEGG enrichment analysis showing the results for differentially expressed genes. The colour and size of bubbles correspond to the P value and the number of enriched genes, respectively. **(C)** GSEA of differentially expressed genes revealed that the PI3K signaling pathway was upregulated in ACC of the submandibular gland. **(D)** Venn diagram of gene set intersections: set 1 is the differentially expressed genes in the normal parotid gland and submandibular gland tissues, and set 2 is the differentially expressed genes in the parotid gland and submandibular gland ACC tissues.

patients with parotid gland ACC (10). Further analysis and comparison indicated that ACC of the parotid gland was characterized by a higher T stage, while ACC of the submandibular gland was characterized by a higher rate of cervical lymph node metastasis and distant metastasis. Although the log-rank test showed that a higher TNM stage and T stage are high-risk factors, the finding that the proportion of stage IV and T4 stage parotid gland ACC was higher than that in the submandibular gland ACC seems paradoxical, as the parotid gland has a larger space for invasion inside and outside the envelope and is prone to a later T stage. Subsequently, a dataset with complete distant metastasis information was selected for further analysis, and submandibular gland ACC had a higher overall metastasis rate than parotid gland ACC, and the lung was the main site of metastasis. In conclusion, compared with parotid gland ACC, submandibular gland ACC has a higher metastasis rate and worse prognosis.

In addition, the aforementioned study based on the SEER database found that the submandibular ACC was more likely to have lymph node metastasis and earlier distant metastasis than the parotid gland in stage IV. Because clinical staging adopts a mixed grading method compared with TNM staging, it cannot reflect the inherent law of tumor occurrence and development. Moreover, the SEER database lacks the specific time and disease progression status of distant metastasis. Therefore, we expanded the sample size as much as possible in a single-centre retrospective cohort to analyse the specific characteristics of distant metastases in submandibular gland ACC and to analyse the difference in the progression rate of lymph node and distant metastases of submandibular gland ACC compared with parotid gland ACC. Limited by the heterogeneity and the small size of the population, we did not observe a significant difference in the distant metastasis time of the two sites of ACC tumors using the log-rank test; however, within 1 year after diagnosis, submandibular gland ACC had a higher rate of distant metastasis ($P<0.05$). At the same time, in patients with T1-2 stage, submandibular gland ACC had a higher rate of cervical lymph node metastasis and distant metastasis than parotid gland ACC at the first diagnosis ($P<0.05$). Further comparison of the metastatic status of patients with T1-2N0 stage parotid gland ACC and submandibular gland ACC showed that patients with submandibular gland ACC had a

higher risk level of distant metastasis (pulmonary metastatic nodules >3 cm or extrapulmonary metastasis). In conclusion, compared with patients with parotid gland ACC, patients with submandibular gland ACC have a risk of early occult metastasis and rapid disease progression, resulting in a poor site-specific prognosis.

To further explore the molecular expression characteristics of ACC in the submandibular gland with high metastasis and poor prognosis, we analyzed the gene mutation characteristics based on the cBioPortal dataset and found that there was a high *MYB/MYBL1-NFIB* fusion ratio in the submandibular gland. Differentially expressed genes were analysed using the GEO database to further verify the differences in expression and abnormal pathways, and we found that the MYB-dominated PI3K pathway was also significantly enriched and upregulated in the submandibular gland ACC. However, the upregulation of genes in the PI3K pathway, including MYB, in the submandibular gland ACC was not due to a difference in expression between normal tissues of the parotid and submandibular glands (Figure 7D). *MYB* fusion mutations (the most common fusion *NFIB*) are hallmark molecular events in the development of ACC, with a mutation frequency of 16-100% (17–19), and high expression of MYB is closely related to the poor prognosis (20). Relevant studies have found that the genes of the PI3K pathway amplified and mutated in various tumors, such as breast cancer and gastric cancer, and this signaling pathway plays a role in cell survival, angiogenesis, lymph node metastasis, and distant metastasis (21, 22). In salivary gland cancers, aggressive tumor types have higher genomic alterations in the PI3K pathway (23). Therefore, the upregulation of the PI3K pathway may be the main reason for the higher rate of lymph node and distant metastasis of submandibular gland ACC than parotid gland ACC. One study found that the administration of PI3K inhibitors to the ACC xenograft mouse model effectively reduces the primary tumor burden and lung metastasis (24). Target therapies against abnormal genetic alterations have shown varying degrees of promise in the clinic as precision medicines of ACC.

Data availability statement

The original contributions presented in the study are included in the article/Supplementary Material. Further inquiries can be directed to the corresponding authors.

Author contributions

Conception and design: MZ and TM. Data analysis: XW, SZ, and GY. Manuscript writing: MZ and TM. Manuscript revision: RS and XC. Funding support: XC. All authors contributed to the article and approved the submitted version.

Funding

This work was supported by grants from the National Natural Science Foundation of China (grant no. 82173312) and the Capital Health Development Research Project (grant no. 2022-2-2057).

Conflict of interest

The authors declare that the research was conducted in the absence of any commercial or financial relationships that could be construed as a potential conflict of interest.

Publisher's note

Supplementary material

The Supplementary Material for this article can be found online at: https://www.frontiersin.org/articles/10.3389/fonc.2022.1021169/full#supplementary-material

SUPPLEMENTARY TABLE 1
Analysis of the age distribution of patients with submandibular gland ACC in the SEER database.

SUPPLEMENTARY TABLE 2
Overall clinical characteristics of 889 patients with submandibular/parotid glands ACC in the SEER database.

References

1. van Weert S, Bloemena E, van der Waal IC, de Bree R, Rietveld DHF, Kuik JD, et al. Adenoid cystic carcinoma of the head and neck: A single-center analysis of 105 consecutive cases over a 30-year period. *Oral Oncol* (2013) 49(8):824–9. doi: 10.1016/j.oraloncology.2013.05.004

2. Ouyang DQ, Liang LZ, Zheng GS, Ke ZF, Weng DS, Yang WF, et al. Risk factors and prognosis for salivary gland adenoid cystic carcinoma in southern china: A 25-year retrospective study. *Medicine* (2017) 96(5):e5964. doi: 10.1097/MD.0000000000005964

3. Bhayani MK, Yener M, El-Naggar A, Garden A, Hanna EY, Weber RS, et al. Prognosis and risk factors for early-stage adenoid cystic carcinoma of the major salivary glands. *Cancer* (2012) 118(11):2872–8. doi: 10.1002/cncr.26549

4. van der Wal JE, Becking AG, Snow GB, van der Waal I. Distant metastases of adenoid cystic carcinoma of the salivary glands and the value of diagnostic examinations during follow-up. *Head Neck* (2002) 24(8):779–83. doi: 10.1002/hed.10126

5. Bobbio A, Copelli C, Ampollini L, Bianchi B, Carbognani P, Bettati S, et al. Lung metastasis resection of adenoid cystic carcinoma of salivary glands. *Eur J Cardiothorac Surg* (2008) 33(5):790–3. doi: 10.1016/j.ejcts.2007.12.057

6. Xu MJ, Wu TJ, van Zante A, El-Sayed IH, Algazi AP, Ryan WR, et al. Mortality risk after clinical management of recurrent and metastatic adenoid cystic carcinoma. *J Otolaryngol Head Neck Surg* (2018) 47(1):28. doi: 10.1186/s40463-018-0273-z

7. Seok J, Lee DY, Kim WS, Jeong W-J, Chung E-J, Jung YH, et al. Lung metastasis in adenoid cystic carcinoma of the head and neck. *Head Neck* (2019) 41(11):3976–83. doi: 10.1002/hed.25942

8. Seethala RR, Hunt JL, Baloch ZW, Livolsi VA, Leon Barnes E. Adenoid cystic carcinoma with high-grade transformation: a report of 11 cases and a review of the literature. *Am J Surg Pathol* (2007) 31(11):1683–94. doi: 10.1097/PAS.0b013e3180dc928c

9. Ferrarotto R, Mitani Y, McGrail DJ, Li K, Karpinets TV, Bell D, et al. Proteogenomic analysis of salivary adenoid cystic carcinomas defines molecular subtypes and identifies therapeutic targets. *Clin Cancer Res* (2021) 27(3):852–64. doi: 10.1158/1078-0432.CCR-20-1192

10. Tasoulas J, Divaris K, Theocharis S, Farquhar D, Shen C, Hackman T, et al. Impact of tumor site and adjuvant radiotherapy on survival of patients with adenoid cystic carcinoma: A SEER database analysis. *Cancers* (2021) 13(4):589. doi: 10.3390/cancers13040589

11. Megwalu UC, Sirjani D. Risk of nodal metastasis in major salivary gland adenoid cystic carcinoma. *Otolaryngol Head Neck Surg Off J Am Acad Otolaryngol Head Neck Surg* (2017) 156(4):660–4. doi: 10.1177/0194599817690138

12. Saitou M, Gaylord EA, Xu E, May AJ, Neznanova L, Nathan S, et al. Functional specialization of human salivary glands and origins of proteins intrinsic to human saliva. *Cell Rep* (2020) 33(7):108402. doi: 10.1016/j.celrep.2020.108402

13. Szanto PA, Luna MA, Tortoledo ME, White RA. Histologic grading of adenoid cystic carcinoma of the salivary glands. *Cancer* (1984) 54(6):1062–9. doi: 10.1002/1097-0142(19840915)54:63.0.CO;2-E

14. Ferrarotto R, Mitani Y, Diao L, Guijarro I, Wang J, Zweidler-McKay P, et al. Activating NOTCH1 mutations define a distinct subgroup of patients with adenoid cystic carcinoma who have poor prognosis, propensity to bone and liver metastasis, and potential responsiveness to Notch1 inhibitors. *J Clin Oncol* (2017) 35(3):352–60. doi: 10.1200/JCO.2016.67.5264

15. Ganly I, Amit M, Kou L, Palmer FL, Migliacci J, Katabi N, et al. Nomograms for predicting survival and recurrence in patients with adenoid cystic carcinoma. *Int Collab Study Eur J Cancer (Oxford Engl 1990)* (2015) 51(18):2768–76. doi: 10.1016/j.ejca.2015.09.004

16. Mu X, Li Y, He L, Guan H, Wang J, Wei Z, et al. Prognostic nomogram for adenoid cystic carcinoma in different anatomic sites. *Head Neck* (2021) 43(1):48–59. doi: 10.1002/hed.26443

17. de Almeida-Pinto YD, Costa S, de Andrade BAB, Altemani A, Vargas PA, Abreu LG, et al. t(6;9)(MYB-NFIB) in head and neck adenoid cystic carcinoma: A systematic review with meta-analysis. *Oral Dis* (2019) 25(5):1277–82. doi: 10.1111/odi.12984

18. Mitani Y, Liu B, Rao PH, Borra VJ, Zafereo M, Weber RS, et al. Novel MYBL1 gene rearrangements with recurrent MYBL1-NFIB fusions in salivary adenoid cystic carcinomas lacking t(6;9) translocations. *Clin Cancer Res* (2016) 22(3):725–33. doi: 10.1158/1078-0432.CCR-15-2867-T

19. Gonda TJ, Ramsay RG. Adenoid cystic carcinoma can be driven by MYB or MYBL1 rearrangements: New insights into MYB and tumor biology. *Cancer Discovery* (2016) 6(2):125–7. doi: 10.1158/2159-8290.CD-15-1470

20. Mitani Y, Li J, Rao PH, Zhao Y-J, Bell D, Lippman SM, et al. Comprehensive analysis of the MYB-NFIB gene fusion in salivary adenoid cystic carcinoma: Incidence, variability, and clinicopathologic significance. *Clin Cancer Res* (2010) 16(19):4722–31. doi: 10.1158/1078-0432.CCR-10-0463

21. Mishra R, Patel H, Alanazi S, Kilroy MK, Garrett JT. PI3K inhibitors in cancer: Clinical implications and adverse effects. *Int J Mol Sci* (2021) 22(7):3464. doi: 10.3390/ijms22073464

22. Chen Y, Mao B, Peng X, Zhou Y, Xia K, Guo H, et al. A comparative study of genetic profiles of key oncogenesis-related genes between primary lesions and matched lymph nodes metastasis in lung cancer. *J Cancer* (2019) 10(7):1642–50. doi: 10.7150/jca.28266

23. Ross JS, Gay LM, Wang K, Vergilio JA, Suh J, Ramkissoon S, et al. Comprehensive genomic profiles of metastatic and relapsed salivary gland carcinomas are associated with tumor type and reveal new routes to targeted therapies. *Ann Oncol* (2017) 28(10):2539–46. doi: 10.1093/annonc/mdx399

24. Liu H, Du L, Wang R, Wei C, Liu B, Zhu L, et al. High frequency of loss of PTEN expression in human solid salivary adenoid cystic carcinoma and its implication for targeted therapy. *Oncotarget* (2015) 6(13):11477–91. doi: 10.18632/oncotarget.3411

frontiers | Frontiers in Oncology

TYPE Original Research
PUBLISHED 17 January 2023
DOI 10.3389/fonc.2022.1096068

OPEN ACCESS

EDITED BY
Ashish V. Chintakuntlawar,
Mayo Clinic, United States

REVIEWED BY
Ari Rosenberg,
The University of Chicago, United States
Giandomenico Roviello,
University of Firenze, Italy

*CORRESPONDENCE
Stefano Cavalieri
stefano.cavalieri@istitutotumori.mi.it

SPECIALTY SECTION
This article was submitted to Head and Neck Cancer, a section of the journal Frontiers in Oncology

RECEIVED 11 November 2022
ACCEPTED 30 December 2022
PUBLISHED 17 January 2023

CITATION
Cavalieri S, Nuzzolese I, Ottini A, Bergamini C, Resteghini C, Colombo E, Alfieri S, Quattrone P, Calareso G, Iacovelli NA, Franceschini M and Licitra L (2023) HER2 status in recurrent/metastatic androgen receptor overexpressing salivary gland carcinoma patients.
Front. Oncol. 12:1096068.
doi: 10.3389/fonc.2022.1096068

HER2 status in recurrent/metastatic androgen receptor overexpressing salivary gland carcinoma patients

Stefano Cavalieri[1,2*], Imperia Nuzzolese[1], Arianna Ottini[1], Cristiana Bergamini[1], Carlo Resteghini[1], Elena Colombo[1], Salvatore Alfieri[1], Pasquale Quattrone[3], Giuseppina Calareso[4], Nicola Alessandro Iacovelli[5], Marzia Franceschini[5] and Lisa Licitra[1,2]

[1]Head and Neck Medical Oncology Department, Fondazione IRCCS Istituto Nazionale dei Tumori, Milan, Italy, [2]Department of Oncology and Hemato-Oncology, University of Milan, Milan, Italy, [3]Pathology Department, Fondazione IRCCS Istituto Nazionale dei Tumori, Milan, Italy, [4]Radiology Department, Fondazione IRCCS Istituto Nazionale dei Tumori, Milan, Italy, [5]Radiotherapy Department, Fondazione IRCCS Istituto Nazionale dei Tumori, Milan, Italy

Background: Overexpression of human epidermal growth factor receptor type 2 (HER2) occurs in almost 25-30% of androgen receptor (AR)-positive salivary gland carcinomas (SGCs), notably salivary duct carcinoma (SDC) and adenocarcinoma not otherwise specified (NOS). In the last years, several studies have reported the clinical benefit of HER2 directed therapies in this setting. This work aims at describing the natural history of AR-positive recurrent/metastatic (R/M) SGC patients, based on HER2 amplification status.

Methods: Consecutive R/M AR-positive SGC patients accessing our Institution from 2010 to 2021 were analyzed. Descriptive statistics and survival analyses were performed to present the clinical characteristics of the selected patients and the outcomes, based on HER2 status. A specific focus was dedicated to patients developing metastases to the central nervous system (CNS).

Results: Seventy-four R/M AR-positive SGC patients (72 men) were analyzed. Median follow-up was 36.18 months (95% CI 30.19-42.66). HER2 status was available in 62 cases (84%) and in 42% the protein was overexpressed (HER2+). Compared with patients with HER2- SGCs, in patients with HER2+ disease, HR for disease recurrence was 2.97 (95% CI 1.44-6.1, p=0.003), and HR for death from R/M disease was 3.22 (95% CI 1.39-7.49, p=0.007). Moreover, the HER2+ group showed a non-significant trend towards a higher prevalence of CNS metastases (40% vs. 24%, p=0.263). Patients developing CNS metastases had shorter survival than those who did not; at bivariate analysis (covariates: CNS disease and HER2 status), HER2 status demonstrated its independent prognostic significance.

Discussion: In our patient population, HER2 amplification was a negative prognostic factor, and it was associated with a non-statistically significant higher risk of developing CNS metastasis. Further studies are needed to explore the

potential clinical benefit of tackling the two biological pathways (AR and HER2) in patients affected by this rare and aggressive malignancy.

KEYWORDS

HER2, androgen receptor, SDC, salivary duct carcinoma, SGC, salivary gland carcinoma, brain metastasis

1 Introduction

Epithelial malignancies arising from the salivary glands (SGCs, salivary gland carcinomas) are rare neoplasms. More than 20 entities are included in the World Health Organization (WHO) classification (1). Specific pathologic types, notably salivary duct carcinoma (SDC) and adenocarcinoma not otherwise specified (NOS) may overexpress androgen receptors (AR). A fraction (average 25-30% up to approximately 40%, depending on the published case series (2, 3) of AR-positive SGCs are characterized by human epidermal growth factor receptor type 2 (HER2) amplification (HER2-positive) (4). AR overexpression is almost definitional in SDCs, and consistently AR-negative SDCs are very rare and this diagnosis should be regarded with skepticism (4). Given that the vast majority of HER2-positive SGC have a SDC histology, the present study is focused on two cohorts: AR-positive HER2-positive; AR-positive HER2-negative.

Similarly to other cancer types, also in SGC both AR and HER2 may be targeted by hormone therapy (5–7), and anti-HER2 agents as trastuzumab (8, 9), trastuzumab plus pertuzumab (10), ado-trastuzumab emtansine (11, 12), trastuzumab deruxtecan (13).

From a prognostic point of view, despite HER2-overexpressing SDCs are known to have worse outcomes than HER2-negative cases (14, 15), their natural history is still unknown. Moreover, both patients with HER2-positive breast and HER2-positive gastric cancers, showed a higher incidence of distant metastases located in the central nervous system (CNS) (16, 17), but in HER2-positive SGCs we lack an in-depth analysis of this feature.

The description of a case series of AR-positive SGCs with available HER2 status may provide further knowledge on this topic.

2 Methods

This was a retrospective observational study aimed at describing the natural history of R/M AR-positive SGC according to HER2 status, with a particular focus on patients with CNS metastases, defined as any distant site at any level of the CNS – including carcinomatous meningitis – deemed unequivocal at clinical and radiological level.

We identified consecutive R/M AR-positive SGC patients accessing our Institution from 2010 to 2021, and we selected cases with availability of HER2 status. HER2 was considered positive when immunohistochemistry (IHC) score was 3+, or 2+ confirmed by an *in situ* hybridization (ISH). Cases with 0, 1+ or 2+ with a negative ISH were considered HER2-negative (3).

For the analysis of the prevalence of CNS metastases, subjects with unavailable HER2 status were included as well, but they were analyzed separately. In all cases, the pathologic diagnosis was reviewed and confirmed by an expert pathologist [PQ] dedicated to the diagnosis of rare head and neck cancers, with more than 20 years of experience in the field.

The following clinical variables were collected: gender, age, histology (SDC, adenocarcinoma NOS) AR status (positive, weak), HER2 status (positive, negative), CNS metastases (present, absent), timing of brain metastases (at primary diagnosis – defined as diagnosed within 3 months from the diagnosis of primary disease – or after therapies), previous treatments (loco-regional therapies for primary disease, treatments for R/M disease), treatments for CNS metastases.

The following time-dependent variables were recorded: disease-free interval (DFI, defined as the interval time between the date of primary tumor diagnosis and the date of R/M disease diagnosis), only for cases without metastatic disease at diagnosis of primary tumor (i.e., for the DFI calculation, subjects with metastatic disease at diagnosis were excluded); CNS-metastasis free survival (CNSmfs), only for cases without CNS metastases at diagnosis of primary tumor; time to first CNS metastasis (TTCNS), only for cases without CNS metastases at diagnosis of primary tumor; overall survival (OS) measured from 3 different timepoints:

OS(a) from primary disease, defined as the interval time between the date of primary tumor diagnosis and the date of death or last follow-up;

OS(b) from R/M disease, defined as the interval time between the date of R/M disease diagnosis and the date of death or last follow-up;

OS(c) from CNS metastases onset, defined as the interval time between the date of CNS metastases diagnosis and the date of death or last follow-up, only for cases with CNS metastases.

Data cut-off date was 31/12/2021. Median follow-up, with the respective 95% confidence interval (CI) was estimated through reverse Kaplan-Meier method, measuring the interval time from the date of R/M diagnosis to the date of death or last follow-up. Hazard ratios (HRs) were estimated with Cox proportional hazard model.

Patients with CNS metastases were classified in four groups according to the disease presentation:

1) upfront CNS disease (interval between primary and CNS disease diagnosis ≤ 3 months),
2) CNS metastases after metastatic disease at diagnosis (DFI ≤ 3 months and interval between metastatic and CNS disease > 3 months),

3) CNS metastases as first disease recurrence after treatment for loco-regional disease (DFI > 3 months and interval between metastatic and CNS disease ≤ 3 months),
4) CNS metastases as subsequent recurrence after palliative treatments for R/M disease diagnosed after treatment failure for loco-regional primary disease (DFI > 3 months and interval between metastatic and CNS disease > 3 months).

Descriptive statistics were provided for the main clinical characteristics of each of these four groups.

Descriptive statistics were performed to present the clinical characteristics of the selected patients. To analyze contingency tables Fisher's exact or chi-squared tests were used, as appropriate.

Time-dependent variables were estimated with Kaplan-Meier method and compared with log-rank test. Multivariable analyses were performed with Cox proportional hazard methods. Statistical analyses were performed using SAS® OnDemand for Academics. Statistical significance was set at 0.05.

The conduction of this retrospective study was approved by the Institutional Ethical Committee on 22/12/2021 (local study identifier INT 270-21).

3 Results

3.1 Natural history according to HER2 status

We identified 74 R/M AR-positive SGC patients, with a median follow-up of 36.18 months (95% CI 30.19-42.66). HER2 status was available in 62 cases (84%). The prevalence of HER2-positive disease was 42% (26 patients), and the main clinical characteristics of the study population are reported in Table 1.

DFI and OS (both from primary and from R/M) were significantly shorter in HER2-positive SGC patients than in HER2-negative subjects (Table 1, Figure 1). In patients with HER2-positive disease, HR for disease recurrence (vs. HER-negative) was 2.97 (95% CI 1.44-6.1, p=0.003). HR for death from R/M disease was 3.22 (95% CI 1.39-7.49) in HER2-positive vs. negative SGC patients (p=0.007).

Nineteen patients (31%) did not receive a loco-regional treatment due to the metastatic disease at presentation. In the R/M setting, androgen deprivation therapy (ADT) was administered in 79% of patients overall (89% of HER2-negative vs. 65% of HER-positive patients, p=0.032). An anti-HER2 directed treatment was administered in 27% of HER-positive SGC patients. Systemic targeted treatments were delivered in three HER-negative cases, one within a clinical trial (olaparib followed by palbociclib), two owed to the evidence of actionable tumor mutations (1 tipifarnib for *HRAS* mutation, 1 dabrafenib and trametinib for *BRAF* mutation).

Further details about treatments are reported in Table 1.

3.2 CNS metastases

Compared with patients with HER2-negative SGCs, the HER2-positive group showed a trend towards higher prevalence of CNS metastases: 40% (10) vs. 24% (9) (p=0.263). Three cases (all HER2-positive) presented with CNS metastases at diagnosis, while in the remaining sixteen cases (7 HER2-positive, 9 HER2-negative) CNS involvement was found at least 6 months after the diagnosis of primary tumor. In these cases, there was a non-statistically significant trend (p=0.083) towards a shorter TTCNS in HER2-positive subjects (Table 1). Compared to HER2-negative disease, in HER-positive SGC patients HR for CNSmfs was 2.88 (95% CI 0.87-6.97, p=0.089), and HR for TTCNS was 2.59 (95% CI 0.85-7.87, p=0.094).

The 5-year CNSmfs was 57% in HER2-positive vs. 79% in HER2-negative SGC patients (p=0.08, median CNSmfs not reached in both cohorts).

Independently of HER2 status, no statistically significant difference was found between SGC patients without CNS metastases and those developing CNS disease, in terms of median OS from the diagnosis of primary tumor: 94.31 months (95% CI 47.6-NR) vs 43.52 months (95% CI 24.41-NR), respectively (p=0.125). Further details about outcomes stratified according to both HER2 status and CNS disease are reported in Supplementary Table 1.

At bivariate analysis considering HER2 status (positive vs. negative) and CNS disease (occurrence of CNS disease ever vs. never), HER2 maintained an independent prognostic significance (HR for OS from primary 4.34, 95% CI 1.71-11.06, p=0.002) and CNS disease status did not (p=0.198, Table 2).

At diagnosis of CNS disease, all patients were treated with CNS lesions radiotherapy (RT), with the exception of two cases (one HER2-positive and one HER-2 negative) who were diagnosed with CNS metastases during systemic treatment for R/M disease. Of note, the patient with HER-2 amplified SGC was on treatment with ADT, at CNS disease (>5 lesions) onset he was treated with chemotherapy, but eventually died after 2 months. The subject with HER-2 negative disease was diagnosed with 2 brain lesions while on ADT, continued hormone therapy beyond progression, and is still alive with stable CNS disease after 13 months from the diagnosis of CNS metastases, at the time of study analysis.

Descriptive analyses on clinical characteristics, treatments, and outcomes in the different clinical scenarios are reported in Supplementary Tables 2 and 3. No statistical analyses were performed due to the limited sample size and number of events in each subgroup.

The majority (68%, n.13) received either stereotactic brain RT (SBRT) or Cyberknife radiosurgery, while 7 cases (37%) received whole brain RT (WBRT).

All the 12 patients developing CNS lesions after metastatic disease (with or without loco-regional SGC at diagnosis) received at least one line of palliative systemic treatment.

After the diagnosis of CNS disease, systemic treatments were administered in 17 cases (89%), while the remaining two cases underwent best supportive care (BSC).

Within the group of 12 patients with unavailable HER2 status only one was found with a CNS metastasis, after 17 months from the diagnosis of the primary SGC. He was treated with two lines of hormone treatment and the single CNS metastasis was treated with Cyberknife radiosurgery.

10.3389/fonc.2022.1096068

TABLE 1 Patient characteristics.

	General	HER2-positive	HER2-negative	p value
Number	62	26 (42%)	36 (58%)	-
Sex				
M	60 (97%)	25 (96%)	35 (97%)	1.0*
F	2 (3%)	1 (4%)	1 (3%)	
Median age	62 years (range 27-78)	57.5 years (range 27-74)	61.5 years (range 39-78)	0.074**
Histologic type				
SDC	51 (82%)	23 (88%)	28 (78%)	0.332*
Adenoca NOS	11 (18%)	3 (12%)	8 (22%)	
Previous condition				
Yes	12 (19%)	4 (15%)	8 (22%)	
RT-induced	8 (13%)	1 (4%)	7 (19%)	
NPC	4	1	3	
Lymphoma	3	–	3	0.746
Other HNSCC	1	–	1	(yes vs. no)*
Ex pleom. ad.	3 (5%)	2 (8%)	1 (3%)	
Pregnancy	1 (2%)	1 (4%)	–	
No	50 (81%)	22 (85%)	28 (78%)	
Treatments				
LR treatment	19 (31%)	11 (42%)	8 (22%)	0.104
None	5 (8%)	3 (12%)	2 (6%)	(yes vs. no)*
Surgery	21 (34%)	6 (23%)	15 (42%)	
Surgery-RT	17 (27%)	6 (23%)	11 (31%)	0.119 (0 vs. ≥ 1)*
Surgery-CRT	7 (11%)	5 (19%)	2 (6%)	
RM disease	20 (32%)	8 (31%)	12 (33%)	0.032 (ADTvs.
Lines of systemic treatments	30 (48%) 5 (8%)	11 (42%) 2 (8%)	19 (53%) 3 (8%)	never ADT)*0.312 (yes vs. no)*
0	49 (79%)	17 (65%)	32 (89%)	
1	36 (58%)	14 (54%)	22 (61%)	
2-3	7 (11%)	7 (27%)	0	
≥4	3 (5%)	0	3 (8%)	
Treatments ADT CT Anti-HER2 Other targeted therapy Palliative RT	23 (37%)	9 (35%)	14 (39%)	
CNS metastases				
Yes	19 (31%)	10 (38%)	9 (25%)	0.278*
No	43 (69%)	16 (62%)	27 (75%)	
Median survival				***
DFI	16.33 months	12.11 months	19.28 months	0.002

(Continued)

TABLE 1 Continued

	General	HER2-positive	HER2-negative	p value
Number	62	26 (42%)	36 (58%)	-
CNSmfs TTCNS	(95% CI 11.57-19.47) NR (95% 62.9-NR)	(95% CI 5.92-15.19) NR (95% 19.15-NR)	(95% CI 15.56-23.09) NR (95% 62.9-NR)	0.08 0.083
OS from primary	19.87 months	18.02 months	27.8 months	0.0007
OS from R/M	(95% CI 14.8-29.24)	(95% CI 5.92-24.64)	(95% CI 12.04-62.89)	0.004
OS from CNS mets	74.48 months (95% CI 46.05-NR) 46.74 months (95% CI 31.32-NR) 18.26 months (95% CI 9.61-NR)	43.52 months (95% CI 20.76-47.6) 25.66 months (95% CI 18.88-32.4) 11.51 months (95% CI 2.11-18.26)	115.79 months (95% CI 58.32-NR) 52.96 months (95% CI 35.99-NR) 23.36 months (95% CI 0.49-NR)	0.133

Adenoca NOS, adenocarcinoma not otherwise specified; CI, confidence interval; CNS, central nervous system; CNSmfs, CNS metastasis-free survival; DFI, disease-free interval; Ex pleom. ad., ex pleomorphic adenoma; F, female; HNSCC, head and neck squamous cell carcinoma; M, male; NR, not reached; OS from primary, overall survival measured from the date of diagnosis of primary tumor; OS from R/M, overall survival measured from the date of diagnosis of recurrent/metastatic tumor; OS from CNS mets, overall survival measured from the date of diagnosis of CNS metastases; RT-induced, radiation-induced; SDC, salivary duct carcinoma.
* Fisher's exact test.
** Mann-Whitney test.
*** log-rank test.

4 Discussion

This retrospective study describes clinicopathological characteristics and outcomes in a cohort of patients with R/M AR-positive SDC and adenocarcinoma NOS according to HER2 status, with a particular focus on CNS metastasis.

HER2 overexpression has been associated with poor prognosis in patients with breast and gastric cancers (18) but its prognostic role remains controversial in SGC.

In line with some prior evidences (14, 15), the current study confirmed HER2 overexpression to be associated with worse outcomes in SGC. A higher risk of recurrence and death was reported in the AR-positive/HER2-positive compared to AR-positive/HER2-negative cohort: DFI and OS (both from primary and from R/M) were significantly shorter (mDFI 12.11 m vs 19.28 m p=0.002; mOS from primary 43.52 m vs 115.79 m p=0.0007; mOS from R/M 25.66 m vs 52.96 m p=0.004 respectively). In patients with HER2-positive disease (vs HER2-negative), HR for disease recurrence was 2.97 (95% CI 1.44-6.1, p=0.003) and HR for death from R/M disease was 3.22 (95% CI 1.39-7.49, p=0.007).

Nevertheless, in other previous studies HER2-overexpression was not related to worse prognosis (19), including a recently published retrospective analysis of 200 patients with SDC and adenocarcinoma NOS treated at the MD Anderson Cancer Center. Although no direct comparisons can be made between retrospective case series published at different Institutions, that study and the present one differ from each other for several reasons. In the US study, only 77% of patients had AR-positive disease, and all disease stages were included (i.e., patients with potentially curable disease at diagnosis or with metastatic disease upfront). In our case series, we included patients with R/M only, not all comers, because only those subjects are treated with antiandrogen or anti-HER2 agents, with the exception of patients receiving off label adjuvant therapy after loco-regional treatments.

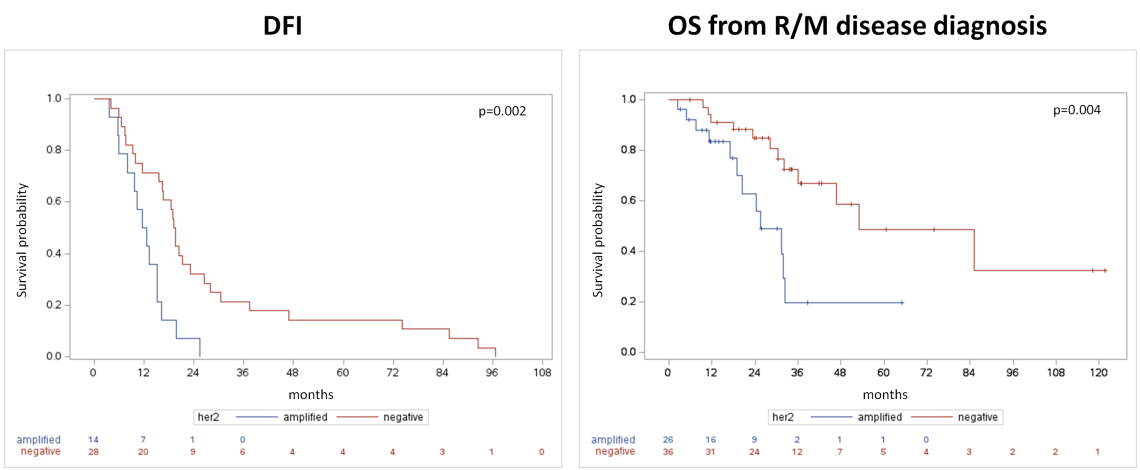

FIGURE 1
Disease-free interval from primary tumor diagnosis (left panel) and overall survival from the occurrence of recurrent/metastatic disease (right panel).

TABLE 2 Bivariate analysis for OS according to HER2 status and presence/absence of CNS disease.

	HR (95% CI)	p value
OS from primary		
HER2-pos (vs. neg)	4.34 (1.71-11.06)	0.002
CNS disease ever (vs. never)	1.76 (0.75-4.14)	0.198
OS from R/M		
HER2-pos (vs. neg)	3.12 (1.33-7.32)	0.009
CNS disease ever (vs. never)	1.63 (0.69-3.85)	0.267

CI, confidence interval; CNS, central nervous system; NR, not reached; OS from primary, overall survival measured from the date of diagnosis of primary tumor; OS from R/M, overall survival measured from the date of diagnosis of recurrent/metastatic tumor.

Moreover, in the MD Anderson study tumors were classified as HER-2 positive if they scored as 2+ or 3+ by IHC, regardless of FISH results (20). In our study, we considered only patients with R/M AR-positive disease and tumors were classified as HER2-positive only if IHC score was 3+ or 2+ with gene amplification by FISH. Even the threshold for AR-positivity was different in the two studies (positivity defined as IHC staining in ≥ 10% of tumor cells in that study versus a combined expression score obtained by summing the scores of staining intensity and extent in our dataset) selecting in our study a population with higher expression of AR and HER2. Finally, a lower prevalence of patients treated with anti-HER2 was observed in our cohort (27%) when compared to the MD Anderson experience. Indeed, in the cited article, more than half (17/32) of HER2-positive SGC patients requiring a first-line systemic therapy were treated with at least one line of anti-HER2-based regimen (10 in first line) (20). Although no direct comparisons can be made between that retrospective series and ours, it is likely that the different regulatory and reimbursement agencies and laws between the US and European Countries might have impacted on this different prevalence.

Thus, the difference between groups with/without AR/HER2 molecular alterations might have become more evident in the present study population. Furthermore, in breast cancer, AR was shown to play an important role in promoting the growth of HER2-positive disease by a functionally significant cross-talk with the HER2 signaling (21).

In our study, a non-statistically significant trend towards a higher risk of CNS metastasis, with shorter CNSmfs (HR 2.88 [95% CI 0.87-6.97]; p=0.089) emerged in HER2-positive compared to HER2-negative cohort. As expected, regardless of HER2 status, the outcomes of patients with CNS metastases were worse than those observed in those without CNS metastases (mOS 43.52m vs 94.31m, although not significant, p=0.125). Nevertheless, after adjustment according to HER2 status, the presence of CNS metastases did not seem to be prognostic *per se*, since this variable lost its prognostic significance at bivariate analysis, while HER2 status did not. This might be explained by the worse prognosis of HER2-amplified SGCs, as known from the literature and as observed in our series. In fact, in the case of neurological involvement, TTCNS (p=0.083) and OS (p=0.133) were shorter, though not significant, also in the HER2-positive group.

It should be noted that only 27% of HER2-positive patients received an anti-HER2 directed treatment, as most patients were treated from 2010 to 2021 when none of these drugs were available for use in clinical practice in Italy. This finding confirms poor outcomes in HER2-positive SGC patients especially if not treated with targeted therapy, as we assume that an additional benefit in clinical outcomes is to be expected by a targeted agent as suggested by recent data (8, 9, 11–13).

In our analysis, there were no statistically significant differences in the clinical characteristics between HER2-positive and HER2-negative populations, but we found a trend for HER2-positive to be younger, less frequently affected by adenocarcinoma NOS, and more frequently affected by CNS metastases. This latter finding resembles the clinical behavior of HER2-positive breast cancer, as confirmed by a recent study of the Unicancer Epidemiological Strategy and Medical Economics (ESME) metastatic breast cancer (MBC) database (n = 16,701): 24.6% of the patients developed brain metastasis, and the risk was higher for patients with HER2-positive/hormone receptor (HR)-negative and triple-negative (TNBC) breast cancer (22).

All these findings confirm the importance of assessing the HER2 status always at diagnosis of SDC and adenocarcinoma NOS, because of its prognostic role, and it should guide the treatment choice, as recommended by major guidelines (23, 24).

With the limit of a small sample size, we observed a 8% prevalence of CNS metastases even in the group with unavailable HER2 status. This underlines the importance to assess a prompt CNS staging at diagnosis in HER2-positive disease and during the follow-up in any AR-positive SGC, even if it does not seem to impact prognosis per se in our bivariate analysis. Further studies are needed to confirm this suggestion, similarly to the current studies on this subject in breast disease. In fact, despite compelling evidence, in HER2 breast cancer, the upfront screening for CNS disease is currently not recommended, due to a lack of data supporting its benefit in terms of overall survival (25). Therefore, the potential benefit from proactive screening strategies in selected patients with increased risk for CNS metastases is being studied in ongoing clinical trials (NCT03881605, NCT03617341, NCT04030507).

In our study, only patients with AR-positive disease were studied, and in this setting the HER2 status was prognostic. This points out the need for more effective treatments for patients with SGC harboring both AR and HER2 overexpression. A retrospective study on SDC or AR-positive adenocarcinoma NOS reported an objective response rate (ORR) to ADT of 55% in the first-line setting and 16.7% for subsequent lines (26), suggesting that ADT as first-line therapy provides a relevant clinical benefit in this setting. Given the encouraging activity in HER2-positive SGC with HER2-targeted therapies (8–10, 12, 27), we can speculate that adding HER2-blockade to ADT may improve survival outcomes. In this scenario,

interestingly, recent *in vitro* experiments showed that enzalutamide, an anti-androgen drug, inhibits the growth of HER2 breast cancer cells (21). This suggests that the activity of AR inhibition might be anticipated in HER2-positive SGCs, even independently of HER2 inhibitors. Clinical trials focused on AR-positive/HER2-positive SGC patients are needed to evaluate this suggestion.

There are some study limitations that need to be considered. This is a retrospective study performed at a single institution. Moreover, in 16% of the case series HER2 status was not available, and this may have produced a bias in the analyses. This lack of information in 12 subjects is mainly due to the fact that this case series was analyzed by collecting consecutive patients treated at our Institution from 2010 to 2021, and the first robust evidence of the activity of anti-HER2 agents in HER2-amplified R/M SGC patients was published in 2019. Therefore, at the time the first patients included in this article were on treatment at our Institution, neither trastuzumab nor any other anti-HER2 drugs were formally approved yet for R/M SGC patients worldwide.

A strength of this study is the number of patients, which is significant for a monocentric cohort of patients with recurrent/metastatic disease only affected by such a rare tumor. Collaborative ongoing efforts such as EURACAN could provide a platform to further investigate these rare entities. Furthermore, only a minority of HER2-positive patients received anti-HER2 drugs, which are known to have an impact on the response of CNS metastases.

5 Conclusions

This study focuses on CNS metastases in SDC and adenocarcinoma NOS patients, suggesting possible connections with HER2 status. Further studies are needed to confirm our findings and to investigate the clinical benefit of tackling the two biological pathways in patients affected by these rare and aggressive malignancies.

Data availability statement

Since the data of this article include sensitive data, they will be made available upon reasonable request to the corresponding Author.

Ethics statement

The studies involving human participants were reviewed and approved by Fondazione IRCCS Istituto Nazionale dei Tumori, Milan, Italy. Written informed consent for participation was not required for this study in accordance with the national legislation and the institutional requirements.

Author contributions

SC and LL contributed to conception and design of the study. PQ reviewed all histological specimens. All authors contributed to data collection and curation. SC organized the database and performed the statistical analysis. SC and IN wrote the first draft of the manuscript. SC, IN, LL, CR, and AO wrote sections of the manuscript. All authors contributed to the article and approved the submitted version.

Conflict of interest

LL declares the following conflicts of interest: research funds donated directly to the institute for clinical trials from Astrazeneca, BMS, Boehringer Ingelheim, Celgene International, Eisai, Exelixis, Debiopharm International SA, Hoffmann-La Roche ltd, IRX Therapeutics, Medpace, Merck-Serono, MSD, Novartis, Pfizer, Roche, Buran; occasional fees for participation as a speaker at conferences/congresses or as a scientific consultant for advisory boards from Astrazeneca, Bayer, MSD, Merck-Serono, AccMed, Neutron Therapeutics, Inc. CR declares honoraria from SunPharma.

The remaining authors declare that the research was conducted in the absence of any commercial or financial relationships that could be construed as a potential conflict of interest.

Publisher's note

Supplementary material

The Supplementary Material for this article can be found online at: https://www.frontiersin.org/articles/10.3389/fonc.2022.1096068/full#supplementary-material

References

1. El-Naggar AK, Chan JKC, Grandis JR, Takata T, Slootweg PJ *WHO classification of head and neck tumours. 4th ed.* Fourth edi. Lyon, France: WHO - IARC (2017).

2. Cavalieri S, Platini F, Bergamini C, Resteghini C, Galbiati D, Bossi P, et al. Genomics in non-adenoid cystic group of salivary gland cancers: one or more druggable entities? *Expert Opin Investig Drugs* (2019) 28:435–43. doi: 10.1080/13543784.2019.1598376

3. Egebjerg K, Harwood CD, Woller NC, Kristensen CA, Mau-Sørensen M. HER2 positivity in histological subtypes of salivary gland carcinoma: A systematic review and meta-analysis. *Front Oncol* (2021) 11:693394/BIBTEX. doi: 10.3389/FONC.2021.693394/BIBTEX

4. Bishop JA, Thompson LDR, Wakely PEJ, Weinreb I. *AFIP atlas: tumors of the salivary glands (fifth series, vol. 5).* ARP Press Arlington, Virginia, USA (2021).

5. Locati LD, Perrone F, Cortelazzi B, Lo Vullo S, Bossi P, Dagrada G, et al. Clinical activity of androgen deprivation therapy in patients with metastatic/relapsed androgen receptor-positive salivary gland cancers. *Head Neck* (2016) 38:724–31. doi: 10.1002/hed.23940

6. Androgen Deprivation Therapy in Advanced Salivary Gland Cancer-ClinicalTrials.gov. Available at: https://clinicaltrials.gov/ct2/show/NCT01969578 [January 9, 2023].

7. Locati LD, Perrone F, Cortelazzi B, Imbimbo M, Bossi P, Potepan P, et al. Activity of abiraterone in rechallenging two AR-expressing salivary gland adenocarcinomas, resistant to androgen-deprivation therapy. *Cancer Biol Ther* (2014) 15:678–82. doi: 10.4161/cbt.28410

8. Takahashi H, Tada Y, Saotome T, Akazawa K, Ojiri H, Fushimi C, et al. Phase II trial of trastuzumab and docetaxel in patients with human epidermal growth factor receptor 2-positive salivary duct carcinoma. *J Clin Oncol* (2019) 37:125–34. doi: 10.1200/JCO.18.00545

9. Lee J, Park S, Jung HA, Lee S-H, Seo S, Kim S-B, et al. Phase II study of trastuzumab-pkrb and docetaxel anhydrous combination therapy in recurrent or metastatic salivary ductal carcinomas (KCSG HN18-08/KM11). *J Clin Oncol* (2022) 40:6018–8. doi: 10.1200/JCO.2022.40.16_SUPPL.6018

10. Kurzrock R, Bowles DW, Kang H, Meric-Bernstam F, Hainsworth J, Spigel DR, et al. Targeted therapy for advanced salivary gland carcinoma based on molecular profiling: results from MyPathway, a phase IIa multiple basket study. *Ann Oncol Off J Eur Soc Med Oncol* (2020) 31:412–21. doi: 10.1016/j.annonc.2019.11.018

11. Li BT, Shen R, Offin M, Buonocore DJ, Myers ML, Venkatesh A, et al. Ado-trastuzumab emtansine in patients with HER2 amplified salivary gland cancers (SGCs): Results from a phase II basket trial. . *J Clin Oncol* (2019) 37:6001–1. doi: 10.1200/jco.2019.37.15_suppl.6001

12. Jhaveri KL, Wang XV, Makker V, Luoh SW, Mitchell EP, Zwiebel JA, et al. Ado-trastuzumab emtansine (T-DM1) in patients with HER2-amplified tumors excluding breast and gastric/gastroesophageal junction (GEJ) adenocarcinomas: results from the NCI-MATCH trial (EAY131) subprotocol q. *Ann Oncol* (2019) 30:1821–30. doi: 10.1093/ANNONC/MDZ291

13. Bando H, Kinoshita I, Modi S, Tsurutani J, Bang Y-J, Iwata H, et al. Trastuzumab deruxtecan (T-DXd) in patients with human epidermal growth factor receptor 2 (HER2)-expressing salivary duct carcinoma: Subgroup analysis of two phase 1 studies. *J Clin Oncol* (2021) 39:6079–9. doi: 10.1200/JCO.2021.39.15_SUPPL.6079

14. Takase S, Kano S, Tada Y, Kawakita D, Shimura T, Hirai H, et al. Biomarker immunoprofile in salivary duct carcinomas: Clinicopathological and prognostic implications with evaluation of the revised classification. *Oncotarget* (2017) 8:59023–35. doi: 10.18632/oncotarget.19812

15. Santana T, Pavel A, Martinek P, Steiner P, Grossmann P, Baněčková M, et al. Biomarker immunoprofile and molecular characteristics in salivary duct carcinoma: clinicopathological and prognostic implications. *Hum Pathol* (2019) 93:37–47. doi: 10.1016/j.humpath.2019.08.009

16. Garcia-Alvarez A, Papakonstantinou A, Oliveira M. Brain metastases in HER2-positive breast cancer: Current and novel treatment strategies. *Cancers 2021 Vol 13 Page 2927* (2021) 13:2927. doi: 10.3390/CANCERS13122927

17. Ghidini M, Petrelli F, Hahne JC, De Giorgi A, Toppo L, Pizzo C, et al. Clinical outcome and molecular characterization of brain metastases from esophageal and gastric cancer: a systematic review. *Med Oncol* (2017) 34:1–10. doi: 10.1007/S12032-017-0919-0/TABLES/2

18. Hennigs A, Riedel F, Gondos A, Sinn P, Schirmacher P, Marmé F, et al. Prognosis of breast cancer molecular subtypes in routine clinical care: A large prospective cohort study. *BMC Cancer* (2016) 16:1–9. doi: 10.1186/S12885-016-2766-3/FIGURES/2

19. Boon E, Bel M, van Boxtel W, van der Graaf WTA, van Es RJJ, Eerenstein SEJ, et al. A clinicopathological study and prognostic factor analysis of 177 salivary duct carcinoma patients from the Netherlands. *Int J Cancer* (2018) 143:758–66. doi: 10.1002/IJC.31353

20. Sousa LG, Wang K, Torman D, Binks BJ, Rubin ML, Andersen CR, et al. Treatment patterns and outcomes of palliative systemic therapy in patients with salivary duct carcinoma and adenocarcinoma, not otherwise specified. *Cancer* (2022) 128:509–18. doi: 10.1002/CNCR.33968

21. He L, Du Z, Xiong X, Ma H, Zhu Z, Gao H, et al. Targeting androgen receptor in treating HER2 positive breast cancer. *Sci Rep* (2017) 7(1):14584. doi: 10.1038/s41598-017-14607-2

22. Pasquier D, Darlix A, Louvel G, Fraisse J, Jacot W, Brain E, et al. Treatment and outcomes in patients with central nervous system metastases from breast cancer in the real-life ESME MBC cohort. *Eur J Cancer* (2020) 125:22–30. doi: 10.1016/J.EJCA.2019.11.001

23. Geiger JL, Ismaila N, Beadle B, Caudell JJ, Chau N, Deschler D, et al. Management of salivary gland malignancy: ASCO guideline. *J Clin Oncol* (2021) 39(17):1909–41. doi: 10.1200/jco.21.00449

24. Alfieri S, Granata R, Bergamini C, Resteghini C, Bossi P, Licitra LF, et al. Systemic therapy in metastatic salivary gland carcinomas: A pathology-driven paradigm? *Oral Oncol* (2017) 66:58–63. doi: 10.1016/j.oraloncology.2016.12.016

25. Cardoso F, Paluch-Shimon S, Senkus E, Curigliano G, Aapro MS, André F, et al. 5th ESO-ESMO international consensus guidelines for advanced breast cancer (ABC 5). *Ann Oncol* (2020) 31:1623–49. doi: 10.1016/J.ANNONC.2020.09.010/ATTACHMENT/A2F41A9B-15CE-4164-8FA7-8C2EFEC32D8B/MMC1.PDF

26. Viscuse PV, Price KA, Garcia JJ, Schembri-Wismayer DJ, Chintakuntlawar AV. First line androgen deprivation therapy vs. chemotherapy for patients with androgen receptor positive recurrent or metastatic salivary gland carcinoma–a retrospective study. *Front Oncol* (2019) 9:701/FULL. doi: 10.3389/FONC.2019.00701/FULL

27. Hainsworth JD, Meric-Bernstam F, Swanton C, Hurwitz H, Spigel DR, Sweeney C, et al. Targeted therapy for advanced solid tumors on the basis of molecular profiles: Results from mypathway, an open-label, phase IIA multiple basket study. *J Clin Oncol* (2018) 36:536–42. doi: 10.1200/JCO.2017.75.3780

frontiers | Frontiers in Oncology

TYPE Original Research
PUBLISHED 23 March 2023
DOI 10.3389/fonc.2023.1153186

OPEN ACCESS

EDITED BY
Ester Orlandi,
National Center of Oncological Hadrontherapy, Italy

REVIEWED BY
Tobias Ettl,
University Medical Center Regensburg, Germany
Davide Lombardi,
University of Brescia, Italy

*CORRESPONDENCE
Feng Han
fcchanf@zzu.edu.cn

SPECIALTY SECTION
This article was submitted to Head and Neck Cancer, a section of the journal Frontiers in Oncology

RECEIVED 29 January 2023
ACCEPTED 10 March 2023
PUBLISHED 23 March 2023

CITATION
Han F (2023) Number of positive lymph nodes affects outcomes in parotid adenoid cystic carcinoma. *Front. Oncol.* 13:1153186. doi: 10.3389/fonc.2023.1153186

Number of positive lymph nodes affects outcomes in parotid adenoid cystic carcinoma

Feng Han*

Department of Pediatric Dentistry, The First Affiliated Hospital of Zhengzhou University, Zhengzhou, Henan, China

Objectives: Survival significance of the number of positive lymph nodes (LNs) in parotid adenoid cystic carcinoma (ACC) remains unknown; thus, this study aimed to determine the impact of the number of positive LNs on the prognosis of parotid ACC.

Methods: Patients with surgically treated parotid ACC were enrolled from the SEER database. The number of positive LNs was analyzed using three models (0 vs 1+, 0 vs 1 vs 2 vs 3 vs 4 vs 4 vs 5 vs 6+, 0/1 vs 2–4 vs 5+), its hazard ratios on disease specific survival (DSS) and overall survival (OS) were assessed using univariate and multivariate Cox analyses.

Results: A total of 1,689 patients were included. In all models, the number of positive LNs was independently related to DSS and OS, model 3 had the highest C-index for DSS [0.83 (95% CI: 0.81–0.85)] and OS [0.82 (95% CI: 0.80–0.84)]. Compared with the 0/1 positive LN group, the 2–4 positive LN group had an HR of 2.81 (95% CI: 1.73–4.56) for DSS and 2.36 (95% CI: 1.58–3.54) for OS. The 5+ LN group had an HR of 20.15 (95% CI: 7.50–54.18) for DSS and 14.20 (95% CI: 5.45–36.97) for OS. No overlap existed in the 95% CI of the HR.

Conclusions: The three prognostic categories based on the number of positive LNs (0/1 vs 2–4 vs 5+) could stratify the DSS and OS in parotid ACC without overlap.

KEYWORDS

parotid gland, adenoid cystic carcinoma, number of positive lymph nodes, survival, AJCC

Introduction

Adenoid cystic carcinoma (ACC) is one of the most common malignancies among all parotid tumors. It is characterized by distant metastasis and perineural infiltration (1), making it remarkably different from other parotid cancers. Although neck nodal metastasis is relatively uncommon, it is still an important prognostic factor in parotid ACC (2). The neck nodal status for parotid cancer is currently deduced from head and neck squamous

cell carcinoma (HNSCC), which is evidently inadequate. Meanwhile, the intraparotid lymph node (LN), which significantly affects prognosis, is not taken into consideration (3, 4). On the other hand, parotid cancer exhibits distinct differences in biology from HNSCC. Contralateral neck LN metastasis is extremely rare in parotid cancer, and this staging fails to distinguish the hazard ratio (HR) of four groups in relation to the prognosis (2, 5). In other words, the 95% confidence interval (CI) of a stage overlaps with the adjacent stages.

Novel LN stagings have been proposed based on the number of positive LNs and/or LN size (6, 7), in which the systems are determined according to the different cutoffs of quantitative LN burden. Both exhibit greater concordance than the current neck nodal classification. However, the two previous studies have analyzed data comprising all major salivary gland histologic types. Thus, whether the findings could be applied for parotid ACC is uncertain.

Therefore, this study aimed to clarify the impact of the number of positive LNs on the prognosis of parotid ACC.

Patients and methods

Study design

All data was obtained from the Surveillance, Epidemiology, and End Results database, which provides information on cancer statistics to reduce the cancer burden among the United States population (8). The profiles of the patients diagnosed with parotid ACC between 2000 and 2019 were reviewed. Patients were excluded as follows: repeated patient ID; a history of other malignancy; non-surgical treatment of primary tumor; unknown number of positive LNs; and number of pathologically examined LNs is smaller than 4 (Figure 1). Information regarding age, sex, race, marital status, tumor size, tumor extension, grade, pathologic tumor stage based on the 8th American Joint Committee on Cancer (AJCC) classification, extranodal extension (ENE), distant metastasis, operation type, radiation, chemotherapy, number of positive LNs, and follow-up were extracted and analyzed.

Ethical approval was not required because the data is publicly accessible.

Variable definition

The disease grade was classified into low, moderate, and high. A low grade was defined as well differentiated; a moderate grade was defined as moderately differentiated; and a high grade was defined as poorly differentiated or undifferentiated. The tumor size was determined based on the Tumor Size Summary (2016+), Collaborative Stage tumor size (2004–2015), and extent of disease (EOD) 10-size (1988–2003). The tumor extension was defined as extracapsular invasion and evaluated based on the Derived EOD 2018 T (2018+), Collaborative Stage extension (2004–2015), and EOD 10-extent (1988–2003). The tumor stage was extrapolated based on the tumor size, tumor extension, and Derived AJCC classification. ENE was formulated based on Derived EOD 2018 N (2018+), Derived AJCC classification, RX Summ–Scope Reg LN Sur (2003+), EOD Regional Nodes (2018+), CS lymph nodes (2004–2015), and EOD 10 - nodes (1988–2003). Distant metastasis was confirmed using the Derived AJCC classification. The type of operation consisted of non-total and total parotidectomy and was decided based on the RX Summ–Surg Prim Site (1998+). The number of positive LN was calculated based on the Regional nodes examined (1988+), Regional nodes positive (1988+), and RX Summ–Scope Reg LN Sur (2003+). The time to surgery (TTS) was defined as the duration between the diagnosis and treatment.

Statistical analysis

Missing data patterns were evaluated on whether they occur at random using the method previously introduced and imputed using

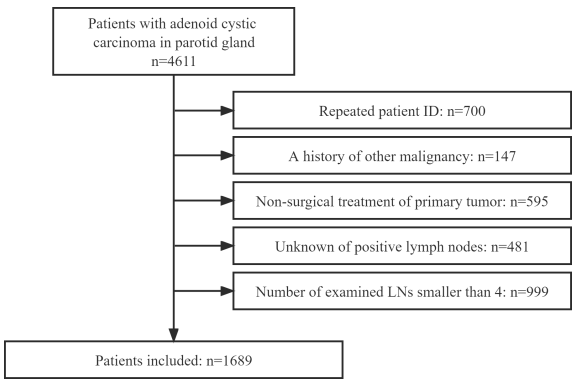

FIGURE 1
Flowchart of the enrolled patients.

multiple imputation by fully conditional specifications, which was implemented using multiple imputation by chained equations (7, 9).

The primary outcome variable was disease-specific survival (DSS) and overall survival (OS). The time of DSS was calculated from the date of surgery to the date of cancer-caused death or last follow-up. Meanwhile, the time of OS was calculated from the date of surgery to the date of overall death or last follow-up.

Three models were constructed using different cutoffs for the number of positive LNs to detect the optimal cutoff. In model 1, the impact was compared between the 0 and 1+ groups. In model 2, the impact was analyzed among the 0, 1, 2, 3, 4, 5, and 6+ groups. In model 3, the impact was determined among the 0/1, 2–4, and 5+ groups.

In all three models, estimated survival functions were generated *via* the Kaplan-Meier method and compared with the logrank test, univariate Cox analysis was used to assess the variables that affect survival significantly. Subsequently, these variables were further validated through multivariate Cox analysis for detecting independent factors. The three models were evaluated using C-index. All statistical analyses were performed using R program version 3.4.3. Statistical significance was set at $p < 0.05$ (two-sided).

Results

Baseline data

A total of 1,689 patients were included with a mean age of 52 ± 17 years, in which 665 (39.4%) were males and 1,024 (60.0%) were females. Caucasian patients accounted for 76.1% of the total population. During the initial treatment, 59.0% of the patients were married. Low-, moderate-, and high-grade disease occurred in 427 (25.3%), 611 (36.2%), and 446 (26.4%) patients, respectively. The tumor stages were distributed as T1/2 in 604 (35.8%) patients and T3/4 in 955 (56.5%) patients. ENE was present in 49 (2.9%) patients. Distant metastasis was present in 90 (5.3%) patients during diagnosis. Total parotidectomy was performed in 1,157 (68.5%) patients. A total of 1,294 (76.6%) and 107 (6.3%) patients received radiotherapy and chemotherapy, respectively.

LN metastasis occurred in 534 (31.6%) patients, in which 282 patients had one positive LN, 108 patients had two positive LNs, 62 patients had three positive LNs, 24 patients had four positive LNs, 16 patients had five positive LNs, and 42 patients had six or more positive LNs.

TABLE 1 Univariate cox analysis of the impact of clinicopathologic variables on disease specific survival.

Variable	p	HR [95%CI]
Age		
<60 (n=1072)		
60-69 (n=335)	0.260	1.15 [0.90-1.45]
70+ (n=282)	0.154	0.81 [0.61-1.08]
Sex		
Male (n=665)		
Female (n=1024)	0.867	0.98 [0.81-1.20]
Race		
White (n=1286)		
Black (n=183)	0.386	1.14 [0.84-1.55]
Others (n=220)	0.618	0.93 [0.69-1.25]
Marital		
Married (n=996)		
Single (n=328)	0.994	1.00 [0.78-1.29]
Others (365)	0.793	0.97 [0.76-1.23]
Grade		
Low (n=427)		
Moderate (n=611)	<0.001	1.89 [1.03-2.99]
High (n=446)	<0.001	2.79 [1.76-4.87]
Tumor stage		
T1+T2 (n=604)		
T3+T4 (n=955)	<0.001	1.95 [1.01-3.26]
Extranodal extension (n=49)	0.177	4.83 [0.77-19.55]
Distant metastasis (n=90)	<0.001	1.77 [1.11-2.46]
Operation type	0.491	1.08 [0.87-1.33]
Non-total (n=532)		
Total (n=1157)		
Radiotherapy (n=1294)	0.859	0.98 [0.78-1.24]
Chemotherapy (n=107)	0.076	1.40 [0.97-2.03]
TTS*(months)		
<3 (n=1422)		
3+ (n=267)	0.424	0.77 [0.41-1.47]

*TTS, time to surgery.

Univariate Cox analysis

Table 1 presents the potential predictors of DSS. Compared to low-grade disease, moderate- and high-grade disease was associated with increased one- and two-fold risk of cancer-caused death, respectively. T3/4 tumors had an HR of 1.95 (95% CI: 1.01–3.26), which was statistically higher than that in T1/2 tumors ($p < 0.001$). Distant metastasis predicted an HR of 1.77 (95% CI: 1.11–2.46) of cancer-caused death. A statistical relationship between age, sex, race, marital, ENE, operation type, radiotherapy, chemotherapy, and TTS and DSS was not noted (all $p > 0.05$).

Table 2 presents the potential predictors of OS. Compared to the younger ones, patients aged 70+ had an additional nearly three-fold risk of overall death. Both moderate- and high-grade disease statistically meant more risk of overall death than low-grade disease

TABLE 2 Univariate cox analysis of the impact of clinicopathologic variables on overall survival.

Variable	p	HR [95%CI]
Age		
<60 (n=1072)		
60-69 (n=335)	0.138	1.16 [0.95-1.42]
70+ (n=282)	<0.001	3.85 [1.58-8.09]
Sex		
Male (n=665)		
Female (n=1024)	0.663	0.96 [0.82-1.14]
Race		
White (n=1286)		
Black (n=183)	0.478	1.10 [0.86-1.42]
Others (n=220)	0.569	0.93 [0.72-1.19]
Marital		
Married (n=996)		
Single (n=328)	0.895	0.99 [0.80-1.22]
Others (365)	0.979	1.00 [0.82-1.22]
Grade		
Low (n=427)		
Moderate (n=611)	<0.001	1.27 [1.09-2.02]
High (n=446)	<0.001	2.18 [1.61-3.70]
Tumor stage		
T1+T2 (n=604)		
T3+T4 (n=955)	<0.001	2.92 [1.02-5.08]
Extranodal extension (n=49)	0.084	3.42 [0.85-13.81]
Distant metastasis (n=90)	<0.001	2.89 [1.54-5.44]
Operation type		
Non-total (n=532)		
Total (n=1157)	0.271	1.10 [0.93-1.32]
Radiotherapy (n=1294)	0.803	1.03 [0.84-1.25]
Chemotherapy (n=107)	0.081	1.33 [0.97-1.82]
TTS*(months)		
<3 (n=1422)		
3+ (n=267)	0.308	0.92 [0.77-1.08]

*TTS, time to surgery.

(both p < 0.001). T3/4 tumors had an HR of 2.92 (95% CI: 1.02–5.08), which was statistically higher than that in T1/2 tumors (p < 0.001). Distant metastasis predicted an HR of 2.89 (95% CI: 1.54–5.44) of overall death. A statistical relationship between sex, race, marital, ENE, operation type, radiotherapy, chemotherapy, and TTS and OS was not noted (all p > 0.05).

Impact of the number of positive LNs

In model 1, the presence of LN metastasis statistically decreased DSS and OS in the univariate and multivariate Cox analyses and was associated with an additional nearly two- and 1.5-fold risk for cancer-caused and overall death, respectively (Tables 3, 4). The 10-year DSS rates for patients with none and 1+ positive LN were 76% (95% CI: 72%-80%) and 52% (95% CI: 46%-58%), respectively, the difference was significant (p<0.001). The 10-year OS rates for patients with none and 1+ positive LN were 65% (95% CI: 61%-69%) and 43% (95% CI: 37%-49%), respectively, the difference was significant (p<0.001) (Figures 2A, D). The C-index for DSS and OS was 0.63 (95% CI: 0.57–0.69) and 0.64 (95% CI: 0.58–0.70), respectively.

In model 2, the univariate Cox analysis reported the statistical association between DSS/OS and the number of positive LNs. In the multivariate Cox analysis, compared with no LN metastasis, one positive LN did not provide additional compromise to DSS, while two or more positive LNs were related to worse DSS. The 10-year DSS rates of the 2, 3, and 4+ LN groups were 51% (95% CI: 41–61%), 54% (95% CI: 36–72%), and 50% (95% CI: 30–70%), respectively. Their HR was comparable, and their 95% CI greatly overlapped. In the 5 and 6+ positive LNs groups, the median DSS time was 37.0 (95% CI: 31.7–42.3) and 25.0 (95% CI: 9.3–40.6) months, respectively. Their 95% CI also apparently overlapped. As for the OS, a similar trend was observed (Tables 3, 4; Figures 2B, E). The C-index for DSS and OS was 0.77 (95% CI: 0.73–0.81) and 0.76 (95% CI: 0.75–0.78), respectively.

In model 3, the univariate Cox analysis described a statistical association between DSS/OS and the number of positive LNs. The 10-year DSS rates in the 0/1, 2–4, 5+ positive LN groups were 74% (95% CI: 70–78%), 60% (95% CI: 54–66%), and 50% (95% CI: 48–52%), respectively, the difference was significant (p<0.001). The 10-year OS rates in the 0/1, 2–4, 5+ positive LN groups were 63% (95% CI: 59–67%), 50% (95% CI: 44–56%), and 9% (95% CI: 1–17%), respectively, the difference was significant (p<0.001) (Figures 2C, F). In the multivariate Cox analysis, compared with the 0/1 positive LN group, the 2–4 positive LN group had an HR of 2.81 (95% CI: 1.73–4.56) for DSS and 2.36 (95% CI: 1.58–3.54) for OS, respectively. The 5+ LN group had an HR of 20.15 (95% CI: 7.50–54.18) for DSS and 14.20 (95% CI: 5.45–36.97) for OS, respectively (Tables 3, 4). The C-index for DSS and OS was 0.83 (95% CI: 0.81–0.85) and 0.82 (95% CI: 0.80–0.84), respectively.

Discussion

The main finding was that LN metastasis was an important prognostic factor for both DSS and OS; however, the negative impact was only observed when at least two positive LNs were present. The three prognostic categories based on the number of positive LNs (0/1 vs 2–4 vs 5+) could predict oncologic outcomes in parotid ACC without overlap and ultimately help triage high-risk patients who may benefit from more aggressive adjuvant therapies.

TABLE 3 Univariate and multivariate Cox analysis of the impact of number of positive lymph nodes on disease specific survival.

Classification	Univariate		Multivariate	
	p	HR [95%CI]	p	HR [95%CI]
Model 1				
0 (n=1155)			Ref	
1+ (n=534)	<0.001	2.60 [2.14-3.15]	<0.001	2.82 [1.82-4.37]
Model 2				
0 (n=1155)			Ref	
1 (n=282)	<0.001	2.13 [1.67-2.71]	0.379	1.53 [0.60-3.91]
2 (n=108)	<0.001	2.50 [1.83-3.43]	<0.001	2.75 [1.61-4.69]
3 (n=62)	<0.001	2.05 [1.27-3.33]	0.047	3.46 [1.08-14.33]
4 (n=24)	<0.001	3.00 [1.67-5.37]	0.045	3.34 [1.03-10.90]
5 (n=16)	<0.001	14.01 [8.07-24.31]	<0.001	15.19 [4.43-52.07]
6+ (n=42)	<0.001	5.90 [3.97-8.78]	<0.001	48.69 [10.33-229.45]
Model 3				
0/1 (n=1437)			Ref	
2-4 (n=194)	<0.001	1.92 [1.55-2.38]	<0.001	2.81 [1.73-4.56]
5+ (n=58)	<0.001	6.43 [4.62-8.94]	<0.001	20.15 [7.50-54.18]

Model 1 confirmed that LN metastasis is an independent predictor of DSS and OS. However, it referred to the metastasis of intraparotid or neck LN, both of which significantly decrease survival. Han et al. (10) analyzed the association between cervical LN involvement and OS in 54 patients and found that node status was the only independent prognostic factor. Moreover, neck LN metastasis was related to nearly an increased five-fold risk of overall death. Feng et al. (11) discussed the significance of intraparotid LN metastasis in 337 patients and reported that the 10-year local control rate was 94% for patients without intraparotid LN

TABLE 4 Univariate and multivariate Cox analysis of the impact of number of positive lymph nodes on overall survival.

Classification	Univariate		Multivariate	
	p	HR [95%CI]	p	HR [95%CI]
Model 1				
0 (n=1155)				
1+ (n=534)	<0.001	2.06 [1.75-2.42]	<0.001	2.26 [1.56-3.27]
Model 2				
0 (n=1155)				
1 (n=282)	<0.001	1.81 [1.48-2.22]	0.739	1.16 [0.50-2.69]
2 (n=108)	<0.001	1.95 [1.48-2.57]	0.029	2.37 [1.28-6.72]
3 (n=62)	0.002	1.89 [1.27-2.82]	0.001	2.16 [1.37-3.40]
4 (n=24)	0.026	1.93 [1.08-3.44]	0.001	4.12 [1.77-9.59]
5 (n=16)	<0.001	9.71 [5.64-16.72]	<0.001	10.67 [3.21-35.49]
6+ (n=42)	<0.001	3.95 [2.72-5.76]	<0.001	32.15 [7.23-143.03]
Model 3				
0/1 (n=1437)				
2-4 (n=194)	<0.001	1.69 [1.41-2.02]	<0.001	2.36 [1.58-3.54]
5+ (n=58)	<0.001	4.48 [3.27-6.14]	<0.001	14.20 [5.45-36.97]

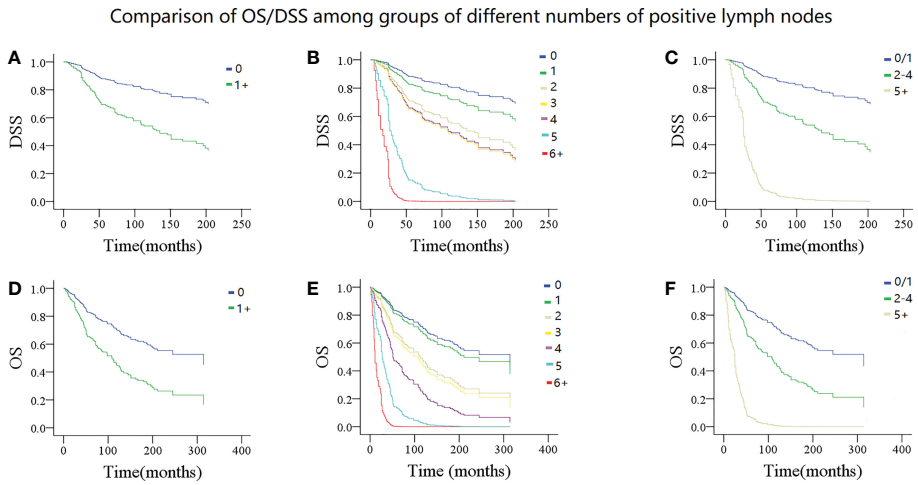

FIGURE 2
Comparison of disease specific survival (DSS) and overall survival (OS) in patients with different numbers of positive lymph nodes. DSS: **(A)** 0 vs 1+; **(B)** 0 vs 1 vs 2 vs 3 vs 4 vs 5 vs 6+; **(C)** 0/1 vs 2-4 vs 5+; OS: **(D)** 0 vs 1+; **(E** 0 vs 1 vs 2 vs 3 vs 4 vs 5 vs 6+; **(F)** 0/1 vs 2-4 vs 5+.

metastasis, 56% for patients with metastasis in no more than two intraparotid LNs, and 22% for patients with metastasis in more than two intraparotid LNs. Moreover, the differences were statistically significant independently. However, model 1 could not explain the effect of LN metastasis on survival as stratified through numbers accurately.

Model 2 provided a more interesting finding. Firstly, this was the first to report that the presence of only one positive LN did not pose any additional compromise in survival compared with the absence of LN metastasis. In many solid cancers, prognosis would be decreased by up to half although there was only one positive LN (12). The obvious difference might be accounted by the unique features of ACC, and that the common cause of death was distant metastasis rather than regional LN metastasis (13). Moreover, LN metastasis was relatively infrequent in ACC (14). This finding offered new insights into the clinical management of parotid ACC. Secondly, the negative impact of LN metastasis on DSS or OS began to appear when there was at least two positive LNs, and the effect did not increase significantly although four positive LNs were detected. A few studies aimed to clarify how different numbers of positive LNs affect survival in ACC. Liu et al. (15) analyzed the outcome of 47 patients with pN+ ACC in the head and neck. They found that in cases with one, two to three, and four positive LNs, the 5-year OS rates were 86.6%, 66.3%, and 60.0%, respectively, and the difference was not significant. This difference from the current study could be contributed by their small sample size and different cutoff values. However, another study reported that a positive LN ratio greater than 0.2 was associated with poorer metastasis-free survival, and a ratio > 0.07 predicted worse DSS (16). However, the ratio was greatly decided by the dissection of the LN, which may be influenced by several uncontrollable factors. Moreover, the method of LN examination varied among different medical centers, and the number, as a variable, was likely to be more stable than the ratio. Thirdly, DSS and OS were greatly inhibited if five or six or more positive LNs were present, and the 95% CI of the survival rates and HR of the two groups apparently overlapped. A study which focused on salivary duct carcinoma (17) reported that the presence of nine or more positive LNs had increased the nearly 11-fold risk of overall death compared to eight or less positive LNs. They also reported in another study that patients with five or more positive LNs were significantly at higher chance of developing cancer-caused death in major salivary gland carcinoma (18).

Model 3 offered the best predictive value for DSS and OS. Its cutoff was determined based on models 1 and 2 with high rationality and reliability, and the three groups had distinct, non-overlapping prognosis and HR. Only a few studies aimed to propose a new LN staging system that will be beneficial for clinical practice. In a study consisting of 307 patients treated for salivary gland carcinoma (6), ENE did not exhibit any negative impact on DSS, OS, locoregional recurrence, or distant metastasis. Moreover, the neck stage based on the 8th AJCC classification could not present a satisfactory OS stratification. However, the new LN system, which was developed based on the number of positive LNs (0 vs 1–3 vs 4+) and/or their maximum diameter (< 20 mm vs 20+ mm) showed better accuracy in OS prediction. In another similar study (7), ENE was also not related to worse OS, and a four-category LN staging system according to the number of positive LNs (0 vs 1–2 vs 3–21 vs 22+) was superior to the current N classification at OS stratification. Boon et al. (19) evaluated the results of 177 patients with salivary duct carcinoma and reported that the absolute number of metastatic LNs (0 vs 1–2 vs 3–15 vs 16+), rather than the traditional cervical stage, was the only significant prognostic factor for OS as shown by the results of a multivariate analysis.

Therefore, four key points could be deduced: (1) ENE may demonstrate little influence on survival; (2) intraparotid LN should be taken into consideration in nodal staging; (3) an LN staging based on the number of positive LNs could be a good surrogate for the current system; and (4) the optimal cutoff for the number of positive LNs varied with the histologic type. Our three prognostic categories provided an accurate discrimination for low-, moderate-, and high-risk patients and could be used as a central predictor of mortality in parotid ACC.

Nevertheless, this study still has some limitations. First, this was a retrospective study; hence, there may be inherent bias. Second, data on lymphovascular invasion and margin status were not available. Third, we only enrolled patients with parotid ACC, it remained unknown whether current finding was suitable for parotid cancers of other histologic types.

In summary, LN metastasis significantly impacts survival in parotid ACC; however, the effect is not apparent until at least two positive LNs are present. Our three prognostic categories based on the number of positive LNs (0/1 vs 2–4 vs 5+) could be used to screen patients with different risks and plan for more aggressive treatment for high-risk patients.

Data availability statement

The datasets presented in this study can be found in online repositories. The names of the repository/repositories and accession number(s) can be found in the article/supplementary material.

Ethics statement

Ethics approval was not required owing to public access of the data.

Author contributions

The author confirms being the sole contributor of this work and has approved it for publication.

Conflict of interest

The author declares that the research was conducted in the absence of any commercial or financial relationships that could be construed as a potential conflict of interest.

Publisher's note

References

1. Fang Y, Peng Z, Wang Y, Gao K, Liu Y, Fan R, et al. Current opinions on diagnosis and treatment of adenoid cystic carcinoma. *Oral Oncol* (2022) 130:105945. doi: 10.1016/j.oraloncology.2022.105945

2. Amit M, Binenbaum Y, Sharma K, Ramer N, Ramer I, Agbetoba A, et al. Incidence of cervical lymph node metastasis and its association with outcomes in patients with adenoid cystic carcinoma. *Int Collab study. Head Neck.* (2015) 37:1032–7. doi: 10.1002/hed.23711

3. Fang Q, Wu J, Du W, Zhang X. Predictors of distant metastasis in parotid acinic cell carcinoma. *BMC Cancer.* (2019) 19:475. doi: 10.1186/s12885-019-5711-4

4. Niu X, Fang Q, Liu F. Role of intraparotid node metastasis in mucoepidermoid carcinoma of the parotid gland. *BMC Cancer.* (2019) 19:417. doi: 10.1186/s12885-019-5637-x

5. de Morais EF, da Silva LP, Moreira DGL, Mafra RP, Rolim LSA, de Moura Santos E, et al. Prognostic factors and survival in adenoid cystic carcinoma of the head and neck: A retrospective clinical and histopathological analysis of patients seen at a cancer center. *Head Neck Pathol* (2021) 15:416–24. doi: 10.1007/s12105-020-01210-7

6. Lombardi D, Tomasoni M, Paderno A, Mattavelli D, Ferrari M, Battocchio S, et al. The impact of nodal status in major salivary gland carcinoma: A multicenter experience and proposal of a novel n-classification. *Oral Oncol* (2021) 112:105076. doi: 10.1016/j.oraloncology.2020.105076

7. Aro K, Ho AS, Luu M, Kim S, Tighiouart M, Clair JM, et al. Development of a novel salivary gland cancer lymph node staging system. *Cancer* (2018) 124:3171–80. doi: 10.1002/cncr.31535

8. Available at: https://seer.cancer.gov/.

9. Ho AS, Kim S, Tighiouart M, Gudino C, Mita A, Scher KS, et al. Metastatic lymph node burden and survival in oral cavity cancer. *J Clin Oncol* (2017) 35:3601–9. doi: 10.1200/JCO.2016.71.1176

10. Han N, Ong H, Liu Z, Ruan M, Yang W, Zhang C. Lymph node involvement predicts poor prognosis in primary tongue adenoid cystic carcinoma: A preliminary study of 54 cases. *J Craniomaxillofac Surg* (2017) 45:589–94. doi: 10.1016/j.jcms.2017.01.012

11. Feng Y, Liu F, Cheng G, Fang Q, Niu X, He W. Significance of intraparotid node metastasis in predicting local control in primary parotid cancer. *Laryngoscope* (2019) 129:2309–12. doi: 10.1002/lary.27701

12. Obinu A, Gavini E, Rassu G, Maestri M, Bonferoni MC, Giunchedi P. Lymph node metastases: Importance of detection and treatment strategies. *Expert Opin Drug Deliv.* (2018) 15:459–67. doi: 10.1080/17425247.2018.1446937

13. Chang CF, Hsieh MY, Chen MK, Chou MC. Adenoid cystic carcinoma of head and neck: A retrospective clinical analysis of a single institution. *Auris Nasus Larynx.* (2018) 45:831–7. doi: 10.1016/j.anl.2017.10.009

14. Zocchi J, Campa M, Bianchi G, Iocca O, Di Maio P, Petruzzi G, et al. Occult neck metastases in head and neck adenoid cystic carcinoma: A systematic review and meta-analysis. *J Clin Med* (2022) 11:4924. doi: 10.3390/jcm11164924

15. Liu Z, Fang Z, Dai T, Zhang C, Sun J, He Y. Higher positive lymph node ratio indicates poorer distant metastasis-free survival in adenoid cystic carcinoma patients with nodal involvement. *J Craniomaxillofac Surg* (2015) 43:751–7. doi: 10.1016/j.jcms.2015.03.040

16. Wo Y, Li S, Wang Y, Lu T, Qin Y, Sun X, et al. Predictors of nodal metastasis and prognostic significance of lymph node ratio and total lymph node count in tracheobronchial adenoid cystic carcinoma. *Cancer Manag Res* (2018) 10:5919–25. doi: 10.2147/CMAR.S182069

17. Qian K, Di L, Guo K, Zheng X, Ji Q, Wang Z. Cervical lymph node metastatic status and adjuvant therapy predict the prognosis of salivary duct carcinoma. *J Oral Maxillofac Surg* (2018) 76:1578–86. doi: 10.1016/j.joms.2018.01.033

18. Qian K, Sun W, Guo K, Zheng X, Sun T, Chen L, et al. The number and ratio of positive lymph nodes are independent prognostic factors for patients with major salivary gland cancer: Results from the surveillance, epidemiology, and end results dataset. *Eur J Surg Oncol* (2019) 45:1025–32. doi: 10.1016/j.ejso.2018.11.008

19. Boon E, Bel M, van Boxtel W, van der Graaf WTA, van Es RJJ, Eerenstein SEJ, et al. A clinicopathological study and prognostic factor analysis of 177 salivary duct carcinoma patients from the Netherlands. *Int J Cancer.* (2018) 143:758–66. doi: 10.1002/ijc.31353

frontiers | Frontiers in Oncology

TYPE Original Research
PUBLISHED 15 June 2023
DOI 10.3389/fonc.2023.1185198

OPEN ACCESS

EDITED BY
Stefano Cavalieri,
(IRCCS), Italy

REVIEWED BY
Nerina Denaro,
IRCCS Ca 'Granda Foundation Maggiore Policlinico Hospital, Italy
Danilo Galizia,
IRCCS Candiolo Cancer Institute, Italy

*CORRESPONDENCE
Makoto Tahara
matahara@east.ncc.go.jp

RECEIVED 13 March 2023
ACCEPTED 09 May 2023
PUBLISHED 15 June 2023

CITATION
Onaga R, Enokida T, Ito K, Ueda Y, Okano S, Fujisawa T, Wada A, Sato M, Tanaka H, Takeshita N, Tanaka N, Hoshi Y and Tahara M (2023) Combination chemotherapy with taxane and platinum in patients with salivary gland carcinoma: a retrospective study of docetaxel plus cisplatin and paclitaxel plus carboplatin. *Front. Oncol.* 13:1185198. doi: 10.3389/fonc.2023.1185198

Combination chemotherapy with taxane and platinum in patients with salivary gland carcinoma: a retrospective study of docetaxel plus cisplatin and paclitaxel plus carboplatin

Ryutaro Onaga[1], Tomohiro Enokida[1], Kazue Ito[1,2], Yuri Ueda[1,3], Susumu Okano[1], Takao Fujisawa[1], Akihisa Wada[1,4], Masanobu Sato[1], Hideki Tanaka[1], Naohiro Takeshita[1], Nobukazu Tanaka[1], Yuta Hoshi[1] and Makoto Tahara[1]*

[1]Department of Head and Neck Medical Oncology, National Cancer Center Hospital East, Kashiwa, Japan, [2]Department of Head and Neck Oncology, Miyagi Cancer Center, Natori, Japan, [3]Department of Otorhinolaryngology-Head and Neck Surgery, Tokyo Medical University, Shinjuku, Japan, [4]Department of Otorhinolaryngology, Nagoya University Graduate School of Medicine, Nagoya, Japan

Background: Despite advances in precision medicine, most patients with recurrent or metastatic salivary gland carcinoma still need conventional chemotherapies, such as the combination of taxane and platinum. However, evidence for these standardized regimens is limited.

Methods: We retrospectively reviewed patients with salivary gland carcinoma treated with a taxane and platinum, which contained docetaxel at a dose of 60 mg/m2 plus cisplatin at a dose of 70 mg/m2 on day 1, or paclitaxel at a dose of 100 mg/m2 plus carboplatin at a dose of area under the plasma concentration-time curve = 2.5 on days 1 and 8 (both on 21-day cycles), between January 2000 and September 2021.

Result: Forty patients with ten adenoid cystic carcinomas and thirty other pathologies were identified. Of these, 29 patients were treated with docetaxel plus cisplatin and 11 with paclitaxel plus carboplatin. For the total population, the objective response rate (ORR) and median progression-free survival (mPFS) were 37.5% and 5.4 months (95% confidence interval: 3.6–7.4 months), respectively. On subgroup analysis, docetaxel plus cisplatin provided favorable efficacy compared with paclitaxel plus carboplatin (ORR: 46.5% *vs.* 20.0%, mPFS: 7.2 *vs.* 2.8 months), and the findings were well retained in patients with adenoid cystic carcinoma (ORR: 60.0% *vs.* 0%, mPFS: 17.7 *vs.* 2.8 months). Grade 3/4 neutropenia was relatively frequent in the docetaxel plus cisplatin (59% *vs.*27%), although febrile neutropenia was uncommon (3%) in the cohort. No treatment-related death was seen in any case.

10.3389/fonc.2023.1185198

Conclusion: The combination of taxane and platinum is generally effective and well-tolerated for recurrent or metastatic salivary gland carcinoma. In contrast, paclitaxel plus carboplatin appears unfavorable in terms of efficacy in certain patients, such as those with adenoid cystic carcinoma.

KEYWORDS

salivary gland carcinoma, cytotoxic chemotherapy, docetaxel, cisplatin, adenoid cystic carcinoma

Introduction

Salivary gland carcinoma (SGC) is a rare malignant tumor which accounts for fewer than 5% of head and neck cancers (1). The disease is classified into over twenty histological types (2), each of which has a distinctive clinical course. In general, surgery and radiotherapy are performed for patients with local disease, whereas systemic therapy is used for those in local treatment is unsuitable, such as subjects with distant metastatic disease (3). However, because of its rarity and various histological types, evidence in support of standard systemic therapies in this patient population remains limited.

Recently, the effectiveness of targeted therapy for specific oncogenic driver alterations in SGC has been established (4–7). Because of the relatively high anti-tumor efficacy and manageable toxicity profile of these agents, the National Comprehensive Cancer Network (NCCN) guidelines state they are a useful therapeutic option for those who harbor the specific alterations (3). However, the majority of patients with SGC do not have these targets, and are accordingly treated with conventional cytotoxic chemotherapy, represented by taxane and platinum as a monotherapy or combination therapy. Of note, docetaxel plus cisplatin and paclitaxel plus carboplatin have been relatively well examined and provided an ORR of 11.5%–54.5% and median overall survival (mOS) of 12–26.5 months in phase II trials and retrospective studies (8–13). Nevertheless, further validation of these conventional therapies is worthwhile, particularly with regard to why treatment efficacy varies among the various histological subtypes. Moreover, no report has compared the efficacy and safety of these two approaches.

Here, we aimed to evaluate the efficacy and safety of taxane and platinum in combination, including docetaxel plus cisplatin and paclitaxel plus carboplatin, in patients with recurrent or metastatic (R/M) SGC. We also performed subgroup analyses by type of regimen and histological subtype to determine whether distinct populations benefit from a specific regimen.

Materials and methods

Patient selection

We retrospectively reviewed SGC patients treated with combination chemotherapy with taxane and platinum from January 2000 to September 2021 at the National Cancer Center Hospital East, Japan. The cut-off date was April 1st, 2022. Inclusion criteria were as follows: (1) pathologically proven SGC, (2) not suitable for local therapy, (3) primary site in a major or minor salivary gland, and (4) receipt of at least one course of combination chemotherapy with taxane and platinum in the R/M setting. To extract patients with these conditions, we used a computer-managed search system based on the prescribed regimens, and we then collected their clinical data from each medical record. Patients without target lesions were excluded from the evaluation of antitumor efficacy. This study was approved by the Institutional review Board of the National Cancer Center Hospital East.

Treatment

The docetaxel plus cisplatin regimen consisted of docetaxel at a dose of 60 mg/m2 plus cisplatin at a dose of 70 mg/m2 on day 1, repeated every 21 days. After completion of six cycles of combination therapy, treatment could continue as maintenance therapy consisting of docetaxel monotherapy at a dose of 60 mg/m2 on day 1, repeated every 21 days. The paclitaxel plus carboplatin regimen consisted of paclitaxel at a dose of 100 mg/m2 plus carboplatin at a dose of area under the plasma concentration-time curve (AUC) = 2.5 on day 1 and 8, repeated every 21 days. Treatment continued until disease progression or the development of intolerable toxicity. If intolerable toxicity to carboplatin appeared, treatment could be continued as maintenance therapy consisting of paclitaxel monotherapy at a dose of 100 mg/m2 on day 1 and 8 every 21 days. The selection of regimen was determined through discussion between the attending physician and the patient themself from the viewpoint of the patient's organ function, age and performance status, and the patient's preference in consideration of expected toxicities and administration schedule (docetaxel plus cisplatin is given in an inpatient setting, while paclitaxel plus carboplatin can be administrated in an outpatient setting). In both regimens, dose modification and delay during the treatment schedule were allowed at the physician's discretion. When combination therapy was discontinued due to toxicity, a switch to maintenance therapy at that time was acceptable in both regimens. Written informed consent for the therapies, including a treatment schedule and expected adverse events, was obtained from each patient. Besides, this study for summarizing their clinical information was approved by the Institutional review Board of the National Cancer Center Hospital East.

10.3389/fonc.2023.1185198

Evaluation of efficacy and statistical analysis

Clinical tumor response to treatment was evaluated radiographically according to primarily Response Evaluation Criteria in Solid Tumors (RECIST) ver. 1.1 using computerized tomography. PFS and OS were calculated by the Kaplan-Meier method and compared using a log-rank test. Hazard ratios were calculated by Cox regression analysis. PFS was calculated from the first day of administration of the taxane and platinum regimen until disease progression or death from any cause. We defined the disease progression of patients with non-target lesions only unequivocal progression containing clinical disease progression. OS was defined as the period from the first admission day of either regimen until death from any cause. Patients who were lost to follow-up were censored at the date of last follow-up. ORR was defined as complete response and partial response rates. Disease control rate (DCR) was defined as complete response, partial response, and stable disease rate. Subgroup analyses by treatment regimen and histological type were performed. Toxicity during the objective treatment period was graded using the Common Toxicity Criteria for Adverse Events (CTCAE version 4.0). All statistical analyses were performed with EZR (version 1.51; Saitama Medical Center, Jichi Medical University, Saitama, Japan), which is a graphical user interface for R (The R Foundation for Statistical Computing, Vienna, Austria; version 4.1.1).

Results

Patient characteristics

Forty patients were identified. Their characteristics are summarized in Table 1. Median age was 60 years (range, 31–77 years), and ECOG performance status (PS) of 0/1/2 was 21/15/3, respectively. Median baseline of creatinine clearance using the Cockcroft-Gault formula was 85.9 mL/min (range, 43.3-140.2). The most common histological type was adenoid cyst carcinoma (AdCC) (n=10), followed by adenocarcinoma not otherwise specified (ANOS) (n=8), salivary duct carcinoma (SDC) (n=8) and Carcinoma ex pleomorphic adenoma (CEPA) (n=6). The positivity of androgen receptor (AR) and human epidermal growth factor receptor 2 (HER2) in representative histological subtypes were 25.0% and 12.5% in ANOS, 62.5% and 37.5% in SDC, 50.0% and 33.3% in CEPA, respectively (Table 1). Furthermore, patient and tumor characteristics according to the histological subtypes (AdCC *vs.* others) and regimens are shown in Supplementary Table 1.

Treatment outcome

For all 40 patients, median follow-up time was 15.8 months (range, 0.8–102.3 months) at the cut-off date. The mPFS and mOS were 5.4 months (95% CI 3.6-7.4 months) and 26.6 months (95% CI 12.9- 48.3 months) in the total population (Figure 1); 4.5 months (95%CI 0.5-17.7)

TABLE 1 Patient and tumor characteristics.

	N = 40 (%)
Median age, years [range]	60 [31–77]
Gender	
Male	26 (65)
Female	14 (35)
ECOG PS	
0	21 (53)
1	15 (38)
2	3 (8)
Primary site	
Parotid gland	22 (55)
Submandibular gland	12 (30)
Minor salivary gland	6 (15)
Histology	
Mucoepidermoid carcinoma	2 (5)
Adenoid cystic carcinoma	10 (25)
Acinic cell carcinoma	1 (3)
Adenocarcinoma, NOS (ANOS)	8 (20)
Salivary duct carcinoma (SDC)	8 (20)
Carcinoma ex pleomorphic adenoma (CEPA)	6 (15)
Poorly differentiated carcinoma	4 (10)
Carcinoma, NOS	1 (3)
Prior systemic therapy line[†]	
0	29 (72.5)
1	9 (22.5)
2	2 (5)
Median baseline of creatinine clearance using the Cockcroft-Gault formula (mL/min) [range]	85.9 [43.3–140.2]
Hormone receptor expression (overall)	
AR-positive and HER2-positive	6 (15)
AR-positive and HER2-negative	5 (13)
Both negative or uncertain	29 (73)
Hormone receptor expression in representative subtypes	
ANOS (n=8)	
AR-positive	4 (25)
HER2-positive	2 (12.5)
SDC (n=8)	
AR-positive	5 (62.5)
HER2-positive	3 (37.5)

(Continued)

10.3389/fonc.2023.1185198

TABLE 1 Continued

	N = 40 (%)
CEPA (n=6)	
AR-positive	3 (50.0)
HER2-positive	2 (33.3)
Prior hormone therapy	
Yes	8 (20)
No	32 (80)
Next-generation sequencing	
Yes	15 (38)
No	25 (62)

[†]The number indicates the treatment line in which chemotherapy and hormone therapy were used as systemic therapy for R/M SGC. AR, androgen receptor; HER2, human epidermal growth factor receptor 2.

and 30.6 months (95%CI 24.3-NA) in the AdCC group, 5.7 months (95%CI 3.2-7.5) and 26.6 months (11.0-39.0 months) in non-AdCC group, respectively. Thirty-two patients had target lesions evaluable by RECIST, and the ORR and DCR in this population were 37.5% and 87.5% in the total population, 33.3% and 0% in the AdCC group, 39.1% and 17.4% in the non-AdCC group, respectively (Table 2 and Supplementary Table 2). Twenty-three patients (72%) achieved any tumor shrinkage with treatment, with a median change in the sum of tumor diameters from baseline of -18.9% (range, -92-+84%). Regarding treatment regimen and reasons for choosing the regimen, 29 patients were treated with docetaxel plus cisplatin, 11 with paclitaxel plus carboplatin; six of 11 patients in the paclitaxel plus carboplatin group requested the regimen preferring its outpatient-based treatment, and the remaining five had medical complications which hamper using cisplatin, such as cardio-pulmonary dysfunction (n=3), renal impairment (n=1) as well as advanced age (> 75 years old, n=1) (Supplementary Table 1). In the docetaxel plus cisplatin group, five patients proceeded to the docetaxel maintenance phase, and two of them terminated the treatment due to disease progression after six docetaxel administrations, and the other two experienced treatment termination due to adverse events after 19 and ten docetaxel administrations each, resulting that one in the group was under treatment with docetaxel monotherapy as of data cut-off(Supplementary Figure 1). Median follow-up time was 19.2 months (range, 0.8–102.3 months) for docetaxel plus cisplatin group and 10.3 months (range, 2.1–38.6 months) for the paclitaxel plus carboplatin group. Although the limited subject number and uneven background between the two groups might have impacted the results, analysis to estimate prognosis by type of treatment regimen was attempted. For PFS, docetaxel plus cisplatin showed a statistically significant prolongation of outcome compared with paclitaxel plus carboplatin (mPFS: 7.2 months *vs.* 2.8 months, log-rank p-value; 0.01, hazard ratio [HR]; 0.39 (95% confidence interval [CI], 0.19-0.83) (Supplementary Figure 2). Further, a trend toward favorability was also seen in the docetaxel plus cisplatin group (mOS: 36.6 months *vs.* 12.9 months, log-rank p-value; 0.25, HR; 0.54 (95%CI, 0.19-1.56). Antitumor efficacy in the 32 patients who were evaluable by RECIST is shown in Figure 2 and Supplementary Table 2. ORR and DCR by docetaxel plus cisplatin and paclitaxel plus carboplatin were 46.5% *vs.* 20.0% and 90.9%, and 80.0%, respectively (Supplementary Table 2). Further detailed assessment with consideration to the impact of histological type on efficacy revealed a distinctive relationship between the two; as one example, docetaxel plus cisplatin showed relatively robust antitumor efficacy in AdCC compared with paclitaxel plus carboplatin (ORR: 60% *vs.* 0%) (Figure 2). Moreover, in the subgroup analysis focusing on the AdCC population in this study at least, the docetaxel plus cisplatin group showed statistically significantly prolonged PFS compared with the paclitaxel plus carboplatin group (mPFS: 17.7 months *vs.* 2.8 months, log-rank p-value; 0.0237, HR; 0.10 (95% CI, 0.01-0.89) (Supplementary Figure 3).

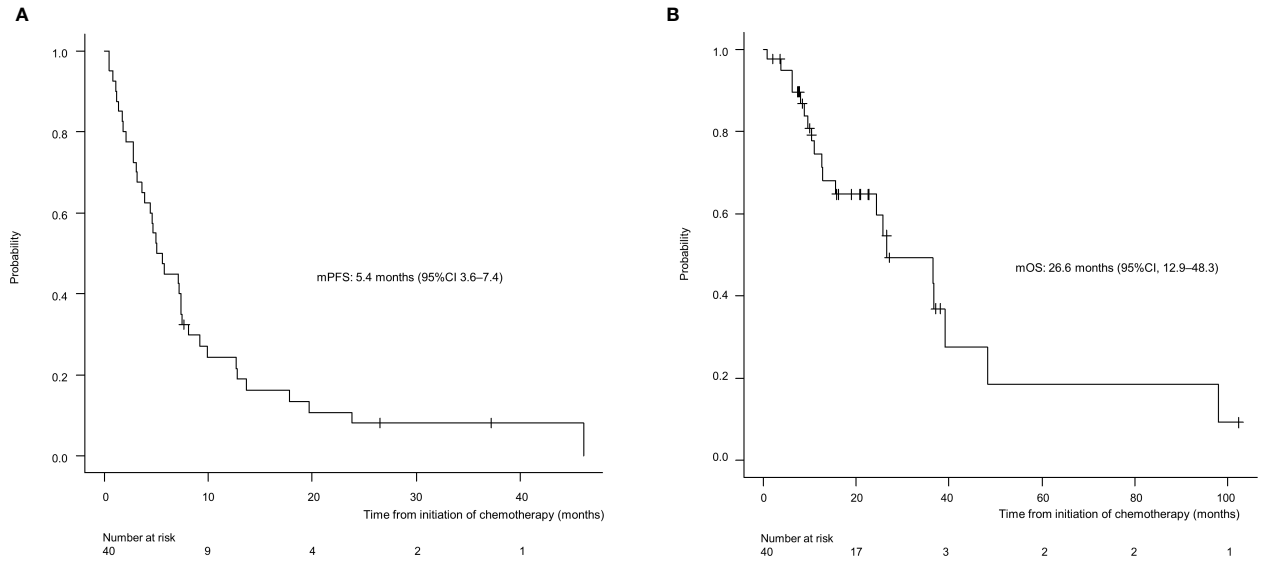

FIGURE 1
Progression-free survival **(A)** and overall survival **(B)** for the entire population (N=40). mPFS, median progression-free survival; CI, confidence interval.

10.3389/fonc.2023.1185198

TABLE 2 Antitumor efficacy in 32 patients who be evaluable by RECIST.

	n = 32[†] (%)
BOR	
Complete response	1 (3)
Partial response	11 (31)
Stable disease	16 (50)
Progressive disease	4 (13)
ORR, %	37.5
DCR, %	87.5
Tumor shrinkage by the treatment	
Yes	23 (72)
No	9 (28)
Mean change in the sum of tumor diameter from baseline, % [range]	-18.9 [-92 to +84]
Mean change in the sum of tumor diameter from baseline, % [range]	-18.9 [-92 to +84]
	n = 32[†] (%)
BOR	
Complete response	1 (3)
Partial response	11 (31)
Stable disease	16 (50)
Progressive disease	4 (13)
ORR, %	37.5
DCR, %	87.5
Tumor shrinkage by the treatment	
Yes	23 (72)
No	9 (28)
Mean change in the sum of tumor diameter from baseline, % [range]	-18.9 [-92 to +84]

[†]Data were analyzed in 32 evaluable patients. BOR, best overall response; ORR, objective response rate; DCR, disease control rate.

Safety

Toxicities experienced during treatment are listed in Table 3. The most common grade 3/4 adverse event was a decrease in neutrophil count (59% in the docetaxel plus cisplatin group and 27% in the paclitaxel plus carboplatin group). Regarding the use of Granulocyte colony-stimulating factors(G-CSF), primary G-CSF prophylaxis (G-CSF administration in the first cycle of chemotherapy before the onset of neutropenia) was not performed in both groups. While ten (37.9%) patients in the docetaxel plus cisplatin group were administered the agent after the occurrence of neutropenia. Furthermore, the age of these patients who recured G-CSF administration tended to higher than those who did not (average age: 64 *vs.* 55, p=0.08). On the other hand, no patients in the paclitaxel plus carboplatin group were given G-CSF throughout the treatment. A few patients experienced febrile neutropenia (3% in the docetaxel plus cisplatin group and 0% in the paclitaxel plus carboplatin group). No treatment-related death was observed in any patient.

Discussion

In this study, we comprehensively evaluated the efficacy and safety of two widely used combination chemotherapies based on taxane and platinum in patients with SGC. Furthermore, in a subgroup analysis, we revealed for the first time that efficacy might differ according to histological subtype; notably, the combination of paclitaxel plus carboplatin showed unfavorable antitumor efficacy and prognosis compared with docetaxel plus cisplatin in patients with AdCC (ORR: 0% *vs.* 60.0%, mPFS: 2.8 months *vs.* 17.7 months, mOS: 24.2 months *vs.* 42.4 months).

Treatment for R/M SGC generally consists of systemic therapy, as with other cancer types. Among therapies, recent progress in precision medicine has led to molecular-targeted therapy for subjects harboring the corresponding therapeutically targetable alteration. However, this treatment is suitable for only a small fraction of the population; moreover, systems for evaluating these alterations have yet to be generalized and widely distributed. For

10.3389/fonc.2023.1185198

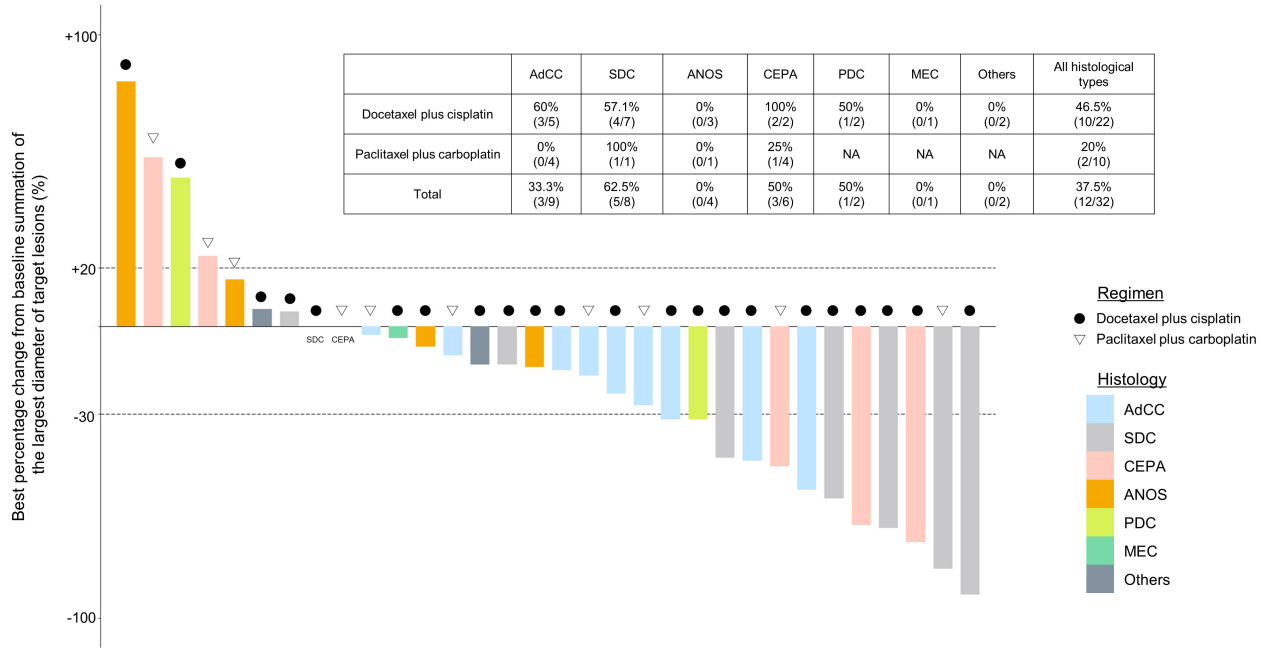

	AdCC	SDC	ANOS	CEPA	PDC	MEC	Others	All histological types
Docetaxel plus cisplatin	60% (3/5)	57.1% (4/7)	0% (0/3)	100% (2/2)	50% (1/2)	0% (0/1)	0% (0/2)	46.5% (10/22)
Paclitaxel plus carboplatin	0% (0/4)	100% (1/1)	0% (0/1)	25% (1/4)	NA	NA	NA	20% (2/10)
Total	33.3% (3/9)	62.5% (5/8)	0% (0/4)	50% (3/6)	50% (1/2)	0% (0/1)	0% (0/2)	37.5% (12/32)

FIGURE 2
Clinical efficacy analysis with waterfall plots of patients evaluable by RECIST (n=32). NA, not applicable; AdCC, Adenoid cystic carcinoma; SDC, Salivary duct carcinoma; ANOS, Adenocarcinoma, NOS; CEPA, Carcinoma ex pleomorphic adenoma, PDC, Poorly differentiated carcinoma; MEC, Mucoepidermoid carcinoma.

instance, the Center for Cancer Genomics and Advanced Therapeutics reported that only 7.8% of all Japanese cancer patients tested for comprehensive genomic profiling underwent drug treatment based on genomic alterations (4). Thus, R/M SGC patients who do not have these targets or the opportunity to receive a companion diagnosis are still treated with conventional cytotoxic chemotherapy. Nevertheless, no standard regimen for these patients has yet been established, as confirmed by the NCCN guidelines,

TABLE 3 Adverse event.

	Any grade		Grade 3/4	
	Docetaxel plus cisplatin	Paclitaxel plus carboplatin	Docetaxel plus cisplatin	Paclitaxel plus carboplatin
	n = 29 (%)	n = 11 (%)	n= 29 (%)	n = 11 (%)
Haematological				
Neutropenia	17 (59)	5 (45)	17 (59)	3 (27)
Febrile neutropenia	1 (3)	0 (0)	1 (3)	0 (0)
Platelet count decreased	1 (3)	0 (0)	1 (3)	0 (0)
Non-haematological				
Malaise	9 (31)	3 (27)	1 (3)	0 (0)
Nausea	10 (34)	5 (45)	0 (0)	0 (0)
Alopecia	4 (14)	3 (27)	0 (0)	0 (0)
Creatinine increased	4 (14)	0 (0)	0 (0)	0 (0)
Diarrhea	4 (14)	2 (18)	0 (0)	0 (0)
Constipation	3 (10)	2 (18)	0 (0)	0 (0)
Dysgeusia	3 (10)	2 (18)	0 (0)	0 (0)

(Continued)

10.3389/fonc.2023.1185198

TABLE 3 Continued

	Any grade		Grade 3/4	
	Docetaxel plus cisplatin	Paclitaxel plus carboplatin	Docetaxel plus cisplatin	Paclitaxel plus carboplatin
	n = 29 (%)	n = 11 (%)	n= 29 (%)	n = 11 (%)
AST increased	3 (10)	0 (0)	0 (0)	0 (0)
ALT increased	3 (10)	0 (0)	1 (3)	0 (0)
Edema	3 (10)	0 (0)	0 (0)	0 (0)
Hyperglycemia	3 (10)	0 (0)	2 (7)	0 (0)
Peripheral sensory neuropathy	2 (7)	5 (45)	0 (0)	0 (0)
Hypomagnesemia	2 (7)	0 (0)	0 (0)	0 (0)
PPE	1 (3)	2 (18)	0 (0)	0 (0)
Hypokalemia	1 (3)	0 (0)	0 (0)	0 (0)
Infusion related reaction	0 (0)	1 (9)	0 (0)	0 (0)

All events were graded according to common toxicity criteria for adverse events version 4.0. AST, aspartate aminotransferase; ALT, alanine aminotransferase; PPE, palmar-plantar erythrodysesthesia.

which also state that no preferred regimen exists. Indirect comparisons suggest that combination therapy, represented by taxane and platinum, is more effective in terms of response rate and progression-free survival than monotherapy (5–7, 14–17) (Table 4). Our present results appear to mirror these recent findings, with efficacy of combination therapy in various histological types showing ORRs ranging from 39%-54.5%, PFS of 6.5-8.4 months, and mOS of 18.8-26.5 months (14, 15, 17). The adverse events of each regimen were tolerable. The most frequent grade 3/4 adverse event was neutropenia (59% with docetaxel plus cisplatin and 27% with paclitaxel plus carboplatin); however, febrile neutropenia occurred in only one case in the docetaxel plus cisplatin group. In contrast, grade 3/4 neutropenia was more common in previous reports, for example at 95% with docetaxel plus cisplatin and 53% with paclitaxel plus carboplatin (14, 17). The reason for these contrasting findings may be the dose difference, as shown in Table 4; generally, the dose per unit time in our regimen was relatively lower than in the other studies. Indeed, the optimal dose of combination chemotherapy with taxane and platinum for SGC patients remains unknown. Nevertheless, our regimens appear to represent a well-balanced therapeutic option in terms of both efficacy and safety.

AdCC is characteristically slow-growing but has a high recurrence rate and is considered to draw a line from other SGC subtypes, at least regarding its treatment strategy; however, evidence on systemic therapy for the disease is not well established. The American Society of Clinical Oncology guidelines and NCCN guidelines recommend lenvatinib, a multi-targeted tyrosine kinase inhibitor, for AdCC (category 2B treatment in the NCCN guidelines), based on the results of phase II trials in a relatively small number of patients (8–10). Antitumor efficacy is modest, however, with an ORR of 10.5-15.6%, and worldwide adoption as the standard of care has not been achieved. Moreover, the disease rarely harbors therapeutically targetable alterations (11). Against this background, exploration of treatment options has continued, including the reevaluation of conventional cytotoxic chemotherapy. Notably, although taxane and platinum as monotherapy has been recognized to provide limited anti-tumor efficacy, as shown in Table 4 (5, 7), the recent phase II trial mentioned above reported that docetaxel plus cisplatin provided an ORR of 54.5% in 11 SGC patients, and that 50% (2/4) of AdCC patients achieved a partial response (12, 17), as similarly seen in our present study (60%, 3/5). In contrast, we found for the first time that paclitaxel plus carboplatin might lead to unfavorable treatment outcome in this population (ORR: 0%, mPFS: 2.8 months). These results, although not conclusive due to the limited patient number and inability to determine the difference in efficacy, may suggest that for AdCC patients who require systemic therapy and are able to tolerate docetaxel plus cisplatin, this regimen is the preferred option, particularly given the encouraging efficacy over that in previous reports of AdCC (ORRs: 15.6-43%) (9, 13, 18, 19).

This study has several limitations. First, the subgroup analysis on the potential impact of the type of regimen (i.e., docetaxel plus cisplatin *vs.* paclitaxel plus carboplatin) on efficacy was hampered by the heterogeneous patient characteristics, including the unbalanced number of enrolled patients between the two, and the lack of clarity in regimen selection due to selection bias from the retrospective study design. A further randomized trial would therefore provide a more conclusive answer for this clinically significant issue. Second, unfortunately, the standardized treatment schedule and dose of the taxane and platinum have yet to be established worldwide, and we also could not reach a conclusive perspective on it, especially in the combination of paclitaxel plus carboplatin, and verification of the meaning of switching to the maintenance of docetaxel in the docetaxel plus cisplatin, through the current work. Third, despite the significance of examining therapeutically targetable alterations in the SGC population, 62% of our present patients were not examined, as the cohort includes the subjects treated before comprehensive genome profiling was covered by insurance in 2019. The remaining patients (38%) had no targetable alterations, at the

TABLE 4 The summary of literature reports on taxane and/or platinum regimen for salivary gland carcinoma.

Author	Year	Phase	Regimen†	N	mPFS(mo)	mOS (mo)	ORR (%)							
							All	AdCC	SDC	ANOS	CEPA	PDC	MEC	Others
Licitra et al.	1991	II	Cisplatin (100mg/m^2, d1)	25	7	14	16 (4/25)	15 (2/13)	NA	0 (0/5)	NA	NA	20 (1/5)	50 (1/2)
Airoldi et al.	2000	II	Paclitaxel (175mg/m^2, d1) Carboplatin (AUC5.5, d1)	14	NA	12.5	14 (2/14)	20 (2/10)	NA	0 (0/1)	NA	0% (0/2)	0 (0/1)	NA
Gilbert et al.	2006	II	Paclitaxel (200mg/m^2, d1)	45	4	12.5	18 (8/45)	0 (0/14)	NA	29 (5/17)	NA	NA	21 (3/14)	NA
Nakano et al.	2016	retro	Paclitaxel (200mg/m^2, d1) Carboplatin (AUC6, d1)	38	6.5	26.5	39 (15/38)	11 (1/9)	39 (7/18)	64 (7/11)				
										4	4	NA	1	2
Okada et al.	2019	retro	Docetaxel (70mg/m^2, d1) Carboplatin (AUC5. d1)	24	8.4	26.4	42 (10/24)	0 (0/1)	50 (6/12)	50 (2/4)	NA	NA	0 (0/1)	33 (2/6)
Fukuda et al.	2021	retro	Paclitaxel (200mg/m^2, d1) Carboplatin (AUC6, d1)	26	8.1	22.3	11.5 (3/26)	11.5 (3/26)	NA	NA	NA	NA	NA	NA
Imamura et al.	2021	II	Docetaxel (75mg/m2, d1) Cisplatin (75mg/m^2, d1)	11	6.6	18.8	54.5	50 (2/4)	67 (2/3)	67 (2/3)	NA	NA	NA	0 (0/1)
Current study.	2023	retro	Docetaxel (60mg/m^2, d1) Cisplatin (70mg/m^2, d1)	22	7.2	36.6	46.5 (10/22)	60 (3/5)	57.1 (4/7)	0 (0/3)	100 (2/2)	50 (1/2)	0 (0/1)	0 (0/2)
			Paclitaxel (100mg/m^2, d1,8) Carboplatin (AUC2.5, d1,8)	10	2.8	12.9	20 (2/10)	0 (0/4)	100 (1/1)	0 (0/1)	25 (1/4)	NA	NA	NA

†All regimens given over three weeks. ORR, objective response rate; mPFS, median progression-free survival; mOS, median overall survival; AdCC, adenoid cystic carcinoma; SDC, salivary duct carcinoma; ANOS, adenocarcinoma, not otherwise specified; CEPA, carcinoma ex pleomorphic adenoma, PDC, poorly differentiated carcinoma; MEC, mucoepidermoid carcinoma; NA, not applicable.

10.3389/fonc.2023.1185198

time at least; however, we should note that this fact might cause a biased result that does not match the current clinical situation and that further study may reveal the true efficacy of these combinations in subjects who do not have such targets, as well as identify predictive markers in patients who would substantially benefit from these regimens.

Conclusion

The combination of taxane and platinum is a chemotherapeutic option for patients with salivary gland carcinoma. In contrast, paclitaxel plus carboplatin may be less effective in certain situations, such as in patients with AdCC.

Data availability statement

The original contributions presented in the study are included in the article/Supplementary Material. Further inquiries can be directed to the corresponding author.

Ethics statement

The studies involving human participants were reviewed and approved by Institutional Review Board of the National Cancer Center Hospital East. Written informed consent for participation was not required for this study in accordance with the national legislation and the institutional requirements.

Author contributions

RO and KI participated in formulating the study concept and design, data curation, data interpretation, and drafting of the manuscript. TE participated in data interpretation and drafting of the manuscript. MT supervised the study and revised the manuscript. All authors provided critical revisions and approved the final manuscript. All authors contributed to the article.

Conflict of interest

MT reports grants and personal fees from Ono Pharmaceutical and Bayer; personal fees from MSD, BMS, Merck Biopharma, Pfizer, Rakuten Medical, Lilly, Boehringer Ingelheim, Eisai, Chugai Pharmaceutical, Daiichi-Sankyo, Janssen Pharmaceutical, Genmab, Astra Zeneca, Abbvie and Astellas, outside the submitted work. TE reports personal fees from Ono Pharmaceutical, Bayer, MSD, and Merck Biopharma outside the submitted work. SO reports personal fees from Ono Pharmaceutical, MSD, BMS, Merck Biopharma. YU reports personal fees from BMS.

The remaining authors declare that the research was conducted in the absence of any commercial or financial relationships that could be construed as a potential conflict of interest.

Publisher's note

Supplementary material

The Supplementary Material for this article can be found online at: https://www.frontiersin.org/articles/10.3389/fonc.2023.1185198/full#supplementary-material

References

1. Guzzo M, Locati LD, Prott FJ, Gatta G, McGurk M, Licitra L. Major and minor salivary gland tumors. *Crit Rev Oncol Hematol* (2010) 74:134–48. doi: 10.1016/j.critrevonc.2009.10.004

2. Seethala RR, Stenman G. Update from the 4th edition of the world health organization classification of head and neck tumours: tumors of the salivary gland. *Head Neck Pathol* (2017) 11:55–67. doi: 10.1007/s12105-017-0795-0

3. *National comprehensive cancer network clinical practice guidelines in oncology, head and neck cancers. version 1.2023*. (2022).

4. Kohno T, Kato M, Kohsaka S, Sudo T, Tamai I, Shiraishi Y, et al. C-CAT: the national datacenter for cancer genomic medicine in Japan. *Cancer Discovery* (2022) 12:2509–15. doi: 10.1158/2159-8290.CD-22-0417

5. Licitra L, Marchini S, Spinazzè S, Rossi A, Rocca A, Grandi C, et al. Cisplatin in advanced salivary gland carcinoma. a phase II study of 25 patients. *Cancer* (1991) 68:1874–7. doi: 10.1002/1097-0142(19911101)68:9<1874::aid-cncr2820680904>3.0.co;2-s

6. Airoldi M, Fornari G, Pedani F, Marchionatti S, Gabriele P, Succo G, et al. Paclitaxel and carboplatin for recurrent salivary gland malignancies. *Anticancer Res* (2000) 20:3781–3.

7. Gilbert J, Li Y, Pinto HA, Jennings T, Kies MS, Silverman P, et al. Phase II trial of taxol in salivary gland malignancies (E1394): a trial of the Eastern cooperative oncology group. *Head Neck* (2006) 28:197–204. doi: 10.1002/hed.20327

8. Geiger JL, Ismaila N, Beadle B, Caudell JJ, Chau N, Deschler D, et al. Management of salivary gland malignancy: ASCO guideline. *J Clin Oncol* (2021) 39:1909–41. doi: 10.1200/jco.21.00449

9. Tchekmedyian V, Sherman EJ, Dunn L, Tran C, Baxi S, Katabi N, et al. Phase II study of lenvatinib in patients with progressive, recurrent or metastatic adenoid cystic carcinoma. *J Clin Oncol* (2019) 37:1529–37. doi: 10.1200/jco.18.01859

10. Locati LD, Galbiati D, Calareso G, Alfieri S, Singer S, Cavalieri S, et al. Patients with adenoid cystic carcinomas of the salivary glands treated with lenvatinib: activity and quality of life. *Cancer* (2020) 126:1888–94. doi: 10.1002/cncr.32754

11. Miller LE, Au V, Mokhtari TE, Goss D, Faden DL, Varvares MA. A contemporary review of molecular therapeutic targets for adenoid cystic carcinoma. *Cancers (Basel)* (2022) 14:992. doi: 10.3390/cancers14040992

12. Imamura Y, Kiyota N, Tahara M, Hanai N, Asakage T, Matsuura K, et al. Systemic therapy for salivary gland malignancy: current status and future perspectives. *Jpn J Clin Oncol* (2022) 52:293–302. doi: 10.1093/jjco/hyac008

13. Laurie SA, Siu LL, Winquist E, Maksymiuk A, Harnett EL, Walsh W, et al. A phase 2 study of platinum and gemcitabine in patients with advanced salivary gland cancer: a trial of the NCIC clinical trials group. *Cancer* (2010) 116:362–8. doi: 10.1002/cncr.24745

14. Nakano K, Sato Y, Sasaki T, Shimbashi W, Fukushima H, Yonekawa H, et al. Combination chemotherapy of carboplatin and paclitaxel for advanced/metastatic salivary gland carcinoma patients: differences in responses by different pathological diagnoses. *Acta Otolaryngol* (2016) 136:948–51. doi: 10.3109/00016489.2016.1170876

15. Okada T, Saotome T, Nagao T, Masubuchi T, Fushimi C, Matsuki T, et al. Carboplatin and docetaxel in patients with salivary gland carcinoma: a retrospective study. *In Vivo* (2019) 33:843–53. doi: 10.21873/invivo.11549

16. Fukuda N, Fujiwara Y, Wang X, Ohmoto A, Urasaki T, Hayashi N, et al. Tumor growth rate as a prognostic factor for metastatic or recurrent adenoid cystic carcinoma of the head and neck patients treated with carboplatin plus paclitaxel. *Eur Arch Otorhinolaryngol* (2021) 278:3037–43. doi: 10.1007/s00405-020-06481-y

17. Imamura Y, Tanaka K, Kiyota N, Hayashi H, Ota I, Arai A, et al. Docetaxel plus cisplatin in recurrent and/or metastatic non-squamous-cell head and neck cancer: a multicenter phase II trial. *Med Oncol* (2021) 38:128. doi: 10.1007/s12032-021-01581-z

18. Dimery IW, Legha SS, Shirinian M, Hong WK. Fluorouracil, doxorubicin, cyclophosphamide, and cisplatin combination chemotherapy in advanced or recurrent salivary gland carcinoma. *J Clin Oncol* (1990) 8:1056–62. doi: 10.1200/JCO.1990.8.6.1056

19. Hong MH, Kim CG, Koh YW, Choi EC, Kim J, Yoon SO, et al. Efficacy and safety of vinorelbine plus cisplatin chemotherapy for patients with recurrent and/or metastatic salivary gland cancer of the head and neck. *Head Neck* (2018) 40:55–62. doi: 10.1002/hed.24933

frontiers | Frontiers in Oncology

TYPE Original Research
PUBLISHED 20 June 2023
DOI 10.3389/fonc.2023.1107134

OPEN ACCESS

EDITED BY
Stefano Cavalieri,
National Cancer Institute Foundation (IRCCS), Italy

REVIEWED BY
Elena Colombo,
Fondazione Istituto Nazionale dei Tumori, Italy
Luigi Lorini,
Humanitas Research Hospital, Italy

*CORRESPONDENCE
Damian T. Rieke
damian.rieke@charite.de

RECEIVED 24 November 2022
ACCEPTED 26 May 2023
PUBLISHED 20 June 2023

CITATION
Rieke DT, Schröder S, Schafhausen P, Blanc E, Zuljan E, von der Emde B, Beule D, Keller U, Keilholz U and Klinghammer K (2023) Targeted treatment in a case series of AR+, HRAS/PIK3CA co-mutated salivary duct carcinoma.
Front. Oncol. 13:1107134.
doi: 10.3389/fonc.2023.1107134

Targeted treatment in a case series of AR+, HRAS/PIK3CA co-mutated salivary duct carcinoma

Damian T. Rieke[1,2,3,4]*, Sebastian Schröder[1], Philippe Schafhausen[5], Eric Blanc[3,6], Erika Zuljan[3,6], Benjamin von der Emde[1], Dieter Beule[3,6], Ulrich Keller[1,4,7], Ulrich Keilholz[2,4] and Konrad Klinghammer[1,4]

[1]Department of Hematology, Oncology and Cancer Immunology, Charité – Universitätsmedizin Berlin, Corporate Member of Freie Universität Berlin and Humboldt-Universität zu Berlin, Berlin, Germany, [2]Comprehensive Cancer Center, Charité – Universitätsmedizin Berlin, Corporate Member of Freie Universität Berlin and Humboldt-Universität zu Berlin, Berlin, Germany, [3]Berlin Institute of Health (BIH) at Charité – Universitätsmedizin Berlin, Berlin, Germany, [4]German Cancer Consortium (DKTK) and German Cancer Research Center (DKFZ), Heidelberg, Germany, [5]Department of Oncology, Hematology, and Bone Marrow Transplantation with Section of Pneumology, University Medical Center Hamburg-Eppendorf, Hamburg, Germany, [6]Core Unit Bioinformatics (CUBI), Berlin Institute of Health at Charité – Universitätsmedizin Berlin, Berlin, Germany, [7]Max-Delbrück-Center for Molecular Medicine, Berlin, Germany

Background and purpose: A subgroup of salivary duct carcinoma (SDC) harbor overexpression of the androgen receptor (AR), and co-occurring mutations in the *HRAS*- and *PIK3CA*-genes. The impact of genomic complexity on targeted treatment strategies in advanced cancer is unknown.

Materials and methods: We analyzed molecular and clinical data from an institutional molecular tumor board (MTB) to identify AR+, *HRAS*/*PIK3CA* co-mutated SDC. Follow-up was performed within the MTB registrational study or retrospective chart review after approval by the local ethics committee. Response was assessed by the investigator. A systematic literature search was performed in MEDLINE to identify additional clinically annotated cases.

Results: 4 patients with AR+ *HRAS*/*PIK3CA* co-mutated SDC and clinical follow-up data were identified from the MTB. An additional 9 patients with clinical follow-up were identified from the literature. In addition to AR overexpression and *HRAS* and *PIK3CA*-alterations, PD-L1 expression and Tumor Mutational Burden > 10 Mutations per Megabase were identified as additional potentially targetable alterations. Among evaluable patients, androgen deprivation therapy (ADT) was initiated in 7 patients (1 Partial Response (PR), 2 Stable Disease (SD), 3 Progressive Disease (PD), 2 not evaluable), tipifarnib was initiated in 6 patients (1 PR, 4 SD, 1 PD). One patient each was treated with immune checkpoint inhibition (Mixed Response) and combination therapies of tipifarnib and ADT (SD) and alpelisib and ADT (PR).

10.3389/fonc.2023.1107134

Conclusion: Available data further support comprehensive molecular profiling of SDC. Combination therapies, PI3K-inhibitors and immune therapy warrant further investigation, ideally in clinical trials. Future research should consider this rare subgroup of SDC.

KEYWORDS

salivary gland cancer, salivary duct carcinoma, targeted therapy, precision oncology, molecular tumor board, head and neck cancer

1 Introduction

Salivary gland cancers (SGC) are a rare group of tumors with an incidence of about 1.3 cases/100,000 individuals in the United States (1). More than 20 distinct malignant subtypes have been described, many of which are defined by recurrent genetic alterations (2).

Salivary duct carcinoma (SDC) is an aggressive high-grade SGC subtype with a dismal prognosis. SDC most commonly arises in the parotid gland and accounts for about 1.8% of major salivary gland tumors in the SEER database (3–5). SDC can arise *de-novo* or ex pleomorphic adenoma (ex-PA) (4). Due to the aggressive nature of this disease, metastatic spread and a need for systemic therapy is frequent (6).

In addition to chemotherapy, targeted treatment strategies are increasingly used in SDC. SDC harbors recurrent molecular alterations such as HER2 and androgen receptor (AR) amplification and overexpression. Furthermore, *FGFR1* amplification, *PIK3CA*, *HRAS* and *TP53* mutations and *PTEN* and *CDKN2A* loss have been described (2, 4, 7, 8). Some of these alterations have been applied as predictive biomarkers for targeted therapy. Previous prospective studies have shown activity of HER2, AR and *HRAS*-directed therapy in SDC (9–11). Additionally, a prospective basket study showed a benefit of targeted therapy (targeting *HER2* amplification, *HER2*, *BRAF* and *PTCH1* mutation and high tumor mutational burden) in a large group of SGC, including SDC (12). No prospective trials supporting the efficacy of PI3K-inhibitors in *PIK3CA*-mutant SDC currently exist. A summary of ongoing and published clinical trials relevant for metastatic salivary duct carcinoma is provided in Table 1.

These results have led to a recommendation of comprehensive molecular analyses (e.g. next-generation panel or whole-exome sequencing) in patients with advanced SDC. These analyses should be done to assess opportunities for targeted therapy, including HER2- or AR-directed treatment (15, 16). Available data correspond to ESMO Scale of Clinical Actionability (ESCAT) scores of II-B (i.e. investigational therapy, alteration-drug match is associated with antitumor activity but magnitude of benefit is unknown) for AR (>70% positivity by immunohistochemistry, IHC) and HER2 (IHC score 3+ or fluorescence *in situ* hybridization positivity) in SGC. A participation in clinical trials is strongly recommended (15–17). The use of immune checkpoint inhibition remains investigational (15, 16). However, the FDA-approval of pembrolizumab in tumors with high tumor mutational burden also includes SGC (18).

In SDC, several targetable molecular alterations occur in recurrent patterns. The resulting subgroups of SDC are mainly defined by HER2- and AR-expression. In a retrospective analysis of 63 SDC samples, 34 samples were AR+/HER2- and harbored

TABLE 1 Published and ongoing clinical trials relevant for salivary duct carcinoma, as identified from a structured search (MEDLINE clinical trials, search term "salivary gland cancer" on 17th May 2023, clinicaltrials.gov, search term "salivary gland AND metastatic" on 17th May 2023).

Studyname (Identifier)	Recruitment status	Intervention	Phase	Reference
EORTC 1206 Androgen Deprivation Therapy in Advanced Salivary Gland Cancer	completed	bicalutamide + triptorelin	II, randomized	NCT01969578
Testing the Anti-Cancer Drug Darolutamide in Patients With Testosterone-driven Salivary Gland Cancers	recruiting	darolutamide	II, nonrandomized	NCT05669664
Abiraterone Acetate in Patients With Castration-Resistant, Androgen Receptor-Expressing Salivary Gland Cancer: A Phase II Trial	completed	abiraterone	II, nonrandomized	(13)
Phase II Study of Enzalutamide for Patients With Androgen Receptor-Positive Salivary Gland Cancers (Alliance A091404)	completed	enzalutamide	II, nonrandomized	(14)
Tipifarnib in recurrent, metastatic HRAS-mutant salivary gland cancer	completed	tipifarnib	II, nonrandomized	(9)
A prospective phase II study of combined androgen blockade in patients with androgen receptor-positive metastatic or locally advanced unresectable salivary gland carcinoma	completed	leuprorelin + bicalutamid	II, nonrandomized	(10)

frequent *PIK3CA* (50%) and *HRAS (41%)* mutations (19). In this study, *HRAS*-mutations were exclusively found in the HER2-/AR+ group and in 93% of cases they co-occurred with a *PIK3CA*-mutation (19). Additionally, no *HRAS* mutations were identified in SDC ex pleomorphic adenoma (19). The co-occurrence of three potentially predictive biomarkers complicates selection for targeted treatment decisions in these rare patients. We here present a case series of patients presenting to an institutional molecular tumor board or identified through a systematic search of the literature to assess outcome of AR+, *HRAS*/*PIK3CA* SDC patients with targeted treatment.

2 Materials and methods

2.1 Patients

Patients with salivary gland cancer presenting to the molecular tumor board (MTB) of the Charité Comprehensive Cancer Center between 2016 and 2022 were analyzed in a retrospective analysis of the MTB database (20). Original histopathological reports for patients classified as adenocarcinoma NOS, carcinoma NOS, invasive ductal carcinoma or carcinoma ex pleomorphic adenoma were considered. Patients with a final histopathological diagnosis of salivary duct carcinoma and molecular results with AR positivity (any immunohistochemistry, IHC staining) and activating *HRAS* and *PIK3CA*-mutations were included in the analysis (Supplementary Figure 1). Next-generation sequencing (NGS) was performed on formalin-fixed, paraffine-embedded tumor tissue for all identified patients, using the SureSelect Custom Library Panel (MH IVD Panel 600+, Agilent Technologies, USA). Library preparation was done using the SureSelectXT Low Input Target Enrichment System (Agilent Technologies, USA). Sequencing was performed on the NextSeq550 system using the NextSeq 500/550 Mid Output Kit v2.5, 300 Cycles (Illumina, USA). Follow-up, including response assessment, progression-free survival (PFS) and overall survival (OS), was performed prospectively within the MTB registrational study or as retrospective chart review. Median follow-up was calculated from the time of diagnosis. No minimum follow-up was required. The analysis was approved by the local ethics committee (Berlin, EA1/305/21).

2.2 Literature search

Systematic literature search (performed by DTR, last updated on 7th November 2022) was performed on MEDLINE using the following terms: "PIK3CA AND HRAS AND SALIVARY" OR "AR AND SALIVARY DUCT CARCINOMA". Studies and case reports providing individual clinical follow-up data for patients with AR+, *HRAS*/*PIK3CA* co-mutated cases were included in the analysis.

2.3 Analysis

Clinical patient characteristics, line and type of treatment, best response, time on treatment, progression-free survival and overall survival were collected, as provided. Best response was assessed by the investigator after a review of CT or MRI radiology reports (complete response, CR; partial response PR; stable disease SD; mixed response, MR; progressive disease, PD). Clinical benefit was defined as CR/PR or SD lasting for at least 6 months. Outcomes with similar treatment strategies (e.g. chemotherapy, androgen deprivation therapy, HER2-directed therapy, HRAS-directed therapy, combination therapy or immune checkpoint inhibition) were summarized. No formal statistical analysis was performed because of insufficient sample size. Cases were consecutively numbered starting with cases retrieved from the internal MTB database and followed by cases identified from the literature.

3 Results

3.1 Patient cohort

Seventeen patients with salivary gland histologies, consistent with SDC, were discussed in the institutional molecular tumor board between 2016 and 2022. After review of final histopathological diagnoses, 4 patients had salivary duct carcinoma with AR expression and *HRAS*/*PIK3CA* mutation and were included in the analysis. These patients (3 male, 1 female) were between 48-79 years old at the time of presentation at the MTB. Activating *HRAS* mutations were identified in the p.Q61 (3 patients) and p.G13 (1 patient) positions. Activating *PIK3CA* mutations were identified in the p.H1047 (3 patients) and p.E545 (1 patients) positions. Additional molecular findings were low to medium HER2-expression in 3 patients, PD-L1 expression in 2 patients, a tumor mutational burden (TMB) > 10 mutations/Megabase (mut/Mb) and an *AR* mutation in 1 patient, each. Median follow-up was 14.5 months. Clinical and molecular findings were summarized in Table 2.

The medline searches revealed 37 and 89 results, respectively. Of these, 4 studies with individual follow-up data for patients with AR+, *PIK3CA*/*HRAS* co-mutated SDC were included after manual review of the identified publications. The publications yielded a total of 9 cases (7 male, 2 female). Age was reported for 5 patients (range 38-65 years). Concurrent molecular alterations were *HER2* amplification and overexpression in 1 and *TP53* mutations in 2 patients, respectively. Clinical and molecular findings in these patients were summarized in Table 3. A consort diagram of patient identification is provided in Supplementary Figure 1.

Overall, 13 patients (10 male, 3 female; median age in 9 evaluable patients 61 years, range 38-79 years) with AR+, *PIK3CA*/*HRAS* co-mutated SDC were identified.

3.2 Treatment

Combined analysis of 13 evaluable patients yielded information on various targeted systemic treatment strategies. Androgen deprivation therapy (ADT) was reported in 7 patients, *HRAS*-directed treatment in 6 patients, immune checkpoint inhibition in 1 patient and combinations of tipifarnib and ADT and alpelisib and ADT in 1 patient, each. Treatment data, including line of treatment,

TABLE 2 Clinical and molecular data for patients identified from the local MTB database.

ID	Age	Gender	Primary Site	Stage at diagnosis	Sites of metastases	Site sequenced	AR (IHC)	HER2 (IHC)	*HRAS* mutation	*PIK3CA mutation*	TMB (Mut/Mb)	Other Alterations
1	48	m	Parotid Gland	pT3pN2bcM1	lung	primary	positive	negative	p.G13V	p.E545K	2.9	*CDKN2A* mutation, PD-L1 CPS 45, *ARID1A* mutation, *TP53* mutation
2	61	f	Submandibular Gland	cT4cN3bcM0	skin	Skin metastasis	80%	2+	p.Q61R	p.H1047L	3.64	PD-L1 CPS 5, *AR* p.R20P
3	54	m	Parotid Gland	pT3N0M0	bone, lung	Bone metastasis	90%	1+	p.Q61K	p.H1047R	2.18	
4	79	m	Parotid Gland	cT4cN1cM1	lung	Lung metastasis	strong positive	1+	p.Q61R	p.H1047R	10.9	*NQO1* mutation

CPS, combined positivity score, f, female, ID, identification number; IHC, immunohistochemistry, m, male, Mut/Mb, mutations per megabase, TMB, tumor mutational burden.

best response and progression-free survival (PFS) are provided, as available, in Table 4 and Figure 1.

3.3 Androgen deprivation therapy

Seven patients were treated with androgen deprivation therapy alone (ADT). Among 6 patients with available data on the specific type of ADT, 3 received bicalutamide and a GnRH-analogue and 3 received bicalutamide alone. Best response was evaluable in 5 patients (1 PR, 1 SD, 3 PD). 6 patients had evaluable PFS (median PFS = 2 months) and 2 of them had PFS > 6 months.

3.4 *HRAS*-directed therapy

The farnesyltransferase inhibitor tipifarnib as a single agent was administered in 6 patients. Among 5 patients with available data, 1 PR, 2 SD and 2 PD were achieved as best responses. PFS data were available for 6 patients and PFS was more than 6 months in 3 patients.

3.5 Combination therapy

One patient received ADT (bicalutamid/GnRH-Analogue) in combination with tipifarnib after prior progression to tipifarnib after 3 months. This patient achieved stable disease for more than 6 months, which was ongoing at the time of data collection. Another patient achieved a partial response with the PI3K-inhibitor alpelisib in combination with ADT (bicalutamide) for more than 12 months (ongoing at time of publication).

3.6 Other treatment

Chemotherapy use with carboplatin/paclitaxel alone was reported in 4 patients. Among 3 patients with available data, 1 PR, 1 MR and 1 PD were reported. The use of alpelisib as monotherapy was only reported for one patient without information on treatment response. Immune checkpoint inhibition was also reported for one patient with a mixed response for 7 months. Following progression on the single-agent PD-1 inhibitor, this patient was treated with a combination of a PD-1 and a CTLA-4 inhibitor, which was followed by disease progression. One patient with concurrent *HER2* amplification received trastuzumab in combination with chemotherapy and achieved a partial response.

3.7 Toxicity

No major (common terminology criteria of adverse events, CTCAE grade 4 or higher) or unexpected toxicities were observed in the 4 patients identified from the MTB database and no dose reductions were required. In published data, a dose reduction

TABLE 3 Clinical and molecular data for patients identified from literature review.Two PIK3CA mutations were identified in patient 12.

ID	Reference	Age	Gender	AR (IHC)	HER2 (IHC)	*HRAS* mutation	*PIK3CA* mutation	Other Alterations	Sequencing technique
5	(21)	64	m	positive	3+	p.Q61R	p.E545K	*HER2* amplification, *TP53* p.R196*, *ACVR2A* p.D177E	NGS
6	(9)	61	m	positive		p.Q61R	mutation	*TP53* mutation	NGS
7	(9)	65	m	n/a		p.Q61R	mutation		NGS
8	(9)	38	m	positive	2+	mutation	mutation		NGS
9	(22)	61	m	positive		p.Q61K	p.E545K		unknown
10	(23)	n/a	f	negative, mRNA pathway score 43.7	positive	p.Q61K	p.H1047R		NGS
11	(23)	n/a	f	positive		p.Q61R	p.E545K		NGS
12	(23)	n/a	m	positive		p.Q61K	p.E545K, p.H1047R		NGS
13	(23)	n/a	m	positive		p.Q61R	p.H1047R		NGS

AR IHC results are provided as described in the respective publications. No AR IHC was provided for patients #7. Results from a qPCR-based AR mRNA pathway activity test (normalized score, 0 lowest, 100 highest) was provided in patient #10.
ID, identification number; IHC, immunohistochemistry; n/a, not available; NGS, next generation sequencing.

because of toxicity was required in six patients (46%) receiving tipifarnib (4 because of cytopenia, 2 because of reversible renal failures), hypoglycemia requiring dose reduction was reported for alpelisib (9, 21). Toxicity data were not reported in the literature for patients receiving antiandrogen therapy in this cohort (22, 23). Available data from combined ADT in SGC reported no CTCAE grade 4/5 events and discontinuation of part of the combined ADT due to adverse events in 2 out of 36 patients (10).

4 Discussion

This is, to the best of our knowledge, the largest clinical case series of AR+, *PIK3CA*/*HRAS* co-mutated salivary duct carcinoma. The co-occurrence of these alterations has been described in previous analyses of this disease but was not associated with prognosis (19). The co-occurrence of these alterations poses a challenge for personalized therapy strategies. It is currently unclear, if response to targeted therapy is different in this subgroup. Despite the low number of patients, the heterogeneity of administered treatments in the cohort and the lack of data on mechanisms of secondary resistances, these results still hold important information because of the rarity of this disease. It should be noted that at least 2/13 patients in the cohort did not receive upfront palliative systemic therapy with ADT or chemotherapy (15, 16). This is likely caused by the lack of guidelines at the time of treatment initiation and a lack of data for the specific situation in AR+, *HRAS*/*PIK3CA* co-mutated tumors. Yet, despite available data and guidelines, current treatment strategies are not satisfactory and there is a lack of prospective clinical trials. The administration of experimental therapies, including immune checkpoint inhibition, will therefore likely remain a reality in these tumors, thus making sharing of real-world data essential.

HER2 overexpression or amplification is a well-defined therapeutic target in SDC (11). HER2 positivity has been found to be mutually exclusive with the AR+, *HRAS*/*PIK3CA* co-mutated subgroup (19). In this cohort, concurrent HER2 expression or amplification was reported in 6 patients with mostly low to moderate staining intensity. One patient was reported to harbor a concurrent *HER2* amplification and received trastuzumab in combination with chemotherapy, achieving a partial response. These results suggest, that HER2-positivity is not entirely mutually exclusive with the here described subgroup and HER2-directed treatment might be an additional option in some of the patients. In addition to HER2-directed antibodies, efficacy of HER2-directed antibody drug conjugates was shown in salivary gland cancer (24).

In the group of patients treated with ADT, a clinical benefit was observed in about a third of the evaluable patients, which is less than the clinical benefit rate of about 75% in previously reported results (10). However, clinical benefit was found in some patients, thus providing evidence of activity and the low number of patients does not allow further conclusions. Furthermore, previous work did not show an impact of oncogenic drivers, including *HRAS* and *PIK3CA* mutations, on the efficacy of ADT but studies on larger cohorts are warranted (10). Therefore, these data do not provide evidence against the use of ADT in the AR+, *HRAS*/*PIK3CA* co-mutated subgroup. Importantly, no data currently exist for the use of abiraterone in castration-resistant AR+, *HRAS*/*PIK3CA* co-mutated SDC. Abiraterone is active as a second line ADT in AR+ salivary gland cancer and might represent an additional treatment strategy for the here reported subgroup (13). Additional data on limited activity with enzalutamide were reported previously (14). In

TABLE 4 Treatment and outcome data for the entire case series.

ID	Treatment #1	Best Response #1	PFS #1	Treatment #2	Best Response #2	PFS #2	Treatment #3	Best Response #3	PFS #3	Treatment #4	Best Response #4	PFS #4	OS
1	Pembrolizumab (off-label)	MR	7 m	Nivolumab/ Ipilimumab (off-label)	PD	3 m	Carboplatin/Paclitaxel (off-label)	MR	3 m	Tipifarnib (compassionate use program)	PR	5 m+	18 m +
2	Carboplatin/Paclitaxel (off-label)	PD	2 m	Tipifarnib (compassionate use program)	PD	3 m	Tipifarnib/ADT (compassionate use program/ off-label)	SD	6 m +				11 m +
3	Carboplatin/Paclitaxel (off-label)	n/a	6 m	ADT (Bicalutamid/ Trenantone) (off-label)	PD	3 m	Tipifarnib (compassionate use program)	SD	10 m +				19 m +
4	Carboplatin/Paclitaxel (off-label)	PR	3 m +										3 m +
5	Carboplatin/Paclitaxel/ Trastuzumab	PR	6 m	Alpelisib /ADT (Bicalutamid)	PR	12 m +							21 m +
6	Carboplatin	n/a	n/a	ADT	n/a	n/a	Tipifarnib	PD	1 m				n/a
7	Cisplatin	n/a	n/a	Tipifarnib	SD	7 m							n/a
8	Alpelisib	n/a	n/a	Tipifarnib	n/a	6 m +							n/a
9	ADT (Bicalutamid/Leuprolide)	n/a	7 m +										n/a
10	ADT (LHRH + bicalutamide) Treatment Sequence Unknown	PD	0 m										10 m
11	ADT (Bicalutamid) Treatment Sequence Unknown	PD	1 m										13 m
12	ADT (Bicalutamid) Treatment Sequence Unknown	SD	1 m										5 m
13	ADT (Bicalutamid) Treatment Sequence Unknown	PR	14 m										44 m

Best response and progression-free survival (PFS) data are indicated for each provided treatment line. + indicates ongoing therapy/survival. Isolated data for androgen deprivation therapy (ADT) but no complete treatment sequences were available for patients 10-13. No high-grade or unexpected toxicities were observed and no dose interruptions were necessary in patients 1-4. ADT, androgen deprivation therapy; ID, identification number; PD, progressive disease; PFS, progression-free survival; SD, stable disease; m, months; MR, mixed response, OS, overall survival; n/a, not available..

10.3389/fonc.2023.1107134

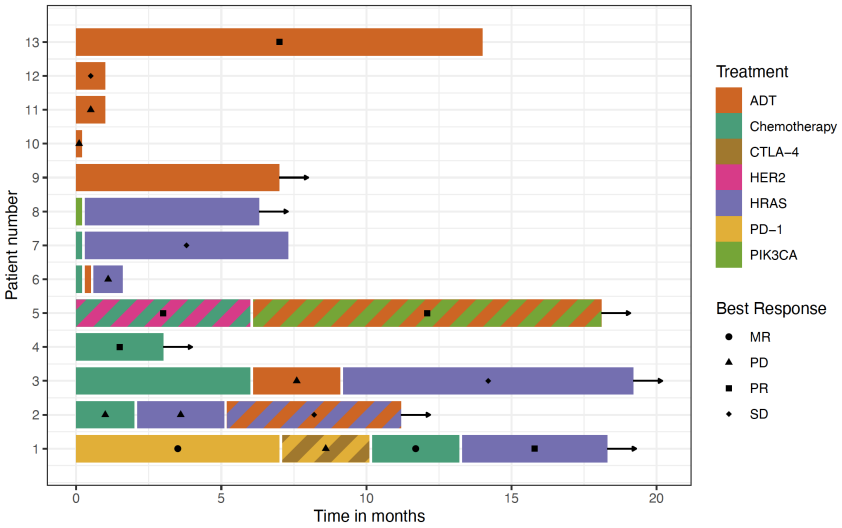

FIGURE 1
treatment sequences are depicted for the entire case series. No complete treatment sequences were available for patients 10-13. Duration of prior treatment was not provided for patients 6-8 (prior treatment indicated by colored bars). Color indicates the type of treatment; striped colors indicate combination therapy. Best responses are indicated. Arrows indicate ongoing therapy.

this phase 2 trial, tumor regressions were also noted among patients with prior ADT (14).

In patients receiving *HRAS*-directed therapy, 1 objective response and clinically meaningful disease stabilizations in about half of the patients was reported. These results are similar to previously reported results in SGC (9). In the same trial, co-occuring *PIK3CA*-alterations or the type of *HRAS* mutation (more common Q61 or less common G13) did also not seem to impact treatment efficacy (9). Again, these data further support the investigation of tipifarnib in the here reported disease subgroup.

Two patients received combination therapy after prior progression of disease. One patient achieved disease stabilization with tipifarnib and ADT after prior progression with tipifarnib monotherapy. In this patient, tipifarnib treatment was continued because of low toxicity and improvement in local symptoms. However, disease stabilization might be mediated by ADT alone. Another patient achieved a partial response with the PI3K-inhibitor alpelisib and ADT. The impact of the individual drugs in this combination therapy can also not be assessed. Further investigation of combination therapies is warranted.

A single agent PI3K-inhibitor was only used in 1 patient and no response data were available. The published results from the NCI-MATCH subprotocol Z1F of Copanlisib in *PIK3CA*-mutated cancer did show activity of the drug in several cancer types, but no SDC were enrolled (25). Additional research is needed to establish the activity of single-agent PI3K-inhibitors in SDC.

The activity of immune checkpoint inhibition also remains to be determined. One patient in the reported cohort achieved a mixed response with single-agent PD-1 blockade for 7 months, followed by disease progression. The same patient then experienced disease progression with combined PD-1 and CTLA-4 inhibition. Immune checkpoint inhibition was administered in this patient because of high PD-L1 expression and the co-occurrence of driver alterations, potentially complicating single-agent targeted treatment. These results suggest, that immune checkpoint inhibitors might be an additional treatment option in some patients. An analysis of 109 patients with advanced SGC in the Keynote-158 study showed an overall response rate of 4.6% in the overall population and 10.7% (n=3/28) in the PD-L1 positive population (26). Only 3 patients in this trial were found to be TMB-high, among which 1 had an objective reponse (26). PD-L1 expression or a high TMB > 10 mut/Mb was reported in 2 patients in the here reported cohort, accordingly.

For untargeted therapies, best data currently exist for carboplatin/paclitaxel use, which is also supported by previous analyses and yields clinically meaningful benefit (27).

In summary, the here provided data show multiple targeted treatment strategies for patients with AR+, *HRAS*/*PIK3CA* co-mutated SDC. Best available evidence, expected toxicities and patient factors need to be considered for a choice of treatment in this rare subgroup. These results support comprehensive molecular profiling of SDC. Additional molecular analyses might help with further establishing active signaling pathways for treatment stratification. Further research is required to establish optimal treatment combinations and sequences, which is a challenge in this rare disease.

Data availability statement

The original contributions presented in the study are included in the article/Supplementary Material. Further inquiries can be directed to the corresponding author.

Ethics statement

The studies involving human participants were reviewed and approved by Charité - Universitätsmedizin Berlin. Written informed consent for participation was not required for this study in accordance with the national legislation and the institutional requirements.

Author contributions

DR, SS, PS and KK provided patient data, DR performed a systematic review of the literature, DR, EZ, BE, DB, EB, UK (8th Author), UK (9th Author) and KK analyzed data. DR, UK (9th Author) and KK wrote the manuscript. All authors contributed to the article and approved the submitted version.

Funding

DR is a participant in the Berlin Institute of Health – Charité Clinical Scientist Program funded by the Charité – Universitätsmedizin Berlin and the Berlin Institute of Health. We acknowledge financial support from the Open Access Publication Fund of Charité – Universitätsmedizin Berlin and the German Research Foundation (DFG).

Conflict of interest

DR has received consultant and/or advisory board and/or speaker fees from Roche, Bayer, Bristol-Myers Squibb and Lilly. PS has received honoraria personal from BMS, MSD, Incyte, SOBI, AOP, Novartis, Alexion, AstraZeneca, BPM, and ROCHE and travel support from BMS, SOBI, AOP, and Novartis. UK 8th Author reports a consulting role for Roche, Janssen-Cilag, Takeda, BMS, Gilead, Hexal, Pfizer, Astra-Zeneca, Pentixapharm and honoraria from Gilead, Amgen, Novartis, BMS, Roche, Takeda, MSD, as well as research funding from Celgene, Takeda, BMS, Roche, Astra-Zeneca, Novartis, MSD, Janssen-Cilag, Pfizer. Other support was declared from Roche, BMS, Gilead, Takeda, Janssen-Cilag and Celgene. UK 9th Author has received advisory board/speaker bureau, trial support, research collaboration or research support from Amgen, AstraZeneca, BMS, Boehringer Ingelheim, Glycotope, Innate, Lilly, Medimmune, MerckSerono, MSD/Merck, Novartis, Pfizer, Roche/Genentech and Sirtex. KK: Advisory Boards, travel grants and speaker's fees: MSD, BMS, Merck, Novartis, Bayer.

The remaining authors declare that the research was conducted in the absence of any commercial or financial relationships that could be construed as a potential conflict of interest.

Publisher's note

Supplementary material

The Supplementary Material for this article can be found online at: https://www.frontiersin.org/articles/10.3389/fonc.2023.1107134/full#supplementary-material

SUPPLEMENTARY FIGURE 1
Consort diagram showing the identification of patients for the final cohort. MTB, molecular tumor board; HNC, head and neck cancer; SGC, salivary gland cancer; SDC, salivary duct carcinoma.

References

1. Helen Lin H, Limesand KH, Ann DK. Current state of knowledge on salivary gland cancers. *Crit Rev Oncog* (2018) 23:139–51. doi: 10.1615/CRITREVONCOG.2018027598

2. Skálová A, Hyrcza MD, Leivo I. Update from the 5th edition of the world health organization classification of head and neck tumors: salivary glands. *Head Neck Pathol* (2022) 16:40–53. doi: 10.1007/S12105-022-01420-1

3. Kleinsasser O, Klein HJ, Hübner G. [Salivary duct carcinoma. a group of salivary gland tumors analogous to mammary duct carcinoma]. *Arch Klin Exp Ohren Nasen Kehlkopfheilkd* (1968) 192:100–5. doi: 10.1007/BF00301495

4. Schmitt NC, Kang H, Sharma A. Salivary duct carcinoma: an aggressive salivary gland malignancy with opportunities for targeted therapy. *Oral Oncol* (2017) 74:40–8. doi: 10.1016/J.ORALONCOLOGY.2017.09.008

5. Jayaprakash V, Merzianu M, Warren GW, Arshad H, Hicks WL, Rigual NR, et al. Survival rates and prognostic factors for infiltrating salivary duct carcinoma: analysis of 228 cases from the surveillance, epidemiology, and end results database. *Head Neck* (2014) 36:694–701. doi: 10.1002/HED.23350

6. Mifsud M, Sharma S, Leon M, Padhya T, Otto K, Caudell J. Salivary duct carcinoma of the parotid: outcomes with a contemporary multidisciplinary treatment approach. *Otolaryngol Head Neck Surg* (2016) 154:1041–6. doi: 10.1177/0194599816636812

7. Ross JS, Gay LM, Wang K, Vergilio JA, Suh J, Ramkissoon S, et al. Comprehensive genomic profiles of metastatic and relapsed salivary gland carcinomas are associated with tumor type and reveal new routes to targeted therapies. *Ann Oncol* (2017) 28:2539–46. doi: 10.1093/ANNONC/MDX399

8. Dalin MG, Desrichard A, Katabi N, Makarov V, Walsh LA, Lee KW, et al. Comprehensive molecular characterization of salivary duct carcinoma reveals actionable targets and similarity to apocrine breast cancer. *Clin Cancer Res* (2016) 22:4623–33. doi: 10.1158/1078-0432.CCR-16-0637

9. Hanna GJ, Guenette JP, Chau NG, Sayehli CM, Wilhelm C, Metcalf R, et al. Tipifarnib in recurrent, metastatic HRAS-mutant salivary gland cancer. *Cancer* (2020) 126:3972–81. doi: 10.1002/CNCR.33036

10. Fushimi C, Tada Y, Takahashi H, Nagao T, Ojiri H, Masubuchi T, et al. A prospective phase II study of combined androgen blockade in patients with androgen receptor-positive metastatic or locally advanced unresectable salivary gland carcinoma. *Ann Oncol* (2018) 29:979–84. doi: 10.1093/ANNONC/MDX771

11. Takahashi H, Tada Y, Saotome T, Akazawa K, Ojiri H, Fushimi C, et al. Phase II trial of trastuzumab and docetaxel in patients with human epidermal growth factor receptor 2-positive salivary duct carcinoma. *J Clin Oncol* (2019) 37:125–34. doi: 10.1200/JCO.18.00545

12. Kurzrock R, Bowles DW, Kang H, Meric-Bernstam F, Hainsworth J, Spigel DR, et al. Targeted therapy for advanced salivary gland carcinoma based on molecular profiling: results from MyPathway, a phase IIa multiple basket study. *Ann Oncol* (2020) 31:412–21. doi: 10.1016/J.ANNONC.2019.11.018

13. Locati LD, Cavalieri S, Bergamini C, Resteghini C, Colombo E, Calareso G, et al. Abiraterone acetate in patients with castration-resistant, androgen receptor-expressing salivary gland cancer: a phase II trial. *J Clin Oncol* (2021) 39:4061–8. doi: 10.1200/JCO.21.00468

14. Ho AL, Foster NR, Zoroufy AJ, Campbell JD, Worden F, Price K, et al. Phase II study of enzalutamide for patients with androgen receptor-positive salivary gland cancers (Alliance A091404). *J Clin Oncol* (2022) 40:4240–9. doi: 10.1200/JCO.22.00229

15. van Herpen C, Vander Poorten V, Skalova A, Terhaard C, Maroldi R, van Engen A, et al. Salivary gland cancer: ESMO-European reference network on rare adult solid cancers (EURACAN) clinical practice guideline for diagnosis, treatment and follow-up. *ESMO Open* (2022) 7:100602. doi: 10.1016/J.ESMOOP.2022.100602/ATTACHMENT/06B11B84-E961-43A3-BB8F-BD5E325E30EE/MMC1.PDF

16. Geiger JL, Ismaila N, Beadle B, Caudell JJ, Chau N, Deschler D, et al. Management of salivary gland malignancy: ASCO guideline. *J Clin Oncol* (2021) 39 (17):1909-41. doi: 10.1200/JCO.21.00449

17. Mateo J, Chakravarty D, Dienstmann R, Jezdic S, Gonzalez-Perez A, Lopez-Bigas N, et al. A framework to rank genomic alterations as targets for cancer precision medicine: the ESMO scale for clinical actionability of molecular targets (ESCAT). *Ann Oncol* (2018) 29:1895–902. doi: 10.1093/ANNONC/MDY263

18. Marcus L, Fashoyin-Aje LA, Donoghue M, Yuan M, Rodriguez L, Gallagher PS, et al. FDA Approval summary: pembrolizumab for the treatment of tumor mutational burden-high solid tumors. *Clin Cancer Res* (2021) 27:4685–9. doi: 10.1158/1078-0432.CCR-21-0327

19. Mueller SA, Gauthier MEA, Blackburn J, Grady JP, Kraitsek S, Hajdu E, et al. Molecular patterns in salivary duct carcinoma identify prognostic subgroups. *Mod Pathol* (2020) 33:1896–909. doi: 10.1038/S41379-020-0576-2

20. Lamping M, Benary M, Leyvraz S, Messerschmidt C, Blanc E, Kessler T, et al. Support of a molecular tumour board by an evidence-based decision management system for precision oncology. *Eur J Cancer* (2020) 127:41–51. doi: 10.1016/j.ejca.2019.12.017

21. Sheth H, Kumar P, Shreenivas A, Sambath J, Pragya R, Madre C, et al. Excellent response with alpelisib and bicalutamide for advanced salivary duct carcinoma with PIK3CA mutation and high androgen receptor expression-a case report. *JCO Precis Oncol* (2021) 5:744–50. doi: 10.1200/PO.20.00436

22. You Y, Wang P, Wan X, Xu L, Gong Y, Zhang W. Androgen deprivation therapy for patients with androgen-Receptor-Positive metastatic salivary duct carcinoma: a case report and review of the literature. *Onco Targets Ther* (2021) 14:3481–6. doi: 10.2147/OTT.S304900

23. van Boxtel W, Verhaegh GW, van Engen-van Grunsven IA, van Strijp D, Kroeze LI, Ligtenberg MJ, et al. Prediction of clinical benefit from androgen deprivation therapy in salivary duct carcinoma patients. *Int J Cancer* (2020) 146:3196–206. doi: 10.1002/IJC.32795

24. Li BT, Shen R, Offin M, Buonocore DJ, Myers ML, Venkatesh A, et al. Ado-trastuzumab emtansine in patients with HER2 amplified salivary gland cancers (SGCs): results from a phase II basket trial. *J Clin Oncol* (2019) 37:6001–1. doi: 10.1200/JCO.2019.37.15_SUPPL.6001

25. Damodaran S, Zhao F, Deming DA, Mitchell EP, Wright JJ, Gray RJ, et al. Phase II study of copanlisib in patients with tumors with PIK3CA mutations: results from the NCI-MATCH ECOG-ACRIN trial (EAY131) subprotocol Z1F. *J Clin Oncol* (2022) 40:1552–61. doi: 10.1200/JCO.21.01648

26. Even C, Delord JP, Price KA, Nakagawa K, Oh DY, Burge M, et al. Evaluation of pembrolizumab monotherapy in patients with previously treated advanced salivary gland carcinoma in the phase 2 KEYNOTE-158 study. *Eur J Cancer* (2022) 171:259–68. doi: 10.1016/J.EJCA.2022.05.007

27. Uijen MJM, Lassche G, van Engen-van Grunsven ACH, Tada Y, Verhaegh GW, Schalken JA, et al. Systemic therapy in the management of recurrent or metastatic salivary duct carcinoma: a systematic review. *Cancer Treat Rev* (2020) 89:102069. doi: 10.1016/J.CTRV.2020.102069

frontiers | Frontiers in Oncology

TYPE Original Research
PUBLISHED 18 August 2023
DOI 10.3389/fonc.2023.1223598

OPEN ACCESS

EDITED BY
Ester Orlandi,
National Center of Oncological Hadrontherapy, Italy

REVIEWED BY
Sara Imparato,
National Center of Oncological Hadrontherapy, Italy
Huiting Zhang,
Siemens Healthineers, China

*CORRESPONDENCE
Lijun Wang
wanglj345@163.com

RECEIVED 16 May 2023
ACCEPTED 28 July 2023
PUBLISHED 18 August 2023

CITATION
Wang Y, Wang L, Huang H, Ma J, Lin L, Liu L, Song Q and Liu A (2023) Amide proton transfer-weighted magnetic resonance imaging for the differentiation of parotid gland tumors.
Front. Oncol. 13:1223598.
doi: 10.3389/fonc.2023.1223598

Amide proton transfer-weighted magnetic resonance imaging for the differentiation of parotid gland tumors

Yihua Wang[1], Lijun Wang[1]*, Haitao Huang[2], Juntao Ma[2], Liangjie Lin[3], Lin Liu[2], Qingwei Song[1] and Ailian Liu[1]

[1]Department of Radiology, First Affiliated Hospital of Dalian Medical University, Dalian, China, [2]Department of Stomatology, First Affiliated Hospital of Dalian Medical University, Dalian, China, [3]Clinical and Technical Support, Philips Healthcare, Beijing, China

Purpose: To assess the usefulness of amide proton transfer-weighted (APTw) imaging in the differentiation of parotid gland tumors.

Materials and methods: Patients with parotid gland tumors who underwent APTw imaging were retrospectively enrolled and divided into groups according to pathology. Two radiologists evaluated the APTw image quality independently, and APTw images with quality score ≥3 were enrolled. The maximum and average values of APTw imaging for tumor lesions (APTmax and APTmean) were measured. The differences in APTmax and APTmean were compared between malignant tumors (MTs) and benign tumors (BTs), as well as between MTs and pleomorphic adenomas (PAs) and between MTs and Warthin tumors (WTs). Independent-samples *t*-test, Kruskal–Wallis *H* test, and receiver operating characteristic (ROC) curve analyses were used for statistical analysis.

Results: Seventy-three patients were included for image quality evaluation. In this study, 32/73 and 29/73 parotid tumors were scored as 4 and 3, respectively. After excluding lesions with quality score ≤2 (12/73), the APTmean and APTmax of MTs were 4.15% ± 1.33% and 7.43% ± 1.61%, higher than those of BTs 2.74% ± 1.04% and 5.25% ± 1.54%, respectively ($p < 0.05$). The areas under the ROC curve (AUCs) of the APTmean and APTmax for differentiation between MTs and BTs were 0.819 and 0.821, respectively. MTs indicated significantly higher APTmean and APTmax values than those of PAs ($p < 0.05$) and WTs ($p < 0.05$). The AUCs of the APTmean and APTmax for differentiation between MTs and PAs were 0.830 and 0.815 and between MTs and WTs were 0.847 and 0.920, respectively.

Conclusion: Most APTw images for parotid tumors had acceptable image quality for APTw value evaluation. Both APTmax and APTmean can be used to differentiate MTs from BTs and to differentiate MTs from subtype parotid gland tumors.

KEYWORDS

parotid gland tumor, magnetic resonance imaging, amide proton transfer-weighted image, pleomorphic adenoma, Warthin tumor

Introduction

Salivary gland tumors account for approximately 2%~5% of all tumors in the head and neck (1, 2), with nearly 80% occurring in the parotid glands. The parotid benign tumors (BTs) and malignant tumors (MTs) account for approximately 80% and 20%, respectively (3). For BTs, local parotidectomy or superficial lobectomy is adopted to protect the facial nerve. For MTs, total parotidectomy is required (4, 5). Preoperative biopsy is helpful for the qualitative diagnosis of parotid gland tumors, but some punctures have the risk of capsule rupture, which will greatly increase the risk of tumor proliferation or implantation (6). Therefore, noninvasive qualitative preoperative diagnosis has become an urgent clinical need.

Magnetic resonance imaging (MRI) is one of the major methods to diagnose tumors of the head and neck with good visualization (7, 8). However, the pathological types of parotid gland tumors are various, and there exists substantial overlap in the appearance of tumors, which limits the role of conventional MRI in characterization and brings great difficulty to the preoperative qualitative diagnosis (9). In the past, diffusion-weighted imaging (DWI), dynamic contrast-enhanced MRI (DCE-MRI), and other functional imaging have been used to evaluate parotid tumors, but the diagnostic ability of one single functional MRI technology is limited (10–12). Rather, multiparametric analysis is usually required to improve diagnostic accuracy (13, 14). However, there are still some challenges in the clinical applications of multiparametric analysis because of the long acquisition time and requirement in the injection of contrast agents in DCE-MRI.

Amide proton transfer-weighted (APTw) imaging is a novel imaging technique that uses endogenous contrast by chemical exchange saturation transfer to indirectly detect mobile proteins and peptides in tissues, which are thought to closely relate to tumor metabolism (15). The clinical utility of APTw imaging has already been demonstrated in glioma, lung cancer, prostate cancer, endometrial carcinoma, and rectal cancer (16–19). Kamitani et al. (20) demonstrated that for parotid tumors, the mean APTw values measured from circle regions of interest (ROIs) in MTs were higher than those in BTs. Bae et al. (21) reported about parotid gland that APTw imaging was superior to conventional MRI contrasts and to advanced functional imaging methods such as DCE-MRI and DWI. However, one limitation of APTw is its vulnerability to hyperintensity artifacts in the parotid gland, resulting in false positives in the evaluation of lesions probably (22, 23). Therefore, in this study, we investigated APTw imaging in parotid lesions in terms of image quality to ensure the accuracy of APTw measurements and evaluated its ability to differentiate among parotid gland tumors.

Abbreviations: APTw, amide proton transfer-weighted; AUC, area under the receiver operating characteristic curve; BT, benign tumor; DWI, diffusion-weighted imaging; DCE-MRI, dynamic contrast-enhanced MRI; ICC, intraclass correlation coefficient; MT, malignant tumor; MRI, magnetic resonance imaging; PA, pleomorphic adenoma; ROI, region of interest; ROC, receiver operating characteristic; WT, Warthin tumor.

Materials and methods

Patients

The institutional review board of our hospital approved our retrospective study (license number: PJ-KS-XJS-2021-18). The patients who participated in this study provided their written informed consent. Inclusion criteria were as follows: 1) the clinical and pathological information was complete; 2) 3.0T MRI examination [including T1-weighted imaging (T1WI), T2-weighted imaging (T2WI), and APTw imaging] was performed within 1 week before treatment; 3) no treatment before MRI examination. Exclusion criteria were as follows: 1) parotid lesions were not clearly visible on images or motion artifacts affected the observation; 2) the tumor diameter was less than 2 cm that it was difficult to define the boundary of the tumor. The flowchart of patient inclusion and exclusion is shown in Figure 1.

Based on inclusion criteria, the imaging and clinical information data of 105 patients with parotid gland tumors in our hospital from September 2020 to October 2022 were retrospectively analyzed. All patients underwent surgical treatment in the Department of Stomatology of our hospital within 1 week after MRI examination. All extracted tumor tissues routinely underwent histopathological examination after the operation. These tissues were embedded in paraffin, stained with hematoxylin–eosin, and examined microscopically.

MRI

APTw imaging was performed using a 3.0T MR scanner (Ingenia CX; Philips Healthcare, Best, Netherlands) with a 32-channel phase-array head coil. In addition, the protocol of conventional MRI was acquired, including the axial T1WI and axial fat-suppressed T2WI. The APTw sequence used in this study is based on Chen et al. (23). The detailed parameters of all MRI sequences are shown in Table 1. The $MTR_{asym(3.5\ ppm)}$ was calculated by the following equation: $MTR_{asym(3.5\ ppm)} = (S_{-3.5\ ppm} - S_{3.5\ ppm})/S_0$, where $S_{-3.5\ ppm}$ is the signal intensity acquired at the saturation frequency of -3.5 ppm, $S_{3.5\ ppm}$ is the signal intensity acquired at the saturation frequency of 3.5 ppm, and S_0 is the reference signal intensity acquired at a saturation frequency of 1,540 ppm (the water frequency was referred to as 0 ppm).

MR image evaluation

APTw images were automatically reconstructed after data acquisition and then transferred to the Intellispace Portal (ISP v9.0, Philips Healthcare) workstation. The image quality evaluation and quantitative measurements of APTw image were implemented by two experienced radiologists in MRI diagnosis independently (radiologist 1 and radiologist 2 had 3 and 20 years of MRI diagnosis experience, respectively) who were blinded to pathological results. With APTw images fused to axial T2WI images, the degree of image quality was judged with a 4-scale scoring system

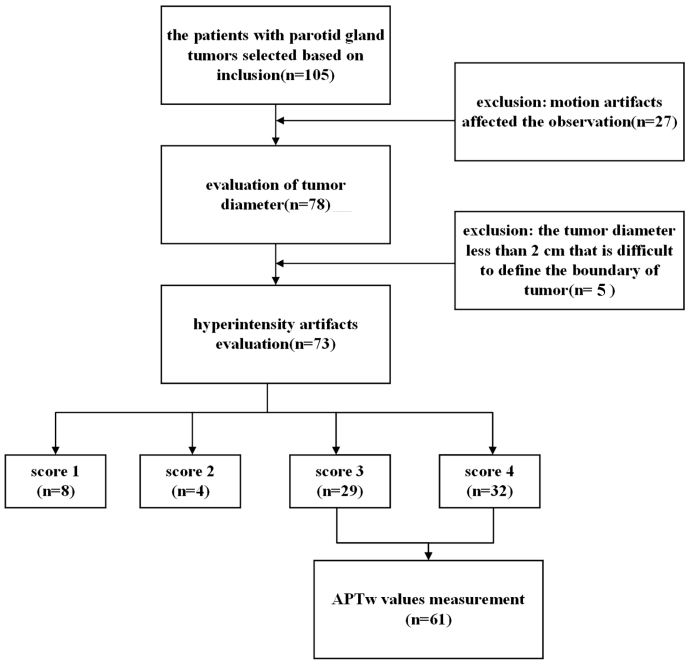

FIGURE 1
Flowchart depicting the patient selection.

according to a previous report (23): 4 = excellent, tumor could be recognized on APTw images without hyperintensity artifacts; 3 = good, hyperintensity artifacts impair less than 50% tumor; 2 = moderate, hyperintensity artifacts impair more than 50% tumor; 1 = poor, the entire tumor is impaired by hyperintensity artifacts.

APTw images with image quality score no higher than 2 were excluded for further analyses. The ROI was carefully drawn on a slice of the fused image showing the maximum lesion to cover the solid part of the tumor as much as possible and exclude the cystic degeneration, necrosis, and hyperintensity artifacts from surrounding tissues (Figure 2). The maximum (APTmax) and the average (APTmean) values were recorded.

Statistical analysis

For statistical analyses of patient information and diagnostic efficacy of APTw, we used SPSS (version 25.0; IBM Corp., Armonk, NY, USA) and MedCalc (version 20 MedCalc Software Ltd., Ostend, Belgium). The interobserver reliability for all APTw values measured by two radiologists was assessed *via* intraclass correlation coefficient (ICC) (excellent, >0.75; good, 0.60~0.74; fair, 0.40~0.59; poor, <0.40). One-sample Kolmogorov–Smirnov test was performed to test the normality of APTmax and APTmean values for both BTs and MTs, as well as patient ages. When continuous variables conformed to the normal distribution, the parameters were expressed as mean ± standard deviation, and independent-samples *t*-test was used for comparisons between BTs and MTs groups; otherwise, they were expressed as median (first quartile, third quartile), and Mann–Whitney U test was used. The Kruskal–Wallis *H* test was used to test the differences of the two parameters among pleomorphic adenomas (PAs), Warthin tumors (WTs), and MTs. The pairwise comparison with Bonferroni correction was made with overall test statistically significant for the above three groups. Receiver operating characteristic (ROC) curve analysis was used to determine the diagnostic value of APTmax and APTmean for the differentiation between MTs and BTs. The threshold criterion was calculated to maximize the Youden index. ROC curves were compared by the method of DeLong et al. (24). $p < 0.05$ was considered statistically significant.

TABLE 1 Scan parameters of T1WI, T2WI, and APTw.

	TR (ms)	TE (ms)	Voxel (mm)	FOV (mm)	Matrix
T_1WI	466	8.1	0.55×0.72×4	200×200×89	364×257×18
T_2WI	2,122	112	0.7×0.7×4	300×300×89	428×428×18
APTw	3,000	7.9	2.5×2.5×2.5	230×221×62	120×140×40

APTw, amide proton transfer-weighted imaging; T1WI, T1-weighted imaging; T2WI,T2-weighted imaging; TR, repetition time; TE, echo time.

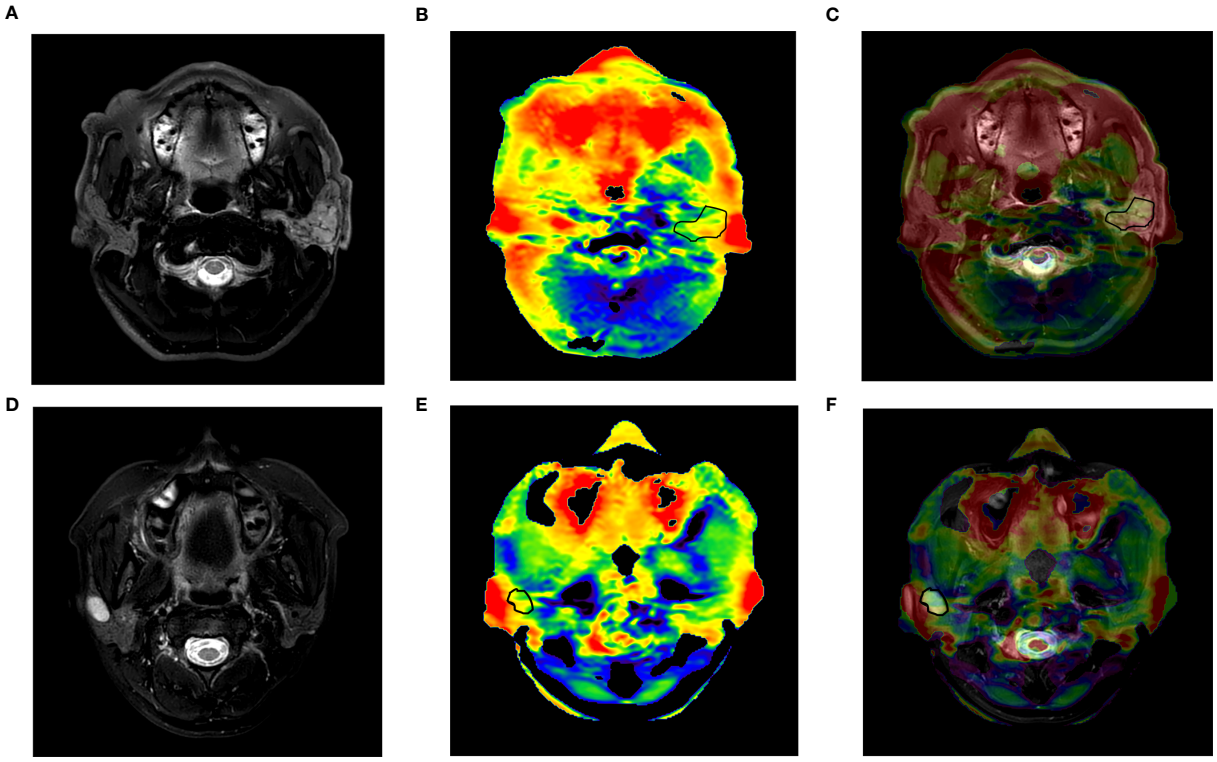

FIGURE 2
(A–C) A 57-year-old man with adenoid cystic carcinoma of the left parotid gland. **(A)** T2WI; **(B)** APTw image; **(C)** APTw image (fused on T2WI) showed an image quality score of 3 with little hyperintensity artifact less than 50% tumor, an APTmean of 5.14%, and an APTmax of 6.75%. **(D–F)** A 30-year-old woman with pleomorphic adenoma of the right parotid gland. **(D)** T2WI; **(E)** APTw image; **(F)** APTw image (fused on T2WI) showed an image quality score of 4, an APTmean value of 1.95%, and an APTmax of 4.9%. APTmax, the maximum value of APTw imaging; APTmean, the average value of APTw imaging; APTw, amide proton transfer-weighted.

Results

Patient characteristics

Among the included 105 patients, 27 patients were excluded because of the incomplete MR scans or severe motion artifacts on images, and five patients were excluded due to the small tumor size and unclear tumor boundary. Finally, we enrolled a total of 73 patients for the next image quality analysis. According to the benign and malignant pathological results, 73 patients who were included for image quality scale analysis were divided into two groups (Table 2). There was no significant difference in age (p = 0.63) between benign and malignant groups.

Score of APTw image quality

Interobserver agreement was excellent, with ICCs = 0.989 for artifact scores of parotid lesions by the two readers. In the evaluation of image quality, 32 out of 73 parotid tumors (43.84%) were considered for score 4, and 29 out of 73 (39.73%) for score 3. Moreover, 5.48% (4/73) and 10.95% (8/73) of tumors were scored 2 and 1, respectively, which showed parotid lesions highly affected by hyperintensity artifacts and were removed in the subsequent measurement of APTw values.

APTw finding and diagnostic performance between BTs and MTs

After excluding the cases with image quality scores ≤2, 61 patients were involved in the quantitative evaluation. Interobserver agreement was excellent, with ICCs = 0.994 and 0.918, respectively, for APTmax and APTmean measurements, and the average values by the two observers were taken for analyses. The APTmean of MTs (4.15% ± 1.33%) was significantly higher than that of BTs (2.74% ± 1.04%) ($p < 0.05$), and the APTmax value of MTs was (7.43% ± 1.61%), similarly higher than that of BTs (5.25% ± 1.54%) ($p < 0.05$) (Table 3, Figure 3).

The threshold of APTmean was 3.98%, and its area under the ROC curve (AUC), sensitivity, and specificity were 0.819, 86.00%, and 72.73%, respectively, for differential diagnosis between BTs and MTs. Moreover, ROC curve analysis indicated that an APTmax of 5.9% was the optimum threshold to distinguish between BTs and MTs, with AUC, sensitivity, and specificity of 0.821, 53.33%, and 82.61%, respectively. There was no significant difference in

TABLE 2 Demographics for patients confirmed by surgery.

	Benign group (n=62)	Malignant group (n=11)
Male : Female	41:21	8:3
Age (years)	25-85 (mean 55.73 ± 15.38)	46-82 (mean 58.00 ± 10.95)
Pathology	32 pleomorphic adenoma	3 mucoepidermoid carcinoma
	21 Warthin tumor	2 acinic cell carcinoma
	8 base cell adenoma	2 adnoid cystic carcinoma
	1 schwannoma	1 salivary duct carcinoma
		1 malignant neurofibroma
		1 non Hodgkin's lymphoma
		1 poorly differentiated carcinoma

diagnostic efficacy between the above parameters (Z = 0.017, p = 0.987) (Table 4, Figure 4).

APTw finding and diagnostic performance among PAs, WTs, and MTs

There were significant differences among these three groups (APTmean, p = 0.03; APTmax, p = 0.02). The pairwise comparisons showed that the APTmean and APTmax values in MTs were significantly higher than those of PAs and WTs, while the difference of the two parameters between PAs and WTs was not significant (p > 0.99, Table 5).

The diagnostic performance of APTmean and APTmax for differentiating among these three groups was shown in Tables 4 and 5. When the thresholds of the APTmean and APTmax were 3.98% and 5.65%, respectively, the optimal diagnostic performance for differentiating between PAs and MTs can be achieved. The AUC, sensitivity, and specificity of the APTmean between PAs and MTs were 0.830, 92.31%, and 72.73%. And the AUC, sensitivity, and specificity of the APTmax between PAs and MTs were 0.815, 76.90%, and 90.90%. Meanwhile, the threshold APTmean value of 3.90% can be used for optimal differential diagnosis between WTs and MTs with AUC, sensitivity, and specificity 0.847, 93.57%, and 72.73%. And the threshold APTmax value of 5.50% can be used for differentiating between WTs and MTs with AUC, sensitivity, and specificity 0.920, 93.75%, and 90.91%. There was no significant difference in diagnostic efficacy between APTmean and APTmax (PAs and MTs: Z = 0.141, p = 0.887; WTs and MTs: Z = 0.707, p = 0.479).

Discussion

In this study, we investigated the image quality of APTw imaging of parotid gland tumors and evaluated the characteristics and diagnostic performance of APTmax and APTmean. APTmean and APTmax in MTs were higher than those in BTs with high diagnostic efficacy. However, APTw imaging based on the current technology may be associated with severe artifacts in parotid glands (16.43% of cases), which can affect the evaluation of tumors.

In the parotid gland, APTw hyperintensity artifacts, diffused from the bone, air, ear, and other surrounding tissues, can affect the display of peripheral lesions and thus the quantitative APTw measurements. In this study, most of the cases with score ≤2 were PAs and WTs, where more than half of the tumors and the surrounding normal parotid gland parenchyma showed significantly hyperintensity. These hyperintensity artifacts were usually spread from the ear and mandible regions around the parotid gland. On the other hand, the area of hemorrhage, necrosis, and cystic degeneration can also contribute to the increase of APTw values due to the increase of mobile water molecule and amide protons. Chen et al. (23) demonstrated that approximately 70.6% of parotid gland lesions had no or small artifacts and the APTw measurements of the lesion would be reliable after excluding cases with poor image integrity and severe artifacts. Takeshi et al. (20) evaluated the difference in APTw values of BTs and MTs by sketching three circular ROIs in the parenchyma of parotid tumors. This measurement method can avoid artifacts of necrosis and cystic degeneration but cannot determine the maximum value of the whole tumors. Therefore, this study evaluated the image quality (83.57% of cases with an acceptable image quality score of 3 or 4) before the overall measurement of lesions, excluded lesions with severe artifacts, and determined reliable cases for analyses. The fusion of APTw with conventional structural images can be helpful for the determination of tumor boundary.

APTw imaging has been widely used in the assessment of tumor metabolism, ischemic penumbra of cerebral infarction, neurodegenerative changes, etc. (25, 26). In previous studies (27), it was found that MTs showed generally higher APTw values due to increased mobile proteins and polypeptides; however, abundant new blood vessels and increased vascular permeability could also lead to significantly increased APTw signal intensity in BTs. Most

TABLE 3 Comparison of APTw values between BT and MT.

	ICC*	MT(n=11)	BT(n=50)	p
APTmax(%)	0.918	7.43 ± 1.61	5.25 ± 1.54	<0.01
APTmean(%)	0.994	4.15 ± 1.33	2.74 ± 1.04	<0.01

*Interobserver agreement was excellent.
APTmax, the maximum value of APTw imaging; APTmean, the average value of APTw imaging; APTw, amide proton transfer-weighted; BT, benign tumor; MT, malignant tumor.

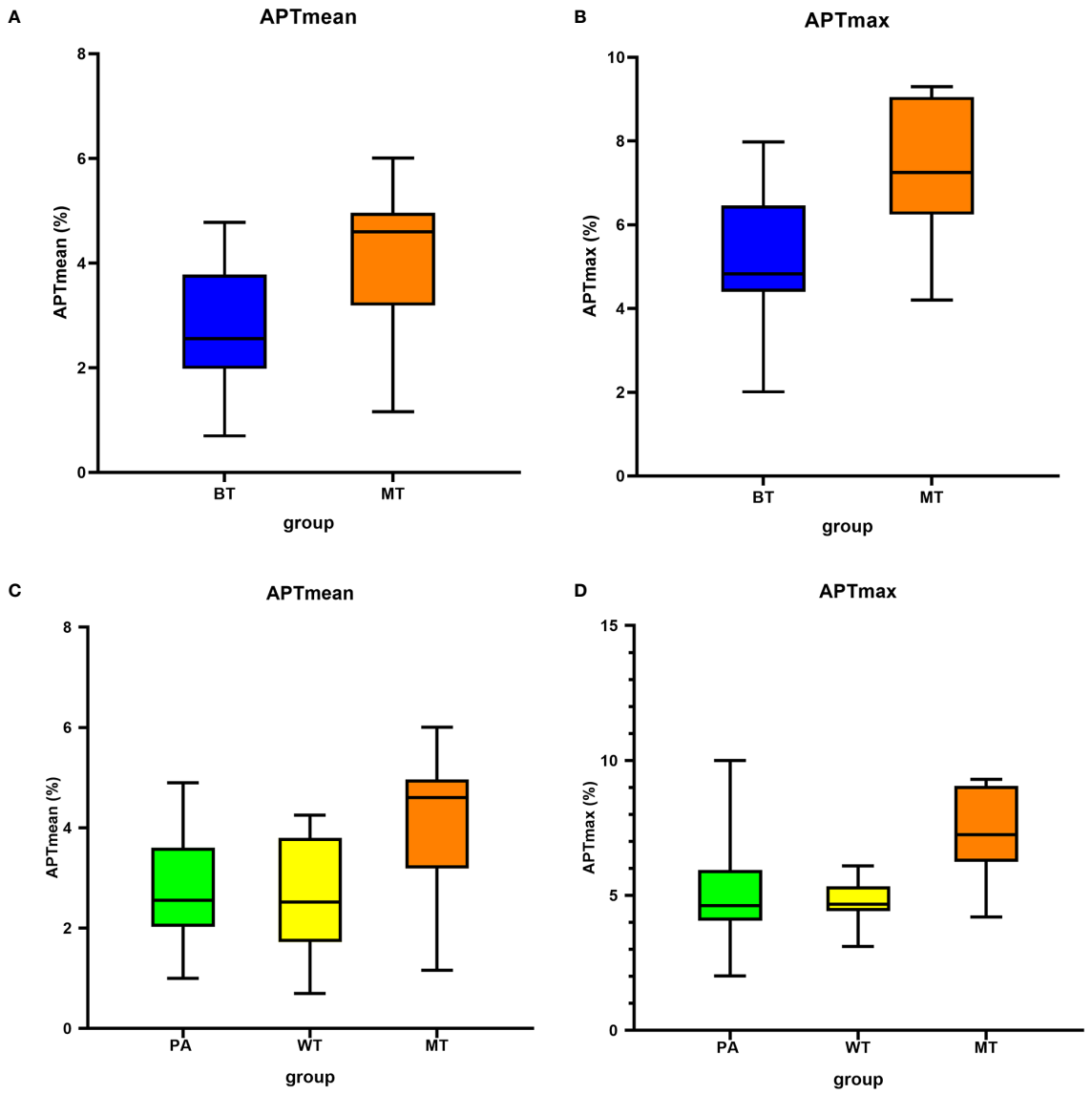

FIGURE 3
Box plots show the comparison of APTmean and APTmax among groups. Line in box represents the median, and the height of the box represents the interquartile range. **(A, B)** Comparison between BT and MT; **(C, D)** comparison among PA, WT, and MT. APTmax, the maximum value of APTw imaging; APTmean, the average value of APTw imaging; BT, benign tumor; MT, malignant tumor; PA, pleomorphic adenoma; WT, Warthin tumor.

studies (20, 28) used the mean APTw value of the lesion to evaluate the overall lesion. Generally, the APTw mean value of MTs is higher than that of BTs, and similar results were also observed in this study. However, in the study of Ochiai et al. (29) on the evaluation of endometrial carcinoma, APTmean values had no significant difference between type I and type II endometrial carcinoma, but APTmax was significantly higher in type II carcinomas than that in type I, which may be due to the heterogeneity of lesion histology. APTmax might indicate the position with the most active metabolism and the highest cell density, which can evaluate heterogeneity of tumors more accurately in some studies (30, 31). The malignant lesions with more active cell proliferation, which showed a higher APTw value, may be related to the capacity of tumor invasion and prognosis. In the study by Law et al. (27), the AUC and sensitivity of the APTw value at the 90th percentage in head and neck tumors were significantly higher than those of the mean APTw value. Therefore, we speculated that the maximum APTw value of the whole lesions may have high diagnostic efficacy between BTs and MTs.

In this study, we excluded the cases showing artifacts that might affect the APTw value measurements and selected the slice with the largest section of lesion for ROI delineation to obtain the mean and maximum APTw values. It was found that in this study, the AUC of the APTmax value was similar to that of the APTmean for differentiation between MTs and BTs, but the APTmax was more specific than the APTmean. Additionally, because of hypercellularity, some functional MRI sequences showed image overlap between WTs and MTs (32, 33). In this study, the

TABLE 4 The ROC curve of the values of APTw to differentiate between groups.

	Cut off value	AUC (95% confidence interval)	Sen(%)	Sp(%)	PPV(%)	NPV(%)
BT vs. MT						
APTmax	5.9%	0.821 (0.702, 0.907)	53.33	82.61	41.67	97.30
APTmean	3.98%	0.819 (0.700, 0.906)	86.00	72.73	53.34	93.48
PA vs. MT						
APTmax	5.65%	0.815 (0.653, 0.923)	76.90	90.90	62.50	95.24
APTmean	3.98%	0.830 (0.671, 0.933)	92.31	72.73	80.00	88.89
WT vs. MT						
APTmax	5.50%	0.920 (0.750, 0.989)	93.75	90.91	90.91	93.75
APTmean	3.90%	0.847 (0.656, 0.955)	93.57	72.73	88.89	83.33

AUC, area under the receiver operating characteristic curve; APTmax, the maximum value of APTw imaging; APTmean, the average value of APTw imaging; APTw, amide proton transfer-weighted; BT, benign tumor; MT, malignant tumor; NPV, negative predictive value; PA, pleomorphic adenoma; PPV, positive predictive value; Sen, sensitivity; Sp, specificity; WT, Warthin tumor.

APTmean also showed false-positive results in the evaluation of MTs, but the APTmax values in the two groups of tumors have less overlap with higher diagnostic efficiency, which may suggest that the APTmax can play a complementary role in the differential diagnosis of parotid gland tumors. Although the overall APTmean and APTmax of BTs were lower, not a few cases of PA exhibited high APTmax signals. Some studies (20, 34, 35) believe that the epithelial and interstitial components of PA are diverse, and mesenchymal-like component is rich in mucoid, which can cause the variety of APTw values and might be the interference for APTw in parotid gland tumor evaluation. Moreover, some MTs (36) were low-grade malignant (such as mucoepidermoid carcinomas), and the increase of cell proliferation was not obvious, with the increase of the APTw value inapparent, which can be difficult to be distinguished from some BTs with more active proliferation. Therefore, the pathological complexity of parotid gland tumors mentioned above led to their diverse imaging manifestations, which also affected the accuracy of the APTmean and APTmax in the diagnosis of parotid gland tumors.

There are some limitations in our study. First, we did not choose the overall volume but the largest slice of tumor for analysis, which may affect the evaluation of tumor heterogeneity. Second, our study did not register imaging results with pathological findings accurately. It is necessary to further explore the relationship between the heterogeneity of imaging manifestations and tissue structure. Third, some previous studies (11, 13) demonstrated a high diagnostic performance with the combination of DCE-MRI and DWI, and this study did not compare APTw-MRI with other functional imaging sequences and investigate whether APTw can further improve the diagnostic performance of other functional sequences. Fourth, this was a small-sample retrospective study, especially, with few other BT types except PAs and WTs, and the malignant group was a small sample and includes different histological patterns. The pathological types were relatively limited, which may cause some errors in the statistics of the results. The low disease prevalence of MTs is the fundamental limiting factor. It is recommended to conduct further research to confirm the clinical impact of our results and the differences between specific sites in a larger cohort.

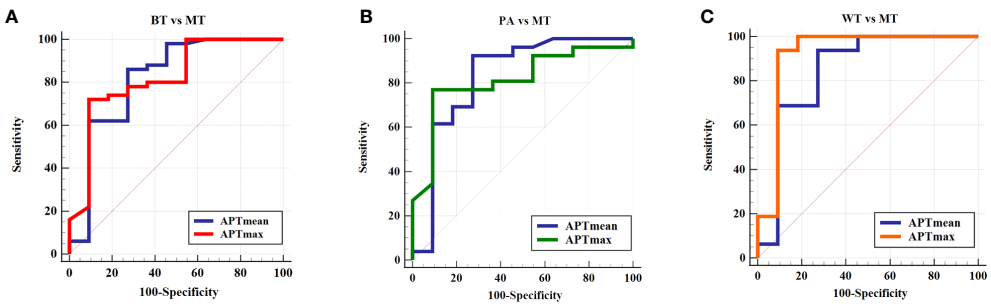

FIGURE 4
ROC curve of the APTmean and APTmax for differentiation between **(A)** BT and MT, **(B)** PA and MT, and **(C)** WT and MT. APTmax, the maximum value of APTw imaging; APTmean, the average value of APTw imaging; BT, benign tumor; MT, malignant tumor; PA, pleomorphic adenoma; WT, Warthin tumor.

TABLE 5 Comparison of APTw values among PA, WT, and MT.

	PA(n=26)	WT(n=15)	MT(n=11)	*p*	*p*		
					PA vs. WT	PA vs. MT	WT vs. MT
APTmax(%)	5.11 ± 1.88	4.67 ± 0.83	7.43 ± 1.61	0.02*	>0.99	<0.01*	<0.01*
APTmean(%)	2.69 ± 0.95	2.58 ± 1.06	4.15 ± 1.33	0.03*	>0.99	<0.01*	<0.01*

*$p < 0.05$.
APTmax, the maximum value of APTw imaging; APTmean, the average value of APTw imaging; APTw, amide proton transfer-weighted; BT, benign tumor; MT, malignant tumor; PA, pleomorphic adenoma; WT, Warthin tumor.

Conclusion

Both APTmax and APTmean values can differentiate benign and malignant parotid gland tumors, which suggested that APTw imaging might be helpful in the differentiation of benign and malignant parotid tumors before surgery. In our study, most APTw images in parotid gland tumors (83.57%) had acceptable image quality for APTw value evaluation. However, the technique still needs to be improved for reduced image artifacts.

Data availability statement

The raw data supporting the conclusions of this article will be made available by the authors without undue reservation.

Ethics statement

The studies involving human participants were reviewed and approved by the Ethics Committee of the First Affiliated Hospital of Dalian Medical University (license number: PJ–KS–XJS–2021-18). The patients/participants provided their written informed consent to participate in this study.

Author contributions

YW: methodology, investigation, data curation, writing—original draft, and writing—review and editing. LW: conceptualization, investigation, writing—review and editing, supervision, and project administration. LJL: software, visualization, and writing—review and editing. HH, JM, and LL: investigation, resources, and data curation. QS: resources and data curation. AL: supervision and project administration. All authors contributed to the article and approved the submitted version.

Funding

This study was supported by the Medical Education Research Project of Liaoning Province (No. 2022-N005-05).

Conflict of interest

Author LJL was employed by company Philips Healthcare, Beijing, China.

The remaining authors declare that the research was conducted in the absence of any commercial or financial relationships that could be construed as a potential conflict of interest.

Publisher's note

References

1. Santana BW, Silva LP, Serpa MS, Borges MD, Moura SR, Silveira MM, et al. Incidence and profile of benign epithelial tumors of salivary glands from a single center in Northeast of Brazil. *Med Oral Patol Oral Cir Bucal* (2021) 26:e108–13. doi: 10.4317/medoral

2. Del Signore AG, Megwalu UC. The rising incidence of major salivary gland cancer in the United States. *Ear Nose Throat J* (2017) 96(3):E13–6. doi: 10.1177/014556131709600319

3. Gupta R, Balasubramanian D, Clark JR. Salivary gland lesions: recent advances and evolving concepts. *Oral Surg Oral Med Oral Pathol Oral Radiol* (2015) 119(6):661–74. doi: 10.1016/j.oooo.2015.02.481

4. Lee DH, Yoon TM, Lee JK, Lim SC. Surgical treatment strategy in Warthin tumor of the parotid gland. *Braz J Otorhinolaryngol* (2019) 85(5):546–50. doi: 10.1016/j.bjorl.2018.04.004

5. Chiesa-Estomba CM, Larruscain-Sarasola E, Lechien JR, Mouawad F, Calvo-Henriquez C, Diom ES, et al. Facial nerve monitoring during parotid gland surgery: a systematic review and meta-analysis. *Eur Arch Otorhinolaryngol* (2021) 278(4):933–43. doi: 10.1007/s00405-020-06188-0

6. Seyhun N, Doğan U, Çalış ZAB, Kaya MF, Hasçiçek SÖ, Turgut S. The role of fine needle aspiration biopsy in deep lobe parotid tumors: Comparison of preoperative cytology and postoperative histopathologic results. *Am J Otolaryngol* (2021) 42(1):102590. doi: 10.1016/j.amjoto.2020.102590

7. El Beltagi AH, Elsotouhy AH, Own AM, Abdelfattah W, Nair K, Vattoth S. Functional magnetic resonance imaging of head and neck cancer: Performance and potential. *Neuroradiol J* (2019) 32(1):36–52. doi: 10.1177/1971400918808546

8. Wang J, Weygand J, Hwang KP, Mohamed AS, Ding Y, Fuller CD, et al. Magnetic resonance imaging of glucose uptake and metabolism in patients with head and neck cancer. *Sci Rep* (2016) 6:30618. doi: 10.1038/srep30618

9. Wei P, Shao C, Tian M, Wu M, Wang H, Han Z, et al. Quantitative analysis and pathological basis of signal intensity on T2-weighted MR images in benign and

Malignant parotid tumors. *Cancer Manag Res* (2021) 13:5423–31. doi: 10.2147/CMAR.S319466

10. Gökçe E. Multiparametric magnetic resonance imaging for the diagnosis and differential diagnosis of parotid gland tumors. *J Magn Reson Imaging* (2020) 52(1):11–32. doi: 10.1002/jmri.27061

11. Mikaszewski B, Markiet K, Smugała A, Stodulski D, Szurowska E, Stankiewicz C. Clinical and demographic data improve diagnostic accuracy of dynamic contrast-enhanced and diffusion-weighted MRI in differential diagnostics of parotid gland tumors. *Oral Oncol* (2020) 111:104932. doi: 10.1016/j.oraloncology.2020.104932

12. Karaman CZ, Tanyeri A, Özgür R, Öztürk VS. Parotid gland tumors: comparison of conventional and diffusion-weighted MRI findings with histopathological results. *Dentomaxillofac Radiol* (2021) 50(4):20200391. doi: 10.1259/dmfr.20200391

13. Xu Z, Zheng S, Pan A, Cheng X, Gao M. A multiparametric analysis based on DCE-MRI to improve the accuracy of parotid tumor discrimination. *Eur J Nucl Med Mol Imaging* (2019) 46(11):2228–34. doi: 10.1007/s00259-019-04447-9

14. Patella F, Franceschelli G, Petrillo M, Sansone M, Fusco R, Pesapane F, et al. A multiparametric analysis combining DCE-MRI- and IVIM -derived parameters to improve differentiation of parotid tumors: a pilot study. *Future Oncol* (2018) 14 (28):2893–903. doi: 10.2217/fon-2017-0655

15. Zhou J, Heo HY, Knutsson L, van Zijl PCM, Jiang S. APT-weighted MRI: Techniques, current neuro applications, and challenging issues. *J Magn Reson Imaging* (2019) 50(2):347–64. doi: 10.1002/jmri.26645

16. Guo Z, Qin X, Mu R, Lv J, Meng Z, Zheng W, et al. Amide proton transfer could provide more accurate lesion characterization in the transition zone of the prostate. *J Magn Reson Imaging* (2022) 56(5):1311–9. doi: 10.1002/jmri.28204

17. Song Q, Tian S, Ma C, Meng X, Chen L, Wang N, et al. Amide proton transfer weighted imaging combined with dynamic contrast-enhanced MRI in predicting lymphovascular space invasion and deep stromal invasion of IB1-IIA1 cervical cancer. *Front Oncol* (2022) 12:916846. doi: 10.3389/fonc.2022.916846

18. Chappell MA, Chen M, Gochberg DF, Goerke S, Heo HY, Jiang S, et al. Review and consensus recommendations on clinical APT-weighted imaging approaches at 3T: Application to brain tumors. *Magn Reson Med* (2022) 88(2):546–74. doi: 10.1002/mrm.29241

19. Meng N, Fu F, Feng P, Li Z, Gao H, Wu Y, et al. Evaluation of amide proton transfer-weighted imaging for lung cancer subtype and epidermal growth factor receptor: A comparative study with diffusion and metabolic parameters. *J Magn Reson Imaging* (2022) 56(4):1118–29. doi: 10.1002/jmri.28135

20. Kamitani T, Sagiyama K, Togao O, Yamasaki Y, Hida T, Matsuura Y, et al. Amide proton transfer (APT) imaging of parotid tumors: Differentiation of Malignant and benign tumors. *Eur J Radiol* (2020) 129:109047. doi: 10.1016/j.ejrad.2020.109047

21. Bae YJ, Choi BS, Jeong WJ, Jung YH, Park JH, Sunwoo L, et al. Amide proton transfer-weighted MRI in the diagnosis of major salivary gland tumors. *Sci Rep* (2019) 9 (1):8349. doi: 10.1038/s41598-019-44820-0

22. Paech D, Zaiss M, Meissner JE, Windschuh J, Wiestler B, Bachert P, et al. Nuclear overhauser enhancement mediated chemical exchange saturation transfer imaging at 7 Tesla in glioblastoma patients. *PloS One* (2014) 9(8):e104181. doi: 10.1371/journal.pone.0104181

23. Chen Y, Wang X, Su T, Xu Z, Wang Y, Zhang Z, et al. Feasibility evaluation of amide proton transfer-weighted imaging in the parotid glands: a strategy to recognize artifacts and measure APT value. *Quant Imaging Med Surg* (2021) 11(6):2279–91. doi: 10.21037/qims-20-675

24. DeLong ER, DeLong DM, Clarke-Pearson DL. Comparing the areas under two or more correlated receiver operating characteristic curves: a nonparametric approach. *Biometrics* (1988) 44:837–45. doi: 10.2307/2531595

25. Chen W, Mao L, Li L, Wei Q, Hu S, Ye Y, et al. Predicting treatment response of neoadjuvant chemoradiotherapy in locally advanced rectal cancer using amide proton transfer MRI combined with diffusion-weighted imaging. *Front Oncol* (2021) 11:698427. doi: 10.3389/fonc.2021.698427

26. Zhang H, Zhou J, Peng Y. Amide proton transfer-weighted MR imaging of pediatric central nervous system diseases. *Magn Reson Imaging Clin N Am* (2021) 29 (4):631–41. doi: 10.1016/j.mric.2021.06.012

27. Law BKH, King AD, Ai QY, Poon DMC, Chen W, Bhatia KS, et al. Head and neck tumors: amide proton transfer MRI. *Radiology* (2018) 288(3):782–90. doi: 10.1148/radiol.2018171528

28. Ju Y, Liu A, Wang Y, Chen L, Wang N, Bu X, et al. Amide proton transfer magnetic resonance imaging to evaluate renal impairment in patients with chronic kidney disease. *Magn Reson Imaging* (2022) 87:177–82. doi: 10.1016/j.mri.2021.11.015

29. Ochiai R, Mukuda N, Yunaga H, Kitao S, Okuda K, Sato S, et al. Amide proton transfer imaging in differentiation of type II and type I endometrial carcinoma: a pilot study. *Jpn J Radiol* (2022) 40(2):184–91. doi: 10.1007/s11604-021-01197-3

30. Gatius S, Cuevas D, Fernández C, ROman-Canal B, Adamoli V, Piulats JM, et al. Tumor heterogeneity in endometrial carcinoma: practical consequences. *Pathobiology* (2018) 85(1-2):35–40. doi: 10.1159/000475529

31. Li B, Sun H, Zhang S, Wang X, Guo Q. The utility of APT and IVIM in the diagnosis and diferentiation of squamous cell carcinoma of the cervix: a pilot study. *Magn Reson Imaging* (2019) 63:105–13. doi: 10.1016/j.mri.2019.08.020

32. Yuan Y, Tang W, Tao X. Parotid gland lesions: separate and combined diagnostic value of conventional MRI, diffusion-weighted imaging and dynamic contrast-enhanced MRI. *Br J Radiol* (2016) 89(1060):20150912. doi: 10.1259/bjr.20150912

33. Yabuuchi H, Kamitani T, Sagiyama K, Yamasaki Y, Hida T, Matsuura Y, et al. Characterization of parotid gland tumors: added value of permeability MR imaging to DWI and DCE-MRI. *Eur Radiol* (2020) 30(12):6402–12. doi: 10.1007/s00330-020-07004-3

34. Ishimatsu K, Nishie A, Takayama Y, Asayama Y, Ushijima Y, Kakihara D, et al. Amide proton transfer imaging for differentiating benign ovarian cystic lesions: Potential of first time right. *Eur J Radiol* (2019) 120:108656. doi: 10.1016/j.ejrad.2019.108656

35. Togao O, Yoshiura T, Keupp J, Hiwatashi A, Yamashita K, Kikuchi K, et al. Amide proton transfer imaging of adult diffuse gliomas: correlation with histopathological grades. *Neuro Oncol* (2014) 16(3):441–8. doi: 10.1093/neuonc/not158

36. Al-Zaher N, Obeid A, Al-Salam S, Al-Kayyali BS. Acinic cell carcinoma of the salivary glands: a literature review. *Hematol Oncol Stem Cell Ther* (2009) 2(1):259–64. doi: 10.1016/s1658-3876(09)50035-0

frontiers | Frontiers in Oncology

TYPE Case Report
PUBLISHED 18 September 2023
DOI 10.3389/fonc.2023.1245043

OPEN ACCESS

EDITED BY
Ester Orlandi,
National Center of Oncological Hadrontherapy, Italy

REVIEWED BY
Maria Pia Foschini,
University of Bologna, Italy
Alessandro Franchi,
University of Pisa, Italy

*CORRESPONDENCE
Giacomo Miserocchi
giacomo.miserocchi@irst.emr.it

†These authors have contributed equally to this work

RECEIVED 23 June 2023
ACCEPTED 23 August 2023
PUBLISHED 18 September 2023

CITATION
Miserocchi G, Bassi M, De Luca G, Calpona S, De Rosa F, Bongiovanni A, Parisi E, Di Menna G, De Vita A, Liverani C, Spadazzi C, Cocchi C, Vanni S, Capelli L, Magnani M, Meccariello G, Vicini C, Campobassi A, Mercatali L and Ibrahim T (2023) High-grade transformation of a polymorphous adenocarcinoma of the salivary gland: a case report and review of the literature.
Front. Oncol. 13:1245043.
doi: 10.3389/fonc.2023.1245043

High-grade transformation of a polymorphous adenocarcinoma of the salivary gland: a case report and review of the literature

Giacomo Miserocchi[1*], Massimo Bassi[2], Giovanni De Luca[3], Sebastiano Calpona[1], Francesco De Rosa[4], Alberto Bongiovanni[1], Elisabetta Parisi[5], Giandomenico Di Menna[6], Alessandro De Vita[1], Chiara Liverani[1], Chiara Spadazzi[1], Claudia Cocchi[1], Silvia Vanni[1], Laura Capelli[7], Massimo Magnani[8], Giuseppe Meccariello[9], Claudio Vicini[9], Angelo Campobassi[2], Laura Mercatali[1†] and Toni Ibrahim[1†]

[1]Preclinic and Osteoncology Unit, IRCCS Istituto Romagnolo per lo Studio dei Tumori (IRST) "Dino Amadori", Meldola, Italy, [2]Maxillofacial Surgery Unit, "Bufalini Hospital", Azienda Unità Sanitaria Locale (AUSL) Romagna, Cesena, Italy, [3]Pathology Unit, "Bufalini" Hospital, Azienda Unità Sanitaria Locale (AUSL) Romagna, Cesena, Italy, [4]Immunotherapy, Cell Therapy and Biobank, IRCCS Istituto Romagnolo per lo Studio dei Tumori (IRST) "Dino Amadori", Meldola, Italy, [5]Radiotherapy Department, Istituto Scientifico Romagnolo per lo Studio e la Cura dei Tumori (IRST), IRCCS, Meldola, Italy, [6]Department of Medical Oncology, IRCCS Istituto Romagnolo per lo Studio dei Tumori (IRST) "Dino Amadori", Meldola, Italy, [7]Biosciences Laboratory, IRCCS Istituto Romagnolo per lo Studio dei Tumori (IRST) "Dino Amadori", Meldola, Italy, [8]Department of Head-Neck Surgery Azienda Unità Sanitaria Locale (AUSL) Romagna, Ear Nose Throat (ENT) Unit, Bufalini Hospital, Cesena, Italy, [9]Otolaryngology and Head-Neck Surgery Unit, Department of Head-Neck Surgeries, Morgagni Pierantoni Hospital, Azienda USL della Romagna, Forlì, Italy

Background: Polymorphous adenocarcinoma (PAC) represents the second most widespread neoplasm of the minor salivary glands. These tumors rarely develop a histological progression from low-grade to high-grade malignancy, named "high-grade transformation" (HGT). Only nine cases are described in literature.

Case description: Here, we describe the case of a 76-year-old male patient with a PAC recurrence of the oral floor displaying HGT, and we explore the tumor cytomorphological features, genomic profiling, and the patient's clinical management. The tumor mass was characterized by poorly atypical cellular elements with vesicular nuclei and comedonecrosis foci. The growth pattern was predominantly solid, tubular, and cribriform. The lesion did not show microsatellite instability or targeted molecular alterations. The case was successfully treated with radical surgery followed by radiotherapy.

Conclusion: We report for the first time the recurrence of a PAC with HGT arising in the oral floor after 20 years from the primary lesion. These preliminary data and the literature analysis enhance the knowledge of this extremely rare disease.

KEYWORDS

polymorphous adenocarcinoma, high-grade transformation, minor salivary gland, gene expression profiling, oral floor

1 Introduction

Polymorphous adenocarcinoma (PAC) is the second most common malignancy of the minor salivary glands (1, 2). The incidence of salivary cancers is estimated to be 4–135 cases per million population per year and approximately 10%–15% are located in the minor salivary glands (3). PACs normally arise as surface papillary epithelial hyperplasia with stippled mucosa covering the cancer mass (4).

These tumors are described as infiltrative epithelial malignancies, showing bland nuclei, poor to moderate cytoplasm, and a variety of cytoarchitectural patterns, including solid, cribriform, tubules, and Indian-file infiltrates (1, 5–7). In the past decades, it is likely than PACs have been misdiagnosed as adenoid cystic carcinomas (AdCCs) (8). From a pathological point of view, the two salivary gland tumors display different cribriform patterns; whereas AdCC presents stromal cores surrounded by tumor parenchyma and thus characterized by basement membrane, PAC exhibits genuine lumina and a variety of myxoid, fibrous, hyalinized, or elastotic stroma with inconspicuous inflammation (1). Moreover, neurotropisms, as targetoid pattern, and perivascular arrangements are often detected. The latest WHO categorization of salivary gland tumors includes the so-called "cribriform adenocarcinoma of minor salivary glands" (CAMSG) under the PAC heading, despite their important differences in clinical behavior (7). Unlike PAC, CAMSG usually arises in the base of the tongue and shows more aggressive clinical behaviors, such as higher risk of lymph node metastasis (7). Moreover, CAMSG tumor cells are characterized by vesicular and pale nuclei with ground-glass appearance and clear to eosinophilic cytoplasm (2).

PACs were initially described as indolent malignancies with low metastatic potential (9). However, recent clinical evidence has reported recurrences in 19% of PACs and extremely rare cases of high-grade transformation (HGT) (10–12), with development of cytological atypia, increased proliferative activity, and necrosis areas (11).

In the literature, nine cases of PAC displaying high-grade features have been described (11–17). These pathological conditions are heterogeneous in terms of clinical outcomes, metastasis onset, and treatments; can arise in both primary tumors and recurrences; and can be located in several sites: palate, nasal cavity, maxillary alveolus, and upper lip.

In this study, we review the state- of- the-art literature on this extremely rare salivary gland cancer, and report the clinical and genomic characterization of a new case of PAC characterized by both high- and low-grade aspects.

2 Case presentation

2.1 Case report

In 2000, a 54- year-old male patient underwent a left neck node dissection of levels 2–5 and multiple biopsies (larynx, base of the tongue, amygdaloglossus sulcus, and tonsil) for a metastatic node with no clinically evident primary lesion. The histology confirmed a malignant lymphadenopathy with the presence of a single lymph node metastasis with extranodal lymphatic vascular infiltration. The primitive lesion was not detected. The metastatic tissue showed a tubular, follicular, and microcystic glandular structure with hyaline stroma and crystalloid and amorphous material deposition. The sample displayed necrotic foci, while cancer cells showed poor nuclear atypia and irrelevant mitotic activity. Immunohistochemical analysis revealed α-SMA positivity in peripheral spindle cells of tubular structures and S100 focal positivity. Thyroglobulin, calcitonin, and chromogranin staining were negative. The other lymph nodes appeared with reactive and aspecific modifications. Therefore, the pathologic diagnosis identified a cribriform variant of a lymph node metastasis with low-grade histologic features and probably originated from a primitive neoplasia of the salivary gland, pathologically staged as TX N1 M0. No adjuvant chemotherapy or other treatments were performed due to the low-grade nature of the lesion.

In January 2020, the patient referred to the Oral and Maxillofacial Surgery Unit of Cesena "Bufalini Hospital" for a swollen nodule in the left of the oral floor. Magnetic resonance imaging (MRI), using T1-weighted high-resolution isotropic volume examination (THRIVE), confirmed the presence of a single lesion in the left portion of the oral floor involving the unilateral sublingual space (Figure 1A). The mass was well delimited and in contact with the mandibular cortex, with no signs of bone infiltration: diameters of 2.4 × 3 cm in the axial sequence, 2 × 2.8 cm in the coronal sequence, and 3. cm in the sagittal sequence. In the loco-regional seat, the bone cortex of the jaw appeared remodeled and thin but not interrupted and with no alteration signal, while reaching the ventral surface of the lingual root and the mylohyoid muscle. A biopsy was subsequently performed. On the back, the lesion was widespread since the ventral surface of the tongue root. The mass reached the left mylohyoid muscle with the removal of adipocytic cleavage floor. However, the lesion did not appear to have passed the muscle and was not extended to the submandibular space. The left submandibular gland was characterized by a poor oversized extra- and intraglandular ductal system. The Wharton duct appeared dilated as probably due to the obstruction/infiltration of the excretory duct by the cancer lesion. The volume of the left parotid gland was poorly increased as compared to its counterpart and showed two formations visible in the deep lobe: one of 10 mm characterized by mixed signal (hypo- and hyper-intense) and the other of 14 mm with hemorrhagic component. An additional formation of 15 mm in the inferior pole of the parotid gland (level IIA) and a neoformation in the left oral floor were revealed.

In February 2020, a biopsy was performed and the pathology report described a glandular parenchyma partially substituted by malignant components with cribriform aspects. Tumor cells appeared monomorphic, without significant atypia, with nuclei of medium dimension, vesicular and no evident nucleolus. The H&E staining revealed the presence of low- and high-grade tumor features (Figures 2A, C–E), with different biomarker expression

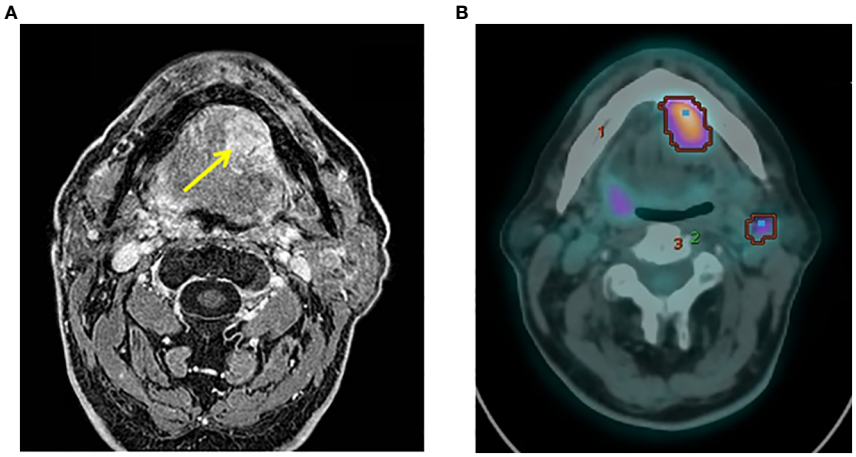

FIGURE 1
Preoperative NMR and PET examinations. **(A)** Axial view of preoperative NMR scan showing the tumor mass (yellow arrow). **(B)** PET images revealed a focal hyperfixation area of the left oral floor and two concomitant areas of radioisotope uptake in the left submandibular and unilateral mandibular seat of the lymph nodes.

on immunohistochemistry assays. The whole tumor tissue was positive for cytokeratin 7 (Figure 2B), while Ki67 staining showed a lower cell proliferation in the low-grade areas with respect to the high-grade counterparts (Figures 2F–H). Cells of the low-grade areas showed higher expression of p63 and lower expression of S100 (Figures 2I–N). The whole tumor areas were negative for p40 (Supplementary Figures 1A, B). Owing to the histological features and to the tumor site, the case was diagnosed as a cribriform variant of a salivary gland PAC and considered as a recurrence with HGT of the metastatic lesion of unknown primary resected in 2000, the lesion being a cribriform variant of a salivary gland PAC. The tumor was classified as a recurrence of the unknown primitive of 2000 due to the very similar histological features.

In March 2020, ^{18}F- fluorodeoxyglucose (^{18}F-FDG) positron emission tomography/computed tomography (PET/CT) images revealed a focal uptake of the left oral floor with a maximum standardized uptake value (SUV) of 9. Two concomitant areas of radiotracer uptake were also present in the left submandibular (SUV max = 4.9) and ipsilateral mandibular (SUV max = 3.8) lymph nodes (Figure 1B). No other uptake areas were detected. Therefore, the MTB (ENT and maxillofacial surgeons, pathologist, radiologist, medical, and radiation oncologists) opted for radical surgery.

In May 2020, the patient underwent complete parotidectomy and dissection of the level 1 lymph node (Figure 3A). The surgery did not require microvascular or local flap reconstruction and no complications arose, allowing patient discharge after 7 days. The pathology report described a well-delimited solid mass (3.5 × 2.5 × 2 cm, weighing 15 g) (Figure 3B), not capsulated and showing marginal foci with infiltrative aspects. The tumor cells were atypical, with vesicular nuclei and evident nucleoli. The growth pattern was mostly solid (Figure 3C), with areas characterized by tubular and cribriform patterns (Figures 3D, E), as well as cystic areas with luminal papillary projections (Figure 3F). Vascular and perineural invasion were present (Figure 3G), together with multiple comedonecrosis foci (Figure 3H). Three lymph node metastases were detected. The degrees of lymph node involvement and growth patterns were variable (solid, cribriform, tubular, papillary, and cystic), but no aspects of extension to perilymphatic soft tissues were detected. The biggest measured was 1.4 cm (Figure 3I); therefore, the disease was staged as pT2, N2b according to TNM classification (18). The patient had no complications after surgery and he was discharged after 7 days.

Because of the presence of multiple lymph node metastases, the MTB referred the patient to adjuvant radiotherapy, completed in August (60 Gy/30 fractions to the tumor bed and ipsilateral nodes, 54 Gy/30 fractions to contralateral nodes). The treatment caused the onset of odynophagia, oral mucositis, and epitheliolysis in the left base of the neck, treated with supportive care and quickly resolved; the single long-term sequela was mild xerostomia.

In May 2023, the patient was still alive and MRI (Supplementary Figure 2) and PET/CT showed no sign of recurrence.

2.2 Molecular characterization

To the best of our knowledge, only one case of PAC with HGT has been molecularly characterized. Here, we performed NGS profiling and microsatellite instability (MSI) status using DNA and RNA extracted by tumor tissue. Sequencing analysis did not detect any alteration in the 52 genes of the NGS panel employed (Supplementary Table 1; Data Sheet 1); MSI status was obtained through the investigation of eight markers (Supplementary Table 2 and Data Sheet 2). The analysis revealed an overlapping stable trend of the curves showed a ΔTm melting temperature (Tm sample − Tm positive control) ≥ −3 (unstable markers are considered for a ΔTm < −3) (Supplementary Figure 3). These results demonstrated the microsatellite stability of the sample.

10.3389/fonc.2023.1245043

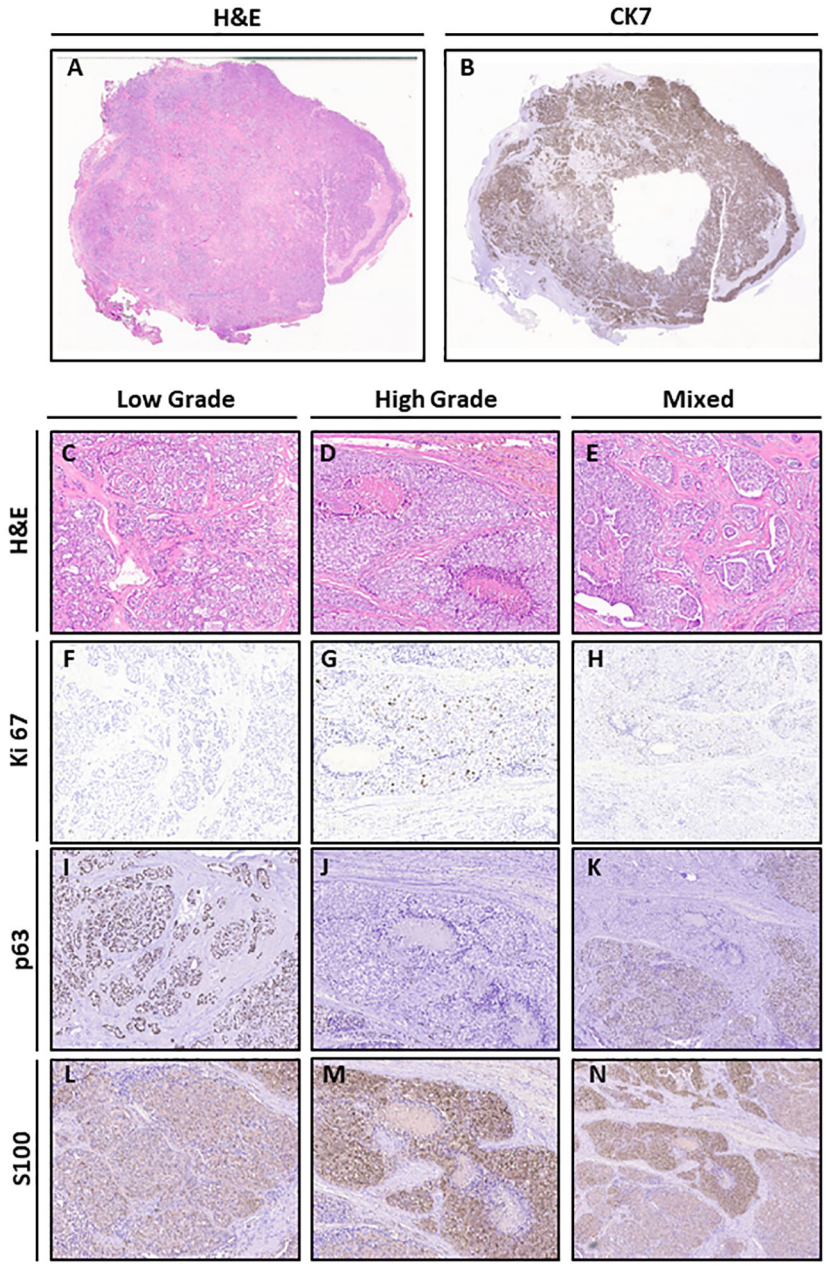

FIGURE 2
Histological features of the lesion. **(A)** H&E (original magnification 1×). **(B)** CK7 (original magnification 1×). **(C–E)** H&E of Low Grade, High Grade (original magnification 10×), and Mixed (original magnification 4×) areas. **(F–H)** Ki67 staining of Low Grade, High Grade (original magnification 10×), and Mixed (original magnification 4×) areas (H&E original magnification 10×). **(I–K)** p63 staining of Low Grade, High Grade (original magnification 10×), and Mixed (original magnification 4×) areas. **(L–N)** S100 staining of Low Grade, High Grade (original magnification 10×), and Mixed (original magnification 4×) areas.

3 Discussion

PAC is a rare malignancy of the minor salivary glands (1, 2), which usually arises in the palate (approximately 60% of all cases), lip, buccal mucosa, alveolar ridge, retromolar region, mouth floor, posterior tongue, and nasal cavity (1, 5, 6, 10, 12). Their nature is generally indolent and clinical outcome is positive, with local recurrence observed in 10%–30% of cases and regional metastases in approximately 15% (19). Histologically, PACs are described as malignant epithelial cancers characterized by heterogenic morphology, cytological uniformity, and an infiltrative growth pattern (7). The last WHO classification also includes CAMSG in the group of PAC variants (7). Different groups consider this aspect controversial and proposed to classify CASG as distinct lesions separated from PACs. Indeed, the two entities show differential diagnosis based on the patient's history and histological examination. PACs are characterized by a heterogeneous group of growth pattern, including cribriform structures, the presence of

10.3389/fonc.2023.1245043

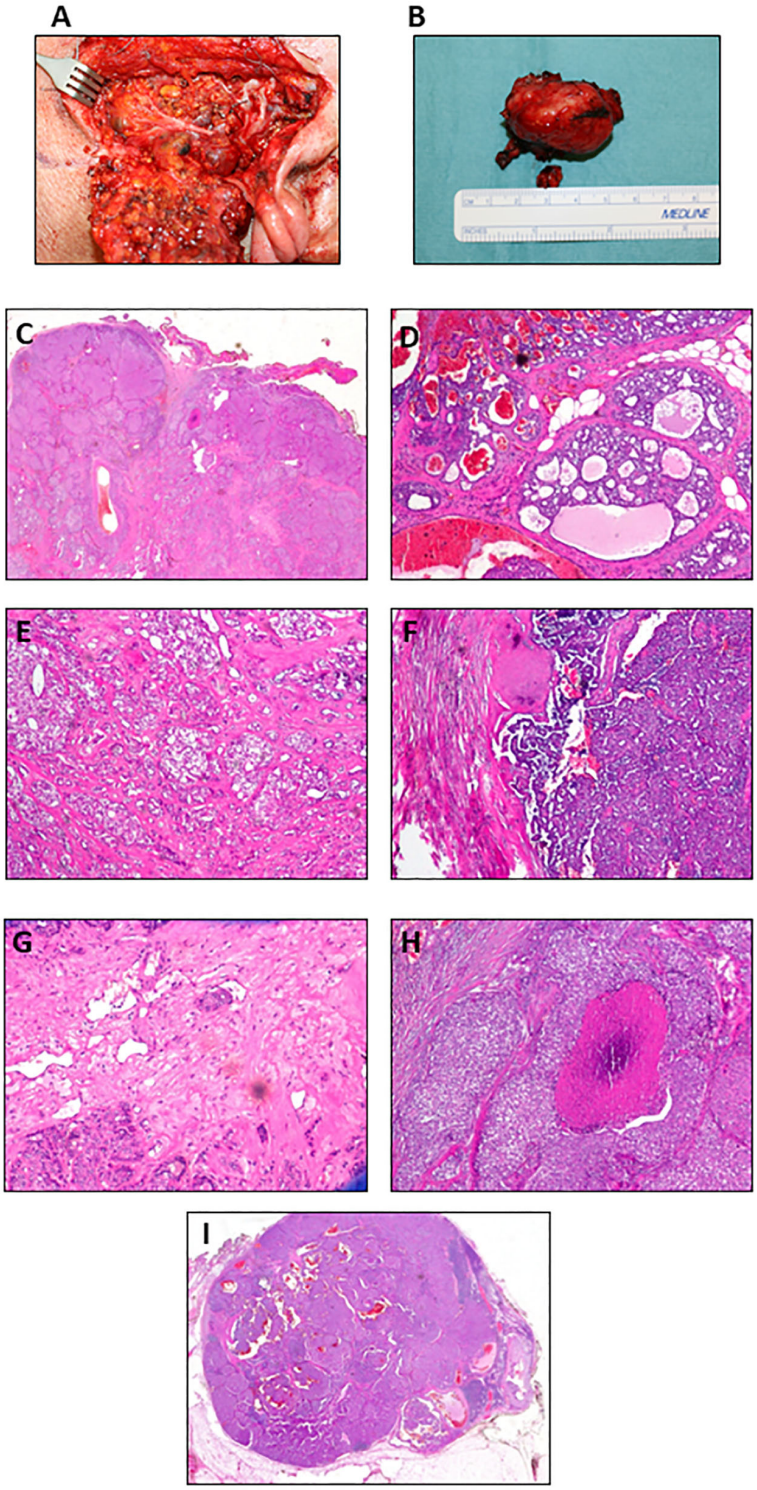

FIGURE 3
Postoperative images of the tumor mass and histological features. **(A)** Intraoperative photograph. **(B)** Lesion surgically excised. H&E images show **(C)** solid (original magnification 5×), **(D)** cribriform with focal infiltration in the perilesional adipose tissue (original magnification 10×), **(E)** cribriform and glandular (original magnification 10×), and **(F)** papillary growth pattern (original magnification 10×). Representative histopathological features: **(G)** vascular neoplastic invasion (original magnification 20×), **(H)** comedonecrosis (original magnification 10×), and **(I)** lymph node metastasis (original magnification 5×).

concentric whorls developed by streaming columns of a single file or narrow trabeculae, and invasion of surrounding tissues and perineural spaces (20). Differently, CAMSGs were cytologically monomorphous with a limited range of growth patterns with a predominance of solid and cribriform structures mixed with a tubular pattern, mild cellular atypia, lymphovascular invasion, and infiltration of adjacent tissues (20, 21). Despite the invasive growth pattern of the two kinds of tumor, the overall prognosis remains favorable. Based on these differences, we have diagnosed the lesion here presented as PAC.

Originally identified as polymorphous low-grade adenocarcinomas (PLGAs), the WHO classification has changed the name in PAC, owing to the occurrence of sporadic cases characterized by a more aggressive pathophysiological feature and morphological appearance (7). These events are extremely rare and entail the progression from a low to high grade. High-grade PAC are characterized by prominent nucleoli, nuclear atypia, a high mitotic count, frequent central hemorrhage, and necrosis (1, 15, 22). Based on the histologic features, cytology, and behavior differences between PACs and CAMSGs, we have diagnosed the lesion here presented as PAC.

In the literature, the first documented case of PAC of the palate showing HGT at relapse was published in 1984 (13): four other cases subsequently reported features of HGT in PAC recurrences (11, 15). Pelkey et al. described two multiple locoregional recurrences displaying histological transformation to high grade after 17 and 26 years (15). The fourth and fifth cases recurred after 11 and 28 years, respectively (11, 17). Here, we report the first documented case of PAC recurrence that occurred 20 years after a lymph node metastasis of unknown primary lesion with low-grade histologic aspects. Although late recurrences were already described, the case here reported shows unusual and unique features not only in the recurrence, but also in the primary tumor. Indeed, the diagnosis of the second lesion as a recurrence with HGT of the undetected primary tumor relies on the same histologic features shared with the lymph node metastasis of 2000. The supposedly spontaneous remission of the primary PAC confirms the low aggressiveness of the disease.

In some instances, high-grade morphological features were also identified in PAC at initial presentation (11, 12, 14, 16). The tumor recurrences arose only in the palate while the cases at the initial presentation also included the site of nasopharynx and maxillary alveolus (14, 16). Therefore, our report describes the first documented case originating from the oral floor.

PAC and AdCC share many growth pattern features, such as solid and cribriform histology or the presence of neurotropism (6, 12): immunohistochemical stainings for the myoepithelial markers α-SMA and p40, positive in AdCC and negative in PAC, help to discriminate between the two entities (12, 23–25).

PACs with HGT —such as the case with our patient —share both high- and low-grade histological characteristics. In particular, high-grade areas are characterized by a solid growth pattern and necrosis or comedonecrosis foci, and low-grade areas show heterogeneous growth patterns (solid, tubular, trabecular, and cribriform are the most represented) (Table 1). Our case presented a prevalent solid growth pattern with some areas with cystic, cribriform, and tubular features.

As previously described, patients affected by PAC present good clinical outcomes, and this aspect is maintained also in the HGT variants. Indeed, four patients were alive and disease-free at the time of the case report publications (11–13) and only one had died from septic shock after an *Escherichia coli* infection of the urinary tract (14). In the other cases, the clinical outcomes were not available. In all cases, surgery represented the first treatment choice. In addition, radiotherapy was used in different modalities: alone (14), in combination with hyperthermia (13), or in combination with chemotherapy (15). In a single instance, the patient was treated with multidrug chemotherapy alone as adjuvant therapy after resection of multiple bilateral nodal metastases in the neck (11).

TABLE 1 Patients' characteristics.

Patient	Sex, age (at surgery)	Site	Metastasis	Primary lesion/ Recurrence	Histological growth patterns	Outcome (months)	Ref.
1	F, 48	Palate	Lymph nodes, mandible	Recurrence	So, Cys, Pa	AWD (NA)	(13)
2	M, 47	Nasal cavity	NA	Primary lesion	So	Died for septic shock	(14)
3	F, 44	Palate	Lymph nodes	Recurrence	So, Crib, Tra, Sin-F	NA	(15)
4	F, 38	Palate	/	Recurrence	Crib, Tub, Tra, Sin-F	NA	(15)
5	M, 66	Palate	/	Recurrence	So, Pa, Crib, Sin-F, Tub	AWD (156)	(11)
6	M, 63	Palate	Lymph nodes	Primary lesion	So, Crib, Tub, Sin-F	AWD (5)	(11)
7	F, 73	Maxillary alveolous	Lymph nodes, abdomen, lung	Primary lesion	So, Crib, Tub, Sin-F	NA	(16)
8	M, 43	Palate	/	Primary lesion	So, Pa, Crib, Sin-F, Tub	AWD (39)	(12)
9	F, 73	Palate	/	Recurrence	So, Tra, Tub	NA	(17)
10	M, 74	Oral Floor	Lymph nodes	Recurrence	So, Cys, Pa, Crib, Tub	AWD (38)	

F, female; M, male; So, solid; Cys, Cystic; Pa, papillary; Crib, cribriform; Tra, trabecular; Sin-F, single-file (Indian-file); Tub, tubule; ADW, alive without disease; NA, not available.
"/" correspond to the absence of Metastasis.

The mutational status of PACs with HGT are poorly described. Currently, only one study investigated the genome profiling of high-grade forms of PAC (17). The genomic analysis revealed a clonal NOTCH2 Q2409* truncating mutation and a MEF2B P315Qfs* frameshift mutation. Moreover, fluorescence *in situ* hybridization (FISH) analysis revealed PRKD2 rearrangement and PRKD1 and PRKD3 wild-type status. We used an NGS multi-biomarker assay to detect variants across cancer-relevant genes from DNA and RNA. No gene mutations were detected, neither in DNA nor in RNA. These results add genomic information on this extremely rare type of cancer, but further and more extended sequencing analysis are warranted to better characterize these diseases.

For the first time here, we explored the MSI status of a PAC with HGT. MSI represents a genetic hypermutability condition driven by DNA mismatch repair system (MMR) mainly associated with endometrial and gastric malignancies (26–28). MSI analysis showed an overlapping stable trend of the curves, and thus, microsatellites were considered stable. Several studies associate higher MSI frequency to young non-smoker patients with H&N SCCs (29, 30) while salivary gland tumors display lower frequency (31). Therefore, the case presented here is consistent with the scientific literature and suggests that HGT does not influence the stability of microsatellites. However, further analyses on different tumor samples are needed to better describe the genetic status of this rare disease.

Taken together, our results and the scientific evidence on these extremely rare malignancies highlight some considerations. HGT in salivary gland carcinomas is a process associated with a more aggressive behavior and poorer prognosis with respect to low-grade forms (22, 32). Conversely, the cases of PAC with HGT described in literature and summarized in this review (Table 1) showed heterogeneous clinical outcomes. Indeed, only in one case did the patient die as a consequence of his tumor (14). These differences suggest that HGT of PAC might be associated with a less aggressive behavior compared to the other salivary gland carcinomas.

Data availability statement

The datasets presented in this article are not readily available because of ethical/privacy restrictions. Requests to access the datasets should be directed to the corresponding author.

Ethics statement

The studies involving humans were approved by IRST-Area Vasta Romagna Ethics Committee. The studies were conducted in accordance with the local legislation and institutional requirements. The participants provided their written informed consent to participate in this study. Written informed consent was obtained from the individual(s) for the publication of any potentially identifiable images or data included in this article.

Author contributions

Conceptualization, GMi, MB, GDL, LM, and TI; methodology, GMi, MB, GDL, SC, FDR, AB, EP, GDM, MM, GMe, CV, and AC; formal analysis, GMi, MB, GDL, SC, FDR, AB, and EP; investigation, GMi, MB, GDL, EP, GDM, ADV, CL, MM, GMe, CV, and AC; data curation, GMi, MB, GDL, ADV, CL, CS, CC, SV, and LC; writing—original draft preparation, GMi, ADV, CL, CS, CC, SV, and LC; writing—review and editing, GMi, MB, GDL, SC, FDR, AB, EP, GDM, MM, GMe, CV, AC, LM, and TI; supervision, LM and TI. All authors contributed to the article and approved the submitted version.

Funding

This work was partly supported by the contribution of Ricerca Corrente by the Italian Ministry of Health within the research line Precision, gender and ethnicity-based medicine and geroscience: genetic-molecular mechanisms in the development, characterization and treatment of tumors.

Conflict of interest

The authors declare that the research was conducted in the absence of any commercial or financial relationships that could be construed as a potential conflict of interest.

Publisher's note

Supplementary material

The Supplementary Material for this article can be found online at: https://www.frontiersin.org/articles/10.3389/fonc.2023.1245043/full#supplementary-material

References

1. Poorten VV, Triantafyllou A, Skálová A, Stenman G, Bishop JA, Hauben E, et al. Polymorphous adenocarcinoma of the salivary glands: reappraisal and update. *Eur Arch Otorhinolaryngol* (2018) 275(7):1681–95. doi: 10.1007/s00405-018-4985-5

2. Mimica X, Katabi N, McGill MR, Hay A, Zanoni DK, Shah JP, et al. Polymorphous adenocarcinoma of salivary glands. *Oral Oncol* (2019) 95:52–8. doi: 10.1016/j.oraloncology.2019.06.002

3. Hay AJ, Migliacci J, Zanoni DK, McGill M, Patel S, Ganly I. Minor Salivary Gland tumors of the Head and Neck- Memorial Sloan Kettering experience. Incidence and outcomes by site and histological type. *Cancer* (2019) 125(19):3354–66. doi: 10.1002/cncr.32208

4. Chi AC, Neville BW. Surface papillary epithelial hyperplasia (rough mucosa) is a helpful clue for identification of polymorphous low-grade adenocarcinoma. *Head Neck Pathol* (2015) 9:244–52. doi: 10.1007/s12105-014-0572-2

5. Evans HL, Luna MA. Polymorphous low-grade adenocarcinoma: a study of 40 cases with long-term follow up and an evaluation of the importance of papillary areas. *Am J Surg Pathol* (2000) 24:1319–28. doi: 10.1097/00000478-200010000-00001

6. El-Naggar AK, Chan JKC, Grandis JR, Takata T, Slootweg PJ. *World Health Organization classification of head and neck tumours*. Lyon, France: International Agency for Research on Cancer (IARC) (2017).

7. Skálová A, Hyrcza MD, Leivo I. Update from the 5th edition of the world health organization classification of head and neck tumors: salivary glands. *Head Neck Pathol* (2022) 16(1):40–53. doi: 10.1007/s12105-022-01420-1

8. Darling MR, Schneider JW, Phillips VM. Polymorphous low-grade adenocarcinoma and adenoid cystic carcinoma: a review and comparison of immunohistochemical markers. *Oral Oncol* (2002) 38(7):641–5. doi: 10.1016/s1368-8375(02)00003-9

9. Nagao T, Gaffey TA, Kay PA, Minato H, Serizawa H, Lewis JE. Polymorphous lowgrade adenocarcinoma of the major salivary glands: report of three cases in an unusual location. *Histopathology* (2004) 44:164–71. doi: 10.1111/j.1365-2559.2004.01799.x

10. Castle JT, Thompson LD, Frommelt RA, Wenig BM, Kessler HP. Polymorphous low grade adenocarcinoma: a clinicopathologic study of 164 cases. *Cancer* (1999) 86:207–19. doi: 10.1002/(SICI)1097-0142(19990715)86:2<207::AID-CNCR4>3.0.CO;2-Q

11. Simpson RHW, Pereira EM, Ribeiro AC, Abdulkadir A, Reis-Filho JS. Polymorphous low-grade adenocarcinoma of the salivary glands with transformation to high-grade carcinoma. *Histopathology* (2002) 41:250–9. doi: 10.1046/j.1365-2559.2002.01439.x

12. Kikuchi K, Nagao T, Ide F, Takizawa S, Sakashita H, Tsujino I, et al. Palatal polymorphous adenocarcinoma with high-grade transformation: A case report and literature review. *Head Neck Pathol* (2019) 13(2):131–9. doi: 10.1007/s12105-018-0916-4

13. Mills SE, Garland TA, Allen JMS. Low-grade papillary adenocarcinoma of palatal salivary gland origin. *Am J Surg Pathol* (1984) 8(5):367–74. doi: 10.1097/00000478-198405000-00005

14. Lloreta J, Serrano S, Corominas JM, Ferrés-Padró E. Polymorphous low-grade adenocarcinoma arising in the nasal cavities with an associated undifferentiated carcinoma. *Ultrastruct Pathol* (1995) 19(5):365–70. doi: 10.3109/01913129509021908

15. Pelkey TJ, Mills SE. Histologic transformation of polymorphous low-grade adenocarcinoma of salivary gland. *Am J Clin Pathol* (1999) 111(6):785–91. doi: 10.1093/ajcp/111.6.785

16. Thennavan A, Rao L, Radhakrishnan R. Polymorphous low-grade adenocarcinoma of maxillary alveolus metastasising to the abdomen: the role of immunomarkers in diagnosis. *BMJ Case Rep* (2013) 8:bcr2013009633. doi: 10.1136/bcr-2013-009633

17. Sebastiao APM, Pareja F, Kumar R, Brown DN, Silveira C, da Silva EM, et al. Genomic analysis of recurrences and high-grade forms of polymorphous adenocarcinoma. *Histopathology* (2019) 75(2):193–201. doi: 10.1111/his.13854

18. Bertero L, Massa F, Metovic J. Eighth Edition of the UICC Classification of Malignant Tumours: an overview of the changes in the pathological TNM classification criteria-What has changed and why? *Virchows Arch* (2018) 472(4):519–31. doi: 10.1007/s00428-017-2276-y

19. Seethala RR. Salivary gland tumors: current concepts and controversies. *Surg Pathol Clin* (2017) 10(1):155–76. doi: 10.1016/j.path.2016.11.004

20. Madhura MG, Veerendra Kumar B, Suma S, Sarita Y. Cribriform adenocarcinoma of minor salivary gland: A mimic of polymorphous low-grade adenocarcinoma. *J Oral Maxillofac Pathol* (2016) 20(3):536–9. doi: 10.4103/0973-029X.190961

21. Raitz R, Martins MD, Araujo VC. A study of the extracellular matrix in salivary gland tumors. *J Oral Pathol Med* (2003) 32(5):290–6. doi: 10.1034/j.1600-0714.2003.00019.x

22. Nagao T. "Dedifferentiation" and high-grade transformation in salivary gland carcinomas. *Head Neck Pathol* (2013) 7:37–47. doi: 10.1007/s12105-013-0458-8

23. Sedassari BT, Dos Santos HT, Pigatti FM, Mussi MCM, Tobouti PL, Altemani A, et al. Doing more with less: the challenging diagnosis of polymorphous low-grade adenocarcinoma in incisional biopsy samples. *Histopathology* (2016) 68(7):1046–54. doi: 10.1111/his.12880

24. Rooper L, Sharma R, Bishop JA. Polymorphous low grade adenocarcinoma has a consistent p63+/p40- immunophenotype that helps distinguish it from adenoid cystic carcinoma and cellular pleomorphic adenoma. *Head Neck Pathol* (2015) 9(1):79–84. doi: 10.1007/s12105-014-0554-4

25. Weinreb I, Piscuoglio S, Martelotto LG, Waggott D, Ng CKY, Perez-Ordonez B, et al. Hotspot activating PRKD1 somatic mutations in polymorphous low-grade adenocarcinomas of the salivary glands. *Nat Genet* (2014) 46(11):1166–9. doi: 10.1038/ng.3096

26. Li K, Luo H, Huang L, Luo H, Zhu X. Microsatellite instability: a review of what the oncologist should know. *Cancer Cell Int* (2020) 13:20. doi: 10.1186/s12935-019-1091-8

27. Bonneville R, Krook MA, Kautto EA, Miya J, Wing MR, Chen HZ, et al. Landscape of MSI across 39 cancer types. *JCO Precis Oncol* (2017) 2017). doi: 10.1200/PO.17.00073

28. Richman S. Deficient mismatch repair: Read all about it (Review). *Int J Oncol* (2015) 47(4):1189–202. doi: 10.3892/ijo.2015.3119

29. Wang Y, Irish J, MacMillan C, Brown D, Xuan Y, Boyington C, et al. High frequency of microsatellite instability in young patients with head-and-neck squamous-cell carcinoma: lack of involvement of the mismatch repair genes hMLH1 AND hMSH2. *Int J Cancer* (2001) 93(3):353–60. doi: 10.1002/ijc.1337

30. Gleich LL, Wang J, Gluckman JL, Fenoglio-Preiser CM. Microsatellite instability as a predictor of survival in head and neck cancer – is there a link with colon cancer? *ORL J Otorhinolaryngol Relat Spec* (2003) 65(4):193–8. doi: 10.1159/000073113

31. Ohki K, Kumamoto H, Ichinohasama R, Suzuki M, Yamaguchi T, Echigo S, et al. Genetic analysis of DNA microsatellite loci in salivary gland tumours: comparison with immunohistochemical detection of hMSH2 and p53 proteins. *Int J Oral Maxillofac Surg* (2001) 30(6):538–44. doi: 10.1054/ijom.2001.0161

32. Skalova A, Leivo I, Hellquist H, Agaimy A, Simpson RHW, Stenman G, et al. High-grade transformation/dedifferentiation in salivary gland carcinomas: occurrence across subtypes and clinical significance. *Adv Anat Pathol* (2021) 28(3):107–18. doi: 10.1097/PAP.0000000000000298

frontiers | Frontiers in Oncology

TYPE Review
PUBLISHED 19 September 2023
DOI 10.3389/fonc.2023.1264287

OPEN ACCESS

EDITED BY
Dietmar Thurnher,
Medical University of Graz, Austria

REVIEWED BY
Stefan Janik,
Medical University of Vienna, Austria
Yuri Ueda,
Tokyo Medical University Hospital, Japan

*CORRESPONDENCE
Ester Orlandi
ester.orlandi@cnao.it

RECEIVED 20 July 2023
ACCEPTED 05 September 2023
PUBLISHED 19 September 2023

CITATION
Locati LD, Ferrarotto R, Licitra L, Benazzo M, Preda L, Farina D, Gatta G, Lombardi D, Nicolai P, Vander Poorten V, Chua MLK, Vischioni B, Sanguineti G, Morbini P, Fonseca I, Sozzi D, Merlotti A and Orlandi E (2023) Current management and future challenges in salivary glands cancer.
Front. Oncol. 13:1264287.
doi: 10.3389/fonc.2023.1264287

Current management and future challenges in salivary glands cancer

Laura D. Locati[1,2], Renata Ferrarotto[3], Lisa Licitra[4,5], Marco Benazzo[6,7], Lorenzo Preda[8,9], Davide Farina[10], Gemma Gatta[11], Davide Lombardi[12], Piero Nicolai[13], Vincent Vander Poorten[14,15], Melvin Lee Kiang Chua[16], Barbara Vischioni[17], Giuseppe Sanguineti[18], Patrizia Morbini[19], Isabel Fonseca[20], Davide Sozzi[21,22], Anna Merlotti[23] and Ester Orlandi[17]*

[1]Department of Internal Medicine and Therapeutics, University of Pavia, Pavia, Italy, [2]Medical Oncology Unit, Istituti Clinici Scientifici Maugeri Istituto di Ricovero e Cura a Carattere Scientifico (IRCCS), Pavia, Italy, [3]Department of Thoracic and Head and Neck Medical Oncology, The University of Texas MD Anderson Cancer Center, Houston, TX, United States, [4]Head and Neck Medical Oncology Unit, Fondazione Istituto di Ricovero e Cura a Carattere Scientifico (IRCCS) National Cancer Institute, Milano, Italy, [5]University of Milan, Milano, Italy, [6]Department of Clinical, Surgical, Diagnostic, and Pediatric Sciences, University of Pavia, Pavia, Italy, [7]Department of Otorhinolaryngology, Fondazione Istituto di Ricovero e Cura a Carattere Scientifico (IRCCS) Policlinico San Matteo, Pavia, Italy, [8]Diagnostic Imaging and Radiotherapy Unit, Department of Clinical, Surgical, Diagnostic, and Pediatric Sciences, University of Pavia, Pavia, Italy, [9]Radiology Institute, Fondazione Istituto di Ricovero e Cura a Carattere Scientifico (IRCCS) Policlinico San Matteo, Pavia, Italy, [10]Azienda Socio-Sanitaria Territoriale (ASST) Spedali Civili di Brescia, Division of Radiology and Department of Medical and Surgical Specialties, Radiological Sciences and Public Health, University of Brescia, Brescia, Italy, [11]Evaluative Epidemiology Unit, Fondazione Istituto di Ricovero e Cura a Carattere Scientifico (IRCCS) National Cancer Institute, Milano, Italy, [12]Department of Otorhinolaryngology - Head and Neck Surgery, University of Study, Brescia, Italy, [13]Unit of Otorhinolaryngology - Head and Neck Surgery, University of Study, Padova, Italy, [14]Otorhinolaryngology-Head and Neck Surgery, Leuven Cancer Institute, University Hospital of Leuven, Leuven, Belgium, [15]Department of Oncology, Section Head and Neck Oncology, Katholieke Universiteit Leuven, Leuven, Belgium, [16]Division of Radiation Oncology, National Cancer Centre Singapore, Singapore, Singapore, [17]Radiation Oncology Clinical Department, National Center for Oncological Hadrontherapy, Pavia, Italy, [18]Department of Radiotherapy, Istituto di Ricovero e Cura a Carattere Scientifico (IRCCS) Regina Elena National Cancer Institute, Roma, Italy, [19]Unit of Pathology, Department of Molecular Medicine, University of Pavia, Foundation Istituto di Ricovero e Cura a Carattere Scientifico (IRCCS) Policlinico San Matteo, Pavia, Italy, [20]Anatomia Patológica, Instituto Português de Oncologia Francisco Gentil, University of Lisbon, Lisbon, Portugal, [21]Department of Medicine and Surgery, School of Medicine University of Milano-Bicocca, Monza, Italy, [22]Maxillofacial Surgery Unit, Fondazione Istituto di Ricovero e Cura a Carattere Scientifico (IRCCS) San Gerardo dei Tintori, Monza, Italy, [23]Department of Radiation Oncology, Santa Croce and Carle Teaching Hospital, Cuneo, Italy

Salivary gland cancers (SGCs) are rare, accounting for less than 5% of all malignancies of the head and neck region, and are morphologically heterogeneous. The diagnosis is mainly based on histology, with the complementary aid of molecular profiling, which is helpful in recognizing some poorly differentiated, borderline, or atypical lesions. Instrumental imaging defines the diagnosis, representing a remarkable tool in the treatment plan. Ultrasound and magnetic resonance are the most common procedures used to describe the primary tumour. The treatment of SGCs is multimodal and consists of surgery, radiotherapy, and systemic therapy; each treatment plan is, however, featured on the patient and disease's characteristics. On 24 June 2022, in the

10.3389/fonc.2023.1264287

meeting "Current management and future challenges in salivary gland cancers" many experts in this field discussed the state of the art of SGCs research, the future challenges and developments. After the meeting, the same pool of experts maintained close contact to keep these data further updated in the conference proceedings presented here. This review collects the insights and suggestions that emerged from the discussion during and after the meeting per se.

KEYWORDS

salivary gland cancer, rare cancer, surgery, heavy particles, targeted therapy

1 Introduction

On June 24, 2022, a one-day meeting entitled "Current management and future challenges in salivary glands cancer" took place at CNAO (Italian National site for Hadrontherapy) in Pavia, Italy. Several international experts in the field have been involved to bring their experience on the management and the research in salivary gland cancers (SGCs). A multidisciplinary overview contributed to turn on the light on these challenging tumours, especially regarding the future research and development. In this review, we describe the current landscape in SGC treatment, focusing on the novelties in diagnosis, surgery, radiotherapy, and systemic therapies that emerged during the meeting.

2 Epidemiological update

SGCs are rare, accounting for less than 5% of all malignancies of the head and neck (HN) region. The WHO Global Cancer Observatory reported 53.583 new diagnoses in 2020 worldwide; the incidence was 0.59 and the mortality 0.23 per 100,000/year (1). Across all European countries, the Eurocare register, which collects data on rare tumours including SGCs, reports an incidence of 0.91 per 100,000/year for malignant epithelial tumours of major salivary glands and 0.43 per 100,000/year for salivary gland-type tumours of the minor salivary glands (2).

The incidence is stable over time, without increment in the risk, except for the elderly population. In 2020, 43% of SGCs occurred in the elderly, causing 12,339 cancer-specific deaths, with a male-to-female ratio of 1.3:1. In the next two decades, the new diagnoses in the elderly age group are expected to account for 80% of the total SGCs diagnoses (3). The review of the Surveillance, Epidemiology and End Results (SEER) Program database indicated that the incidence of major salivary glands and salivary gland-type cancers in patients over 65 years was 4 and 7 times higher, respectively, than that reported in younger patients and the overall 5-year survival rates were significantly better in young than in elderly subjects who, more frequently, presented histotypes with poor prognosis (e.g. salivary duct cancer) or unspecified histotypes (3). Indeed, almost half of SGCs cases from the SEER dataset presented at diagnosis with localized disease, without significant differences between major salivary glands and salivary gland-type carcinomas, while elderly patients were diagnosed more frequently at a metastatic stage (3).

3 Pathological classification and molecular characterization

The diagnosis of SGCs may be challenging to the pathologist because it is a morphologically heterogenous group of neoplasms. The characteristics of each neoplasm have been specified in the updated SGCs classification which the World Health Organization (WHO) has recently released (4). The most important novelties are i) the introduction of molecular data to define new entities; ii) the attention to cytological findings according to the Milan System; iii) the attention to high-grade transformation which may determine a negative prognosis (5). Many types of SGCs (e.g. mucoepidermoid carcinoma, adenoid cystic carcinoma, acinic cell carcinoma, secretory carcinoma, polymorphous adenocarcinoma, hyalinizing clear cell carcinoma, mucinous adenocarcinoma, and microsecretory adenocarcinoma) are defined according to the presence of recurrent genomic alterations, such as gene fusions and tightly tumour-type specific mutations (Table 1).

Recurrent gene defects become, therefore, valuable and helpful for use in diagnostically challenging cases, not only for examining poorly differentiated lesions but also for recognizing borderline or atypical lesions. The next-generation sequencing approach may contribute to clarifying some heterogeneous groups, such as adenocarcinoma, not otherwise specified (NOS) (8). However, most entities are defined based on histology and immunohistochemistry findings, and molecular characterization is not mandatory for the diagnosis (9). However, molecular diagnosis can be supplementary in terms of providing information on biological behaviour, as well as, the suitability of a patient to targeted therapies. Indeed, some gene defects can help to identify some potential targets for therapy; currently, the predictive role of molecular alterations is still not relevant, except for the *RET* and *NTRK* genes translocation that can be targeted by specific inhibitors (e.g. selpercatinib or pralsetinib for *RET* and entrectinib or larotrectinib for *NTRK*) (10, 11); androgen receptor overexpression in salivary duct carcinoma handled with androgen deprivation therapy (12, 13), and HER2 overexpression/

10.3389/fonc.2023.1264287

TABLE 1 Salivary gland cancer, according to the presence of recurrent genomic alterations (6, 7).

Histotype	Molecular alterations	Fusion (major)	Fusion (alternative)
Adenoid cystic carcinoma	*NOTCH1* mutation; *EGFR* and *KIT* overexpression	*MYB-NFIB*	*MYBL1-NFIB*
Mucoepidermoid carcinoma	*PI3KCA, POU6F2, BRCA1/2; CDKN2A* mutation	*CRTC1-MAML2*	*CRTC3-MAML2*
Acinic cell carcinoma	*CDKN2A* and *PPP1R13B* deletion	*NR4A3*	*HTN3-MSANTD3*
Secretory carcinoma	*PRSS1, MLH1, MUTYH*, and *STK11* mutation	*ETV6-NTRK3*	*ETV6-RET; ETV6-MET*
Hyalinising clear cell carcinoma	Not reported	*EWSR1-ATF1*	*EWSR1-CREM; EWSR1-CREB1*
Intraductal carcinoma	*KRAS* and/or *PI3KCA* mutations	*NCOA4-RET*	*TRIM27-RET*
Carcinoma ex pleomorphic adenoma	HER-2 overexpression and *ERBB2* amplification; *HRAS* mutation; *PI3KCA* mutations; *PTEN* loss	*PLAG1-HMGA2, NFIB-PLAG1*	*CTNNB1, LIFR, FGFR1*
Salivary duct carcinoma	AR overexpression; HER-2 overexpression and *ERBB2* amplification; *BRAF, HRAS, PI3KCA, EGFR* and *NF1* mutation; *PTEN* loss	*PLAG1-CTNNB1*	
Myoepithelial carcinoma	*KRAS* and *HRAS* mutation; *SMARCB1* deletion	*TGFBR3-PLAG1*	*PLAG1; HMGA2; EWSR1*

amplification treated with trastuzumab, since other HER2 targeted agents available perhaps generalize to HER2 targeted therapies (14).

Another aspect of novelty in the new classification is the attention to the high-grade transformation/dedifferentiation. High-grade transformation is associated with aggressive clinical behaviour and poor prognosis, regardless of the background histotypes. Adenoid cystic adenocarcinoma (ACC) more frequently undergoes high-grade transformation, usually *de novo* at the initial presentation and, more rarely, at recurrence. The presence of high-grade transformation may be detrimental to morphological diagnosis because of the partial or total loss of distinct morphology of background histotype; in this case, molecular features may be useful to characterize the tumour. The genetic bases which determine the shift toward high-grade transformation have been not completely elucidated yet (15).

Some unresolved issues still exist in the WHO Classification 2022: for example, the definition of mucinous adenocarcinomas or to classify the oncocytic carcinoma no more as an independent entity.

The classification of WHO 2022 reserves an important role to cytology in the diagnosis, introducing the Milan System for reporting. The Milan System provides a very practical SGC classification from a cytological point of view (Table 2).

4 Radiological diagnosis of malignant tumours from both major and minor salivary glands

Imaging plays essential role in treatment planning, in terms of tumour characterization and of locoregional spread detection. Ultrasound (US) imaging with high frequency is the first examination and can be considered conclusive, in case of small lesions or clinically defined and/or confined to the superficial lobe of the parotid gland. In most cases, US can distinguish between benign and malignant tumours, as benign lesions present regular and well-defined margins, a homogeneous hypoechoic structure, and demarcated vessel distribution, while malignant tumours are poorly defined with an irregular shape, blurred margin, and hypoechoic, heterogenous internal architecture and perfusion. However, in some cases as in lower-grade lesions, benign and malignant salivary gland tumours may have a similar US patterns. They appear well-defined and may display a lobulated border and homogeneous internal architecture, as well as, pleomorphic adenomas may have an irregular shape with heterogeneous echo structures. Similarly, about 60% of benign and 50% of malignant tumours are poorly vascularized, while all Warthin tumours, 15% of pleomorphic adenomas, and 38.8% of malignant tumours are well-vascularized (17). Thus, although US is a sensitive and specific

TABLE 2 Diagnostic categories in the Milan System for Reporting Salivary Gland Cytopathology (16).

Diagnostic category
I. Non diagnostic
II. Non-neoplastic
III. Atypia of Undetermined Significance (AUS)
IV. Neoplasm
IVA. Neoplasm: benign
IVB. Neoplasm: salivary gland neoplasm of uncertain malignant potential (SUMP)
V. Suspicious for Malignancy
VI. Malignant

Diagnostic category correlates with the risk of malignancy (ROM), tier I ROM 25%, tier II ROM 10%, tier III ROM 20%, tier IVA ROM < 5%, tier IVB ROM 35%, tier V ROM 60%, tier VI ROM 90%.

technique, about 18-20% of specimens remain non-diagnostic and indeterminate (18).

US is frequently used to perform biological sampling and fine-needle aspirate cytology (FNAC), as in experienced hands is inexpensive, easy to perform, well-tolerated, and safe. Core-needle biopsy (CNB) has a higher sensitivity in diagnosing malignant neoplasms and allows tumour characterization and grading in most of the cases. The technique is less operator-dependent and has a lower rate of indeterminate and non-diagnostic specimens (19). It is, however, more cumbersome with some potential complications and that is why, in the recent ESMO/EURACAN guidelines, a stepped approach is recommended, performing CNB in patients where FNAC is inconclusive (20).

Besides US, magnetic resonance (MRI) represents the imaging technique of choice as it can provide both a morphological and structural analysis by combining conventional and functional sequences. It is valuable to characterize lesions especially when clinical and US evaluations are doubtful or cyto-histological sampling is not conclusive or difficult to perform MRI may have a role in surgical planning in presence of symptoms suggestive of malignancy (such as pain, paralysis of the VII nerve, and lymphadenopathies) and in case of large lesions or lesions involving the deep lobe of the parotid gland (21, 22).

Functional MRI procedures contribute to better discrimination and describe specific types of SGCs. Diffusion-weighted (DWI)-MRI sequence and dynamic contrast-enhanced (DCE) can differentiate pleomorphic adenoma from Warthin tumours. In DCE, the degree of tumour enhancement is plotted against time and the acquired signal generates a time-intensity curve; four time-intensity curves have been characterized. Most pleomorphic adenomas have a type A curve (time to peak was more than 120 seconds), while almost all Warthin tumours have a type B curve (time to peak was 120 seconds or less with high washout ratio, ≥30%); most malignant tumours are characterized by a type C curve (time to peak was 120 seconds or less with low washout ratio, <30%), which is a criterion for predicting salivary gland malignancy with 79% sensitivity and 95% specificity (23). MRI also allows an investigation of the relationship between facial nerves and tumoural mass and the presence of perineural spread. Therefore, the combination of conventional MR and functional imaging contributes to better defining the tumour and helps in treatment planning (21) (Table 3).

Computed Tomography (CT) represents an alternative when MRI is contraindicated or represents an additional exam in cases of suspected involvement of bony structures. CT is less sensitive than MRI in detecting the presence of perineural diffusion, in such cases it may demonstrate enlargement or erosion of skull base foramina (17).

In presence of histologically confirmed malignant lesions, especially if high grade, CT examination can be extended to thorax and abdomen for staging purpose (17).

Some differences can be accounted for major and minor salivary gland imaging. First of all, the anatomy of the minor salivary gland is different, as minor glands are located especially in the oral cavity (mostly lips, posterior 1/3 of the hard palate, base of the tongue), in oro- and nasopharynx, paranasal sinuses, larynx, and trachea, with a submucosal location. The anatomic site of the primary tumour influences the choice of the imaging acquisition protocol. In the differential diagnosis of minor SGCs, it should be noted that the rate of malignant tumours is higher than in major SGCs, with pleomorphic adenoma, mucoepidermoid carcinoma, and ACC being the most common histological type (Table 4). Other histotypes have sites and patterns overlapping; therefore, imaging is not enough to give a diagnosis in most cases.

The differential diagnosis should encompass other entities, namely "tumour mimickers", including mucocele, IgG4-related disease (26), and necrotizing sialometaplasia. Local invasion and a permeative growth pattern are features of ACC, with the involvement of bone, and soft tissue. Perineural spread of minor SGCs involves maxillary (tumours arising from hard palate and spheno-palatine area) and mandibular nerves (tumours arising from nasopharynx), VII cranial nerves, mostly via interconnections with V cranial nerves, and lower cranial nerves (tumour arising from nasopharynx extending to the skull base). All these characteristics of the tumours of minor salivary glands reflect on imaging protocols in terms of field-of-view and spatial resolution. The field of view should be adapted to the site that should be visualized and the resolution should be maximized to identify all lesions.

TABLE 3 Conventional MRI features in pleomorphic adenoma, Warthin tumour, and malignant tumour (24, 25).

Type of lesion	Typical MR Characteristics	Contrast-enhancement pattern	Additional characteristics
Pleomorphic adenoma	Low signal on T1w, bright signal on T2w Well-defined, lobulated margins with hypointense capsule	Marked heterogeneous nodular enhancement	Cellular subtypes or with fibrosis content associated with low T2 signal
Warthin tumour	Cystic portions with high signal on unenhanced T1w and intermediate-to-high signal on T2w	Solid portions with low-intermediate enhancement	Located in the inferior portion of the parotid gland, often bilateral
Malignant tumours	low signal on T2w (high cellularity). Undefined borders, invasion of surrounding structures. Macroscopic perineural spread. Lymphadenopathies	Homogeneous or heterogeneous contrast-enhancement. Necrosis and cystic changes are not specific features	Low-grade lesions may have MRI features comparable to benign lesions (homogeneous signal intensity, well defined borders and capsule-like rim enhancement)

MRI, magnetic resonance imaging T1w, T1 weighted; T2w, T2 weighted.

TABLE 4 Clinical and radiological features of the most common tumours in minor salivary glands.

Histotype	Pleomorphic adenoma	Mucoepidermoid carcinoma	Adenoid cystic carcinoma
Radiological pattern	Usual MRI-CT pattern DWI -	Imaging findings variable, depending on grade	DWI + Permeative growth pattern
Anatomic site	Hard palate, upper lip	Palate	Paranasal sinus (30%), oral cavity
Typical features	Rarely malignant	Children and young adults	Perineural spread

MRI, magnetic resonance imaging; CT, computerized tomography; DWI, diffusion-weighted magnetic resonance imaging.

5 Surgery of salivary glands cancers: current status and recent advances

Surgery is often the upfront treatment for all SGCs; however, the most important prognostic factors (e.g. high-grade lesion, high pT-category, perineural spread, especially if microscopic) that may affect the outcomes are not often available before surgery. The Vander Poorten Scoring System may help in estimating prognosis and decision making. This index allows for a weighted estimate of an individual patient's prognosis in both the pre- and the post-operative situation (27, 28), and by now has been repeatedly externally validated (29–33) and it is also available as a nomogram (34).

The main principles of surgery are complete resection (R0) with adequate margins and the preservation (or restoration) of vital function. Regarding the definition of "adequate margins", no relevant differences have been observed between negative and close (< 5 mm) margins for all SGC sites (35), except for the oral cavity. For ACC, there is consensus that a close margin (R1) resection makes sense in enhancing local control in combination with postoperative radiotherapy as compared to using radiotherapy alone (35, 36). In this respect, patients with an expected R2 margin are preferably sent for primary radiotherapy, and heavy ion therapy is preferred in this situation (20).

The vast majority of high-grade tumours require a combination of surgery and radiotherapy, although the most efficacious technique for radiotherapy delivery e.g., photons versus protons versus carbon ion therapy remains undefined. In the adjuvant setting, the use of platinum-based chemoradiotherapy was well tolerated but up to now did not demonstrate any survival improvement, compared to radiotherapy alone in patients with high-risk salivary gland cancers (37). Indeed, the use of concomitant chemoradiation in adjuvant setting is discouraged by the recent guidelines (20, 38), outside of clinical trials; the RTOG-1008 trial (NCT01220583) has completed recruitment, and currently, we await the first results.

5.1 Surgery for MiSGC

Minor SGCs are rare and heterogeneous in terms of histology, grade, and site of origin. In these tumours, negative prognostic factors are advanced stage at presentation including advanced T classification, positive margins (R1), positive nodes, perineural and – especially for ACC – intraneural spread (39), sinonasal and nasopharyngeal site of origin, lymph node ratio, and high-grade. Survival is quite good, but high-grade tumours are associated with a dismal prognosis (40). The surgical management of minor SGCs is particularly challenging and should be centralized in centres with large experience. Transoral surgery, transnasal endoscopic surgery, and combined transoral-transnasal techniques are becoming common surgical procedures to manage minor SGCs of oropharyngeal or sinonasal origin (41). Since the past 2 decades, transoral surgery is traditionally performed using laser microscopic surgery, through laryngoscopes and oropharyngoscopes, but the surgeon is limited by the line of sight through a positioned scope, while only a tangential cutting plane can be used. Frequent repositioning of scopes results in a piecemeal resection, and the technique needs a demanding learning curve. In specific indications and given good exposure, the Da Vinci ® robot for transoral surgery can result in improved maneuverability and visualization, thus overcoming the limits of transoral laser microsurgery and giving access to selected tumours that are otherwise hard to approach. The underlying idea is to use a minimally invasive natural orifice surgery, reducing the interference with surrounding tissues when compared to traditional transcervical/transmandibular approaches. Current evidence in the use of this technique in minor SGCs concerns tumours located in the oropharynx at the base of the tongue and, very rarely, supraglottic locations; limited evidence is available on the advantages of robotic surgery for parapharyngeal SGCs of minor and major salivary gland origin (42, 43). Based on the experience with squamous cell carcinomas (SCC), it is suggested that, in selected patients, transoral surgery can result in a shorter recovery and hospital stay and better functional outcomes than open approaches; in selected patients with SCC in the salvage setting, the transoral approach also shows functional and oncological superiority (44). We should, however, remain careful in extrapolating this experience with SCC to SGCS of minor salivary gland origin, the latter having a known tendency to submucosal spread and perineural invasion, complicating a good resection. To date, the data supporting this approach in SGCs remain limited and often related to small case series and retrospective studies with potential inclusion bias (42, 43). Nevertheless, transoral robotic surgery, followed by adjuvant radiotherapy, should be considered a valuable option in the multidisciplinary management of minor SGCs, achieving durable disease-free survival in well-selected patients (43). In the same line, endoscopic endonasal resection can be applied in the nasopharynx (in SGCs without involvement of the internal carotid artery, and with minimal skull base extension) and in the sinonasal tract and skull base (45). The combination of endoscopic and transoral approaches, e.g. in the endoscopic-assisted maxillectomy, has the dual advantage of better delineating the posterior margin by drilling the pterygomaxillary junction while avoiding facial incisions (46).

For ACC located in the nasopharynx and in the sinonasal tract, the main issue is the nerve invasion, not only limited to perineural invasion and inflammation but also including intraneural invasion, which resulted as an independent predictor of poor prognosis (39). In particular, definitive upfront radiotherapy should be considered for ACC of the nasopharynx.

5.2 Surgery for Major SGCs

The surgery of major SGCs consists in most of the cases in superficial parotidectomy or total parotidectomy, to obtain a complete resection with adequate free surgical margins (47). The extent of resection performed may differ according to the local extension and specific growth pattern of the tumour (48). The debate on parotidectomy is still open: a superficial parotidectomy can be sufficient and adequate for superficial lobe lesions and in presence of normal mobility and functioning of the VII nerve, while total conservative parotidectomy is preferred when deep lobe parotid lymph nodes are at risk or involved (49). Both ASCO and ESMO/EURACAN guidelines (20, 38) suggest that at least parotidectomy with the removal of additional parotid tissue should be recommended for advanced or high-grade cancer, if it is deemed to not place the facial nerve at significant risk, but the latter is obviously related to the experience of the surgeon. Prophylactic deep lobe parotidectomy may be indicated with high-grade tumours and in presence of lymph node involvement, especially using the en bloc technique that limits the risk to facial nerve damage (50). Total parotidectomy for small malignant tumours is not supported by significant evidence as no randomized clinical trials are available and the local recurrence rate is very low in the early stage, if adequately treated with postoperative radiotherapy (51–53). Nevertheless, current guidelines promote total parotidectomy in tumours with pre-operative known type and high-grade (20, 38). Total parotidectomy is indicated for a tumour in the deep lobe, retromandibular area, upper part of the stylomandibular tunnel, and in presence of obvious malignant tumours with extraparenchymal extension or neck metastasis. Mandibulotomy should be considered (but surely is not always needed) for deep lobe malignant tumours, or parapharyngeally recurring pleomorphic adenomas. Reconstructive surgery is aimed at minimizing aesthetic deformity and maximizing the functionality in radical parotidectomy with VII nerve sacrifice. Classical combinations are static reconstruction, free fasciocutaneous or muscle flaps for soft tissue and skin replacement, and free nerve cable grafting to restore the sacrificed facial nerve; new developments resulting in better and quicker recovery are the use of vascularized nerve grafts and of the masseteric nerve transfer (41).

6 Radiotherapy: when, how, and where

According to ASCO and ESMO/EURACAN Guidelines (20, 38), postoperative radiotherapy should be offered to all patients with ACC, and for the other SGC types for high-grade tumours, positive margins, perineural invasion, lymphovascular invasion, lymph node metastases, and pT3-4 tumours; it should also be considered an option for patients with close margins or intermediate-grade tumours (38). Radiotherapy should be suggested also to patients who are not eligible for surgical resection because of the extent of the disease or in case of anticipated R2 resection or the presence of clinical comorbidities. Elective nodal irradiation is indicated for a selected group of patients with high-grade tumours or advanced T status that did not undergo neck dissection at the time of the primary resection.

The scenario is different for low-grade SGCs (e.g. low-grade mucoepidermoid carcinoma, classical acinic cell carcinoma, myoepithelial carcinoma, all polymorphous adenocarcinomas). No data from randomized studies are currently available on the role of radiotherapy in low-grade SGCs and recommendations mainly derive from retrospective studies and expert opinions. The treatment paradigm of a malignant low-grade tumour consists of surgical resection in all salivary sites, followed by postoperative radiotherapy in presence of the risk factors mentioned above or in case of recurrence and it should be accounted for that almost 50% of low-grade SGCs (54) and almost 30% of ACC have at least one high-risk feature (55). On the other hand, radiotherapy is not suggested in pT1 and pT2 low-grade cancers without additional negative prognostic factors; indeed, in a study cohort on more than 800 patients with surgically treated SGCs, the use of post-operative radiotherapy did not change the survival rates in the subset of patients with stage I/II, close margins (< 1 mm) and low- or intermediate-risk histologic type (56). But one should remain cautious in that there is still inevitable selection bias in this institutional cohort, even if there is correction for confounding via multivariate analysis.

For ACC, the standard treatment consists of radical surgery and postoperative radiotherapy, especially for locally advanced disease and in presence of the risk factors mentioned above. Due to its well-known radioresistance, ACC remains a major challenge for radiation oncologists. Its horseshoe shape often embraces or intersects radiosensitive structures following neural pathways: indeed, high conformational radiotherapy techniques are required to reduce the dose delivered to normal structures avoiding radiation induced severe toxicities. In this regard, particles, including protons, neutrons and carbon ions, with different physical features appear to reduce the low-to-moderate dose of photon radiotherapy (RT) by inverting the depth dose profile of energy deposition through the matter. In contrast to photons, the dose at the beam entrance is relatively lower than in the Bragg peak, where most energy is deposited in a limited depth interval with a consequently reduced irradiation of healthy tissues along the beam path. In addition, neutrons and carbon ion radiation therapy (CIRT) show several advantages compared to photons. In particular carbon ions have a superior relative biological effectiveness (RBE) that is estimated at least a 2–3-fold factor in comparison to photons and protons. Neutrons and carbon ions entered the clinical practice from some decades. Good local control (LC) rates from early neutron studies on SGCs, including the pivotal phase III trial conducted by Radiation Therapy Oncology Group (RTOG) and Medical Research Council (MRC) in the 1980's were unfortunately reached at the expense of considerably higher late toxicities

compared to photons (57). Thus, it led to the investigation of CIRT therapy for these tumours, ACC, particularly when surgery is not an option. In addition to the dosimetric advantages with steep dose gradients beyond the Bragg peak, steering of carbon ions is much more convenient than for neutrons. The interest in carbon ion arose in Germany (58) and Japan (59, 60) and rapidly spread around the world, with many particle facilities that are built even in Europe and China. Evidence that ACC may benefit from CIRT, alone or in combination with photons based intensity modulated RT in terms of LC, overall survival (OS) and toxicity, including R2 and inoperable cases has been reported in the latest years (61–64). Especially in Akbaba et al. for paranasal sinuses after CIRT boost it was reported higher toxicity rate (>G3) in the postoperative intensitiy modulated radiotherapy (IMRT) + CIRT cases in comparison to the primary IMRT + CIRT, with comparable results in terms of LC (58). In a series of 184 patients with ACC of the head and neck treated with CIRT at CNAO from January 2013 to June 2020 worse OS was reported for patients with any gross tumour volume (GTV) at pre-CIRT MRI compared to macroscopically resected patients (p=0.008), with shorter OS in patients after debulking surgery and unresected patients (43% and 54% 5 years OS) compared to R1 postoperative patients with macroscopic disease at pre CIRT MRI (78% OS) and patients with microscopic disease (93%, p=0.014).

It is difficult to exhaustively delineate the toxicity scenario of CIRT as different prescription doses, different biological models for dose prescriptions, and different dose constraints are used in each centre. In addition, some discrepancies are observed in the way to evaluate the impact of therapy, especially for example on brain toxicity. Consensus initiatives are necessary to standardize as much as possible treatments with CIRT and the evaluations of toxicity during the follow-up as it has been proposed for proton therapy (65). Proton therapy can be used to achieve a good dose distribution in complex ACC volumes and may be potentially advantageous over advanced photon techniques in selected cases and for children and young adults to reduce low dose splash of conventional photon RT. High local control was achieved in a Japanese series of 25 patients (3-year LC 63%) (66) and in another American series of 19 patients (2-year OS 93) (67) treated with radical proton therapy. An excellent outcome (5-year LC 93%) was reported in a French series of 23 patients treated with mixed photon/proton beams when post-surgical flap insertion is performed or in young patients (68). It is important to remember that each tumour localization and histology needs a specific approach. In paranasal sinuses and palate, the most common histological subtype is squamous cell carcinoma, and rarer variants are olfactory neuroblastoma, adenocarcinoma, mucoepidermoid carcinoma, ACC, undifferentiated sinonasal carcinoma, neuroendocrine carcinoma, and chordoma. Postoperative radiotherapy is indicated almost in all patients and treatment recommendations are agnostic to histological subtypes. However, some attention should be paid in presence of a positive margin, in proximity to crucial structures, and according to the status of the reconstructed flap and irradiation of the neck.

Some issues of radiotherapy are still present in paranasal sinuses, although many advances have been done in this field in the last years (69). The tumour clinical target volume dosimetry is challenging as the dose is often limited to respect the constraints of critical structures and is particularly critical in unresectable diseases. In some cases, excessive doses with hotspots >10% of the prescribed dose to the skull base, skin, and flap can occur; it should be cautious to avoid exceeding doses within critical structures such as optic nerve and chiasm or to cause other equally debilitating complications including flap necrosis, ocular infections, eating difficulty as all these side effects can compromise short- and long-term quality of life (70). Finally, the anatomical volume to be included in case of perineural invasion remains controversial, in particular no consensus exists to treat electively the skull base only when a named nerve is involved or include it routinely even when a microscopic perineural inflammation is reported.

7 Neck involvement in salivary gland cancer

The treatment of salivary gland cancer with clinically negative lymph nodes is still unclear. In this patients category we need to look at the presence of the risk factors for occult neck disease and deciding to treat the neck when the probability, based on the combined presence of different risk factors, exceeds the threshold of 15–20%. Risk factors predicting micrometastases are clinical characteristics, such as age (>54 years), pain, facial nerve dysfunction and stage >T2, and pathological as intermediate- or high-grade tumour, extraglandular soft tissue invasion and lymphatic invasion (71). A different distribution of occult metastases in the neck in cN+ and cN0 has been reported (72). The rate of occult nodal disease ranges from 10.2 and 22.4% in patients with cN0 parotid cancer (73) and from 10 to 40% in patients with cN+ parotid cancer (48). According to the ESMO/EURACAN/EURACAN and NCCN guidelines, management of cN0 can be different according to the primary site and the presence of high-risk features. Elective neck dissection is suggested in case of major salivary gland cancer in presence of "high-grade and/or T3–4 tumours" (20, 74). Elective RT could be a second option in high-risk patients that end up in this category depending on definitive histopathology of the resected primary (71). In case of primary from minor salivary glands of the head and neck or sublingual gland, elective neck dissection is always recommended (20, 74). In patients with cN+ all levels of the neck are involved, as well as intra and peri-parotid nodes (72, 75, 76). Considering the classical TNM of squamous cell carcinoma of the upper airways, SGCs have a peculiar biology as no contralateral nodal involvement is described, rarely metastases measure more than 6 cm in diameter, and the role of extra-nodal extension is at least debatable. This biology reflects on a different impact of nodal involvement: the quantitative burden of nodal disease is an important determinant with a progressive impact on prognosis, while extranodal extension does not seem to impact on prognosis (77). Intraparotid nodal involvement is another negative prognostic factor that should be included in treatment planning (78). The inclusion of the intraparotid lymph node status into the lymph node assessment with the log odds of pN+ led to robust prognostication, regardless of the T status (79). Therefore, the intraparotid node

should be assessed after surgery in every single case and, definitively, a novel N staging system tailored to major salivary glands should be evaluated.

8 Systemic therapies for recurrent/metastatic salivary gland cancers

Systemic therapies for recurrent/metastatic SGCs are chemotherapy and targeted therapy for ACC and chemotherapy, targeted therapy, hormonal therapy, and immunotherapy for non-ACC. It is not clear which is the best therapeutic approach because randomized trials are lacking. Chemotherapy provides a low response rate in ACC (5-22%), while in other histotypes the response rate ranges from 30 to 40%. However, the effect on overall survival has not been demonstrated yet, but there is a potential impact on quality of life (80). Chemotherapy is generally reserved for palliative care for an advanced disease that is not manageable with local therapies such as surgery and/or radiation (80). ACC is a biphasic tumour consisting of myoepithelial and epithelial cells, with *MYB/MYB L1-NFIB* rearrangements which occur in almost 65% of cases. The rate of distant failure after curative treatment ranges from 40 to 50%, and approximately 15% of cases have an aggressive disease course. No standard of care system therapy for patients with metastatic disease is currently available, and chemotherapy, anti-angiogenic agents, and checkpoint inhibitors have limited activity. Noteworthy, despite the biological variability of the disease, all patients are treated in the same way. The aggressiveness of ACC depends on its molecular profile and, in particular, on the mutational status of the *NOTCH 1* gene. About 15% of patients show mutations in *NOTCH 1* gene, most of them are located in the negative regulation PEST domain. *NOTCH*-mutated patients have a peculiar phenotype with a solid component, bone and liver metastases, and advanced stage IV (81); *NOTCH 1* mutations have been associated with a worse prognosis (82).

In proteogenomic studies, consensus clustering identified two distinct ACC subtypes, ACC-I (37%) and ACC-II (63%). ACC-I had strong upregulation of *MYC*, *MYC* target genes, and mRNA splicing, enrichment of NOTCH-activating mutations, and dramatically worse prognosis. ACC-II exhibited upregulation of TP63 and receptor tyrosine kinases (AXL, MET, and EGFR) and a less aggressive clinical course. TP63 and MYC were sufficient to assign tumours to ACC subtypes, which was validated in one independent cohort by IHC and two additional independent cohorts by RNA-sequencing (83).

The presence of multiple targetable protein/pathways alterations in each ACC subtype provides opportunities for combination therapy for this disease (83). Potential drug targets in ACC-I are PRMT5, NOTCH 1 (84), and BCL2, while in ACC-II these are EGFR, AXL, and MEK/AKT pathways (83). Xenograft models of ACC-I were responsive to PRMT5 inhibition with a block of tumour growth (85); AL101 determined tumour regression in *NOTCH* activated ACC-I models and further synergic activity was observed when used in combination with BCL2 inhibitor or palbociclib (86). The ACCURACY study investigated the response to the NOTCH inhibitor AL101 in patients with recurrent and/or metastatic ACC harbouring *NOTCH* activating mutations (87), while the response rate was overall low (8.3 to 14.6%), the disease control rate was 66.7-70.7% and clinical benefit was noted in a proportion of patients. To better understand the biologic changes induced by pharmacologic NOTCH inhibition in NOTCH-mutated ACC and guide rationale combinatorial therapy, a window of opportunity trial is currently being conducted with the gamma-secretase inhibitor AL101. AXL is another promising target for therapy; in preclinical models inhibition of AXL by an antibody-conjugated drug blocked tumour growth (88). TROP2 expression is moderate to high in 86% of ACC, especially in ACC-II (89) and sacituzumab govitecan can be potentially employed in SGC.

Tumor microenvironment resulted as different in two ACC subtypes: in ACC-I more epithelial tumour cells and intratumoural natural killer cells were counted, with a higher expression of Ki67 and B7-H4 and in the stroma more immune cells and cytotoxic T cells were observed; in ACC-II there was a higher density of fibroblasts and myoepithelial p63+ tumour cells (90). To modulate the tumour microenvironment, axitinib and avelumab were used in combination in recurrent/metastatic ACC, providing disease control in most patients without significantly increasing the response rate of historical data with axitinib alone (91).

Non-ACC is a highly heterogenous group of diseases, with many druggable molecular targets. For instance, SDC is an aggressive tumour characterized by overexpression of androgen receptor in 80-90% of cases, HER2 overexpression with higher variability (16-83%), and *PI3KCA*, *HRAS*, and *BRAF* mutations in a lower rate (92). Androgen receptor (AR+) expression supports the use of androgen deprivation therapy and several agents as enzalutamide, abiraterone acetate, apalutamide- have been employed to treat AR+ disease, with favourable outcomes in terms of progression-free survival and overall survival (13). For tumour overexpressing HER2, the use of Herceptin seemed to be reasonable, but in a phase II study, trastuzumab given as a single agent showed a low activity (93). The combination of trastuzumab with docetaxel improved the outcomes with an overall response rate of 70.2% (94). Many other trials are currently ongoing with anti-HER2 agents including new anti HER2 agents (95). The secretory carcinoma carries *ETV6-NTRK3* or *ETV6-RET* fusion in almost all patients and can be treated with entrectinib (96) or larotrectinib (97). Immunotherapy alone cannot provide a significant clinical benefit, especially in ACC (98). Indeed, only high-grade tumours as salivary duct seem to be enriched by PD-L1, compared to ACC, generally defined as immune-excluded tumour (99). Data from recent clinical trials with single agent immunotherapy (e.g. pembrolizumab, nivolumab) are quite disappointing in term of objective response rate (12% at maximum with pembrolizumab) and progression-free survival (median, 4 months (100–103). Results seem to improve with nivolumab and ipilimumab (104). Remarkable, activity of this combination is higher in SDC (25%) compared to non-ACC (16%) and ACC (6%), respectively,

suggesting that immunotherapy is promising for very selected histotypes. However, immune-checkpoints have been tested in small patients cohorts with mixed histotypes, further evidence are warranted to deepen the role of immune modulation in SGCs. In addition, there is an urgent need for predictive biomarkers to guide both the therapy and development of effective immuno-oncology combination strategies.

As also recommended in the ESMO/EURACAN/EURACAN guidelines (20), targeted therapy for advanced salivary gland cancers should be based on molecular profiling: indeed, MyPathway phase IIa multiple basket study achieved a 63% of overall response rate with chemotherapy-free regimens matched to specific molecular alteration (105). Clinical trials, however, are warranted in these neglected cancers.

9 Conclusion

The current landscape of SGCs is rapidly evolving and impressive advances have been done in the last few years in many fields, including molecular characterization, surgery, radiotherapy, and the development of novel systemic therapies. We have learned that is mandatory to work in research networks to optimize the efforts. Networks are crucial to allow the organization and management of international clinical trials in rare diseases, as SGCs; specific research plans are warranted to support the research in this field.

Author contributions

LDL: Conceptualization, Supervision, Writing – original draft, Writing – review & editing. RF: Writing – review & editing. LL: Writing – review & editing. MB: Writing – review & editing. LP: Writing – review & editing. DF: Writing – review & editing. GG: Writing – review & editing. DL: Writing – review & editing. PN: Writing – review & editing. VV: Writing – review & editing. MC: Writing – review & editing. BV: Writing – review & editing. GS: Writing – review & editing. PM: Writing – review & editing. IF: Writing – review & editing. DS: Writing – review & editing. AM: Writing – review & editing. EO: Writing – review & editing, Conceptualization, Supervision, Writing – original draft.

Acknowledgments

The authors wish to thank Dr. Elisa Sala, PhD medical writer, for her writing assistance.

Conflict of interest

LDL received conference honoraria/advisory board fees from: Lilly, MSD, EISAI, Roche, Bayer, Merck Serono, Istituto Gentili Srl, New Bridge; RF had consulting or Advisory Role in Regeneron, Sanofi, Prelude Therapeutics, Elevar Therapeutics, Guidepoint, Expert Connect, Remix, Eisai, Bioatla, Coherus in the past 24 months and received Research Funds Inst from Prelude, Ayala, Merck, Genentech, Pfizer, Rakuten, Nanobiotix, EMD Serono, ISA, Viracta, and Gilead in the past 24 months; LL received Research funds donated directly to the institution for clinical trials from:

Adlai Nortye, Astrazeneca, BMS, Debiopharm International SA, Eisai, Eli Lilly and Company, Exelixis, Hoffmann-La Roche ltd, Isa Therapeutics, Kura Oncology, Merck-Serono, MSD, Merck Sharp&Dome Corp, Nektar Therapeutics, Novartis, Regeneron, Roche, Sanofi, Syneos, Sun Pharmaceutica and received occasional fees for participation as a speaker at conferences/congresses or as a scientific consultant for advisory boards from: Adlai Nortye, Astrazeneca, Bicara Therapeutics, DRG part of Clarivate, Genmab US, GlaxoSmithKline, Bayer, Mirati Therapeutics, MSD, Merck-Serono, Merck Healthcare KGaA, Neutron Therapeutics Inc, Seagen International BmbH.

The remaining authors declare that the research was conducted in the absence of any commercial or financial relationships that could be construed as a potential conflict of interest.

Publisher's note

References

1. WHO. Available at: https://gco.iarc.fr/today/data/factsheets/cancers/2-Salivary-glands-fact-sheet.pdf.

2. RareCancer. Available at: www.rarecancer.net.

3. Colombo E, Van Lierde C, Zlate A, Jensen A, Gatta G, Didone F, et al. Salivary gland cancers in elderly patients: challenges and therapeutic strategies. *Front Oncol* (2022) 12:1032471. doi: 10.3389/fonc.2022.1032471

4. IARC. Available at: https://publications.iarc.fr/.

5. Skalova A, Hyrcza MD, Leivo I. Update from the 5th edition of the world health organization classification of head and neck tumors: salivary glands. *Head Neck Pathol* (2022) 16:40–53. doi: 10.1007/s12105-022-01420-1

6. Na K, Hernandez-Prera JC, Lim JY, Woo HY, Yoon SO. Characterization of novel genetic alterations in salivary gland secretory carcinoma. *Mod Pathol* (2020) 33:541–50. doi: 10.1038/s41379-019-0427-1

7. Bishop J. *Tumors of the Salivary Glands AFIP ATLASES OF TUMOR AND NON-TUMOR PATHOLOGY*. ARP Press, Rockville, Maryland (2021).

8. Bishop JA, Sajed DP, Weinreb I, Dickson BC, Bilodeau EA, Agaimy A, et al. Microsecretory adenocarcinoma of salivary glands: an expanded series of 24 cases. *Head Neck Pathol* (2021) 15:1192–201. doi: 10.1007/s12105-021-01331-7

9. Zhang C, Gu T, Hu Y, Sun J, Xia R, Tian Z, et al. Reevaluation of salivary lymphadenoma: A subgroup identified as warthin-like mucoepidermoid carcinoma

following molecular investigation for MAML2 rearrangement. *Arch Pathol Lab Med* (2021) 145:744–52. doi: 10.5858/arpa.2019-0702-OA

10. Suzuki K, Harada H, Takeda M, Ohe C, Uemura Y, Kawahara A, et al. Clinicopathological investigation of secretory carcinoma cases including a successful treatment outcome using entrectinib for high-grade transformation: a case report. *BMC Med Genomics* (2022) 15:6. doi: 10.1186/s12920-022-01155-6

11. Weinreb I, Bishop JA, Chiosea SI, Seethala RR, Perez-Ordonez B, Zhang L, et al. Recurrent RET gene rearrangements in intraductal carcinomas of salivary gland. *Am J Surg Pathol* (2018) 42:442–52. doi: 10.1097/PAS.0000000000000952

12. Boon E, van Boxtel W, Buter J, Baatenburg de Jong RJ, van Es RJJ, Bel M, et al. Androgen deprivation therapy for androgen receptor-positive advanced salivary duct carcinoma: A nationwide case series of 35 patients in The Netherlands. *Head Neck* (2018) 40:605–13. doi: 10.1002/hed.25035

13. Locati LD, Cavalieri S, Bergamini C, Resteghini C, Colombo E, Calareso G, et al. Abiraterone acetate in patients with castration-resistant, androgen receptor-expressing salivary gland cancer: A phase II trial. *J Clin Oncol* (2021) 39:4061–68. doi: 10.1200/JCO.21.00468

14. Limaye SA, Posner MR, Krane JF, Fonfria M, Lorch JH, Dillon DA, et al. Trastuzumab for the treatment of salivary duct carcinoma. *Oncologist* (2013) 18:294–300. doi: 10.1634/theoncologist.2012-0369

15. Skalova A, Leivo I, Hellquist H, Agaimy A, Simpson RHW, Stenman G, et al. High-grade transformation/dedifferentiation in salivary gland carcinomas: occurrence across subtypes and clinical significance. *Adv Anat Pathol* (2021) 28:107–18. doi: 10.1097/PAP.0000000000000298

16. Rossi ED, Baloch Z, Pusztaszeri M, Faquin WC. The Milan System for Reporting Salivary Gland Cytopathology (MSRSGC): an ASC-IAC-sponsored system for reporting salivary gland fine-needle aspiration. *J Am Soc Cytopathol* (2018) 7:111–18. doi: 10.1016/j.jasc.2018.02.002

17. David E, Cantisani V, De Vincentiis M, Sidhu PS, Greco A, Tombolini M, et al. Contrast-enhanced ultrasound in the evaluation of parotid gland lesions: an update of the literature. *Ultrasound* (2016) 24:104–10. doi: 10.1177/1742271X15626611

18. Zbaren P, Triantafyllou A, Devaney KO, Poorten VV, Hellquist H, Rinaldo A, et al. Preoperative diagnostic of parotid gland neoplasms: fine-needle aspiration cytology or core needle biopsy? *Eur Arch Otorhinolaryngol* (2018) 275:2609–13. doi: 10.1007/s00405-018-5131-0

19. Hurry KJ, Karunaratne D, Westley S, Booth A, Ramesar K, Zhang TT, et al. Ultrasound-guided core biopsy in the diagnosis of parotid neoplasia: an overview and update with a review of the literature. *Br J Radiol* (2022) 95:20210972. doi: 10.1259/bjr.20210972

20. van Herpen C, Vander Poorten V, Skalova A, Terhaard C, Maroldi R, van Engen A, et al. Salivary gland cancer: ESMO-European Reference Network on Rare Adult Solid Cancers (EURACAN) Clinical Practice Guideline for diagnosis, treatment and follow-up. *ESMO Open* (2022) 7:100602. doi: 10.1016/j.esmoop.2022.100602

21. Coudert H, Mirafzal S, Dissard A, Boyer L, Montoriol PF. Multiparametric magnetic resonance imaging of parotid tumors: A systematic review. *Diagn Interv Imaging* (2021) 102:121–30. doi: 10.1016/j.diii.2020.08.002

22. Liang YY, Xu F, Guo Y, Wang J. Diagnostic accuracy of magnetic resonance imaging techniques for parotid tumors, a systematic review and meta-analysis. *Clin Imaging* (2018) 52:36–43. doi: 10.1016/j.clinimag.2018.05.026

23. Yabuuchi H, Matsuo Y, Kamitani T, Setoguchi T, Okafuji T, Soeda H, et al. Parotid gland tumors: can addition of diffusion-weighted MR imaging to dynamic contrast-enhanced MR imaging improve diagnostic accuracy in characterization? *Radiology* (2008) 249:909–16. doi: 10.1148/radiol.2493072045

24. Friedman ER, Saindane AM. Pitfalls in the staging of cancer of the major salivary gland neoplasms. *Neuroimaging Clin N Am* (2013) 23:107–22. doi: 10.1016/j.nic.2012.08.009

25. Zaghi S, Hendizadeh L, Hung T, Farahvar S, Abemayor E, Sepahdari AR. MRI criteria for the diagnosis of pleomorphic adenoma: a validation study. *Am J Otolaryngol* (2014) 35:713–8. doi: 10.1016/j.amjoto.2014.07.013

26. Sasaki T, Takahashi K, Mineta M, Fujita T, Aburano T. Immunoglobulin G4-related sclerosing disease mimicking invasive tumor in the nasal cavity and paranasal sinuses. *AJNR Am J Neuroradiol* (2012) 33:E19–20. doi: 10.3174/ajnr.A2495

27. Vander Poorten V, Guntinas-Lichius O. Prognostic scoring for Malignant salivary gland neoplasms. *Adv Otorhinolaryngol* (2016) 78:71–82. doi: 10.1159/000442127

28. Vander Poorten VL, Balm AJ, Hilgers FJ, Tan IB, Loftus-Coll BM, Keus RB, et al. The development of a prognostic score for patients with parotid carcinoma. *Cancer* (1999) 85:2057–67. doi: 10.1002/(SICI)1097-0142(19990501)85:9<2057::AID-CNCR24>3.0.CO;2-F

29. Vander Poorten VL, Hart AA, van der Laan BF, Baatenburg de Jong RJ, Manni JJ, Marres HA, et al. Prognostic index for patients with parotid carcinoma: external validation using the nationwide 1985-1994 Dutch Head and Neck Oncology Cooperative Group database. *Cancer* (2003) 97:1453–63. doi: 10.1002/cncr.11254

30. Poorten VV, Hart A, Vauterin T, Jeunen G, Schoenaers J, Hamoir M, et al. Prognostic index for patients with parotid carcinoma: international external validation in a Belgian-German database. *Cancer* (2009) 115:540–50. doi: 10.1002/cncr.24015

31. Lu CH, Liu CT, Chang PH, Yeh KY, Hung CY, Li SH, et al. Validation and comparison of the 7(th) edition of the american joint committee on cancer staging system and other prognostic models to predict relapse-free survival in asian patients with parotid cancer. *J Cancer* (2016) 7:1833–41. doi: 10.7150/jca.15692

32. Paderno A, Tomasoni M, Mattavelli D, Battocchio S, Lombardi D, Nicolai P. Primary parotid carcinoma: analysis of risk factors and validation of a prognostic index. *Eur Arch Otorhinolaryngol* (2018) 275:2829–41. doi: 10.1007/s00405-018-5122-1

33. Westergaard-Nielsen M, Moller S, Godballe C, Grau Eriksen J, Larsen SR, Kiss K, et al. Prognostic scoring models in parotid gland carcinoma. *Head Neck* (2021) 43:2081–90. doi: 10.1002/hed.26672

34. Peeperkorn S, Meulemans J, Van Lierde C, Laenen A, Valstar MH, Balm AJM, et al. Validated prognostic nomograms for patients with parotid carcinoma predicting 2- and 5-year tumor recurrence-free interval probability. *Front Oncol* (2020) 10:1535. doi: 10.3389/fonc.2020.01535

35. Amit M, Na'ara S, Trejo-Leider L, Ramer N, Burstein D, Yue M, et al. Defining the surgical margins of adenoid cystic carcinoma and their impact on outcome: An international collaborative study. *Head Neck* (2017) 39:1008–14. doi: 10.1002/hed.24740

36. Mendenhall WM, Morris CG, Amdur RJ, Werning JW, Hinerman RW, Villaret DB. Radiotherapy alone or combined with surgery for adenoid cystic carcinoma of the head and neck. *Head Neck* (2004) 26:154–62. doi: 10.1002/hed.10380

37. Gebhardt BJ, Ohr JP, Ferris RL, Duvvuri U, Kim S, Johnson JT, et al. Concurrent chemoradiotherapy in the adjuvant treatment of high-risk primary salivary gland Malignancies. *Am J Clin Oncol* (2018) 41:888–93. doi: 10.1097/COC.0000000000000386

38. Geiger JL, Ismaila N, Beadle B, Caudell JJ, Chau N, Deschler D, et al. Management of salivary gland Malignancy: ASCO guideline. *J Clin Oncol* (2021) 39:1909–41. doi: 10.1200/JCO.21.00449

39. Amit M, Binenbaum Y, Trejo-Leider L, Sharma K, Ramer N, Ramer I, et al. International collaborative validation of intraneural invasion as a prognostic marker in adenoid cystic carcinoma of the head and neck. *Head Neck* (2015) 37:1038–45. doi: 10.1002/hed.23710

40. Hay AJ, Migliacci J, Karassawa Zanoni D, McGill M, Patel S and Ganly I. Minor salivary gland tumors of the head and neck-Memorial Sloan Kettering experience: Incidence and outcomes by site and histological type. *Cancer* (2019) 125:3354–66. doi: 10.1002/cncr.32208

41. Meulemans J VLC, Delaere P, Vranckx JJ, Vander Poorten V. New developments in surgery for Malignant salivary gland tumors. *Critical Issues Head Neck Oncol* (2023) 19:315–26. doi: 10.1007/978-3-031-23175-9_19

42. Bollig CA, Wang K, Llerena P, Puram SV, Pipkorn PJ, Jackson RS, et al. National analysis of oropharyngeal salivary gland Malignancies treated with transoral robotic surgery. *Otolaryngol Head Neck Surg* (2022) 166:886–93. doi: 10.1177/01945998211031161

43. Schoppy DW, Kupferman ME, Hessel AC, Bell DM, Garland EM, Damrose EJ, et al. Transoral endoscopic head and neck surgery (eHNS) for minor salivary gland tumors of the oropharynx. *Cancers Head Neck* (2017) 2:5. doi: 10.1186/s41199-017-0024-2

44. White H, Ford S, Bush B, Holsinger FC, Moore E, Ghanem T, et al. Salvage surgery for recurrent cancers of the oropharynx: comparing TORS with standard open surgical approaches. *JAMA Otolaryngol Head Neck Surg* (2013) 139:773–8. doi: 10.1001/jamaoto.2013.3866

45. Ferrari M, Zanoletti E, Taboni S, Cazzador D, Tealdo G, Schreiber A, et al. Resection of the internal carotid artery in selected patients affected by cancer of the skull base. *Head Neck* (2022) 44:1030–42. doi: 10.1002/hed.26967

46. Deganello A, Ferrari M, Paderno A, Turri-Zanoni M, Schreiber A, Mattavelli D, et al. Endoscopic-assisted maxillectomy: Operative technique and control of surgical margins. *Oral Oncol* (2019) 93:29–38. doi: 10.1016/j.oraloncology.2019.04.002

47. Deschler DG, Eisele DW. Surgery for primary Malignant parotid neoplasms. *Adv Otorhinolaryngol* (2016) 78:83–94. doi: 10.1159/000442128

48. Lombardi D, McGurk M, Vander Poorten V, Guzzo M, Accorona R, Rampinelli V, et al. Surgical treatment of salivary Malignant tumors. *Oral Oncol* (2017) 65:102–13. doi: 10.1016/j.oraloncology.2016.12.007

49. Olsen KD, Moore EJ. Deep lobe parotidectomy: clinical rationale in the management of primary and metastatic cancer. *Eur Arch Otorhinolaryngol* (2014) 271:1181–5. doi: 10.1007/s00405-013-2616-8

50. Olsen KD, Quer M, de Bree R, Vander Poorten V, Rinaldo A, Ferlito A. Deep lobe parotidectomy-why, when, and how? *Eur Arch Otorhinolaryngol* (2017) 274:4073–78. doi: 10.1007/s00405-017-4767-5

51. Chen AM, Granchi PJ, Garcia J, Bucci MK, Fu KK and Eisele DW. Local-regional recurrence after surgery without postoperative irradiation for carcinomas of the major salivary glands: implications for adjuvant therapy. *Int J Radiat Oncol Biol Phys* (2007) 67:982–7. doi: 10.1016/j.ijrobp.2006.10.043

52. Herman MP, Werning JW, Morris CG, Kirwan JM, Amdur RJ, Mendenhall WM. Elective neck management for high-grade salivary gland carcinoma. *Am J Otolaryngol* (2013) 34:205–8. doi: 10.1016/j.amjoto.2012.11.012

53. Kirkbride P, Liu FF, O'Sullivan B, Payne D, Warde P, Gullane P, et al. Outcome of curative management of Malignant tumours of the parotid gland. *J Otolaryngol* (2001) 30:271–9. doi: 10.2310/7070.2001.19527

54. Cho JK, Lim BW, Kim EH, Ko YH, Oh D, Noh JM, et al. Low-grade salivary gland cancers: treatment outcomes, extent of surgery and indications for postoperative

adjuvant radiation therapy. *Ann Surg Oncol* (2016) 23:4368–75. doi: 10.1245/s10434-016-5353-6

55. Zenga J, Parikh AS, Emerick KS, Lin DT, Faquin WC, Deschler DG. Close margins and adjuvant radiotherapy in acinic cell carcinoma of the parotid gland. *JAMA Otolaryngol Head Neck Surg* (2018) 144:1011–16. doi: 10.1001/jamaoto.2018.0788

56. Hanson M, McGill M, Mimica X, Eagan A, Hay A, Wu J, et al. Evaluation of surgical margin status in patients with salivary gland cancer. *JAMA Otolaryngol Head Neck Surg* (2022) 148:128–38. doi: 10.1001/jamaoto.2021.3459

57. Laramore GE, Krall JM, Griffin TW, Duncan W, Richter MP, Saroja KR, et al. Neutron versus photon irradiation for unresectable salivary gland tumors: final report of an RTOG-MRC randomized clinical trial. Radiation Therapy Oncology Group. Medical Research Council. *Int J Radiat Oncol Biol Phys* (1993) 27:235–40. doi: 10.1016/0360-3016(93)90233-l

58. Akbaba S, Ahmed D, Mock A, Held T, Bahadir S, Lang K, et al. Treatment outcome of 227 patients with sinonasal adenoid cystic carcinoma (ACC) after intensity modulated radiotherapy and active raster-scanning carbon ion boost: A 10-year single-center experience. *Cancers (Basel)* (2019) 11:1705. doi: 10.3390/cancers11111705

59. Hayashi K, Koto M, Demizu Y, Saitoh JI, Suefuji H, Okimoto T, et al. A retrospective multicenter study of carbon-ion radiotherapy for major salivary gland carcinomas: Subanalysis of J-CROS 1402 HN. *Cancer Sci* (2018) 109:1576–82. doi: 10.1111/cas.13558

60. Koto M, Demizu Y, Saitoh JI, Suefuji H, Tsuji H, Okimoto T, et al. Definitive carbon-ion radiation therapy for locally advanced sinonasal Malignant tumors: subgroup analysis of a multicenter study by the Japan carbon-ion radiation oncology study group (J-CROS). *Int J Radiat Oncol Biol Phys* (2018) 102:353–61. doi: 10.1016/j.ijrobp.2018.05.074

61. Akbaba S, Ahmed D, Lang K, Held T, Mattke M, Hoerner-Rieber J, et al. Results of a combination treatment with intensity modulated radiotherapy and active raster-scanning carbon ion boost for adenoid cystic carcinoma of the minor salivary glands of the nasopharynx. *Oral Oncol* (2019) 91:39–46. doi: 10.1016/j.oraloncology.2019.02.019

62. Akbaba S, Bostel T, Lang K, Bahadir S, Lipman D, Schmidberger H, et al. Large german multicenter experience on the treatment outcome of 207 patients with adenoid cystic carcinoma of the major salivary glands. *Front Oncol* (2020) 10:593379. doi: 10.3389/fonc.2020.593379

63. Jensen AD, Poulakis M, Nikoghosyan AV, Welzel T, Uhl M, Federspil PA, et al. High-LET radiotherapy for adenoid cystic carcinoma of the head and neck: 15 years' experience with raster-scanned carbon ion therapy. *Radiother Oncol* (2016) 118:272–80. doi: 10.1016/j.radonc.2015.05.010

64. Sulaiman NS, Demizu Y, Koto M, Saitoh JI, Suefuji H, Tsuji H, et al. Multicenter study of carbon-ion radiation therapy for adenoid cystic carcinoma of the head and neck: subanalysis of the Japan carbon-ion radiation oncology study group (J-CROS) study (1402 HN). *Int J Radiat Oncol Biol Phys* (2018) 100:639–46. doi: 10.1016/j.ijrobp.2017.11.010

65. De Roeck L, van der Weide HL, Eekers DBP, Kramer MC, Alapetite C, Blomstrand M, et al. The European Particle Therapy Network (EPTN) consensus on the follow-up of adult patients with brain and skull base tumours treated with photon or proton irradiation. *Radiother Oncol* (2022) 168:241–49. doi: 10.1016/j.radonc.2022.01.018

66. Morimoto K, Demizu Y, Hashimoto N, Mima M, Terashima K, Fujii O, et al. Particle radiotherapy using protons or carbon ions for unresectable locally advanced head and neck cancers with skull base invasion. *Jpn J Clin Oncol* (2014) 44:428–34. doi: 10.1093/jjco/hyu010

67. Linton OR, Moore MG, Brigance JS, Summerlin DJ, McDonald MW. Proton therapy for head and neck adenoid cystic carcinoma: initial clinical outcomes. *Head Neck* (2015) 37:117–24. doi: 10.1002/hed.23573

68. Pommier P, Liebsch NJ, Deschler DG, Lin DT, McIntyre JF, Barker FG2nd, et al. Proton beam radiation therapy for skull base adenoid cystic carcinoma. *Arch Otolaryngol Head Neck Surg* (2006) 132:1242–9. doi: 10.1001/archotol.132.11.1242

69. Vedrine PO, Thariat J, Merrot O, Percodani J, Dufour X, Choussy O, et al. Primary cancer of the sphenoid sinus–a GETTEC study. *Head Neck* (2009) 31:388–97. doi: 10.1002/hed.20966

70. Liang ZG, Kusumawidjaja G, Kazmi F, Wee JTS, Chua MLK. Intensity-modulated radiotherapy for paranasal sinuses and base of skull tumors. *Oral Oncol* (2018) 86:61–8. doi: 10.1016/j.oraloncology.2018.09.010

71. Vander Poorten V, Locati L, Licitra L. *Surgery for Malignant Parotid Tumors Salivary Gland Cancer*. Springer, Heidelberg, Germany (2019) p. 45–67.

72. Ali S, Palmer FL, DiLorenzo M, Shah JP, Patel SG and Ganly I. Treatment of the neck in carcinoma of the parotid gland. *Ann Surg Oncol* (2014) 21:3042–8. doi: 10.1245/s10434-014-3681-y

73. Warshavsky A, Rosen R, Muhanna N, Ungar O, Nard-Carmel N, Abergel A, et al. Rate of occult neck nodal metastasis in parotid cancer: A meta-analysis. *Ann Surg Oncol* (2021) 28:3664–71. doi: 10.1245/s10434-020-09331-7

74. NCCN. Head and neck. (2023). Available at: https://www.nccn.org/guidelines/guidelines-detail?category=1&id=1437

75. Chisholm EJ, Elmiyeh B, Dwivedi RC, Fisher C, Thway K, Kerawala C, et al. Anatomic distribution of cervical lymph node spread in parotid carcinoma. *Head Neck* (2011) 33:513–5. doi: 10.1002/hed.21479

76. Yoo SH, Roh JL, Kim SO, Cho KJ, Choi SH, Nam SY, et al. Patterns and treatment of neck metastases in patients with salivary gland cancers. *J Surg Oncol* (2015) 111:1000–6. doi: 10.1002/jso.23914

77. Aro K, Ho AS, Luu M, Kim S, Tighiouart M, Clair JM, et al. Development of a novel salivary gland cancer lymph node staging system. *Cancer* (2018) 124:3171–80. doi: 10.1002/cncr.31535

78. Guntinas-Lichius O, Thielker J, Robbins KT, Olsen KD, Shaha AR, Makitie AA, et al. Prognostic role of intraparotid lymph node metastasis in primary parotid cancer: Systematic review. *Head Neck* (2021) 43:997–1008. doi: 10.1002/hed.26541

79. Kouka M, Koehler B, Buentzel J, Kaftan H, Boeger D, Mueller AH, et al. Role of intraparotid and neck lymph node metastasis in primary parotid cancer surgery: A population-based analysis. *Cancers (Basel)* (2022) 14:2822. doi: 10.3390/cancers14122822

80. Laurie SA, Licitra L. Systemic therapy in the palliative management of advanced salivary gland cancers. *J Clin Oncol* (2006) 24:2673–8. doi: 10.1200/JCO.2005.05.3025

81. Ferrarotto R, Heymach JV. Taking it up a NOTCH: a novel subgroup of ACC is identified. *Oncotarget* (2017) 8:81725–26. doi: 10.18632/oncotarget.20879

82. Ferrarotto R, Mitani Y, Diao L, Guijarro I, Wang J, Zweidler-McKay P, et al. Activating NOTCH1 mutations define a distinct subgroup of patients with adenoid cystic carcinoma who have poor prognosis, propensity to bone and liver metastasis, and potential responsiveness to notch1 inhibitors. *J Clin Oncol* (2017) 35:352–60. doi: 10.1200/JCO.2016.67.5264

83. Ferrarotto R, Mitani Y, McGrail DJ, Li K, Karpinets TV, Bell D, et al. Proteogenomic analysis of salivary adenoid cystic carcinomas defines molecular subtypes and identifies therapeutic targets. *Clin Cancer Res* (2021) 27:852–64. doi: 10.1158/1078-0432.CCR-20-1192

84. Ferrarotto R, Eckhardt G, Patnaik A, LoRusso P, Faoro L, Heymach JV, et al. A phase I dose-escalation and dose-expansion study of brontictuzumab in subjects with selected solid tumors. *Ann Oncol* (2018) 29:1561–68. doi: 10.1093/annonc/mdy171

85. Carter J. PRMT5 inhibition downregulates MYB and NOTCH1 signaling, key molecular drivers of adenoid cystic carcinoma. *Cancer Res* (2021) 81 (13_Supplement):1138. doi: 10.1158/1538-7445.AM2021-1138

86. Ferrarotto R. 1789P - The gamma secretase inhibitor AL101 combined with other drugs for dual targeting of Notch dysregulated tumors. *Ann Oncol* (2021) 32: S1222. doi: 10.1016/j.annonc.2021.08.1732

87. Ferrarotto R. Results of ACCURACY: A phase 2 trial of AL101, a selective gamma secretase inhibitor, in subjects with recurrent/metastatic (R/M) adenoid cystic carcinoma (ACC) harboring Notch activating mutations (Notchmut). *J Clin Oncol* (2022) 40:6046. doi: 10.1200/JCO.2022.40.16_suppl.6046

88. Humtsoe JO, Kim HS, Leonard B, Ling S, Keam B, Marchionni L, et al. Newly identified members of FGFR1 splice variants engage in cross-talk with AXL/AKT axis in salivary adenoid cystic carcinoma. *Cancer Res* (2021) 81:1001–13. doi: 10.1158/0008-5472.CAN-20-1780

89. Wolber P, Nachtsheim L, Hoffmann F, Klussmann JP, Meyer M, von Eggeling F, et al. Trophoblast cell surface antigen 2 (Trop-2) protein is highly expressed in salivary gland carcinomas and represents a potential therapeutic target. *Head Neck Pathol* (2021) 15:1147–55. doi: 10.1007/s12105-021-01325-5

90. Guimaraes de Sousa L NF, McGrail DJ, Li K, Marques-Piubelli ML, Ferri Borgogno S, Dai H, et al. Single-cell immune mapping of adenoid cystic carcinoma (ACC) reveals potential therapeutic targets for the aggressive solid subtype. *J Clin Oncol* (2022) 40:6090. doi: 10.1200/JCO.2022.40.16_suppl.6090

91. Ferrarotto R, Sousa LG, Feng L, Mott F, Blumenschein G, Altan M, et al. Phase II clinical trial of axitinib and avelumab in patients with recurrent/metastatic adenoid cystic carcinoma. *J Clin Oncol* (2023) 41:2843–51. doi: 10.1200/JCO.22.02221

92. Cavalieri S, Platini F, Bergamini C, Resteghini C, Galbiati D, Bossi P, et al. Genomics in non-adenoid cystic group of salivary gland cancers: one or more druggable entities? *Expert Opin Investig Drugs* (2019) 28:435–43. doi: 10.1080/13543784.2019.1598376

93. Haddad R, Colevas AD, Krane JF, Cooper D, Glisson B, Amrein PC, et al. Herceptin in patients with advanced or metastatic salivary gland carcinomas. A phase II study. *Oral Oncol* (2003) 39:724–7. doi: 10.1016/s1368-8375(03)00097-6

94. Takahashi H, Tada Y, Saotome T, Akazawa K, Ojiri H, Fushimi C, et al. Phase II trial of trastuzumab and docetaxel in patients with human epidermal growth factor receptor 2-positive salivary duct carcinoma. *J Clin Oncol* (2019) 37:125–34. doi: 10.1200/JCO.18.00545

95. Di Villeneuve L, Souza IL, Tolentino FDS, Ferrarotto R, Schvartsman G. Salivary gland carcinoma: novel targets to overcome treatment resistance in advanced disease. *Front Oncol* (2020) 10:580141. doi: 10.3389/fonc.2020.580141

96. Drilon A, Li G, Dogan S, Gounder M, Shen R, Arcila M, et al. What hides behind the MASC: clinical response and acquired resistance to entrectinib after ETV6-NTRK3 identification in a mammary analogue secretory carcinoma (MASC). *Ann Oncol* (2016) 27:920–6. doi: 10.1093/annonc/mdw042

97. Le X, Baik C, Bauman J, Gilbert J, Brose MS, Grilley-Olson JE, et al. Larotrectinib treatment for patients with TRK fusion-positive salivary gland cancers. *Oncologist* (2022), oyac080. doi: 10.1093/oncolo/oyac080

98. Imamura Y, Kiyota N, Tahara M, Hanai N, Asakage T, Matsuura K, et al. Systemic therapy for salivary gland Malignancy: current status and future perspectives. *Jpn J Clin Oncol* (2022) 52:293–302. doi: 10.1093/jjco/hyac008

99. Linxweiler M, Kuo F, Katabi N, Lee M, Nadeem Z, Dalin MG, et al. The immune microenvironment and neoantigen landscape of aggressive salivary gland carcinomas

differ by subtype. *Clin Cancer Res* (2020) 26:2859–70. doi: 10.1158/1078-0432.CCR-19-3758

100. Cohen RB, Delord JP, Doi T, Piha-Paul SA, Liu SV, Gilbert J, et al. Pembrolizumab for the treatment of advanced salivary gland carcinoma: findings of the phase 1b KEYNOTE-028 study. *Am J Clin Oncol* (2018) 41:1083–88. doi: 10.1097/COC.0000000000000429

101. Fayette J, Even C, Digue L, Geoffrois L, Rolland F, Cupissol D, et al. NISCAHN: A phase II, multicenter nonrandomized trial aiming at evaluating nivolumab (N) in two cohorts of patients (pts) with recurrent/metastatic (R/M) salivary gland carcinoma of the head and neck (SGCHN), on behalf of the Unicancer Head & Neck Group. *J Clin Oncol* (2019) 37:6083. doi: 10.1200/JCO.2019.37.15_suppl.6083

102. Even C, Delord JP, Price KA, Nakagawa K, Oh DY, Burge M, et al. Evaluation of pembrolizumab monotherapy in patients with previously treated advanced salivary gland carcinoma in the phase 2 KEYNOTE-158 study. *Eur J Cancer* (2022) 171:259–68. doi: 10.1016/j.ejca.2022.05.007

103. Niwa K, Kawakita D, Nagao T, Takahashi H, Saotome T, Okazaki M, et al. Multicentre, retrospective study of the efficacy and safety of nivolumab for recurrent and metastatic salivary gland carcinoma. *Sci Rep* (2020) 10:16988. doi: 10.1038/s41598-020-73965-6

104. Vos JL, Burman B, Jain S, Fitzgerald CWR, Sherman EJ, Dunn LA, et al. Nivolumab plus ipilimumab in advanced salivary gland cancer: a phase 2 trial. *Nat Med* (2023). doi: 10.1038/s41591-023-02518-x

105. Kurzrock R, Bowles DW, Kang H, Meric-Bernstam F, Hainsworth J, Spigel DR, et al. Targeted therapy for advanced salivary gland carcinoma based on molecular profiling: results from MyPathway, a phase IIa multiple basket study. *Ann Oncol* (2020) 31:412–21. doi: 10.1016/j.annonc.2019.11.018

frontiers | Frontiers in Oncology

TYPE Original Research
PUBLISHED 14 November 2023
DOI 10.3389/fonc.2023.1229493

OPEN ACCESS

EDITED BY
Andreas Mock,
National Center for Tumor Diseases Heidelberg (NCT), Germany

REVIEWED BY
Paris Liokatis,
LMU Munich University Hospital, Germany
Han-Sin Jeong,
Sungkyunkwan University, Republic of Korea

*CORRESPONDENCE
Lei Wang
wanglei03029114@163.com

RECEIVED 26 May 2023
ACCEPTED 27 October 2023
PUBLISHED 14 November 2023

CITATION
Wang L and Shi W (2023) Metastatic lymph node burden impacts overall survival in submandibular gland cancer.
Front. Oncol. 13:1229493.
doi: 10.3389/fonc.2023.1229493

Metastatic lymph node burden impacts overall survival in submandibular gland cancer

Lei Wang[1,2]* and Weihong Shi[1,2]

[1]Department of Stomatology, The Third Affiliated Hospital of Xinxiang Medical University, Xinxiang, China, [2]Department of Oral Medicine, School of Stomatology, Xinxiang Medical University, Xinxiang, China

Objective: To assess the effect of the number of positive lymph nodes (LNs) on the overall survival (OS) of patients with submandibular gland cancer (SmGC).

Methods: Patients who had undergone neck dissection for SmGC were retrospectively enrolled in this study. The effect of the American Joint Committee on Cancer (AJCC) N stage, the number of positive LNs, LN size, LN ratio, and extranodal extension (ENE) on OS and recurrence-free survival (RFS) was evaluated using Cox analysis. Prognostic models were proposed based on the identified significant variable, and their performance was compared using hazard consistency and discrimination.

Results: In total, 129 patients were included in this study. The number of positive LNs rather than LN ratio, LN size, and ENE was associated with OS. A prognostic model based on the number of positive LNs (0 vs. 1–2 vs. 3+) demonstrated a higher likelihood ratio and Harrell's C index than those according to the 7th/8th edition of the AJCC N stage in predicting OS and RFS.

Conclusions: The effect of LN metastasis on OS and RFS was mainly determined by the number of positive LNs. A validation of this finding is warranted in adenoid cystic carcinomas that were not included in this study.

KEYWORDS

submandibular gland cancer, overall survival, AJCC stage, lymph node metastasis, number of positive lymph nodes

Introduction

Salivary gland cancer, which accounts for approximately 3–5% of all head and neck cancers, is a relatively uncommon malignancy (1). Neck stage is an important factor that affects disease progression. It is determined by the 8th American Joint Committee on Cancer (AJCC) classification, and it is formulated based on head and neck squamous cell carcinoma (2). However, the two types of tumors show distinct differences in biological

behavior (3), which leads to the question of whether the direct application of this classification in salivary gland cancer is possible.

Current literature has proposed alternative lymph node (LN) evaluation methods in patients with salivary gland cancer. Among these methods, the number of positive LNs and extranodal extension (ENE) have shown the greatest potential (4–8). A four-category N stage based on the number of positive LNs (0 vs. 1–2 vs. 3–21 vs. 22+) was proposed by Aro et al. (4). This system provides excellent survival stratification across all histologic types. Similarly, a three-category N stage based on the number of positive LNs and ENE was introduced by Lee et al. (5). This system was superior to the AJCC N stage, enabling a more precise prognostic stratification. Similar results have also been confirmed in other studies (6–8). However, although the two subgroups have apparent differences in proportions and disease prognosis, the origin of cancer from the submandibular and parotid glands was analyzed as one variable in these studies (9). The presence of an additional lymphatic drainage pathway and positive parotid LN in parotid cancer, but no neck LN metastasis, decreases disease control (10). Thus, the relationship of these two factors to the prognosis of submandibular gland cancers (SmGCs) remains unclear.

Therefore, the current study aimed to assess the prognostic significance of LN metastasis burden and ENE in SmGCs.

Methods

This study was approved by the Xinxiang Medical University Institutional Research Committee (No. CR2021670), and written consent was obtained from all patients before the initial treatment. The study was conducted according to the tenets of the Declaration of Helsinki.

Study design

The medical records of patients who underwent surgical treatment for SmGCs between January 2000 and December 2022 were retrospectively reviewed. The inclusion criteria were as follows: the disease was primary; neck dissection had been performed; the number of LNs examined was ≥10; and the follow-up data could be obtained via outpatient follow-ups, WeChat, email, telephone, or letters. The demographic characteristics, pathology, treatment, and follow-up information were also collected.

Study variables

All histopathologic sections were reassessed by two head and neck pathologists to confirm the diagnosis. The tumor and neck stages were graded according to the 7th/8th edition of the AJCC classification. The histologic grade was classified as low, intermediate, and high based on the 5th edition of the World Health Organization Classification of salivary gland tumors. Perineural invasion (PNI) was considered positive if tumor cells entailed either proper perineural or intraneural invasion. Lymphovascular invasion (LVI) was considered positive if tumor cells were present within a lymphovascular vessel. ENE was considered positive if tumor cells were present outside the capsule of the metastatic LN. LN size was defined as the largest diameter of metastatic LNs.

The primary outcome evaluated in this study was the overall survival (OS). The secondary outcome was the recurrence-free survival (RFS). OS time was calculated from the date of surgery to the date of death or the last follow-up; this was censored at 60 months if the duration was longer than five years. RFS time was calculated from the date of surgery to the date of first recurrence or the last follow-up and was censored at 60 months if the duration was longer than five years.

Treatment principle

Frozen sections of the submandibular gland tumor were obtained routinely in cases where a malignant neoplasm was suspected. Therapeutic neck dissection was performed in cases with pathological or clinically positive LNs. Prophylactic neck dissection was performed in cases with a T3/4 tumor, surrounding tissue invasion, or other adverse features. The extent of neck dissection included at least ipsilateral levels I–III.

Statistical analysis

The association between the clinicopathologic factors and OS was initially evaluated using univariate analysis. The factors identified as significant in univariate analysis were then assessed using the Cox model. The hazard ratio (HR) of the number of positive LNs, which was assessed as 0 vs. 1 vs. 2 vs. 3 vs. 4+, was calculated to distinguish the effect of different LN metastasis burdens on OS. Subsequently, the optimal cut-off was determined by using binary recursive partitioning analysis (RPA).

Four Cox regression models were constructed during the second analysis. Hazard consistency and discrimination were used to evaluate the two models. Hazard consistency referred to the homogeneity of patients within the same subgroup with similar outcomes; this was reflected by the likelihood ratio. A value of > 0.5 indicated good hazard consistency. On the other hand, hazard discrimination referred to the difference in outcomes between patients of different subgroups with demonstrably different outcomes. It was reflected by Harrell's C-concordance index. A higher hazard discrimination value indicated better discrimination.

OS and RFS were analyzed using the Kaplan-Meier method and compared using the log-rank test. All analyses were performed using R 3.4.3 (R Core Tea, Vienna, Austria). A p-value0.05 was considered statistically significant.

Results

Baseline data

In total, 129 patients (56 men and 73 women; mean age: 48 ± 18 years) were included in this study. The tumor stage was T1 in 15 patients, T2 in 36 patients, T3 in 54 patients, and T4 in 24 patients. The 8th edition of the AJCC N stage was N0 in 59 patients, N1 in 31 patients, N2 in 26 patients, and N3 in 13 patients. The 7th edition of the AJCC N stage was N0 in 59 patients, N1 in 35, N2 in 24, and N3 in 11 patients. ENE was observed in 15 patients, PNI in 27 patients, and LVI in 24 patients. Positive margins were observed in five patients. The most common histopathologic type observed was mucoepidermoid carcinoma (MEC; n=84), followed by myoepithelial carcinoma (n=20) (Table 1; Supplementary Table 1). The histologic grade was low in 17 patients, intermediate in 75, and high in 37.

Beyond levels I–III, level IV was dissected in 77 patients. Among these patients, level V was resected in 18 patients. The median and mean number of examined LNs were 29 (range: 11–46) and 28 ± 10, respectively. Among the patients with metastatic disease, 31 had one positive LN, 20 had two positive LNs, 13 had three positive LNs, and 6 had four or more positive LNs. The mean number of positive LNs was 1.9 ± 1.0.

Adjuvant radiotherapy was performed in 87 patients with a median dose of 56 Gy. Among these patients, 28 patients also received adjuvant chemotherapy. The median follow-up duration was 5.3 (range: 0.2–17) years. Forty patients died during the study period; 29 deaths among these were caused by the disease.

Univariate analysis

In the univariate analysis, tumor stage, the 7th and 8th neck stages, histologic grade, PNI, positive margin, the ratio of positive to total LNs, and treatment were statistically related to OS (Log-rank test, all $p<0.05$). In contrast, ENE, nodal yield, and level involvement type had no significant effect on OS (Log-rank test, p=0.107, p=0.692, and p=0.554, respectively) (Table 2).

TABLE 1 Histologic type distribution of submandibular gland cancer.

Cancer type	N
High grade (n=37)	
Mucoepidermoid carcinoma	22
Duct carcinoma	10
Adenocarcinoma not otherwise specified	5
Intermediate grade (n=75)	
Mucoepidermoid carcinoma	55
Myoepithelial carcinoma	20
Low grade (n=17)	
Mucoepidermoid carcinoma	7
Acinic cell carcinoma	5
Pleomorphic low-grade adenocarcinoma	3
Basal cell carcinoma	1
Epithelial-myoepithelial carcinoma	1

Prognostic model construction

In multivariate model 1, tumor stage, histologic grade, PNI, positive margin, and treatment were included. The number of positive LNs was associated with OS in the univariate analysis (Figure 1C). In the Cox analysis, compared with no LN metastasis, the presence of one and two metastatic LNs showed an HR of 1.89, 95% CI [1.22–3.47] and 2.02 [1.47–5.79], respectively, groups of three and four or more positive LNs had an HR of 4.78 [2.16–10.33] and 5.0 [2.33–18.17], respectively, it is likely that OS decreased with the increase of metastatic LN burden (Table 3). Other independent factors included stage T3/4 (2.87 [1.34–5.67], p=0.011; 4.29 [1.91–18.12], p<0.001), high histologic grade (3.18 [1.33–17.58], p<0.001), and positive margin (5.18 [2.02–18.38], p<0.001).

After RPA analysis, additional subgroups based on the number of metastatic LNs were formulated (model 2; 0 vs. 1–2 vs. 3+). The three subgroups had significantly different OS rates in the univariate analysis (Figure 1D). Multivariate model 2 revealed that compared with the no metastasis group, the groups of 1–2 and 3+ positive LNs had a HR of 1.99, 95% CI [1.35–4.26] and 4.98 [2.31–16.99]. The two subgroups also had statistically significant differences in terms of the impact on prognosis indicated by HRs (Table 3). Other independent factors included stage T3/4 (3.91 [1.58–8.43], p=0.001/6.806 [3.12–20.73], p<0.001), high histologic grade (5.02 [2.01–18.33], p<0.001), PNI (2.12 [1.47–4.87], p=0.028), and positive margin (4.08 [2.13–9.05], p<0.001). This model demonstrated a likelihood ratio of 0.574 and a Harrell's C index of 0.703.

Comparison with the AJCC N stage

Based on the univariate analysis, a multivariate model 3 including tumor stage, neck stage defined by the 7th AJCC neck stage, histologic grade, PNI, positive margin, and treatment was constructed to assess the reliability of the 7th edition of the AJCC N stage in predicting OS. Compared with the N0 stage, LN metastasis significantly decreased the OS. However, the HRs of N2 (4.21 [1.90–12.64]) and N3 (4.38 95% CI [2.05–15.38]) were comparably high (Figure 1B; Table 3). Other independent factors included stage T3/4 (2.33 [1.28–5.44], p=0.016/4.39 [2.12-8.36], p<0.001), high histologic grade (3.22 [1.81–9.13], p<0.001), PNI (1.98 [1.22–3.23], p=0.011), and positive margin (5.30 [2.11–16.15], p<0.001). This model demonstrated a likelihood ratio of 0.427 and a Harrell's C index of 0.689.

Another multivariate model 4 was developed to evaluate the reliability of the 8th edition of the AJCC N stage. Compared with the N0 stage, N1 (HR 1.80 95%CI [0.83–3.33]) disease did not significantly alter the OS, and the negative impact of LN metastasis did not occur until the development of N2 (6.38 [2.78–15.37]) disease. The groups of N2 and N3 had analogous HRs (Figure 1A;

TABLE 2 Univariate analysis of predictors for overall survival in submandibular gland cancers.

Factors	p	HR[95%CI]
Age (<50/≥ 50)	0.328	2.87[0.78-6.39]
Sex (Male/female)	0.113	2.16[0.35-20.53]
Tumor stage		
T1		ref
T2	0.432	1.90[0.64-4.28]
T3	0.024	2.35 [1.28-7.69]
T4	<0.001	3.17[1.45-9.24]
7th Neck stage		
N0		ref
N1	0.327	1.90 [0.87-4.67]
N2	0.011	2.89 [1.45-8.73]
N3	<0.001	4.07[1.90-10.37]
Extranodal extension	0.107	3.11[0.85-18.22]
8th Neck stage		
N0		ref
N1	0.425	1.88 [0.69-6.14]
N2	0.010	2.26 [1.37-9.52]
N3	<0.001	4.67[1.66-11.53]
Number of positive lymph nodes		
0		ref
1	0.043	1.86 [1.36-6.48]
2	0.028	2.13 [1.44-8.19]
3	<0.001	4.38 [1.80-10.67]
4+	<0.001	5.39 [2.11-15.26]
Number of positive lymph nodes		
0		ref
1-2	0.034	2.05 [1.42-7.59]
3+	<0.001	5.00 [1.94-14.32]
Pathologic type (Mucoepidermoid cancer/others)	0.489	2.10[0.50-8.66]
Histologic grade		
Low		ref
Intermediate	0.111	2.90 [0.62-13.27]
High	<0.001	6.29[2.01-17.63]
Perineural invasion	0.016	2.97[1.45-8.17]
Lymphovascular invasion	0.247	3.03[0.75-7.26]
Positive margin	0.037	4.17[1.56-8.99]
Level involvement type (I-III/IV-V)	0.554	2.88[0.64-8.22]
Nodal yield (~29/29+)	0.692	3.16[0.42-18.57]
Treatment*		
S		ref
S+R	0.135	1.89 [0.45-7.62]
S+R+C	0.036	2.18[1.26-7.90]

(Continued)

TABLE 2 Continued

* S, surgery; R, radiotherapy; C, chemotherapy.

Table 3). Other independent factors included stage T3/4 (2.52 [1.32–6.18], p=0.017/4.30 [2.01–8.75], p<0.001), high histologic grade (4.23 [1.99–10.43], p<0.001), PNI (2.12 [1.33–6.44], p=0.031), and positive margin (7.33 [2.67–17.44], p<0.001). This model demonstrated a likelihood ratio of 0.401 and a Harrell's C index of 0.671.

Both models had inferior likelihood ratios and Harrell's C indices compared with the model based on the number of metastatic LNs (0 vs. 1–2 vs. 3+).

Second outcome variable analysis

RFS was an essential supplement to OS for prognosis evaluation. All the 7th and 8th AJCC N stages, and LN metastasis burden exhibited a significant impact on RFS (Figure 2) (Log-rank test, all with p<0.001). Still, prognostic model based on the number of metastatic LNs (0 vs. 1–2 vs. 3+) showed a likelihood ratio of 0.543 and a Harrell's C index of 0.689, it was superior to those in models according to the the 7th (likelihood ratio: 0.468; Harrell's C index: 0.674) and 8th (likelihood ratio: 0.453; Harrell's C index: 0.645) AJCC N stages.

Discussion

The most valuable finding in the current study was that the number of metastatic LNs offered better OS stratification than the 7th and 8th editions of the AJCC N stage, it could provide additional information while screening real patients at high risk of mortality.

Neck status is an important prognostic factor as mentioned, and the survival rate could decrease by half even with only one metastatic LN (11, 12). The 7th edition of the AJCC N stage evaluated the number, size, and laterality of positive LNs. In contrast, ENE was considered in the 8th edition of the AJCC N stage (2). Although both stages were formulated based on head and neck squamous cell carcinoma (3), the occurrence of contralateral neck LN metastasis in major salivary gland cancer was very uncommon, and the prognostic significance of ENE has remained controversial (13–15). Therefore, some scholars aimed to develop other alternative N stages. Aro et al. (4) were the first to uncover the phenomenon and enrolled 4520 cases of salivary gland cancers in their study. It was observed that OS worsened without plateauing as the number of metastatic LNs increased. The mortality risk was obvious for those with up to four LNs and then gradually stabilized in those with additional LNs> 4.

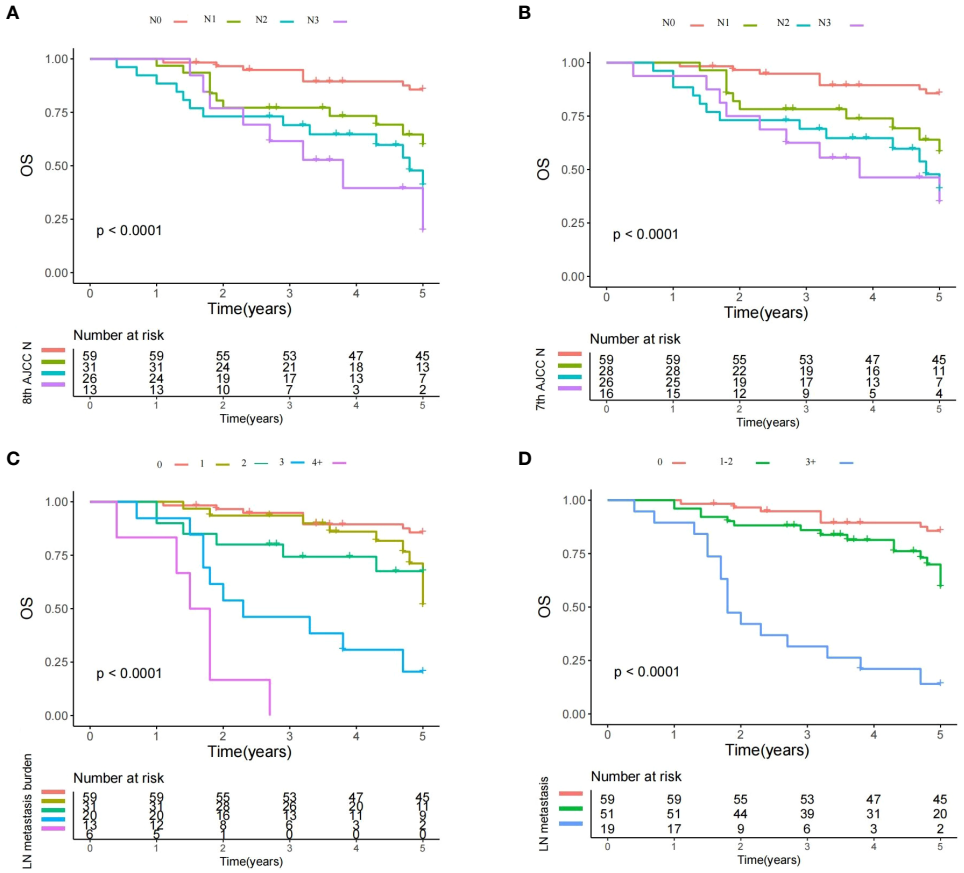

FIGURE 1
Overall survival plots of different lymph node (LN) status. **(A)** Survival plot for the 8th AJCC N stage: a significant difference existed among the N0, N1, N2, and N3 groups (Log-rank test, p<0.001); **(B)** Survival plot for the 7th AJCC N stage: a significant difference existed among the N0, N1, N2, and N3 groups (Log-rank test, p<0.001); **(C)** Survival plot for the LN metastasis burden: significant difference existed among groups with different metastatic burden (Log-rank test, p<0.001); and **(D)** Survival plot for different number of metastatic LNs: significant difference existed among the different subgroups (Log-rank test, p<0.001).

Aro et al. might be the first to demonstrate a new LN assessment method based on the number of metastatic LNs (0 vs. 1-2 vs. 3-21 vs. ≥22), its prognostic model exhibited greater accuracy than the 8th edition of the AJCC N stage in predicting OS (4). Lombardi et al. (8) introduced three novel N-classifications according to the number of metastatic nodes (0 vs. 1–3 vs. ≥ 4) and/or their maximum diameter (<20 mm vs. ≥ 20 mm) that showed better performance in OS stratification. Lin et al. (14) showed a three-category LN evaluation method of 1 vs. 2-7 vs. 8+ metastatic LNs exhibited better DSS and OS predictive efficacy than AJCC N stage based on 895 patients with T-4N-3M0 parotid gland carcinoma. Han et al. (15) compared the prognostic value of three models according to the number of metastatic LNs, and found neck classification of 0/1 vs. 2-4 vs. 5+ positive LNs had the best survival prediction in 1689 parotid adenoid cystic cancer patients. Elhusseiny et al. (16) reported that >4 metastatic LNs were associated with worse survival in major salivary gland cancer. Although these studies confirmed the effect of the number of positive LNs on survival in salivary gland cancer, SmGC was not included for analysis (14, 15), or SmGC only accounted for a very small proportion (less than 10%) of this sample size (4, 8, 16). The two main differences, intraglandular LN presence and surgical strategy, between the parotid and submandibular glands, led to the necessity of validating the impact of the number of positive LNs on SmGC.

We noted that the impact was mainly influenced by the number of positive LNs rather than the ratio of positive to total examined LNs or LN size or level involvement type in SmGC. This finding is significant in that it revealed the inadequacy of the AJCC N stage as the presence of one positive LN could indicate N1, N2, or N3 stage in the AJCC N stage; however, patients with one metastatic LN had comparable OS independent of other LN factors. In addition, this study provided the underlying mechanism for explaining the superiority of prognostic model based on the number of metastatic LNs with a higher likelihood ratio and Harrell's C index.

Nevertheless, conflicted results have been reported by other studies. Cho et al. (17) analyzed the outcome of 99 patients with SmGC. They reported that the ratio of positive to total LNs> 0.15 was related to a nearly 3-fold or higher increase in the risk of locoregional recurrence, distant metastasis, and death. Level IV/V metastasis tended to promote distant metastasis or disease recurrence. However, the authors did not provide the data of the

TABLE 3 Prognostic model construction based on different lymph node (LN) evaluation methods.

Multivariate analysis	p	HR [95%CI]
Model 1		
Number of metastatic LNs		
0		ref
1	0.015	1.89 [1.22-3.47]
2	0.003	2.02 [1.47-5.79]
3	<0.001	4.78 [2.16-10.33]
4+	<0.001	5.0 [2.33-18.17]
Tumor stage		
T1		ref
T2	0.244	1.90 [0.76-5.33]
T3	0.011	2.87 [1.34-5.67]
T4	<0.001	4.29 [1.91-18.12]
Histologic grade		
Low		ref
Intermediate	0.117	2.52 [0.54-12.11]
High	<0.001	3.18 [1.33-17.58]
PNI[&]	0.327	2.08 [0.75-8.31]
Positive margin	<0.001	3.18 [1.33-17.58]
Treatment*		
S		ref
S+R	0.522	1.94 [0.57-6.13]
S+R+C	0.275	3.06[0.64-15.43]
Model 2		
Number of metastatic LNs		
0		ref
1-2	0.002	1.99[1.35-4.26]
3+	<0.001	4.98[2.31-16.99]
Tumor stage		
T1		ref
T2	0.278	2.19[0.73-6.16]
T3	0.001	3.91 [1.58-8.43]
T4	<0.001	6.806 [3.12-20.73]
Histologic grade		
Low		ref
Intermediate	0.221	2.08[0.72-12.74]
High	<0.001	5.02 [2.01-18.33]
PNI	0.028	2.12 [1.47-4.87]
Positive margin	<0.001	4.08 [2.13-9.05]
Treatment		
S		ref
S+R	0.517	3.21[0.73-17.22]
S+R+C	0.367	4.05[0.62-20.18]
Model 3		
AJCC 7th N stage		
N0		ref
N1	0.023	1.78 [1.25-4.02]
N2	<0.001	4.21 [1.90-12.64]
N3	<0.001	4.38 [2.05-15.38]
Tumor stage		
T1		ref
T2	0.175	1.99 [0.82-4.57]
T3	0.016	2.33 [1.28-5.44]
T4	<0.001	4.39 [2.12-8.36]
Histologic grade		
Low		ref
Intermediate	0.190	2.04 [0.69-7.43]
High	<0.001	3.22 [1.81-9.13]
PNI	0.011	1.98 [1.22-3.23]
Positive margin	<0.001	5.30 [2.11-16.15]
Treatment		
S		ref
S+R	0.326	2.45 [0.74-6.38]
S+R+C	0.222	3.26 [0.62-9.00]
Model 4		
AJCC 8th N stage		
N0		ref
N1	0.125	1.80[0.825-3.33]
N2	<0.001	6.38 [2.11-17.62]
N3	<0.001	6.77 [2.78-15.37]
Tumor stage		
T1		ref
T2	0.275	1.98 [0.61-5.38]
T3	0.017	2.52 [1.32-6.18]
T4	<0.001	4.30 [2.01-8.75]

TABLE 3 Continued

Multivariate analysis	p	HR [95%CI]
Histologic grade		
Low		ref
Intermediate	0.523	3.21 [0.43-8.15]
High	<0.001	4.23 [1.99-10.43]
PNI	0.031	2.12 [1.33-6.44]
Positive margin	<0.001	7.33 [2.67-17.44]
Treatment		
S		ref
S+R	0.633	3.17 [0.73-8.13]
S+R+C	0.524	4.05 [0.62-10.08]

* S, surgery; R, radiotherapy; C, chemotherapy.
& PNI, Perineural invasion.

least number of required examined LNs, which prevented further clinical application. Shi et al. (18) divided 376 patients with major salivary gland cancer into three groups: extent 1 referred to level I or parotid LN metastasis, extent 2 referred to level II–IV metastasis, and extent 3 referred to level V or bilateral or rare LN metastasis. Cox analysis revealed clear OS curve separation, whereas the AJCC N classification failed to discriminate the prognosis of the N1 and N2 groups. If the two variables were incorporated into the same Cox analysis, the former would remain an independent prognostic factor, whereas the AJCC N classification would lose significance. We failed to validate the association between the level involvement type and OS, and the difference was partially explained by different inclusion criteria. Unfortunately, no more similar literature was available for comparison.

ENE is another critical prognostic factor that is usually a reliable indicator for the requirement of adjuvant chemotherapy and poor prognosis in patients with head and neck squamous cell carcinoma (19). However, its role in salivary gland cancer has not been studied,

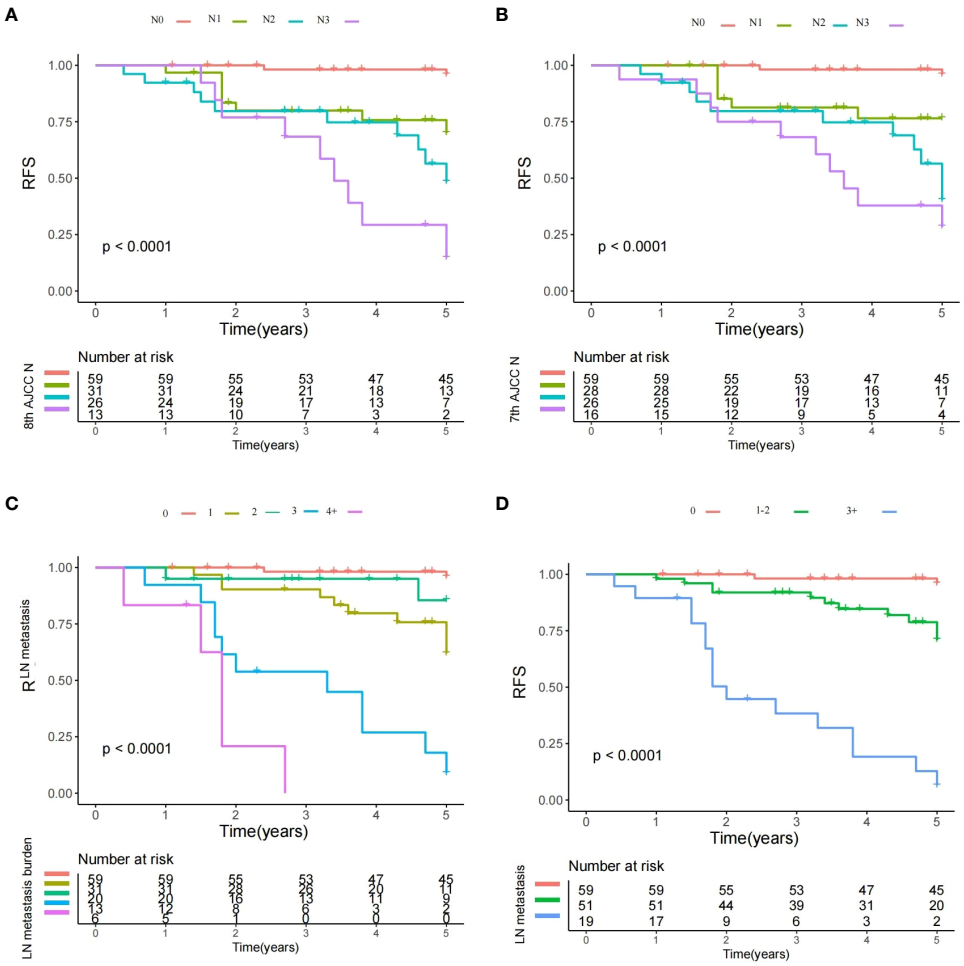

FIGURE 2
Recurrence-free survival plots of different lymph node (LN) status. **(A)** Survival plot for the 8th AJCC N stage: significant difference existed among the N0, N1, N2, and N3 groups (Log-rank test, p<0.001); **(B)** Survival plot for the 7th AJCC N stage: significant difference existed among the N0, N1, N2, and N3 groups (Log-rank test, p<0.001); **(C)** Survival plot for the LN metastasis burden: significant difference existed among groups with different metastatic burden (Log-rank test, p<0.001); and **(D)** Survival plot for different number of metastatic LNs: significant difference existed among the different subgroups (Log-rank test, p<0.001).

and the reported conclusions were contradictory. Lee et al. (5) reported both LN+ number and ENE were independently associated with OS and that the effect of ENE was comparable with that of two or more positive LNs. Their proposed N stage (N0: 0 LN+; N1: 1 LN+; N2: ≥2 LN+ or ENE) had better OS prediction than the 7th/8th edition of the AJCC N staging. However, in a study by Hsieh et al. (13), 51% of the sample developed ENE and had a higher possibility of the incidence of advanced N stage and a greater number of positive LNs, LVI, and PNI. Nevertheless, the OS was like that of those without ENE after adjusting for the number of positive LNs. Comparable results were also described by other authors and us (4, 7, 8, 10, 17), which elucidated that ENE in salivary gland cancer might not demonstrate any influence on survival but was correlated directly with adverse pathologic features that affected the prognosis (10). Thus, the further discussion of the current AJCC N stage and the superiority of our prognostic model based on LN metastasis burden were emphasized.

The current study had some limitations that must be acknowledged. First, there was inherent bias due to the retrospective design of the study. Second, our findings were based on a single constitution; thus, external validation is required before clinical application. Lastly, we did not enroll patients with adenoid cystic carcinoma; hence, it remained unknown whether the finding was suitable for other salivary gland cancers.

In summary, LN metastasis significantly affected OS in SmGC, and the impact was mainly determined by the number of positive LNs rather than other LN factors. A validation of this finding is warranted in adenoid cystic carcinomas that were not included in this study.

Data availability statement

The original contributions presented in the study are included in the article/Supplementary Material. Further inquiries can be directed to the corresponding author.

Ethics statement

The studies involving humans was approved by Xinxiang Medical University Institutional Research Committee. The studies were conducted in accordance with the local legislation and institutional requirements. The participants provided their written informed consent to participate in this study. Written informed consent was obtained from the individual(s) for the publication of any potentially identifiable images or data included in this article.

Author contributions

The authors made all the contributions: study design, manuscript writing, selection of studies and study quality evaluation, data analysis, and the revision of the manuscript. All authors contributed to the article and approved the submitted version.

Funding

The author(s) declare that no financial support was received for the research, authorship, and/or publication of this article.

Conflict of interest

The authors declare that the research was conducted in the absence of any commercial or financial relationships that could be construed as a potential conflict of interest.

Publisher's note

Supplementary material

The Supplementary Material for this article can be found online at: https://www.frontiersin.org/articles/10.3389/fonc.2023.1229493/full#supplementary-material

References

1. Carlson ER, Schlieve T. Salivary gland Malignancies. *Oral Maxillofac Surg Clin North Am* (2019) 31:125–44. doi: 10.1016/j.coms.2018.08.007

2. Zanoni DK, Patel SG, Shah JP. Changes in the 8th edition of the American joint committee on cancer (AJCC) staging of head and neck cancer: rationale and implications. *Curr Oncol Rep* (2019) 21:52. doi: 10.1007/s11912-019-0799-x

3. Chow LQM. Head and neck cancer. *N Engl J Med* (2020) 382:60–72. doi: 10.1056/NEJMra1715715

4. Aro K, Ho AS, Luu M, Kim S, Tighiouart M, Clair JM, et al. Development of a novel salivary gland cancer lymph node staging system. *Cancer* (2018) 124:3171–80. doi: 10.1002/cncr.31535

5. Lee H, Roh JL, Cho KJ, Choi SH, Nam SY, Kim SY. Positive lymph node number and extranodal extension for predicting recurrence and survival in patients with salivary gland cancer. *Head Neck* (2020) 42:1994–2001. doi: 10.1002/hed.26135

6. Qian K, Sun W, Guo K, Zheng X, Sun T, Chen L, et al. The number and ratio of positive lymph nodes are independent prognostic factors for patients with major salivary gland cancer: Results from the surveillance, epidemiology, and End Results dataset. *Eur J Surg Oncol* (2019) 45:1025–32. doi: 10.1016/j.ejso.2018.11.008

7. Terada H, Suzuki H, Hanai N, Nishikawa D, Koide Y, Hasegawa Y. Prognostic value of lymph node density for major salivary gland carcinoma without clinical lymph node metastasis. *Am J Otolaryngol* (2020) 41:102304. doi: 10.1016/j.amjoto.2019.102304

8. Lombardi D, Tomasoni M, Paderno A, Mattavelli D, Ferrari M, Battocchio S, et al. The impact of nodal status in major salivary gland carcinoma: A multicenter experience and proposal of a novel N–classification. *Oral Oncol* (2021) 112:105076. doi: 10.1016/j.oraloncology.2020.105076

9. Svider PF, Blasco MA, Raza SN, Shkoukani M, Sukari A, Yoo GH, et al. Head and neck cancer. *Otolaryngol Head Neck Surg* (2017) 156:10–3. doi: 10.1177/0194599816674672

10. Fang Q, Zhang X, Dai L, Luo R, Yuan J. Association between factor of parotid lymph node and prognosis in parotid cancer. *Eur J Surg Oncol* (2023) 49(8):1405–10. doi: 10.1016/j.ejso.2023.04.002

11. Fang Q, Wu J, Du W, Zhang X. Predictors of distant metastasis in parotid acinic cell carcinoma. *BMC Cancer* (2019) 19:475. doi: 10.1186/s12885-019-5711-4

12. Fang Q, Wu J, Liu F. Oncologic outcome and potential prognostic factors in primary squamous cell carcinoma of the parotid gland. *BMC Cancer* (2019) 19:752. doi: 10.1186/s12885-019-5969-6

13. Hsieh CE, Hung CY, Lin CY, Chen JS, Chang KP, Aithala SP, et al. High metastatic node number, not extranodal extension, as a node-related prognosticator in surgically treated patients with nodal metastatic salivary gland carcinoma. *Head Neck* (2019) 41:1572–82. doi: 10.1002/hed.25603

14. Lin X, Lin Q, Chen X, Wang D. Number of positive lymph nodes combined with the logarithmic ratio of positive lymph nodes predicts long-term survival for patients with node-positive parotid gland carcinoma after surgery: a SEER population-based study. *Eur Arch Otorhinolaryngol* (2023) 280:2541–50. doi: 10.1007/s00405-023-07848-7

15. Han F. Number of positive lymph nodes affects outcomes in parotid adenoid cystic carcinoma. *Front Oncol* (2023) 13:1153186. doi: 10.3389/fonc.2023.1153186

16. Elhusseiny KM, Abd-Elhay FA, Kamel MG, Abd El Hamid Hassan HH, El Tanany HHM, Hieu TH, et al. Examined and positive lymph nodes counts and lymph nodes ratio are associated with survival in major salivary gland cancer. *Head Neck* (2019) 41:2625–35. doi: 10.1002/hed.25742

17. Cho WK, Roh JL, Cho KJ, Choi SH, Nam SY, Kim SY. Lymph node ratio predictive of recurrence, distant metastasis, and survival in submandibular gland carcinoma patients. *J Cancer Res Clin Oncol* (2019) 145:1055–62. doi: 10.1007/s00432-019-02876-5

18. Shi X, Liu XK, An CM, Wei WJ, Tao Y, Ji Y, et al. Anatomic extent of lymph node metastases as an independent prognosticator in node-positive major salivary gland carcinoma: A study of the US SEER database and a Chinese multicenter cohort. *Eur J Surg Oncol* (2019) 45:2143–50. doi: 10.1016/j.ejso.2019.06.029

19. Gau M, Fonseca A, Ozsahin M, Fayette J, Poupart M, Roux PE, et al. Prognostic impact of extranodal extension in resected head and neck squamous cell carcinomas in the era of postoperative chemoradiation: A retrospective monocentric study. *Oral Oncol* (2021) 123:105605. doi: 10.1016/j.oraloncology.2021.105605

Frontiers in Oncology

Advances knowledge of carcinogenesis and tumor progression for better treatment and management

The third most-cited oncology journal, which highlights research in carcinogenesis and tumor progression, bridging the gap between basic research and applications to imrpove diagnosis, therapeutics and management strategies.

Discover the latest Research Topics

See more →

Frontiers

Avenue du Tribunal-Fédéral 34
1005 Lausanne, Switzerland
frontiersin.org

Contact us

+41 (0)21 510 17 00
frontiersin.org/about/contact